Final Report
Integrated Commercial Carbon Capture and Storage (CCS) Prefeasibility Study at Rock Springs Uplift, Wyoming

May 30, 2019

SUBMITTED UNDER FUNDING OPPORTUNITY ANNOUNCEMENT

DE-FE0029302

SUBMITTED BY

Center for Economic Geology Research
School of Energy Resources, University of Wyoming, Energy Innovation Center
1020 E. Lewis Street
Laramie, WY 82071

PRINCIPAL INVESTIGATORS

Dr. Fred McLaughlin
(307) 766-6685
(307) 766-6078 (fax)
derf1@uwyo.edu

Kipp Coddington, Esq.
(307) 766-6731
(307) 766-6078 (fax)
kcodding@uwyo.edu

BUSINESS POINT OF CONTACT

Cindy Ishkanian
(307) 766-6896
(307) 766-6078 (fax)
cishkani@uwyo.edu

SUBMITTED TO

U.S. Department of Energy
National Energy Technology Laboratory

EXECUTIVE SUMMARY

To establish the potential of safe, long-term commercial-scale carbon capture & storage (CCS) in southwestern Wyoming, the University of Wyoming formed a CCS coordination team (CCT) to complete a Phase I CarbonSAFE pre-feasibility study adjacent to the region's largest coal-fired power plant, the Jim Bridger Plant (JBP). The study's primary objective was to evaluate the potential of storing 50+ million metric tons of anthropogenic carbon dioxide (CO_2) in stacked reservoirs over a period of 25 years. In addition, this integrated study evaluated related aspects of carbon capture utilization & storage (CCUS) at the study site, including: (1) the CO_2 character of post-combustion flue gas from JBP and the technical capacity for retrofitting proven commercial-scale CO_2 capture technology relative to CO_2 source character and technological constraints; (2) utilization of the existing CO_2 pipeline network in the immediate vicinity of JBP for enhanced oil recovery (CO_2-EOR) and utilizing that network as part of a regional hub for CO_2 storage from other anthropogenic sources; (3) assessment of the challenges and benefits of meeting all of CarbonSAFE programmatic Phase I goals relative to Wyoming's carbon management regulatory framework; and (4) assessment of the community and environmental factors that may impact CCS at JBP.

With respect to storage, we analyzed the potential of stacked Mesozoic reservoirs at the study site, focusing on the Entrada and Nugget sandstones. The reservoir response to injection simulations varied greatly between formations, though they both were capable of CO_2 storage. The Entrada Sandstone is relative thin (~40') and heterogeneous; storage using one injection and production well was limited to 1.2 Mt over 25 years at the study site. The Nugget Sandstone is much thicker (> 400') and generally homogeneous; storage using one injection and production well approached 15.0 Mt over 25 years; this scenario suggests that the storage potential in the Nugget Sandstone is close to the estimated P90 calculation of 9.6 Mt/mi^2 as models indicate a storage potential of 8.3 Mt/mi^2 at saturation. Both reservoirs' storage capacity benefited greatly from coupling an injection well with an offset production well; total storage capacity increased and reservoir pressure stayed below critical thresholds. This indicates that implementing a pressure management strategy at the study site would optimize storage and decrease risk. Seals associated with the targeted reservoirs were shown to be capable of retaining the potential storage volumes, and the site benefits from multiple seal redundancies (i.e. > 7,000' of seal formations).

Furthermore, assessment of different reservoir variables (e.g., fluid composition, pressure, etc.) indicates all reservoirs at the study site are isolated. Storage assessments from Mesozoic reservoirs were coupled with simulations from the site's Paleozoic reservoirs (the Weber Sandstone and Madison Limestone), which were the focus of previous study. The fully integrated stacked reservoir pre-feasibility studies suggest that the Nugget and Madison formations alone could safely store 50 million metric tons of CO_2 within the study site. Furthermore, both formations are true saline reservoirs near JBP, making them ideal target reservoirs for CO_2 sequestration.

Analysis of Wyoming's laws and regulations confirm that the State has a favorable policy environment for CCS/CCUS. In addition to clarifying spore space ownership and providing for unitization of storage rights, Wyoming has enacted laws that clarify requirements for CCS projects by: (1) setting permitting procedures (Wyo. Stat. § 35-11-313 (2017)); (2) providing for post-closure monitoring, verification and accounting (MVA) via a trust fund approach (id. § 35-11-318); (3) specifying that the injector, not the

pore space owner, is generally liable (id. § 34-1-513); (4) clarifying that production rights are dominant but cannot interfere with storage (id. § 30-5-501); and (5) providing a certification procedure for CO_2 incidentally stored during EOR (id. § 30-5-502). Additionally, the Wyoming Department of Environmental Quality (WYDEQ) filed for Underground Injection Code (UIC) Class VI primacy with the U.S. Environmental Protection Agency (EPA), a factor that is anticipated to facilitate the future permitting of CCS sites within the State. This project also defined a strategy for implementing an insurance program to cover long-term risk associated with CCS at the project site, which is a first of its kind study for the State.

The project's economic models estimated that the following revenues collectively are sufficient to finance the project over its lifespan if CO_2 utilization is coupled with CCS via the following strategies: (1) sales of CO_2 for EOR (approximately $69 million/year); (2) use of CO_2 tax credits such as amended §45Q and §48A (approximately $484 million total); and (3) sales of low-carbon electricity and marketable carbon offset/credits into carbon-constrained markets (approximately $11-$17 million/year) to West Coast consumers. These revenue estimates are broadly consistent with other studies that concluded arbitrage in JBP retail electricity sales between California and Wyoming could help to support the cost of deploying CCS at JBP. The models also indicate that maintaining a successful business case for long-term CCS -- wherein associated capture, transportation and operational costs are fully addressed at JBP -- is reliant on numerous external factors that complicate predictions.

This study suggests that this site meets the CarbonSAFE program's requirements of being able to feasibly store 50+ million metric tons of CO_2 over 25 years within the site's stacked reservoirs, especially if coupled with pressure management strategies. This study suggests that the Nugget Sandstone and the Madison Limestone are two of the best reservoirs in the State with respect to overall storage capacity. In addition, the site's proximity to existing CO_2 transportation networks, CO_2-EOR opportunities, ability to sell to markets that value low-carbon electricity, Wyoming's existing carbon regulatory framework, and a public that is well-educated with respect to energy markets and issues collectively increase the potential for implementing commercial-scale CCS adjacent to the JBP.

With respect to the available technical and non-technical site data, and the reservoir quality at the study site, we suggest that this site is capable of moving directly into Phase III of the CarbonSAFE program.

TABLE OF CONTENTS

Chapter I: Project Management and Execution

Kipp Coddington
Director, Energy Policy, & Economics
Center for Economic Geology Research
School of Energy Resources, University of Wyoming
1020 E. Lewis Street, Energy Innovation Center
Laramie, WY 82071

Section 1.1: Project Introduction

This project is an integrated carbon capture & storage (CCS) pre-feasibility assessment of the storage of 50+ million metric tons of carbon dioxide (CO_2) from partner PacifiCorp's coal-fired Jim Bridger Plant (JBP) in the Rock Springs Uplift (RSU) in southwestern Wyoming. In addition to benefiting from Wyoming's favorable CCS laws, the project possess three unique attributes that make it compelling as the future site of a large-scale (50+ million metric tons of CO_2) integrated CCS facility:

First, an immediately adjacent and previously studied saline storage complex. The identified storage complex is the RSU, one of the most intensively studied saline storage sites in the United States. Immediately south of JBP, the RSU was the subject of several successful initial deep reservoir characterization studies between 2009 and 2014, including the 2009-2011 U.S. Department of Energy's (DOE) Wyoming Carbon Underground Storage Project (WY-CUSP). For WY-CUSP, the University of Wyoming's (UW) Carbon Management Institute (CMI) drilled a ~10,800 ft. characterization well (WY-CUSP Test Well; also known as the RSU #1) and collected core and subsurface data from deeper reservoirs in the RSU in the immediate vicinity of JBP. *Significantly, WY-CUSP and related legacy investigations confirmed that two deeper reservoirs at the RSU -- the Weber Sandstone and Madison Limestone -- alone have sufficient capacity to store 50+ million metric tons of CO_2 (Surdam ed., 2013).* By investigating shallower reservoirs that presumably are less costly to access, this CarbonSAFE pre-feasibility project builds upon and benefits from this voluminous amount of favorable RSU reservoir characterization legacy data.

Second, a major coal-fired CO_2 source that is at the forefront of carbon management policy. JBP is at the forefront of carbon management struggles between coal states like Wyoming and West Coast states that rely upon imported fossil energy but require the same to be low carbon. California shortly will recognize CCS as a carbon mitigation compliance technology which means that JBP could be poised to sell low-carbon electricity into the California market at a premium. JBP similarly is positioned to potentially play an important role in efforts to integrate the western transmission grid, with a CCS-equipped JBP potentially serving as that grid's "clean coal" anchor.

Third, immediate access to Wyoming's existing CO_2 pipeline infrastructure and CO_2-EOR markets. JBP is a mere 11 to 16 miles away from Wyoming's existing CO_2 pipeline infrastructure, which traverses the State in a rough SW-NE direction, ultimately passing near the coal-fired Dry Fork Station (DFS) in Gillette in the State's northeast corner. That pipeline's proximity to major coal-fired CO_2 emitters such as JBP and DFS, as well as to depleting oil fields, create favorable flexibilities for both saline storage and CO_2 enhanced oil recovery (CO_2-EOR). JBP's CO_2 could be stored locally in the RSU or transported elsewhere in Wyoming for storage. Some portion of JBP's CO_2 similarly could be transported for CO_2-EOR elsewhere in the State, thereby improving the project's economics. For these and other reasons, the

project site is anticipated to be the future anchor for carbon capture utilization & storage (CCUS) in the Rocky Mountain region.

Section 1.2: Project Management Summary

The Project Management Plan was successfully prepared, updated as necessary and implemented according to schedule, with no issues noted.

Section 1.3: Developing the CCS Coordination Team

A CCS coordination team (CCT) was convened at the beginning of the project (Figure 1.1.1). The CCT consisted of the following members: (1) UW's CMI; (2) PacifiCorp; (3) Advanced Resources International, Inc.; (4) UW's Enhanced Oil Recovery Institute; (5) KKR; (6) WellDog; (7) UW's Center for Energy Economics & Public Policy; (8) UW's College of Law; (9) the Office of the Governor of Wyoming; and (10) the Wyoming Infrastructure Authority. All team members possessed substantial experience with CCS/CCUS projects and policies. Through in-person meetings and teleconferences, the CCT collaborated closely throughout the project, ultimately leading it to a successful conclusion.

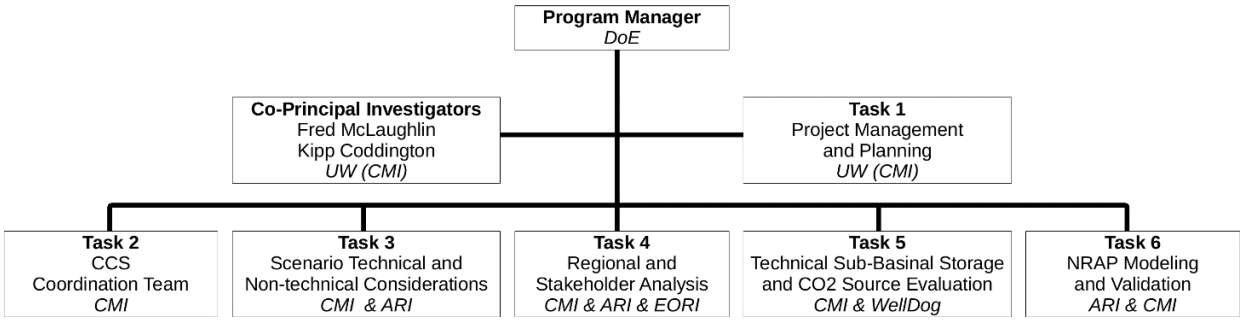

Figure 1.1.1: CarbonSAFE Phase I project organization chart.

Chapter 1 Conclusion

Under the guidance and leadership of an experienced CCT, the Phase I CarbonSAFE prefeasibility study at the RSU was successfully completed in accordance with the project management plan. The two deeper reservoirs at the RSU -- the Weber Sandstone and Madison Limestone -- alone have sufficient capacity to store 50+ million metric tons of CO_2.

Chapter II: Scenario Technical and Non-Technical Analysis

Charles Nye, Tara Righetti, Ben Cook, Thomas Moore, and Erin Phillips
Center for Economic Geology Research
School of Energy Resources, University of Wyoming
1020 E. Lewis Street, Energy Innovation Center
Laramie, WY 82071

In past work the RSU has been treated as an omnibus site that is roughly delimited by the geologic structure (Roehler, 1977). However, this area makes up most of central Sweetwater County and is too large for a feasibility assessment at the level of detail that will be sought in later phases of the CarbonSAFE program (NETL, 2013). In acknowledgement of this scoping challenge, the activities described in this chapter challenged the idea that the RSU was a monolithic single location, and drew out heterogeneous factors within the study area that suggest one specific location over another.

The work in this chapter was divided between finding and evaluating factors. The first (described in section 2.1) describes factors that might influence the project's choice of source, transport, and storage options. That phase also identified the factors' presence in a scenario as beneficial, no effect, or detrimental. In the second phase (described in section 2.2). The importance of these factors was assessed both in competition with each other and as part of 6 scenarios. The result was a list of ranked scenarios with specific ~1 sq mile locations, with recognition that some projects could need an area ~10 times larger for the subsurface CO_2 and pressure plumes.

Section 2.1: Source, Transport, & Storage Factors Identification

The first work of this project included identification of factors that might affect the final scenario. These factors were listed in the Task 3.0 Deliverable "Identified Factor List" which was provided to the program officer June 30, 2017. The factors presented in the deliverable have been updated as the project progressed and now contain more information than before. The deliverable was assembled with input from legal, economic, and technical project team members. The factors below are divided among six categories: (1) Legal; (2) Economic; (3) Environmental; (4) Geologic; (5) Partnership and Outreach; and (6) Engineering Factors, which are summarized below (Table 2.1.1).

Table 2.1.1. Factors identified for scenario selection and their effect on the project.

Factor	Source	Transport	Storage
Legal Factors			
Federal (BLM) Ownership of Surface and Mineral Interests	O	+/-	+/-
Few Private Landowners	O	+/-	+/-
State Land Sections	O	O	O
State, Federal, and Local Laws and Regulations	-	+/-	O
Sage Grouse habitat	O	-	-
National Historic Preservation Act	O	-	-
Economic Factors			
Increasing Distance to Injection Site	-	-	O
Single Point Source of CO2 versus Multiple Source Plants	+/-	-	O
Depth of Injection Site	O	O	+/-
High Oil Prices	+	+/-	+
45Q or Other Tax Incentives	+	O	O
Environmental Factors			
Protected species or their critical habitat	-	-	O
Presence of a waterbody	-	-	O
Protected areas	O	-	O
Geologic Factors			
Potential for stacked storage	O	O	+
Compartmentalization of reservoir	O	O	+/-
Sufficiently high porosity in reservoir	O	O	+
High permeability in reservoir	O	O	+/-
Available subsurface data set (logs and seismic)	O	O	+
Faulting	O	-	+/-
Continuous seal with sufficiently low porosity and permeability	O	O	+
Reservoir depth between ~3000 ft and ~13000 ft	O	O	+
High salinity storage formations	O	O	+
Cementation in reservoir	O	O	-
Reservoir and seal heterogeneity	O	O	-
Confirmed valuable minerals	O	O	-
Developed Oil and Gas reservoirs	O	-	+
Partnership and Outreach Factors			
Synergy with CO2 producers	+	+	+
Negative public perception	-	-	-
Engineering Factors			
Source of over 2Mtonnes/year	+	-	-
Large distance between Source and Storage sites	O	-	-
High Initial CO2 Purity	+	+	+
Traditional Source	+	O	O
Competent and dipping rock strata	O	-	-

Section 2.1.1 Legal Factors

Most identified legal factors apply to all of the RSU study area. For example, the checkerboard ownership of BLM and private owners that resulted from the construction of the transcontinental railroad applies to all considered locations. Two exceptions are the Sage Grouse habitat and National Historic Preservation Act which selectively apply to only some parts of the RSU. The first four of the following six factors apply almost everywhere in the RSU, and the last two apply heterogeneously.

Federal (BLM) Ownership of Surface and Mineral Interests

Source: ( ) No effect
Transport: (+) (-) The BLM is responsible for granting rights-of-way (ROW) for CO_2 pipelines that cross federal land managed by the Department of Interior (DOI). Pursuant to the Mineral Leasing Act of 1920 (MLA), the BLM can impose common carrier requirements on pipelines across federal lands.

Obtaining a ROW from the BLM may be time consuming compared to state permitting and regulation, and the decision to grant a ROW could trigger a National Environmental Policy Act (NEPA) analysis (-). The large percent of ownership means contracting with fewer parties (+) but conversely an adverse decision by the BLM on whether to grant a ROW could preclude development of the project due to BLM's ownership of half every development area (-).
Storage: (+) (-) Pore space is neither a leasable mineral under the MLA nor is it a locatable mineral under the General Mining Law of 1872. It is unclear precisely how the BLM would grant injection/storage rights within pore space on land managed by the DOI and whether a decision to grant injection rights without a surface use would require a NEPA analysis. The current guidance (IM No. CO-2016) suggests that BLM should grant an easement for wastewater injection into federal pore space, and it is possible that DOI would adopt a similar approach for pore space utilization for carbon storage. Uncertainty on the procedure for obtaining injection rights on federal land is unfavorable (-). It is favorable, however, to have fewer parties with which to contract, thus making it more feasible to obtain injection rights to at least 80% of the unit area, as required by Wyoming law (+). Conversely, it is unfavorable in that an adverse decision from DOI on the grant of an easement would make obtaining an injection unit more difficult due to the land ownership pattern, called a checkerboard, wherein each alternating section is federal.

Few Private Landowners

Source: ( ) No effect
Transport: (+) (-). It is favorable to have fewer landowners with which to contract for easements and right of ways (+). It is unfavorable in that certain parties may have a de facto ability to block development of transportation infrastructure due to their considerable land positions, thus enabling them to stop the project or to negotiate for much higher consideration for pipeline easements (-). In the RSU area there are four significant landowners.
Storage: (+) (-) It is favorable to have fewer owners with which to contract (+). It is unfavorable in that a decision not to join by any one landowner could result in an inability to obtain injection rights to 80% of the unit as required by Wyoming law (-) or could make obtaining any such rights more costly (-).

State Land Sections

Source: ( ) No effect
Transport: ( ) No effect
Any transportation infrastructure crossing State land sections will require either an easement or right of way. This requirement is neither favorable nor unfavorable although historically, the Office of State Lands and Investments (OSLI) has been supportive of comparable projects.
Storage: ( ) No effect
Pore space and injection rights will need to be obtained from OSLI for any area within the unit that is owned by the State. If surface injection facilities are located on State lands, the project will need to acquire either a Temporary Use Permit (TUP) or a Special Use Lease (SUL) from OSLI as approved by the State Board of Land Commissioners (Board). Obtaining a TUP or SUL is estimated to take 3-6 months.

State, Federal, and Local Laws and Regulations

Source: (-) It is unfavorable that the possibility that capture of CO_2 might trigger new source review or other permitting or requirements under the U.S. Clean Air Act (CAA), thus potentially deterring participation from industrial CO_2 providers.

Transport: (+) (-) Any transportation infrastructure must comply with state requirements for citing, construction, liability, and safety. It is unclear under Wyoming law whether a CO_2 pipeline for carbon storage can procure easements by condemnation and, if so, how just compensation would be ascertained. Safety compliance of the CO_2 pipeline while in operation would be the responsibility of the Department of Transportation as is the case for all other pipelines per the U.S. Pipeline and Hazardous Materials Safety Administration.
Storage: ( ) No effect
Surface operations must comply with local zoning. It is likely that the project would need to obtain a variance or special use permit or a county conditional use permit. Any injection well would require a Class VI Underground Injection Control (UIC) permit under the U.S. Safe Drinking Water Act (SDWA) issued either by U.S. EPA or the Wyoming Department of Environmental Quality if, at the time of such permitting, Wyoming had obtained state primacy for implementation of the Class VI permitting program. All injection and storage operations must comply with state and federal environmental laws, including, without limitation, the CAA, the Clean Water Act (CWA) and the Endangered Species Act (ESA). Carbon dioxide streams that are injected in Class VI wells are conditionally excluded from classification as hazardous wastes under the U.S. Resource Conservations & Recovery Act (RCRA).

Sage Grouse habitat

Source: ( ) No effect
Transportation: (-) Any surface disturbing activities within an area designated as sage grouse core area will require conservation offsets or mitigation. Total surface disturbance may be limited to a fraction of the total land area.
Storage: (-) Any surface disturbances within an area designated as sage grouse core area will require conservation offsets or mitigation. Total surface disturbance may be limited to a fraction of the total land area. Further, surface injection operations within core areas could be limited to certain times of year to avoid interference with mating.

National Historic Preservation Act

Source: ( ) No effect
Transportation: (-) A survey to find any historic sites will be required before any surface disturbing activities can occur in the RSU area. Upon finding an historic site it must be moved or documented before disturbance may occur. Waivers for sites that are of minimal historical value are common following expedient documentation. The density of sites at the RSU is less than in the PRB so while detrimental to the project, there is a much lower probability of the National Historic Preservation Act (NHPA) causing a delay than elsewhere in Wyoming.
Storage: (-) As with transport, some details of the well siting may require NHPA documentation, accommodation, or translocation.

Section 2.1.2 Economic Factors

Of the factors studied in this work, economic factors perhaps do the best job of drawing out the trade-offs inherent in any saline carbon storage project. All analysis was performed early in this project, on 2017 technology with 2017 dollar values. The exact costs have since changed slightly, but the relative importance of the tradeoffs remains similar. Among the most important conclusions was that shallower storage depths could offset the costs of longer transport. This offset suggests that when designing pipelines teams should consider surface distance in the same function that considers storage depth. As explained in Section 2.2, the RSU has a steep enough dip that a project there could save money by

transporting CO_2 a greater distance so long as more than 15 wells are necessary for the project. This quantity is a reasonable expectation because monitoring wells play an essential role in MVA plans (Greenberg et al., 2017).

Most of the following five factors may seem intuitive, but the interplay between them can be counterintuitive, with the storage-depth versus transport-distance tradeoff being the most dramatic. Another conclusion is that the project benefits from high oil prices. This suggests that high oil prices might not only reduce CO_2 emissions into the atmosphere, but also encourage implementation of capture projects that further reduce emissions. Finally, the project will benefit from various tax credits.

Increasing Distance to Injection Site

Source: (-) Increasing the pipeline span may require additional CO_2 compression at the source, increasing both capital costs and electricity requirements.
Transport: (-) Increasing the pipeline span can dramatically increase the transport-related costs of the project. While there are some economies of scale in building longer pipelines, it does little to offset the additional expense of building longer lines. The 10" diameter pipeline required to transport 100 mmcfd of CO_2 is estimated to cost around $900-$950 thousand per mile for longer distances of 20-35 miles, rising to around $1.25 million per mile for short distances (< 5 miles). While unlikely for the anticipated scenarios, any additional pumping for pressure maintenance on the pipeline over long distances would add additional capital expenses and electricity charges for storage operations.
Storage: ( ) No effect

Single Point Source of CO_2 versus Multiple Source Plants

Source: (-) (+) The capital and operating costs of required capture technology can vary substantially based on the flue-gas characteristics of the source plant and the scale of operation. Multiple point sources will not benefit from economies of scale, but may be much more efficient at CO_2 capture if they have relatively pure CO_2 streams before processing. If the multiple sources are proximate, some processing facilities such as dehydration and compression may be shared.
Transport: (-) Multiple point sources can increase the complexity of the pipeline systems required to gather and transport CO_2 to the injection site. Each point source will have to have a spur pipeline adequate for volumes, their own CO_2 meters (~ $250,000), and a tie-in manifold added to the pipeline if not sharing a single compression station.
Storage: ( ) No effect

Depth of Injection Site

Source: ( ) No effect
Transport: ( ) No effect
Storage: (-) (+) Drilling depth increases the cost of the wells, but not at the magnitude of other factors. Drilling and completion costs are currently estimated at $200 per foot of depth plus fixed costs for surface equipment at $250,000-$500,000 per well. The injection sites contemplated for the Rock Springs Uplift (RSU) area mostly range from 4,600' to 9,600' but in some cases up to 14,000' feet deep resulting in drilling and completion costs of $920,000, $1.92 million, and $2.8 million per well, respectively. With well cost differences of $1-$2 million per well, choosing a site with shallow depths can offset the cost of 1-2 miles of additional pipeline. If three wells are required at the storage site, the shallower wells would offset roughly 3-6 miles of additional pipeline.

High Oil Prices

Source: (+) High oil prices could benefit the project because the price of CO_2 for EOR operations has historically been pegged to the WTI Oil price with a fixed component around $0.50 per mcf for transportation plus 1-2% of the WTI oil price. High oil prices -- even if volatile -- would result in more revenue and allow more expensive source capture technologies to be used economically.
Transport: (-) (+) High oil prices, as above, result in more revenue and would allow a larger transport distance to be economic. There is a minor interference as high oil prices may result in oils and gas development. Such development may result in competition for services shared with oil and gas development such as pipeline construction.
Storage: (+) High oil prices, as above, result in more revenue and would allow deeper wells to be economic. The oil price would need to be slightly higher than strict economics requires because the high costs of implementing CO_2-EOR often require sustained high oil prices before operators commit to such projects. Thus, sustained high oil prices are an overall benefit to the project economics (and vice versa).

45Q or Other Tax Incentives

Source: (+) The current 45Q tax credit is beneficial to the project because CO_2 sequestration projects receive a tax credit of $20 per ton provided certain conditions are met, including a limit as to the aggregate tons eligible for the credits. The availability of the tax credits act as a partial revenue stream, which can help alleviate the capture cost.
Transport: ( ) No effect
Storage: ( ) No effect

Section 2.1.3 Environmental Factors
The environmental factors in this work focused on regulation that protected local flora and fauna, and geographic features such as waterways and national parks. Readily apparent concerns such as direct atmospheric release of CO_2 were not considered here because many of the geologic factors address those. Most of these factors affect the transport decision because that component stands to disrupt the greatest area of land.

Protected species or their critical habitat

Source: (-) Being near a protected species or their critical habitat is unfavorable because the ESA would require mitigation if fitting capture equipment caused new disruption to an endangered, threatened, proposed, or candidate species around the source.
Transport: (-) Similarly, transport near critical habitat is unfavorable because the ESA would require either mitigation or rerouting of transport pipeline if that disturbance affected these species.
Storage: ( ) No effect

Presence of a waterbody

Source: (-) The presence of a waterbody is unfavorable because CWA and SDWA place extra requirements on construction that has the potential to affect waterbodies.
Transport: (-) The presence of a waterbody near the transport pipeline is unfavorable because the CWA and SDWA require mitigation with best management practices for construction that will increase erosion, or cross drainages.

Storage: ( ) No effect

Protected areas

Source: ( ) No effect
Transport: (-) Transport through a protected area (national or state park, national monument, area of historical or cultural significance) in unfavorable because the NHP, Antiquities Act, and other acts would require it to be re-routed.
Storage: ( ) No effect

Section 2.1.4 Geologic Factors

Much of this project's pre-feasibility study was directed at geologic factors. Accordingly there were many factors to consider that almost exclusively affect the storage component of the project. The following 13 factors quickly state why a given geologic property is important to the project.

Potential for stacked storage

Source: ( ) No effect
Transport: ( ) No effect
Storage: (+) Stacked storage is favorable because it would increase storage capacity and reduce lateral extent of a CO_2 plume. Performing MVA for stacked formations with roughly equal area of reviews is about as challenging as performing MVA for a single formation with that same area of review. As a result stacked storage allows more CO_2 to be stored without a proportional increase in MVA effort.

Compartmentalization of reservoir

Source: ( ) No effect
Transport: ( ) No effect
Storage: (+) (-) Compartmentalization could be favorable because it can improve CO_2 trapping and reduce area of review. However, if the compartments are entirely isolated from each other compartmentalization can prove unfavorable because a formation's storage capacity would be greatly reduced, requiring more injection wells, and possibly brine production.

Sufficiently high porosity in reservoir

Source: ( ) No effect
Transport: ( ) No effect
Storage: (+) High porosity is favorable because it directly results in greater total storage capacity. Due to the correlation between porosity and permeability (Kozeny, 1927; Carman, 1937), it normally would also allow higher safe injection rates. Injection rates cannot be guaranteed, but total injected volume can be.

High permeability in reservoir

Source: ( ) No effect
Transport: ( ) No effect
Storage: (+) (-) High permeability in the target reservoirs is favorable up to a point. Common permeability ranges allow a larger amount of CO_2 to be safely injected per well per year. However, if

the permeability is excessive the CO_2 plume becomes extremely mobile and buoyancy forces result in inefficient use of reservoir thickness.

Available subsurface data set (logs and seismic)

Source: ( ) No effect
Transport: ( ) No effect
Storage: (+) While there is some well-log and seismic data is available across all of the RSU, there is a particular concentration at the site of the plugged and abandoned RSU#1 well. This means that characterization of the subsurface will have greater accuracy the closer a relevant study area is to the RSU#1 site.

Faulting

Source: ( ) No effect
Transport: (-) Faults near a transport pipeline pose a small but significant structural challenge necessitating more expensive joints in construction and extra monitoring for damage caused by fault activation.
Storage: (+) (-) Faulting can be beneficial for storage if it provides large-scale compartmentalization that could contain a CO_2 plume. However, faulting can also be detrimental if the fault is conductive or results in an offset in the seal system which compromises its integrity.

Continuous seal with sufficiently low porosity and permeability

Source: ( ) No effect
Transport: ( ) No effect
Storage: (+) A continuous seal with low porosity and permeability is favorable because it would contain a CO_2 plume and prevent leakage. The thickness of this seal also reduces risk that it could be compromised over its whole thickness. In the RSU the Baxter shale appears to be a good seal regional seal that offers ultimate protection against release.

Reservoir depth between ~3000 ft and ~13000 ft

Source: ( ) No effect
Transport: ( ) No effect
Storage: (+) Almost all saline reservoirs at the RSU are at depths greater than ~3000 ft and accordingly would keep CO_2 in the supercritical state. Depths should be less than ~13000 ft because injection at deeper levels increases well costs due to the added necessity of reservoir pressure management during injection. Only a few reservoirs do not meet that criterion.

High salinity storage formations

Source: ( ) No effect
Transport: ( ) No effect
Storage: (+) High salinity (TDS>10,000 mg/L) is favorable because the UIC program of the SDWA does not apply to such reservoirs. If this could not be achieved, an aquifer exemption would be needed.

Cementation in reservoir

Source: ( ) No effect
Transport: ( ) No effect
Storage: (-) Cementation in reservoir in unfavorable because it reduces porosity. Variable cementation within a reservoir could pose problems because it would introduce uncertainty into reservoir characterization. If the cementation were carbonate, it could enhance ultimate mineral trapping, but this was not considered significant enough to alter this factor's categorization.

Reservoir and seal heterogeneity

Source: ( ) No effect
Transport: ( ) No effect
Storage: (-) Locations that have significant reservoir and seal heterogeneity are unfavorable because it generally increases uncertainty in characterization. One of the few methods to assess and address these effects is 3D seismic acquisition.

Confirmed valuable minerals

Source: ( ) No effect
Transport: ( ) No effect
Storage: (-) An area with confirmed valuable minerals are unfavorable for saline storage because, if CO_2 was stored in an area that conflicted with the minerals estate, the minerals could become harder to produce. This could potentially result in reduced cooperation from the owners of the mineral rights or even legal proceedings for mineral trespass.

Developed Oil and Gas reservoirs

Source: ( ) No effect
Transport: (-) Developed oil and gas reservoirs on the path planed for a would-be pipeline are unfavorable because surface transport will need to negotiate crossing and interfering with Oil and Gas infrastructure.
Storage: (+) Developed oil and gas reservoirs are favorable because they indicate reservoir capacities, trapping mechanisms, holding capacities, competent sealing systems, and formation fluids that are likely saline.

Section 2.1.5 Partnership and Outreach Factors

Partnership and Outreach factors consider the social and inter-organizational relationship challenges a CarbonSAFE project might face. These factors are not only the broadest and difficult to define but also carry the greatest risk. For example, losing public support would stall a project's advance regardless of the technical merit of the planned work.

Synergy with CO_2 producers (e.g., Jim Bridger Plant, trona mines)

Source: (+) Synergy with producers is favorable as the choice to add a capture plant to the producer's facility is an important part of generating the supercritical CO_2 for transport and storage.
Transport: (+) Transport from a producer's facility will necessarily cross some associated land holdings and possibly interfere with existing infrastructure such as pipelines. Negotiating the details of a solution to these challenges would be easier if the producer is supportive of the project in general.

Storage: (+) Synergy with producers is favorable, especially if storage is on producer's property. Other areas that benefit include collaborative production of media kits and supportive publicity.

Negative public perception

Source: (-) Negative public perception of the CO_2 source is unfavorable.
Transport: (-) A negative public perception of transporting CO_2, especially close to population centers, could adversely affect the outcomes of the project.
Storage: (-) A negative public perception of CO_2 storage, especially close to population centers, could adversely affect the outcomes of the project.

Section 2.1.6 Engineering Factors
The following five engineering factors describe characteristics that would either greatly increase or decrease the engineering challenge of implementing a proposed carbon storage plan.

Source of over 2 Mmt/year

Source: (+) A source of over 2 Mmt/year is favorable because capture does not need to be as efficient and sales of the surplus CO_2 for EOR can offset a greater fraction of the costs.
Transport: (-) The more CO_2 that must be transported for either EOR or saline storage, the wider the diameter required for a pipeline. Pipeline diameters scale almost all associated parts of the transport component (McCoy, 2008) not only greatly increasing expense but also limiting material and design options.
Storage: (-) A source of over 2 Mmt/year necessitates either more wells or higher injection rates, which put more pressure on the formation and equipment. This detriment could be offset by periodically diverting CO_2 in excess of the required amount to other uses such as EOR fields.

Large distance between Source and Storage sites

Source: ( ) No effect
Transport: (-) Large distance between source and storage sites is unfavorable because pipeline costs increase linearly with distance, but at roughly 20 mile intervals a booster compressor station is needed. These stations cause cost to nearly double and add operating expenses.
Storage: (-) Large distance between source and storage sites is unfavorable because the CO_2 may not arrive onsite at adequate pressure and may need to be compressed at the wellhead to maintain down-well injection targets.

High Initial CO_2 Purity

Source: (+) High initial CO_2 purity is favorable because capture technologies such as the amine process are most efficient when capturing an already mostly pure stream. Capture of less pure CO_2 streams is costly compared to industrial sources with purer streams of CO_2.
Transport: (+) Unless extensive dehydration and purification can be undertaken at the capture plant, a less pure CO_2 would be corrosive. Transport of species other than CO_2 inefficiently uses pipeline transport capacity.
Storage: (+) Injection of CO_2 benefits from high initial CO_2 purity for the same reasons of lower corrosiveness and higher efficiency. Additionally, storage benefits from pure CO_2 because contaminating species also reduce the compressibility of supercritical CO_2, making the solution less dense.

Traditional Source

Source: (+) Using a traditional source such as a flue stack is favorable because capture technologies have been traditionally designed to fit flu gas stacks. This manages R&D costs and construction costs during retro-fitting.
Transport: ( ) No effect
Storage: ( ) No effect

Competent and dipping rock strata

Source: ( ) No effect
Transport: (-) Competent and dipping rock strata are unfavorable because they result in rough terrain which is difficult to transport CO_2 across.
Storage: (-) Competent and dipping rock strata are unfavorable because they can deflect drilling which increases the challenge of casing and instrumenting.

Section 2.2: Factors Assessment

Following generation of the above factors and an analysis of their effect on a project, the team developed six scenarios based on permutations of source and storage options, discarding those that could not be feasibly linked by a transport component.

In Sweetwater County there are five CO_2 producers that can generate more than half a metric ton of CO_2 annually. These include the largest CO_2 source in Wyoming, the JBP), which is a coal-fired producer of about 11.8Mmt CO_2/yr. The other four producers are trona plants which taken together produce 90% of the United States' soda ash, an important precursor to household products and chemicals (Wyoming Mining Association, 2018). These four trona plants average 1.35Mmt CO_2/yr each and are clustered ~20km northwest of Green River, Wyoming. Accordingly the team identified two sources: JBP, and this cluster of four trona plants.

As in much of Wyoming, storage formations in Sweetwater County are plentiful. The most significant structural trap is the RSU, a very large anticline between the JBP and the city of Rock Springs. West of Rock Springs most units remain, as deposited, in sub-horizontal strata (Root, Glass, and Lane, 1973). In that area structure would not enhance trapping, and all trapping would be assured by stratigraphy. While past work has also considered the Moxa Arch, it was deemed outside the study area for this project.

The storage formations of interest at the RSU include two previously studied units (the Madison limestone and Webber sandstone) and two new formations (the Entrada sandstone and Nugget sandstone). Each of these has a personal seal and all are under the Baxter shale which is a regional seal. In the sub-horizontal area near the trona plants these same units are present, but at greater depth, and so storage could include focus on the Mesaverde group with a Lewis seal, or the Frontier sandstone which would allow use of the Baxter shale's superior sealing properties.

Transport from the JBP to the sub-horizontal strata west of Rock Springs or in the other direction, from the trona producers to the RSU, would be challenging, but not impossible, because these sources and sinks are separated by ~80km. The following six scenarios avoid that 80 km transport option because the factor analysis of Section 2.1 showed transport was very detrimental to carbon storage projects.

There are two general groups of scenarios because there are two sources. In eastern Sweetwater County there is the JBP, and in western Sweetwater county there are four large (> 0.5 Mmt CO_2/year) trona producers. At each of these sites we consider an on-site option and a proximal State-section. There are two additional options for JBP. The first additional option is low-distance transport to the fly-ash disposal pits, which may be located over a fault system and/or a better section of reservoir. The second additional option is transport to the crest of the anticline, which offers the same formations at a shallower, though still sufficient, depth.

Section 2.3: Scenario Assessment

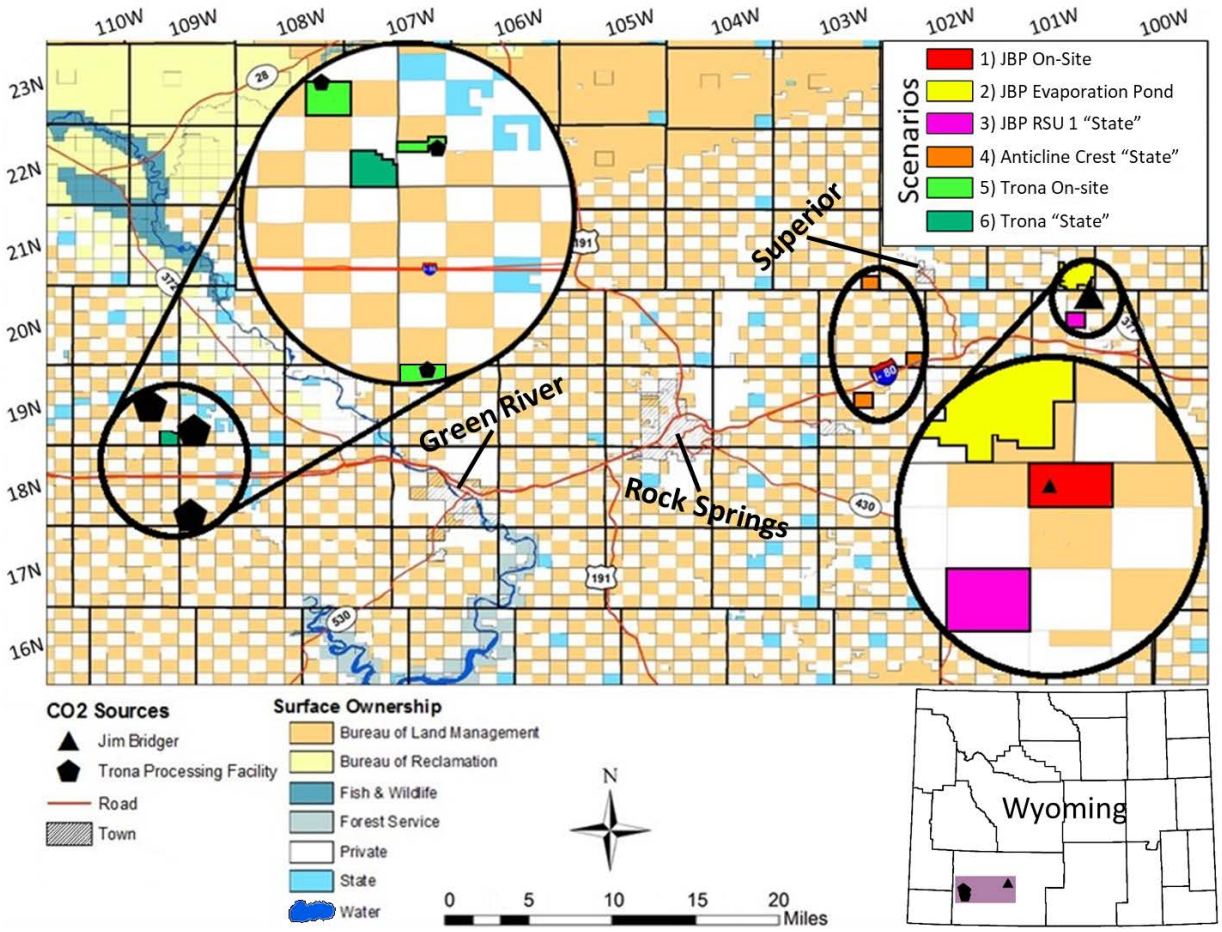

Figure 2.3.1. Land Surface Ownership and the Six Scenarios

Western Sweetwater County: Trona	Eastern Sweetwater County: JBP
● The lower-ranked scenarios are near a set of Trona Processing Plants (black pentagons). ● To source enough CO_2 for this project three of the plants are needed. Buy-in by additional plants would enhance the project economics. ● These scenarios use State and private land. ● The challenge they face is CO_2 capture because trona processing produces CO_2 two different ways: combustion and chemical reaction. ○ Combustion CO_2 is impure, but can be captured with conventional methods. ○ Chemically evolved CO_2 is almost 100% pure but produced in a reaction vessel ill-suited for traditional capture methods. ● Injection could be per-plant or at a central location.	● The top-ranked scenarios are near the Jim Bridger Plant (black triangle). ● These scenarios use State and private land. ● The challenge they face is injection rights. ● Pore space in Wyoming is owned by the surface estate. ● Both BLM and the private ranchers have enough stake that either could stall project development. So outreach is very important. ● Injection on the anticline crest requires expensive transport, but was estimated by Task 4 models to be net-cheaper if more than ~15 wells are drilled, because shallower wells save more than transport adds.

Table 2.3.1. A General Comparison of the Western and Eastern Sweetwater County Scenarios

1) JBP On-site: Very low transport costs, simpler legal challenges, and average reservoir properties make this scenario very attractive. Most target reservoirs are very deep.
CO_2 Source: JBP (11.8 Mmt CO_2/year)
CO_2 Transport: From JBP to elsewhere in the same section of T20N-R101W
CO_2 Storage: Entrada Formation, Nugget Formation, Weber Sandstone, and/or Madison Limestone

2) JBP Evaporation Pond: This area overlies a seismic anomaly which could be a fault system and/or an area of better permeability and porosity.
CO_2 Source: JBP (11.8 Mmt CO_2/year)
CO_2 Transport: From JBP north to one of the four southeast sections of T21N-R101W
CO_2 Storage: Entrada Formation, Nugget Formation, Weber Sandstone, and/or Madison Limestone

3) JBP RSU 1 "State": This scenario has the best geologic constraint due to proximity to the RSU #1 well which was extensively characterized with high resolution logs and ~900ft of core.
CO_2 Source: JBP (11.8 Mmt CO_2/year)
CO_2 Transport: From JBP southwest to the central state section in T20N-R101W
CO_2 Storage: Entrada Formation, Nugget Formation, Weber Sandstone, and/or Madison Limestone

4) Anticline Crest "State": Transport in this scenario will be expensive, and complicated by geography, however shallower wells could result in net savings. Preliminary estimates suggest that this scenario becomes economically favorable if over ~15 wells are needed.
CO_2 Source: JBP (11.8 Mmt CO_2/year)
CO_2 Transport: From JBP west/southwest to the anticline crest (13-16 miles)
CO_2 Storage: Entrada Formation, Nugget Formation, Weber Sandstone, and/or Madison Limestone

5) Trona On-site: This scenario would use one or more wells per trona producer with zero or near-zero transport. Trona CO_2 capture technologies are poorly described, but may produce a stream with high purity, saving costs. Wyoming produces 90% of US soda ash from this trona.
CO_2 Source: Tronox Westvaco, Tata Chemicals, Ciner, and Solvay Chemicals, Inc. (5.4 Mmt CO_2/year)
CO_2 Transport: From each trona plant to an on-site location less than a mile away
CO_2 Storage: Mesaverde Group, Frontier Formation, and/or Muddy Sandstone

6) Trona "State": This scenario would gather the CO_2 of the two or three largest Wyoming trona producers and store it under state section T19N-R110W-S36.
CO_2 Source: Tronox Westvaco, Tata Chemicals, Ciner, and Solvay Chemicals, Inc. (5.4 Mmt CO_2/year)
CO_2 Transport: From each trona plant to the southeast state section in T19N-R110W.
CO_2 Storage: Mesaverde Group, Frontier Formation, and/or Muddy Sandstone.

Chapter II Conclusion

The project team favors Scenario #1 JBP On-site. This scenario benefits from a steady CO_2 source, proximity of the storage site to the CO_2 source, and its location on the property of the CO_2 provider. Additionally, since the CO_2 provider owns a significant portion of the surface in the area, achieving the super majority of interest (80%) required by Wyoming law is more likely. The following assessments focus on this scenario.

Chapter II References

Carman, P. (1937), Fluid flow through a granular bed, Trans. Institute of Chemical Engineering, 15, 150–167.

Greenberg, S.A.; Bauer, R.; Will, R.; Locke, R., II; Carney, M.; Leetaru, H.; Medler, J. (2017), *Geologic carbon storage at a one million tonne demonstration project: Lessons learned from the Illinois Basin—Decatur Project*. Energy Procedia, 114, 5529–5539. DOI: https://doi.org/10.1016/j.egypro.2017.03.1913

Kozeny, Josef. (1927), *Uber kapillare Leitung der Wasser in Boden, Sitzungsber*. Akademie der Wissenschaften. Wien, 136, 271–306.

Mccoy, Sean T (2008) The Economics of CO2 Transport by Pipeline and Storage in Saline Aquifers and Oil Reservoirs Thesis for Carnegie Mellon University. April 2009.

NETL (2017), Best Practices Manual Site Screening, Site Selection, and Site Characterization for Geologic Storage Projects Accessed May, 2019: https://www.netl.doe.gov/sites/default/files/2018-10/BPM-SiteScreening.pdf

Root, F.K., Glass, G.B., and Lane, D.W. (1973), *Sweetwater County, Wyoming: Geologic Map Atlas and Summary of Economic Mineral Resources*. Wyoming Geological Survey, County Resource Series, No 2. Accessed May, 2019: https://www.wsgs.wyo.gov/products/wsgs-1973-crs-02.pdf

Roehler, Henry W. (1977), *Geologic map of the Rock Springs Uplift and adjacent areas, Sweetwater County, Wyoming* DOI: https://doi.org/10.3133/ofr77242

Wyoming Mining Association (2018), Trona. Accessed May, 2019: https://www.wyomingmining.org/minerals/trona/

Chapter III: Economic, Regulatory, Environmental, & Stakeholder Analysis

Section 3.1: Economic Assessment

Ben Cook
College of Business/Enhanced Oil Recovery Institute
University of Wyoming
1000 E. University Ave, Dept. 3985
Laramie, WY 82070

I. ECONOMIC MODEL OVERVIEW

A. Techno-Economic Basis

The economic model and assessment for the RSU area consists of four principle components:

(1) the capital and operating costs of constructing an amine capture system sized for a flue gas stream of 340-380 MWs;
(2) a geologic saline storage site within a 2.5-mile radius of the plant which includes a 15-mile CO_2 pipeline for CO_2-EOR opportunities in the region;
(3) a revenue and equity-sizing module incorporating options for CO_2 sales, premiums on sales of "green electrons" (e.g., electricity sales to carbon-constrained jurisdictions, such as the State of California), monetization of carbon offsets/credits, and the earning of tax credits; and
(4) a trust account module for accumulating sufficient funds for post-injection site care (PISC) and long-term liability (LTL).

More cost-effective technologies may emerge in the future, but at this time the most deployed technology for large-scale industrial capture at power plants is amine capture. The techno-economic aspects of the amine system and storage site are largely based on the documentation for the Integrated Environmental Control Model (IECM 9.5, 2017) developed by Carnegie Mellon/NETL, and the FE/NETL CO_2 Saline Storage Cost Model (NETL 2017).

While capital costs (CAPEX) have been calibrated so that the model can roughly duplicate the NRG W.A. Parish Petro Nova facilities (Armpriester 2017), the maintenance and operating (OPEX) expenses are largely linked to consumable pricing and the ratio of non-fuel OPEX to CAPEX in IECM 9.5. Power and fuel usage volumes are paid according to regional pricing paths for electricity, natural gas, and coal to allow for dynamic scenario modeling of these commodities.

Due to the differences in geography and weather conditions from existing facilities, the model largely ignores cost reductions from economies of scale or learning, with CAPEX and OPEX expressed in terms of 2016 averages.

B. Modules

The Excel-based modeling approach taken allows for both discrete and stochastic scenario analysis, along with adjustments to the various equipment requirements of the facility.

Carbon Capture System: The "Carbon Capture System Block" is composed of six major cost components: (1) the amine system, (2) low-pressure steam source, (3) compression and dehydration, (4) a cooling tower, (5) a water treatment/demineralization plant, and (6) flue-gas tie-in and control.

CO_2 Transport Pipelines: The "Pipeline System Block" calculates CAPEX and OPEX for two pipelines, one to the geologic storage site and another for CO_2 sales. Also included are calculations for the number of CO_2 meters/gauges, and any required pressure boosting stations in the case of long-distance transportation.

Saline Storage Injection Site & Post-Inject Site Care: The "Storage Site Block" includes cost estimates for three main elements: (1) pre-injection site characterization which includes seismic surveys, permits, and test wells; (2) the operating phase includes the drilling and completion of injection wells, monitoring wells and periodic seismic; and (3) the PISC to plug the wells, observe the site and conduct periodic seismic over the 50-year period.

Tax Equity, CO_2 Sales, and Other Revenues: The "Capital & Revenue Block" contains assumptions related to the pricing of CO_2 sales to CO_2-EOR customers, investment tax credits and potential tax credits such as those under amended section 45Q, and the option to earn marketable carbon offsets or to sell "Green Electrons" at a premium to normal electricity. The ability to pre-sell tax-credits in a tax-equity arrangement is central to facilitating private capital to finance the project.

Energy & Commodity Pricing: The "Pricing Path Block" includes pricing assumptions for of WTI Crude Oil, PRB Coal, Henry Hub Gas, Commercial and Industrial Gas, as well as Industrial and Wholesale Electricity rates. Depending the plant configuration chosen, these different consumable prices factor differently into the model results.

Capital Structure, Insurance, Trust Accounts & Long-Term Liability: The "Capital Structure Block" adjusts the mix debt and equity to ensure sufficient capital sources are available to finance the project, and that operational cash flows are sufficient to cover both debt service and the maintenance of the project. The "Insurance and Trust Account Block" includes general liability coverage, and the management of two trust accounts for PISC and LTL.

C. Scenario Results

Pre-Feasibility Estimate of Anticipated Capital and Operating Costs:

The estimated CAPEX and OPEX costs of implementing the scenarios considered (see Table 3.1) will be in the range of $758-$956 million and $54-$103 million, respectively, based upon the project's economic model.

While subject to change as conditions unfold, these CAPEX and OPEX estimates assume: (1) an amine capture system sized for a 380 MW flue gas stream; (2) saline storage site within 2.5 miles of the JBP and includes a 15-mile CO_2 pipeline for regional CO_2-EOR opportunities; (3) utilization of JBP's coal-based steam cycle as discussed in the Sargent & Lundy assessment and the purchase of power at wholesale prices in the lowest cost scenario; (4) adequate injection facilities to store 50 $MMtCO_2$ over 25 years as established in the RSU; and (5) funds for PISC and LTL are deposited in trust accounts during the operating period.

In order to finance the project, it is assumed that: (1) no more than 30% of the project if financed by debt; (2) 95% of the CO_2 can be sold for EOR at roughly 2% of prevailing oil prices; (3) some revenues from

tradable CO_2 offsets can be earned for the saline storage share of capture, and (4) the utilization of section 45Q and section 48 tax credits for tax-equity financing arrangements.

Potential Sources of Revenue:

The economic model considers all potential sources of revenue and capital: (1) sales of CO_2 for EOR (approximately $69 million in revenue per year); (2) CO_2 capture tax credits such as amended section 45Q and section 48 tax credits (approximately $484 million in tax-equity); and (3) sales of low-carbon electricity and marketable carbon offset/credits into carbon-constrained West Coast markets (approximately $11-$17 million in revenue). Collectively, these revenues should be sufficient to finance the project's lowest-cost version (Table 3.1).

Section 3.1 Conclusion

Constructing and operating a carbon capture system which is integrated into the operation of an existing facility requires careful planning and engineering to reduce the risks inherent in large complex projects. The recent on-budget successful completion of NRG's Petra Nova capture project at the W.A. Parish Generating Station demonstrates that successful execution on such projects is indeed possible, and can strengthen confidence in potential partners and capital markets for future endeavors.

The primary techno-economic baseline for evaluating the financial prospects of an amine capture system on a 380 MW flue-gas stream from the JBP was built utilizing the IECM 9.5 and FE/NETL Saline Storage models. Costs were calibrated to match discussion with industry and the realizations at the Petra Nova project. The model also incorporates various opportunities for revenue recognition, and accounts for PISC and LTL utilizing payments into trust accounts during the 25-year operating period.

The major design decisions will include the source of steam for the amine process, and evaluating the need for a cooling tower and water treatment plant. Two major sources of OPEX are tied to the price at which the facility is charged for electricity, and the cost of natural gas in the case of a gas-fired steam source.

The lowest cost option considered would involve utilizing the coal fired steam cycle of the host plant, and requires power purchased at wholesale rates. Under such a scenario, the facilities would cost an estimated $787 million, with around $54 million in annual OPEX. Financing such a project could include up to 30% debt, but would require 95% of CO_2 to be sold for EOR, some earnings from tradable CO_2 allowances, and the significant tax equity from section 45Q tax credits.

Basic Assumptions	Steam Source	Power & Fuel Rates	CAPEX	Year-One OPEX	Total OPEX	All-In Costs	All-In Costs per Ton
380 MW Flu-Gas Stream (50 MtCO2 over 25 years) <u>Included Components:</u> – Amine System – Cooling Tower – Water Treatment – Compression – Pipelines – Storage Site – PISC/LTL Trust Payments – Insurance – Owner's Costs – Debt Reserve (one-half payment) – Working Capital (30% year-one OPEX) – 30% Debt Funded	Co-Gen, Steam plus Power	No Power Purchased Gas at Henry Hub ($3/Mcf)	$949 M	$66 M	$1,578 M	$2,527 M	$50.69
		No Power Purchased Gas at Industrial ($4.3/Mcf)	$951 M	$74 M	$1,783 M	$2,734 M	$54.86
		No Power Purchased Gas at Commercial ($7/Mcf)	$956 M	$92 M	$2,210 M	$3,166 M	$63.52
	Natural Gas Axillary Boiler	Power at Wholesale ($25/MWh) Gas at Henry Hub ($3/Mcf)	$747 M	$65 M	$1,545 M	$2,292 M	$45.99
		Power at Wholesale ($25/MWh) Gas at Industrial ($4.3/Mcf)	$749 M	$72 M	$1,725 M	$2,475 M	$49.65
		Power at Wholesale ($25/MWh) Gas at Commercial ($7/Mcf)	$754 M	$87 M	$2,100 M	$2,854 M	$57.26
		Power at Industrial ($70/MWh) Gas at Henry Hub ($3/Mcf)	$754 M	$88 M	$2,120 M	$2,874 M	$57.67
		Power at Industrial ($70/MWh) Gas at Industrial ($4.3/Mcf)	$754 M	$99 M	$2,395 M	$3,149 M	$54.16
		Power at Industrial ($70/MWh) Gas at Commercial ($7/Mcf)	$758 M	$103 M	$2,495 M	$3,253 M	$65.28

Basic Assumptions	Steam Source	Power & Fuel Rates	CAPEX	Year-One OPEX	Total OPEX	All-In Costs	All-In Costs per Ton
	Coal Plant Steam Cycle Integration	Power at Wholesale ($25/MWh) PRB Coal ($12.50/short-ton)	$787 M	$54 M	$1,273 M	$2,060 M	$41.34
		Power at Industrial ($70/MWh) PRB Coal ($12.50/short-ton)	$792 M	$70 M	$1,668 M	$2,460 M	$49.36

Table 3.1. Rock Springs Uplift/Jim Bridger Capture Plant Design & Economic Scenarios

Section 3.1 References

Integrated Environmental Control Model, Current Public Version 9.5 (2017), Carnegie Mellon University, Department of Engineering & Public Policy. Available at: https://www.cmu.edu/epp/iecm/

National Energy Technology Laboratory, (2017). "FE/NETL CO_2 Saline Storage Cost Model. U.S. Department of Energy." Last Update: Sep 2017 (Version 3) https://www.netl.doe.gov/research/energy-analysis/searchpublications/vuedetails?id=2403

Armpriester, Anthony, (2017). "W.A. Parish Post Combustion CO_2 Capture and Sequestration Project Final Public Design Report." United States. Retrieved from http://www.osti.gov/scitech/servlets/purl/1344080

U.S. Department of Energy, National Energy Technology Laboratory. (2014). "Acquisition and Development of Selected Cost Data for Saline Storage and Enhanced Oil Recovery (EOR) Operations." Prepared by Advanced Resources International. DOE/NETL-2014/1658. http://www.netl.doe.gov/File%20Library/Research/Energy%20Analysis/Publications/saline-and-eor-operation-cost-estimation-recommendations-ari-final-7-2.pdf

McCollum, David L. and Joan M. Ogden, (2006). "Techno-Economic Models for Carbon Dioxide Compression, Transport, and Storage & Correlations for Estimating Carbon Dioxide Density and Viscosity." Institute of Transportation Studies, University of California, Davis, Research Report UCD-ITS-RR-06-14.

Farhat K., Koplin J., Lewis D., Peterlin S., Simms R., (2013). "Financial Assessment of CO2 Capture and Storage with Electricity trading in the U.S.: Role of Interim Storage and Enhanced Oil Recovery." Energy Procedia 37 (2013) 7512-7525.

Cook, Benjamin R. (2012). "Wyoming's Miscible CO_2 Enhanced Oil Recovery Potential in Main Pay Zones: An Economic Scoping Study." University of Wyoming, Enhanced Oil Recovery Institute.

Loganathan, Kavithaa (2014). “Water Management through Water Treatment Technologies.” IETP Final Report prepared by Canadian Natural Resources Limited for the Government of Alberta’s Innovative Energy Technology Program (IETP). Accessed online, November 2017 at http://www.energy.alberta.ca/4229.asp.

U.S. Energy Information Administration (EIA 2016). “Trends in U.S. Oil and Natural Gas Upstream Costs.” Independent Statistics & Analysis, report prepared by EIA and IHS Global Inc. https://www.eia.gov/analysis/studies/drilling/pdf/upstream.pdf

Dooley, James J., Chiara Trabucchi, Lindene Patton (2009). “Tipping Fees Can’t Save us from the Tipping Point: The Need to Create Rational Approaches to Risk Management that Motivate Geologic CO_2 Storage Best Practices.” Energy Procedia, Volume 1, Issue 1, 2009, Pages 4583-4590.

Section 3.2: Legal Assessment

Tara Righetti
Associate Professor of Law, University of Wyoming College of Law
Director, Academic Program in Professional Land Management
School of Energy Resources, University of Wyoming
1000 E. University Ave, Dept. 3035
Laramie, WY 82071

Pore Space Ownership and Obtaining Injection Rights

The proposed scenarios are located in an area of Wyoming where the land ownership pattern is referred to as the "checkerboard," meaning that every alternating section (~640 acres) is federally owned. Due to this ownership pattern, any project will need to include injection rights in federally owned pore space. There is no leasing program or established guidance on obtaining injection rights for CCUS into federal pore space and as a result the project could be subject to delays as a process is developed, during environmental analysis, and potential legal challenge.

The interspersed sections in the checkerboard are privately owned and may include split estate configurations where the owner of the surface is different than the owner of the underlying minerals. Wyoming Statute 34-1-152 statutorily vests ownership of the pore space in the owner(s) of the surface. The mineral estate is dominant over the surface estate - including the pore space - meaning that surface uses are subordinate to use of the land as is necessary for mineral extraction. Although Wyoming requires mineral developers to make reasonable accommodation of existing surface uses, the surface owner may not use pore space in a way that damages, interferes with, or otherwise diminishes the mineral estate. These constraints may limit potential development sites within the project area and also subject the project to legal challenge from mineral owners regarding potential impacts to hydrocarbon or coal resources.

Transportation

Due to the checkerboard land ownership pattern, any pipelines constructed for transportation of CO_2 will require right-of-ways (ROW) across both private and federal land. BLM has authority to issue ROW for CO_2 pipelines pursuant to the Mineral Leasing Act (MLA). Pipeline developers receiving a ROW pursuant to the MLA are required to operate the pipeline as a common carrier. The siting, permitting, and construction, and transportation of CO_2 pipelines across private land in Wyoming is regulated according to state law. Although pipelines enjoy broad condemnation authority in Wyoming, state law prohibits use of eminent domain for carbon capture and sequestration projects, although it is unclear whether this prohibition would apply to a pipeline transporting CO_2 for both sequestration and utilization.

Safety of CO_2 pipelines is regulated by the Department of Transportation's Pipeline and Hazardous Materials Safety Administration (PHMSA) pursuant to the Hazardous Liquid Pipeline Safety Act of 1979 (HLPSA). Wyoming has accepted responsibility for enforcement of HLPSA requirements and has obtained Certification pursuant to Section 60105(a). In addition to HLPSA requirements, Wyoming's Department of Transportation mandates specific casing and siting requirements for hazardous liquid pipelines facilities within the state highway system right-of-way.

Although unlikely, a release of CO_2 during transport could result in fines as well as civil and criminal liability pursuant to Wyoming Statute §35-11-201 and §35-11-901 as well as federal environmental laws.

Injection

Prior to injection, project proponents must obtain a Class VI permit from EPA and the creation of an injection unit by the Wyoming Oil and Gas Conservation Commission. EPA regulations categorize

facilities that inject carbon dioxide for long term storage purposes as Class VI wells under the Underground Injection Control program. Presently, no state has primacy to administer the EPA Class VI injection program, however, the Wyoming Department of Environmental Quality anticipates that Wyoming will have primacy to administer the program before the proposed project implementation. The project will be obligated to comply with all regulations for Class VI wells, including reporting.

The Wyoming Oil and Gas Conservation Commission has authority to create injection units for CCUS pursuant to Wyoming Statute §35-11-315. Unitization plans approved by the Commission will not become effective until the unitization plans has been signed or ratified in writing by the owners representing no less than eighty percent (80%) of the total unit capacity as per Wyoming Statute §35-11-316(c). Accordingly, unless the project can be contained within one section, the project cannot progress without grant of an easement for injection from BLM as well as approval from one or more private pore space owners within the unit area.

Section 404 of the Clean Water Act requires a permit for any "utility line" crossing requiring discharge of dredge or fill material into waters of the United States. Carbon dioxide pipelines are considered a utility line, and accordingly developers of pipelines must obtain either a general (nationwide) or individual permit for the project.

During injection there is a potential of low frequency but catastrophic risk of events with impacts to air, water, earth, public health, and soil, either with or without a seismic event. These could result in liability under a number of federal and state laws or expose the project to tort liability under theories of trespass, nuisance, negligence, and strict liability.

Storage

Although Wyoming has authority to establish a "special revenue account" for the "measurement, monitoring and verification of geologic sequestration sites following site closure," it has not waived its immunity from suit or assumed liability for "geologic sequestration sites or the carbon dioxide and associated constituents injected into those sites." Ownership and operation of a CO_2 storage facility presents long term liability for adverse impacts to property, environment, or human health resulting from either transboundary migration outside the injection unit and surface releases of CO_2. The project will address long-term liability issues through one or more vehicles: (1) commercial insurance; (2) negotiations with project participants; and/or (3) negotiations with the State of Wyoming Legislature.

General Laws Applicable to the Project

The National Environmental Policy Act (NEPA)

NEPA requires an environmental impact statement (EIS) to be prepared whenever a project proposal, "involves a major federal action that will significantly affect the quality of the human environment." Due to the federal lands and permits involved in the contemplated project, an Environmental Impact Statement or Environmental Assessment will be required. The NEPA process can be lengthy and expensive, and subject to legal challenge.

Clean Air Act

Carbon Dioxide and other greenhouse gases are included under the Clean Air Act's definition of "air pollutant." Accordingly, a mass release of carbon dioxide during the project could subject project proponents to administrative, civil, and criminal penalties or require permitting revisions for capture facilities.

Clean Water Act
The project will require adherence to all rules and regulations related to Class VI wells, discussed above, including permitting, geological site characterization and financial responsibility, well construction, mechanical integrity testing and monitoring, well plugging, post injection site care, and site closure.

Resource Conservation and Recovery Act
Carbon dioxide injected into a Class VI well enjoys a conditional exclusion from the definition of "hazardous waste" under RCRA.

National Historic Preservation Act
The NHPA requires federal agencies to consult with the Advisory Council to limit impacts to historic properties and accordingly any such impacts will need to be considered in project siting.

Species Conservation and Habitat Mitigation
Wyoming has proactively addressed concerns regarding the declining population of the Greater Sage Grouse with a multi-agency Sage Grouse Conservation Strategy. This strategy limits surface disturbances within core habitat and requires habitat mitigation, both of which may affect surface facilities and project timing and costs. In addition to Sage Grouse Conservation measures, the project must consider and comply with the Endangered Species Act and other species conservation acts. Project planning and implementation should be designed to avoid take of protected species.

Section 3.3: Environmental Assessment

Tom Moore
Research Scientist, Center for Economic Geology Research
School of Energy Resources, University of Wyoming
1020 E. Lewis Street, Energy Innovation Center
Laramie, WY 82071

The goal of the environmental assessment (EA) is to evaluate environmentally sensitive areas and potential impacts in the region, including which Task 3 factors affect these sensitivities the most. This assessment includes the major biome and inorganic environmental concerns with regard to the suggested source, transport, and storage components for a phase 1 pre-feasibility study investigating a large scale CCS project surrounding the RSU. This EA includes an overview of protected species and their habitat, surface water, ground water, air quality, protected areas, cultural resources, and population centers as described in the national energy technology laboratory (NETL) Best Management Practices (BMP) manual (NETL, 2013). Topography and animal migration corridors have also been evaluated to identify scenarios that could portend mitigation. Additionally all NEPA documents related to the RSU area have been compiled to guide the environmental considerations past project have included in the area of interest (AOI).

Protected Species. The U.S. Fish and Wildlife Service (USWS) official species list (USWS, 2017), compiled in fulfillment of the USWF Endangered Species Act of 1973 (ESA) section7(c), identifies 29 protected species within the AOI. No critical habitat (defined as essential to the species), of any protected species are identified in the AOI of this study. However, there are six threatened species with potential habitat (defined as habitat that could support species) in the AOI. The species include the Yellow-billed Cuckoo (*Coccyzus americanus*) a bird, Ute ladies-tresses *(Spiranthes diluvialis*) an orchid, and the Bonytail Chub (*Gila elegans*), Colorado Pikeminnow *(Ptychocheilus lucius),* Humpback Chub *(Gila cypha),* and the Razorback Sucker *(Xyrauchen texanus)* all fish. Potential habitat for the Ute ladies-tresses and critical habitat of the Yellow-billed Cuckoo as well as the four fish species can be avoided.

The Yellow-billed Cuckoo inhabits cottonwood-dominated habitat in the arid intermountain west (Cornell, 2017). These areas can generally be avoided during the site selection and the construction phases of the project by buffering riparian areas. Critical habitat for the Yellow-billed Cuckoo has been identified in the Seedskadee National Wildlife Refuge. This wildlife refuge is located 7 miles north of the Trona plants and is outside the AOI, however the AOI encompasses potential Yellow-billed Cuckoo habitat (Figure 3.3.1). The Ute ladies-tresses, is an orchid that prefers moist soil found proximal to wetland and riparian areas (ECOS, 2017). Potential Ute ladies-tresses habitat follows wetland and riparian corridors (Figure 3.3.1). The four endangered Colorado fish species do not have critical habitat in the AOI, however the entire AOI does drain into the Colorado River basin. Discharge into AOI waterbodies should be avoided when possible. As the RSU CO_2 storage project is expected to be zero discharge, it is unlikely to affect ephemeral streams located in the AOI or have a significant impact on stream habitat or water quality.

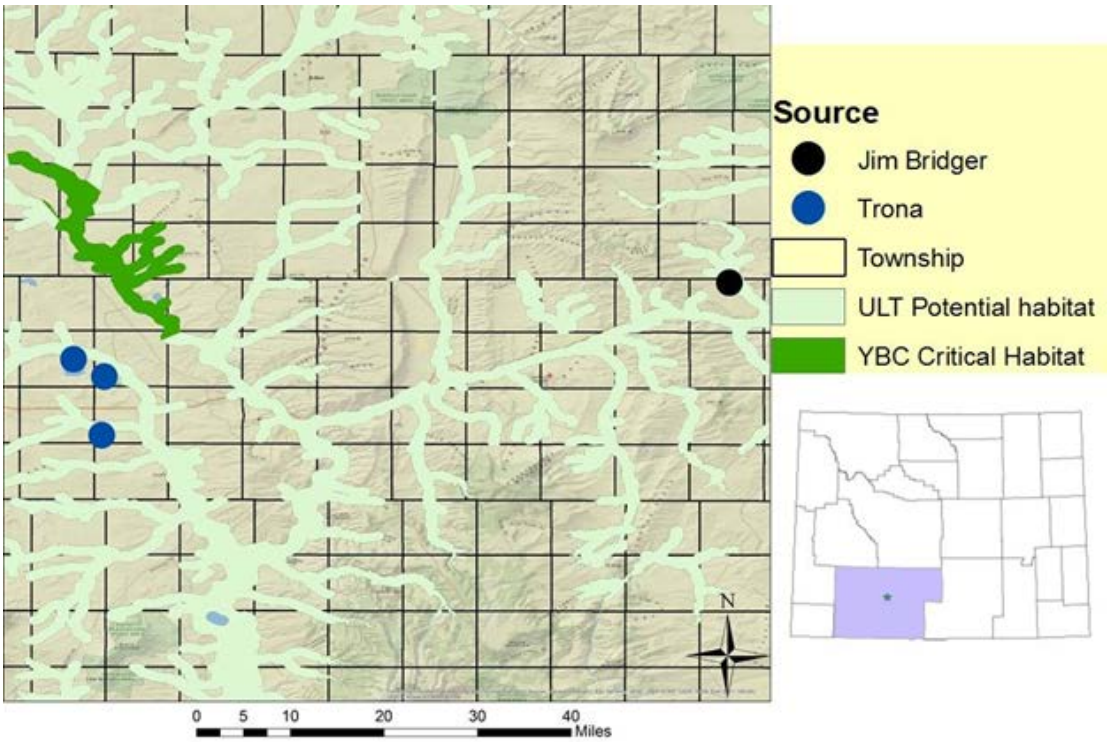

Figure 3.3.1. Potential habitat of the Ute ladies-tresses (ULT) and critical habitat of the Yellow-billed Cookoo (YBC) (USFWS, 2012; 2016)

The Migratory Bird Treaty Act and the Bald and Golden Eagle Protection Act protect bird species native to the AOI. Twenty-three migratory birds of conservation concern have been observed within the AOI. Six species reside in the AOI year round, one species uses the AOI as winter habitat, and the remaining sixteen species use the AOI during migration and breeding periods (Table 3.3.1). Two of these birds, the Golden eagle and Bald eagle are raptors, which prefer sparse grassland habitat with trees to perch on. Bald eagles also frequent riparian and wetland areas (Figure 3.3.2). A raptor nest survey will be required in later phases of this project. The project will also be required to consider the sixteen species that migrate and breed in the AOI, and mitigate impacts from construction during these sensitive periods. The majority of these birds are sparse grassland and shrub species. There are three wetland and four riparian species, although the bald eagle, curlew, and Mountain plover also frequent wetland and riparian habitat. Areas for site selection and CO_2 pipe routing that avoid high impact areas will be preferentially selected (Figure 3.3.2). These concerns can be mitigated by strategically timing construction during breeding and migration periods (Table 3.3.1) and by avoiding sensitive areas. The Greater sage grouse (*Centrocercus urophasianus*) is a candidate species for ESA protection, however there are no leks or core habitat (defined as habitat designated by the state) identified in the AOI. The closest core habitat is approximately 5 miles north of the JBP.

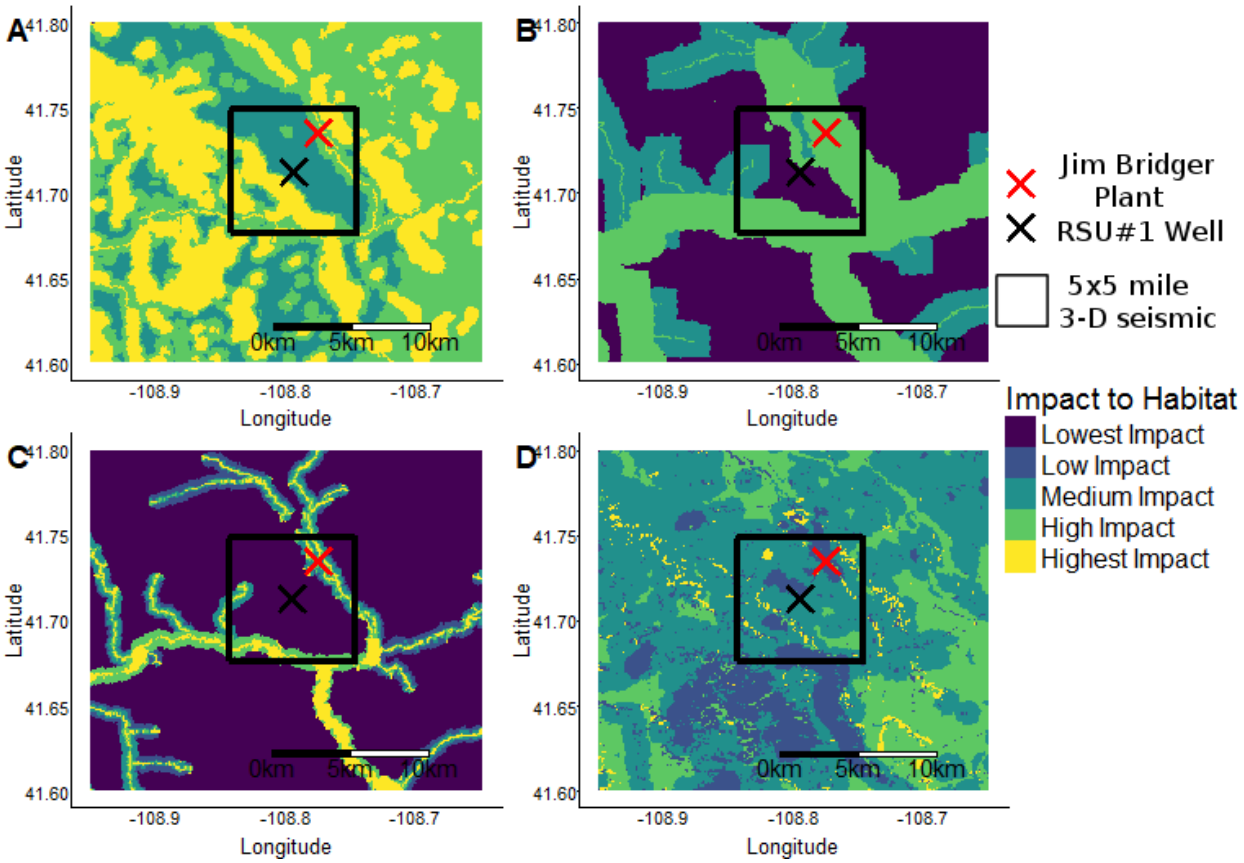

Figure 3.3.2: A map displaying the importance of habitat to A) raptors, B) wetland bird species, C) riparian bird species, D) grassland bird species, and the potential impact developing the area may be (pulled from: Pocewicz et al., 2013)

Table 3.3.1. Protected bird species habitat and periods of sensitivity compiled from Cornell 2017.

Habitat	Species	Use	Timing
Riparian	Willow flycatcher Fox sparrow Olive-sided flycatcher Calliope hummingbird	Migration/Breeding Breeding Breeding Migration	Jun-Jul May-Jul Jun-Jul Mar-May & Jul-Sep
Wetland	American bittern Western grebe Snowy plover	Breeding Breeding Breeding	Apr-Jul Jun-Aug Mar-Apr

Habitat	Species	Use	Timing
Sparse Grassland	Black Rosy finch	Winter	Dependent
	Brewers sparrow	Breeding	Jun-Jul
	Burrowing owl	Breeding	Mar-Aug
	Ferruginous hawk	Breeding	Apr-Jul
	Greater Sage grouse	Year-round	Mar-Aug
	Loggerhead shrike	Breeding	Mar-Jun
	Long billed curlew	Breeding	Apr-Jul
	Mountain plover	Breeding	Apr-Aug
	Sage thrasher	Breeding	May-Jul
	Short-eared owl	Year-round	Apr-May
	Swainson's hawk	Breeding	Apr-Jun
	Cassins finch	Year-round	May-Jun
	Pinyon jay	Year-round	Feb-Jul
	Rufous hummingbird	Migration	Mar-May & Jul-Sep
Raptor	Bald eagle	Year-round	Apr-Aug
	Golden eagle	Year-round	Apr-Aug

Wetlands & Streams. Two federal acts protect waterbodies, the Safe Drinking Water Act (SDWA) and the Clean Water Act (CWA). Wetlands are protected by section 404 of the CWA, which regulates discharge of dredged and fill material into streams and wetlands (EPA, 2002). Construction of new roads, CO_2 pipeline, and well-pads could potentially fall under the prevue of section 404 of the CWA. Additionally wetlands affected by construction may need to be replaced at a 1:1 or 2:1 ratio (USEPA, 2002). All project scenarios have the potential to cross and affect wetlands, streams, and riparian areas. A series of maps were created to guide site selection and CO_2 piping to minimize negative impacts of the project (Figure 3.3.3).

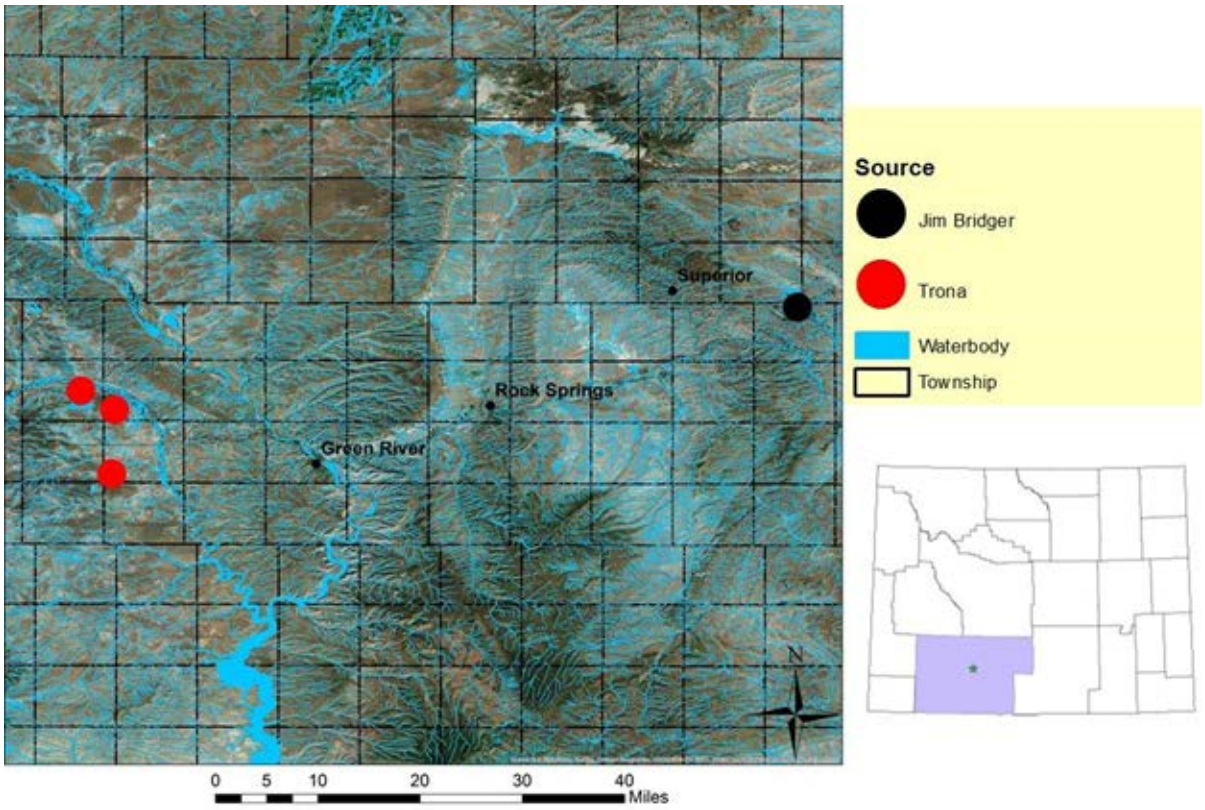

Figure 3.3.3. Surveyed riparian and wetland areas in the area of study (USFWS, 2009).

Groundwater. Groundwater is protected by the SDWA which regulates the water by its designated uses defined by the USEPA. The storage reservoirs selected for this study either: (1) have a salinity exceeding 10,000 ppm total dissolved solids (TDS); or (2) further salinity data needs to be collected to determine the groundwater salinity. Salinity distribution maps were created from the USGS National Produced Waters Geochemical Database v2.2 (Blondes et al., 2016) for targeted reservoirs. Associated seals have been identified for each reservoir; location of wells that penetrate the reservoir seals are shown in Figure 3.3.4.

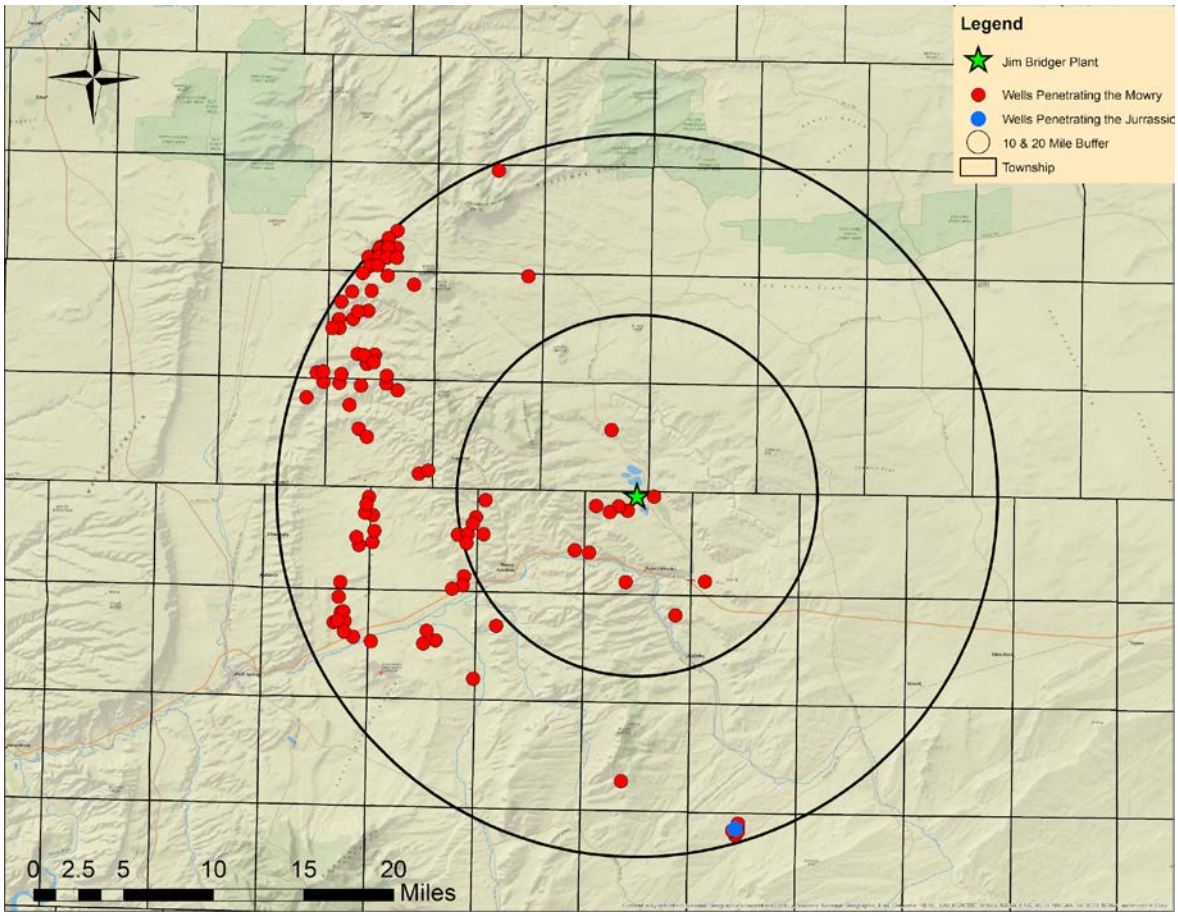

Figure 3.3.4. Wells (WOGCC, 2017) penetrating the overlying Mowry seal and the seal overlying the targeted Jurassic reservoirs seal.

Air Quality. Data have been compiled from the EPA Facility Level Information on Greenhouse gasses Tool (FLIGHT) and Wyoming Department of Environmental Quality (WDEQ) inventories to summarize emissions from the JBP. JBP's yearly emissions have averaged 13.5 million tonnes CO_2, 1.6 million tonnes CH_4, and 227 tonnes N_2O from 2010-2015 (USEPA, 2017). The WDEQ has reported the 2008-2013 average regulated emissions from the Jim Bridger plant's four stacks (Table 3.3.2) (WDEQ, 2017). The short-term construction process would be detrimental to regional air quality, however, the long-term effects will decrease greenhouse gas emissions.

Table 3.3.2. Average tonnes/year of regulated emissions from the Jim Bridger Plant (WDEQ 2017).

Pollutant	CO	NO_X	SO_2	CH_2O	C_6H_6	Pb	Hg	HF	HCl	PM-10	PM-25
Tons/year	0.596	2.42	0.861	0.016	0.025	0.0026	0.0067	0.630	2.417	0.341	0.164

Protected areas. Protected areas including national parks, wildlife refuges, state parks, and national monuments, all of which lie outside the locations being considered for this project. The closest protected area to the AOI is the Seedskadee National Wildlife Refuge located 7 miles north of the trona plants.

Cultural Resources. The natural resource and energy explorer (NREX) was used to map published surveys of cultural artifacts and sites found within the AOI. The number and location of these sites and artifacts does not appear to significantly affect any proposed scenario, although continued awareness and slight mitigation will be needed. Communication has been maintained with the Wyoming State Historic Preservation Office (SHPO) throughout the course of this assessment. A survey of these sites is recommended during later project development under the advisement of the Wyoming SHPO.

Population Centers. Though the study area is sparsely populated, there are several population centers surrounding the RSU (Figure 3.3.5). The largest is Rock Springs, with a population of 23,755 that is 24 miles to the west of the JBP (USCB, 2016). Each town, as well as privately owned ranches, and housing developments have been mapped and are considered in scenario selection. It is unlikely that any scenario will affect a population center.

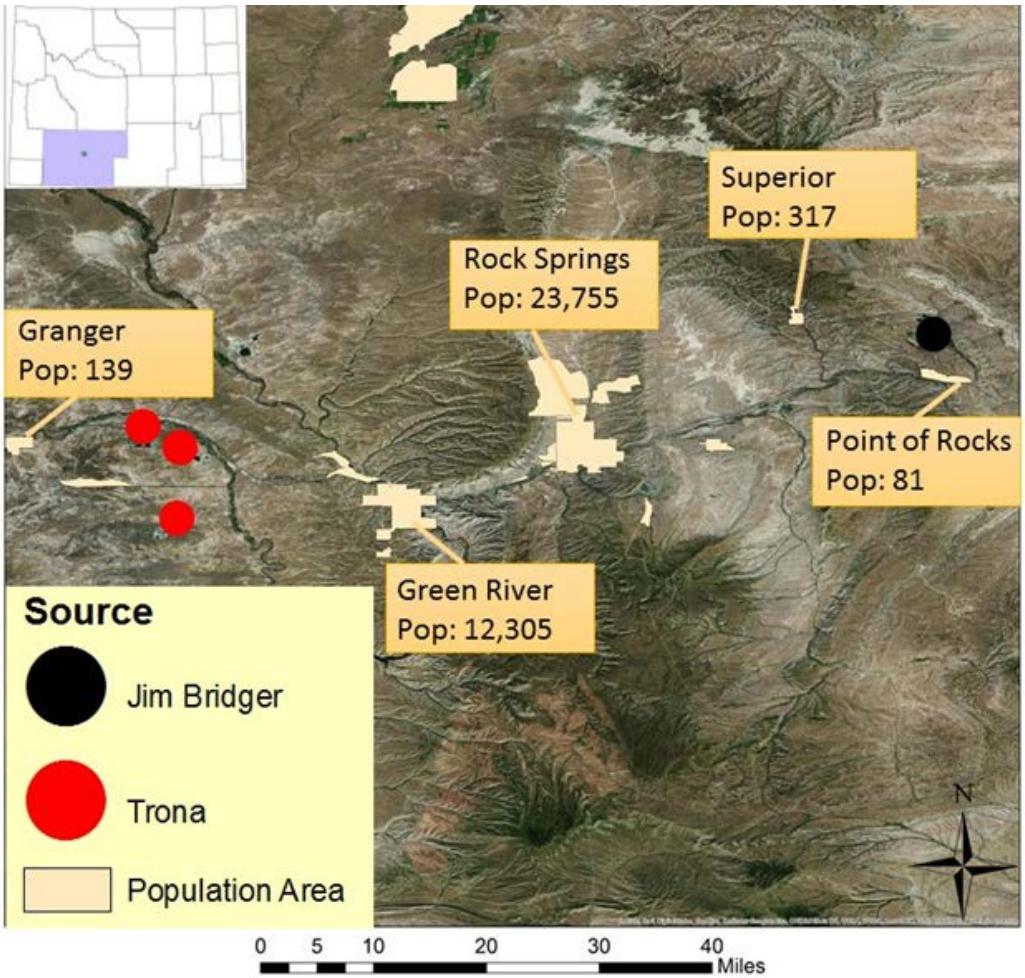

Figure 3.3.5. Population centers and their population surrounding the Jim Bridger and Trona plants (USCB, 2016)

Topography. Soil type is identified as relatively erosive using data from the Natural Resource Conservation Service (NRCS) Soil Survey Geographic (SSURGO) database (USDA-NRCS, 2016). A slope map was generated, and includes areas of mass movement. Based on this information, the areas directly surrounding the JBP and the trona area are between 0 to 5 degrees. Higher slopes are associated with drainages and the RSU. Areas above 15 degrees slope should be avoided for site selection, and are

correlated with mass movement events (Figure 3.3.6). Any increase in distance for CO_2 transport is more likely to cross areas with slopes over 15 degrees.

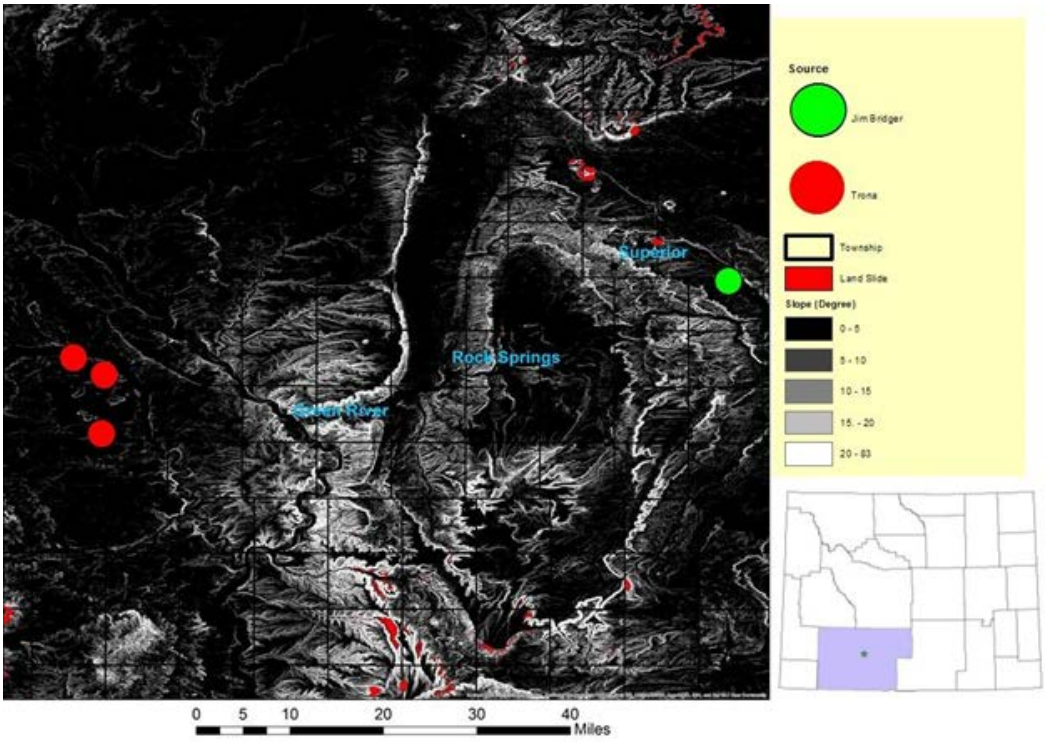

Figure 3.3.6. Slope steepness in the area of study processed from a USGS 10 meter digital elevation map (USGS, 2009) and the surveyed extents of historic mass movement events (WRDS 2009)

Migration Corridors. Big game migration corridors and critical habitat were mapped (Figure 3.3.7) and will be considered with respect to scenario selection. Both mule deer (*Odocoileus hemionus*) and pronghorn (*Antilocapra Americana*) migration corridors have the potential to be affected by the construction and operation of a project site, though impacts should be minimal.

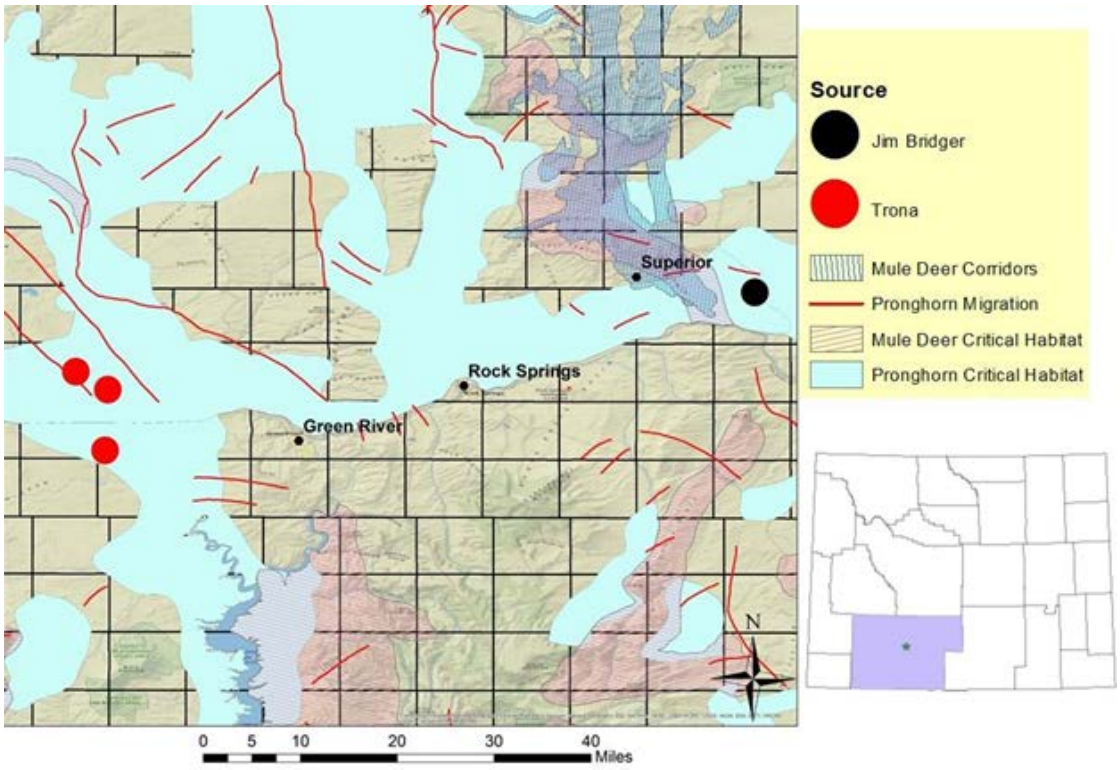

Figure 3.3.7. Mule deer and pronghorn habitat in the study area (USFWS, 2017b).

Section 3.3 References

Blondes, M.S. Gans, KD. Rowan, E.L. Thordsen, J.J. Reidy, M.E. Engle, M.A. Kharaka, Y.K. Thomas, B. (2016). U.S. Geological Survey national produced waters geochemical database. https://energy.usgs.gov/EnvironmentalAspects/EnvironmentalAspectsofEnergyProductionandUse/ProducedWaters.aspx#3822349-data. Accessed: 8/1/2017.

Cornell (2017). The Cornell lab of ornithology. http://www.birds.cornell.edu/Page.aspx?pid=1478. Accessed: 8/1/2017.

ECOS (2017). Environmental conservation online system. https://ecos.fws.gov/ecp/. Accessed: 8/1/2017.

Pocewicz, A. W.A. Estes Zumpf, M.D. Andersen, H.E. Copeland, D.A. Keinath, H.R. Griscom (2013). Modeling the distribution of migratory bird stopovers to inform landscape-scale siting of wind development. PLoS ONE 8 (10): e75363

NETL (2013). Site screening, selection, and initial characterization for storage of CO_2 in deep geologic formations. https://www.netl.doe.gov/File%20Library/Research/Carbon-Storage/Project-Portfolio/BPM-SiteScreening.pdf. Accessed: 5/23/2017.

USCB (2016). United States Census Bureau quick facts. https://www.census.gov/quickfacts. Accesses: 8/08/2017.

USDA-NRCS (2016). Soil Survey Geographic (SSURGO) for Wyoming.

USEPA (2017). Facility level information on greenhouse gasses tool (FLIGHT). https://ghgdata.epa.gov. Accessed: 8/01/2017.

USEPA (2002). Federal Water Pollution Control Act. https://www.epw.senate.gov/water.pdf. Accessed: 5/23/2017.

USFWS (2017a). Species List, consultation code: 06E13000-2017-SLI-0266.

USFWS (2017b). Big game. https://wgfd.wyo.gov/Wildlife-in-Wyoming/Geospatial-Data/Big-Game-GIS-Data. Accessed: 8/1//2017.

USFWS (2016). FWS critical habitat for threatened and endangered species dataset. https://catalog.data.gov/dataset/fws-critical-habitat-for-threatened-and-endangered-species-datasetf6b00. Accessed: 8/1/2017.

USFWS (2012). Area of influence ranges for 18 critical species in Wyoming. http://www.fws.gov/Wyominges/Pages/WYES_GISdata.html. Accessed: 8/1//2017.

USFWS (2009). A system for mapping riparian areas in the western United States. http://www.fws.gov/wetlands/data/Data-Download. Accessed: 8/1//2017.

USGS (2009). Digital elevation model for Wyoming 10 meter. http://viewer.nationalmap.gov/viewer. Accessed: 8/1//2017.

WDEQ (2017). Wise view and oil and gas production (OGER) database. http://qrywiz.wyo.gov/. Accessed: 8/1//2017.

WOGCC (2017). Wyoming oil and gas commission database. http://wogcc.state.wy.us/legacywogcce.cfm. Accessed: 8/1//2017.

WRDS (2009). Landslides per county basis for Wyoming. http://www.wrds.uwyo.edu/wrds/wsgs/hazards/landslides/county/county.html. Accessed: 8/1//2017.

Section 3.4: Community and Public Outreach/Assessment

Kipp Coddington
Director, Energy Policy & Economics
Center for Economic Geology Research
School of Energy Resources, University of Wyoming
1020 E. Lewis Street, Energy Innovation Center
Laramie, WY 82071

The CCT successfully established and implemented a community and public outreach plan/assessment (Outreach Plan).

Stakeholder engagement is considered a critical component for successful deployment of any CCS/CCUS project. The development of a regional storage complex that can accommodate up to 50 million tonnes of CO_2 from multiple sources presents not only complex geologic considerations, but presents unique challenges for engaging stakeholders and generating an environment in which a CarbonSAFE-type project can be successfully implemented.

The public and project stakeholders have various and diverse perspectives, and have the ability to act on those perspectives in various ways with varying levels of influence and control. Understanding the nuances of stakeholder opinion, power and perspective is necessary to the development of a stakeholder engagement strategy that can reduce program/project risk, while creating buy-in and understanding about program/project objectives. Lack of attention to stakeholder engagement can increase project risk and create an environment in which public action can be at cross-purposes with project goals. These "cross-purposes" can, in some severe cases, significantly impact or even derail a project. In order to move the RSU CarbonSAFE project to the next phase, a strong stakeholder engagement strategy is needed along with full and proper execution of that strategy.

Work Flow:

The Outreach Plan consisted of the following seven tasks:

1) Contextual understanding and parameter definition
2) Assessment and data collection
3) Data analysis
4) Strategy development
5) Implementation
6) Evaluation
7) Refinement

Detailed Work Breakdown:

Task 1: Contextual Understanding and Parameter Definition:
This activity included identifying and defining the goals and objectives of the stakeholder engagement process along with determining the methodologies and tools to be used to collect data from stakeholders. There was also consideration of synergistic activities and how the stakeholder engagement process would interact and affect other tasks. During this assessment task, determination for stakeholder designation was determined.

The CCT identified public acceptance of the project within the city of Rock Springs and the surrounding area as the primary goal and objective of the Outreach Plan. Outside of the city of Rock Springs, the

project site is sparsely populated. Plus, the CCT benefitted from the knowledge that the citizens of the area had previously accepted a similar project conducted by the University of Wyoming.

Task 2: Assessment and Data Collection:
This task included research by the CCT to provide insights into potential stakeholders in the area. Stakeholders were identified and their views ascertain from prior public statements and responses to media about the project. Although it was originally envisioned that a workshop would be held, the activities took place without the need for a workshop for several years: (1) the citizen's favorable views regarding CCS/CCUS were readily obtainable from third-party sources; and (2) holding a workshop was deemed to be premature given that this was pre-feasibility study.

Task 3: Data Analysis:
Analysis of publicly available information regarding public perception of CCS/CCUS in the Rock Springs area confirmed that acceptance was likely. The area readily accepted similar work conducted by University of Wyoming researchers several years ago. Relevant city and county officials viewed CCS/CCUS as a business development opportunity. To the extent lands owned by the State of Wyoming were involved, those officials also supported CCS/CCUS.

Task 4: Strategy Development:
The CCT decided on the following strategy for further implementation of the Outreach Plan if a CCS/CCUS project were to be developed at the RSU; (1) more specific project educational materials will be created; (2) meetings will be held with local officials; and (3) public meetings will be held. Favorable outcomes from these activities are anticipated.

Task 5: Implementation:
Given the CCT's conclusion that the local area is favorably inclined to accept CCS/CCUS, the CCT decided to defer implementation of "on-the-ground" public outreach activities until such time as a CCS/CCUS project is developed at the RSU.

Task 6: Evaluation:
As noted, the CCT's evaluation was that the local area is favorably inclined to accept CCS/CCUS, with no material opposition expected.

Task 7: Refinement:
The CCT concluded that its original Outreach Plan did not need to be refined.

Section 3.5: 3-D Visualization & Outreach.

Tom Moore and Thomas Koenig
Center for Economic Geology Research
School of Energy Resources, University of Wyoming
1020 E. Lewis Street, Energy Innovation Center
Laramie, WY 82071

A 3-D model was created using ESRI's ArcScene for visualization of the Nugget and Frontier sandstones. The overlying sealing units, the Baxter and Mowry formations, are also represented. The visualization is intended to educate third parties about the project at the RSU. Such a tool can bring individuals into an immersive 3-D environment to show them the depths and thicknesses of the formations being studied. See Figures 3.5.1, 3.5.2, 3.5.3, and 3.5.4 below. These tools and images are ideal for simply describing geologic storage for outreach and educational purposes.

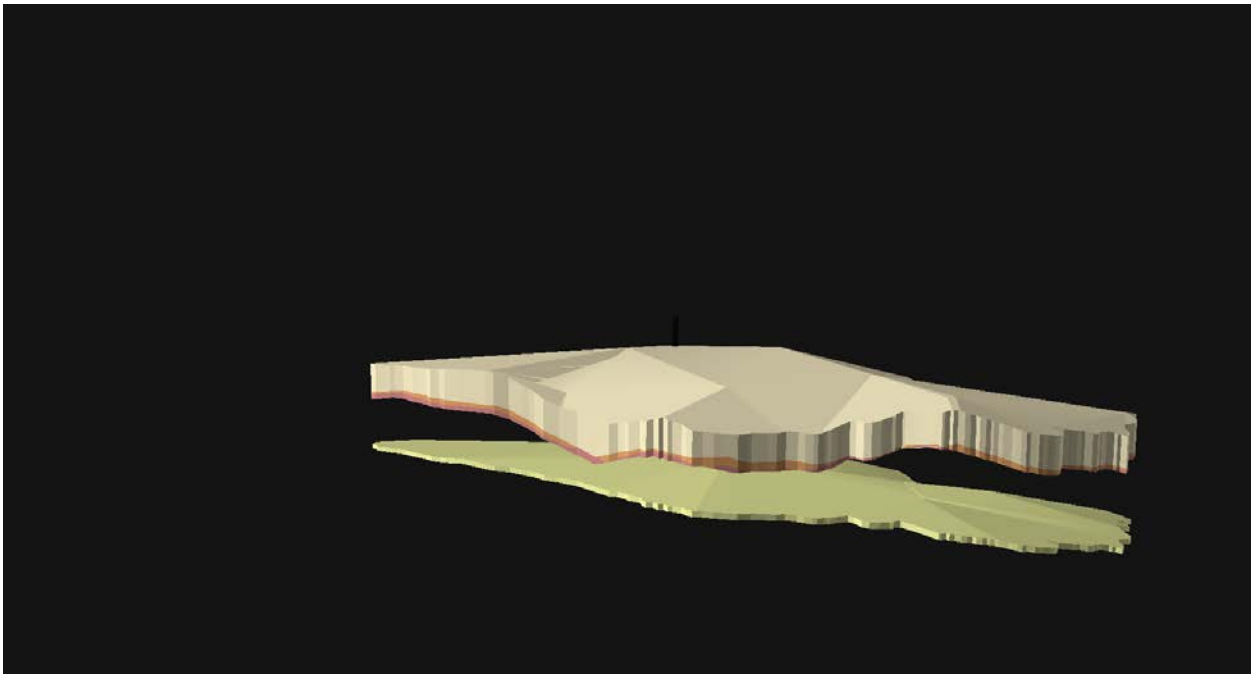

Figure 3.5.1. A 3-D rendering of the Baxter (off-white), Mowry (brown), Frontier (pink), and Nugget (yellow) formations in the study area

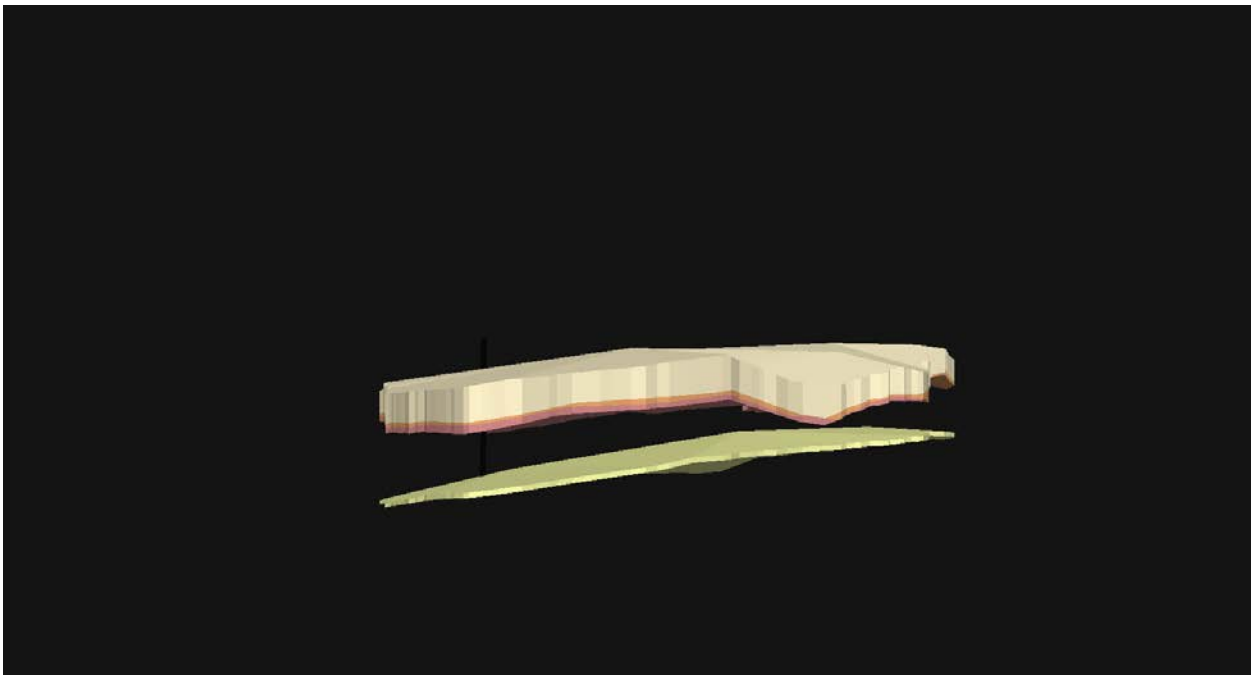

Figure 3.5.2. A 3-D rendering of the Baxter (off-white), Mowry (brown), Frontier (pink), and Nugget (yellow) formations in the study area

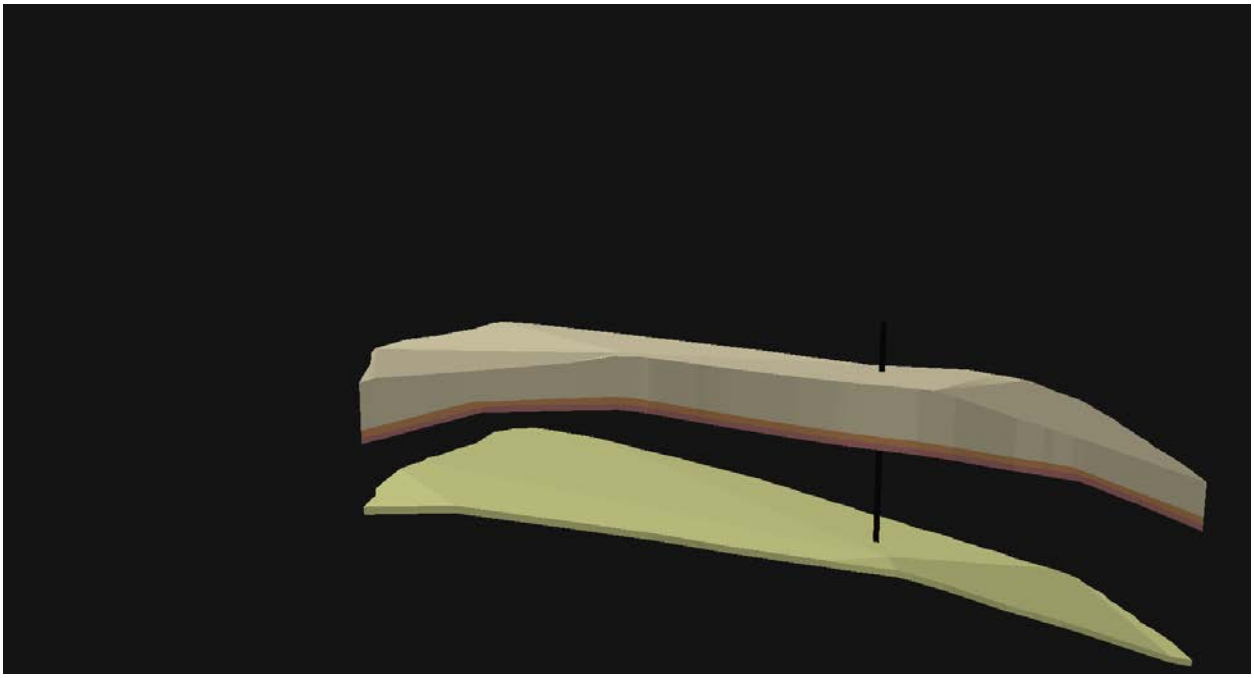

Figure 3.5.3. A 3-D rendering of the Baxter (off-white), Mowry (brown), Frontier (pink), and Nugget (yellow) formations in the study area.

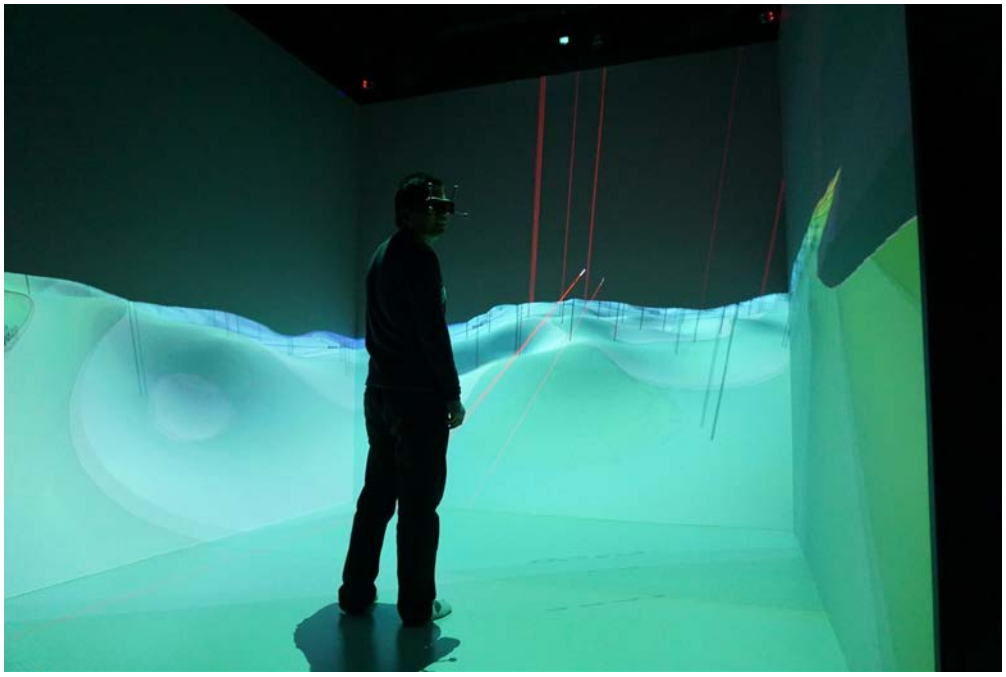

Figure 3.5.4. An isopach map rendered in the 3-D cave in the Energy Innovation Center, University of Wyoming.

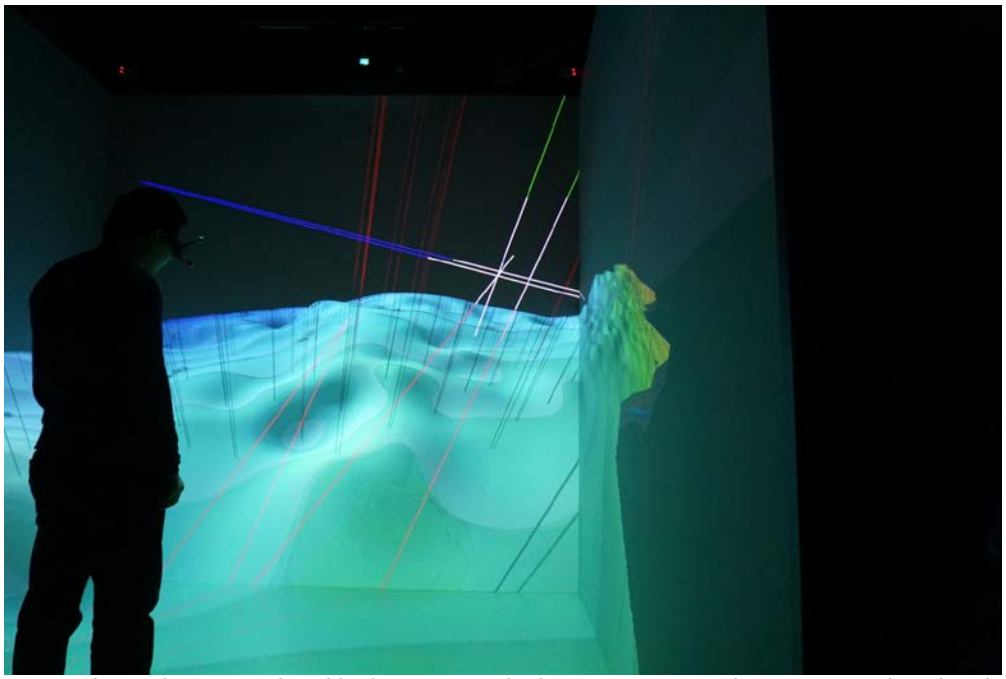

Figure 3.5.5. An isopach map rendered in the 3-D cave in the Energy Innovation Center, University of Wyoming showing wells and other subsurface data.

Chapter IV: Technical Site & Geologic Evaluation

Section 4.1: CO_2 Technical Evaluation.

Tom Moore and Ben Cook
Center for Economic Geology Research
School of Energy Resources, University of Wyoming
1020 E. Lewis Street, Energy Innovation Center
Laramie, WY 82071

CO_2 Source Analysis

JBP's yearly 2010-2015 emissions have averaged 13.5 million metric tons CO_2, making it the largest emitter of CO_2 in Wyoming (USEPA, 2017). In Phase I, the project team retained Sargent & Lundy (S&L) to provide a high-level feasibility evaluation regarding retrofitting CO_2 capture technology at JBP. After assessing JBP's background, location & siting, process considerations, steam requirements, processing & cooling water requirements and auxiliary power requirements, S&L concluded that JBP Units 3 and 4 are "good potential candidates [for] integration of a CO_2 capture facility in conjunction with Wyoming's CarbonSAFE project [and] [i]n fact, the current configuration and operation of the units result in a more cost-effective host site than other facilities which may not have sufficient land, emission control equipment and space capacity." The makeup of the flue gas scales with the output of the power plant, and peaks at approximately 15 percent (Figure 4.1.1).

S&L recommended Units 3 and 4 based on their longer life expectancies, and specifically recommended Unit 4 because it will be less expensive to retrofit with CO_2 capture technology as it has increased fan capacity. Unit 4 typically runs between 302 and 455 MW with an average of 386 MW (Figure 4.1.2). From 2010 to 2015, Unit 4 emitted an annual average of 3.0 million metric tons of CO_2 (WDEQ, 2017). S&L estimated a 90% capture efficiency for approximately 2.7 million metric tons per year. At this rate, 50 million tons of CO_2 can be captured and thereafter stored by the Project's 18th year, leaving another seven years (and 18 million tons of CO_2) to be "utilized" economically.

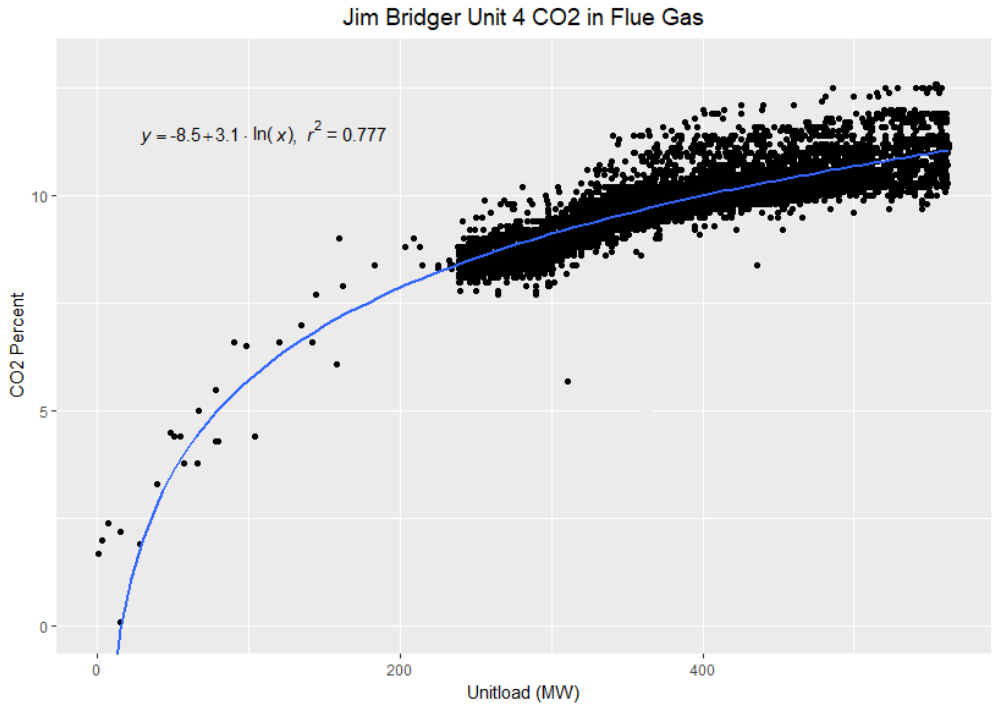

Figure 4.1.1. The percentage of CO_2 in the makeup of the flue gas emitted by unit 4 of the JBP

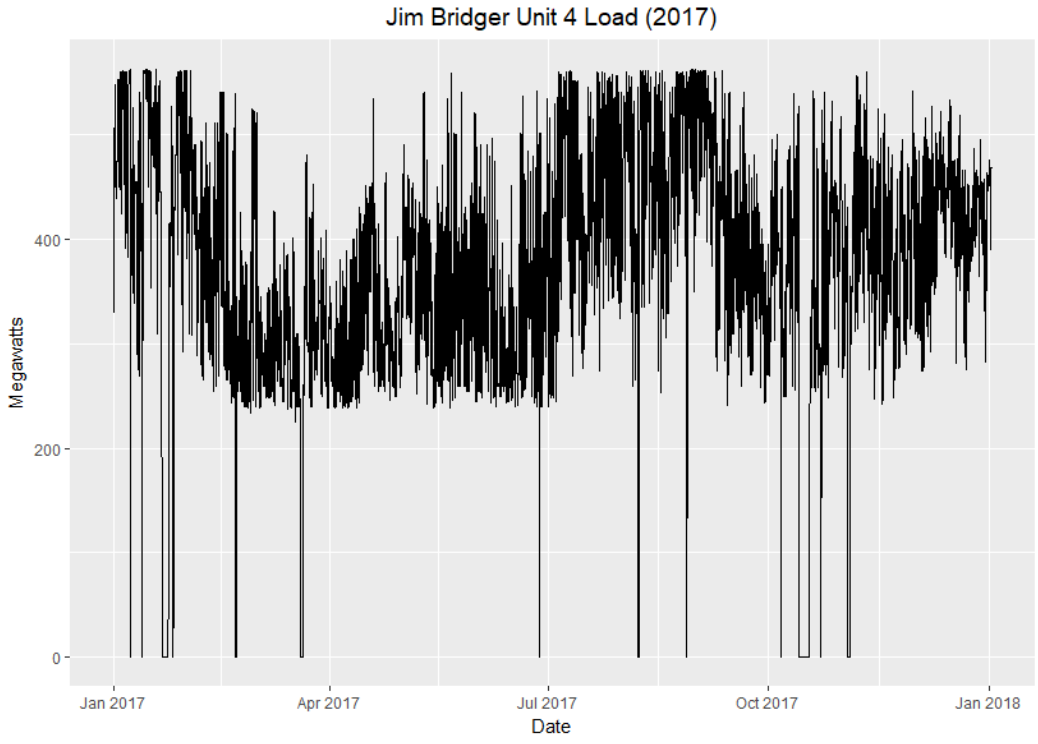

Figure 4.1.2. Power produced from unit 4 of the JBP

As discussed above, the team is addressing "single CO_2 source" risks by assessing local trona processing facilities as additional sources for a potential hub configuration around JBP. JBP's immediate proximity to Wyoming's existing CO_2 infrastructure also creates the potential of connecting both JBP and the local trona processing facilities to other sources and sinks across Wyoming.

Pipeline Requirements

The preferred CO_2 storage complex is immediately adjacent to JBP, minimizing the distance for which CO_2 must be transported -- indeed, the transportation distance should be approximately one mile. At this distance CO_2 can be compressed onsite without any subsequent compression (McCoy, 2009). The relatively short amount of required pipeline should be readily constructible, as discussed above.

CO_2 Pipeline ROW

We envision no CO_2 pipeline ROW issues for numerous reasons: (1) the minimal anticipated transportation distance (one mile or less); (2) surface ownership -- i.e., much if not all of the pipeline ROW will be on the property of team member JBP; (3) robust existing CO_2 infrastructure in the immediate vicinity of JBP (Figure 4.1.3); and (4) favorable Wyoming law and policy regarding CO_2 pipelines.

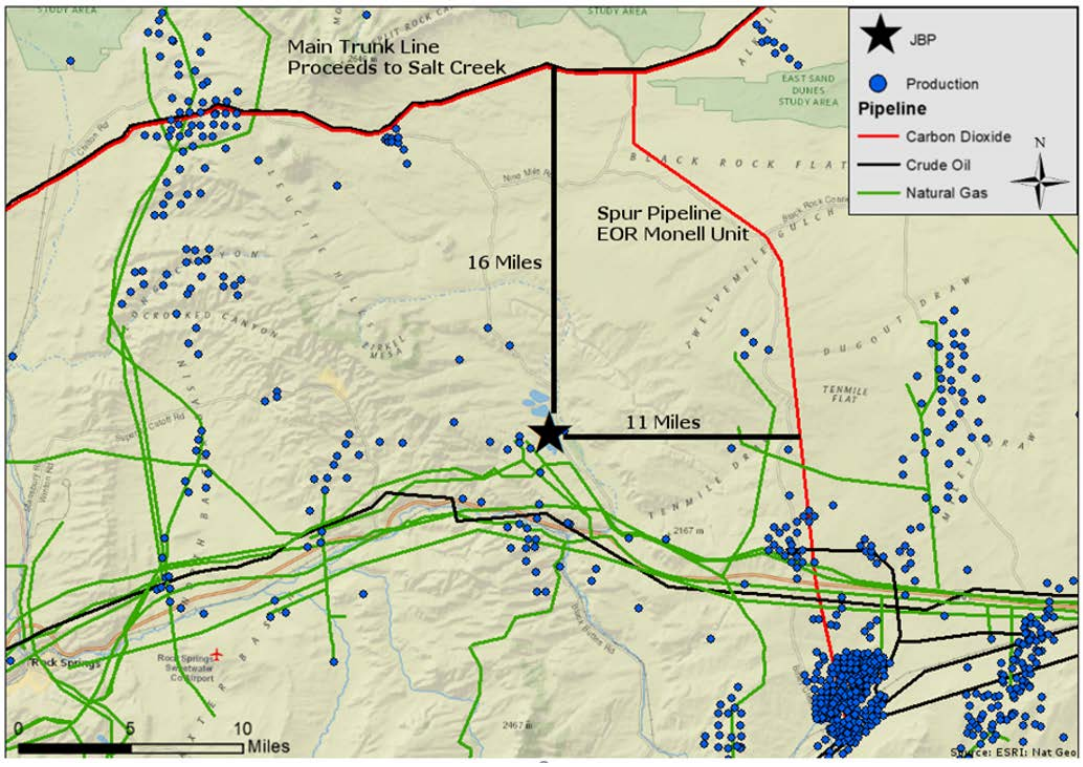

Figure 4.1.3. Map of CO_2 pipelines and oil and gas production wells in the vicinity of JBP.

Section 4.1 References

USEPA (2017). Facility level information on greenhouse gasses tool (FLIGHT). https://ghgdata.epa.gov. Accessed: 8/01/2017.

WDEQ (2017). Wise view and oil and gas production (OGER) database. http://qrywiz.wyo.gov/. Accessed: 8/1//2017.

Section 4.2: Subsurface Description

Scott Quillinan, Zunsheng Jiao, J. Fred McLaughlin, Yuri Ganshin, Heng Wang, Davin Bagdonas, Matthew Johnson, Tom Moore, Charles Nye, and Erin H.W. Phillips
Center for Economic Geology Research
School of Energy Resources, University of Wyoming
1020 E. Lewis Street, Energy Innovation Center
Laramie, WY 82071

Introduction: Regionally, the project's study area is a 5 mi^2 area on the northeastern limb of the RSU that encompasses: (1) JBP; (2) the WY-CUSP Test Well; and (3) the Jim Bridger 3-D seismic survey. The RSU is a large (~50 x 70 mile) asymmetric anticline with over 10,000 feet of proven structural and stratigraphic closure (Deng, et al., 2012; Surdam editor, 2013). High-level technical sub-basinal evaluations of reservoir/seal rocks in basins across Wyoming benefit from prolific subsurface data resources. The study area's suite of high-resolution WY-CUSP legacy data includes a 3-D seismic survey and wells with accompanying data (e.g., logs, production history), including the WY-CUSP Test Well from which CMI collected core and fluid samples from the RSU's deepest intervals.

Pre-feasibility geologic interpretation, modeling, and simulation assessments, coupled with prior geologic characterization work, confirm that Mesozoic and Paleozoic reservoirs at the study area have a high potential for long-term, commercial-scale CO_2 storage. In order of decreasing depth, the reservoir and seal systems directly below JBP are: (1) lower dolomitic units of the Mississippian Madison Limestone (reservoir) and the upper limestone unit of the same formation plus overlying carbonate and shale units of the Mississippian/Pennsylvanian Amsden Formation (seals); (2) eolian sands in the Pennsylvanian/Permian Weber Sandstone (reservoir) and tight shale/redbed/carbonate/evaporite units in the Permian Phosphoria Formation, Triassic Dinwoody Formation and Chugwater Group (seals); and (3) eolian sands in the Jurassic Nugget and Entrada sandstones (reservoirs) and tight shale/carbonate/evaporite units in the Jurassic Gypsum Spring, Sundance and Morrison formations (seals). Previous studies have focused on defining the CO_2 storage and retention capacity of the deeper Madison and Weber reservoir/seal systems (Surdam editor, 2013). The study area's Jurassic reservoir/seal systems have yet to be evaluated beyond pre-feasibility, and no physical data (core, fluids, etc.) are available in the study area.

Storage Reservoirs: Within the RSU, the four targeted storage reservoirs are: (1) Entrada Sandstone; (2) Nugget Sandstone; (3) Weber Sandstone; and (4) Madison Limestone. All four are saline (>10,000 ppm total dissolved solids (TDS)) and located at depths (>9,000 feet) sufficient to contain CO_2 in a supercritical state. The team's understanding of the deeper Weber and Madison are based primarily upon the results of prior RSU characterization studies. *As noted above, WY-CUSP and related legacy investigations confirmed that the Weber and Madison alone have sufficient capacity to store 50+ million metric tons of CO_2 near JBP (Surdam editor, 2013).* More details about all four targeted reservoirs follow.

Entrada Sandstone. At the study area, the Entrada Sandstone is 55 ft. thick and approximately 9,000 ft. deep, based upon interpretations of WY-CUSP Test Well data. Regional core analyses, correlated with data from the WY-CUSP Test Well, identify an upper and lower member within the formation. The lower Entrada consists of fine- to medium-grained, moderately to well-sorted dune and interdune sands. The upper Entrada consists of very fine grained, well-sorted sands. At the study area, the best reservoir interval is 30 ft. thick, with porosity that ranges from 9 to 15%.

Nugget Sandstone. The Nugget Sandstone is a very promising reservoir. At the study area, the Upper Triassic/Lower Jurassic Nugget Sandstone is 465 ft. thick and approximately 9,200 ft. deep. The Nugget

is comprised of eolian sands, with some fluvial interdune deposits (Johnson, 2005). A generalized lithologic description derived from the WY-CUSP Test Well mud log identifies sandstone, fine- to medium-grained, subangular, and well-sorted, with occasional loose clay fragments and quartz grains with iron stain. Density–neutron porosity logs indicate heterogeneous but continuous porosity throughout the Nugget averaging 6 to 21.5% (mean 12.8%) (Figure 4.2.1a). Zones exhibiting higher porosity also exhibit higher permeability, based on resistivity curve separation. Calculated permeability ranges from 0.1 to over 1000 mD (mean 81.6 mD) (Figure 4.2.1a). Gas shows were negligible during drilling below the Cretaceous section, and the neutron density curves show no gas effect, suggesting no risk to mineral estates associated with CO_2 storage.

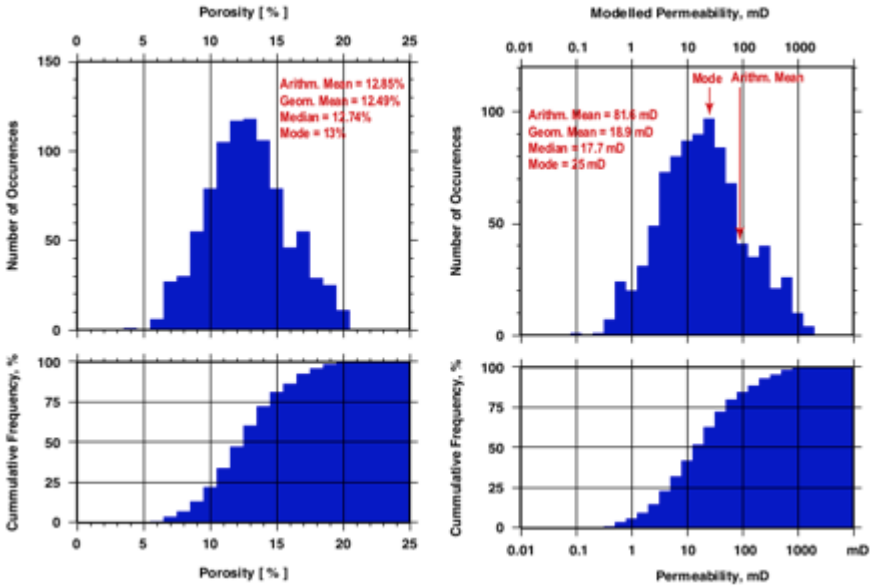

Figure 4.2.1a. (Left) Porosity distribution within the Nugget Sandstone (9,216 - 9,660 ft. depth interval; 889 data samples). Ordinary histogram (top left); cumulative histogram (bottom left). (Right) Permeability distribution within the Nugget Sandstone (9,216 - 9,660 ft. depth interval; 889 data samples). Ordinary histogram (top right); cumulative histogram (bottom right)

Initial assessments indicated that the Nugget has greater storage potential than the Entrada, and therefore pre-feasibility efforts focused on furthering Nugget storage evaluations using available data. The team combined published porosity and permeability data with ten Nugget Sandstone core sample collected from the Brady unit 11-11 well (API# 4903720422, less than 25 miles south of the study area). The relationship between porosity and permeability is shown in Figure 4.2.1b; published data include wells within 25 miles of JBP and show relatively strong correlation between porosity and permeability. This has allowed the team to develop preliminary porosity and permeability models using the study area's legacy data. The preliminary heterogeneous permeability property model for the Nugget Sandstone shows that most permeability is within the tens of millidarcy across the study area, but that some zones likely have permeability in the hundreds of millidarcies (Figure 4.2.1c). An averaged permeability map of the Nugget Sandstone within the study area, derived from seismic velocity data, suggests relatively high zones of permeability adjacent to the JBP (Figure 4.2.1d).

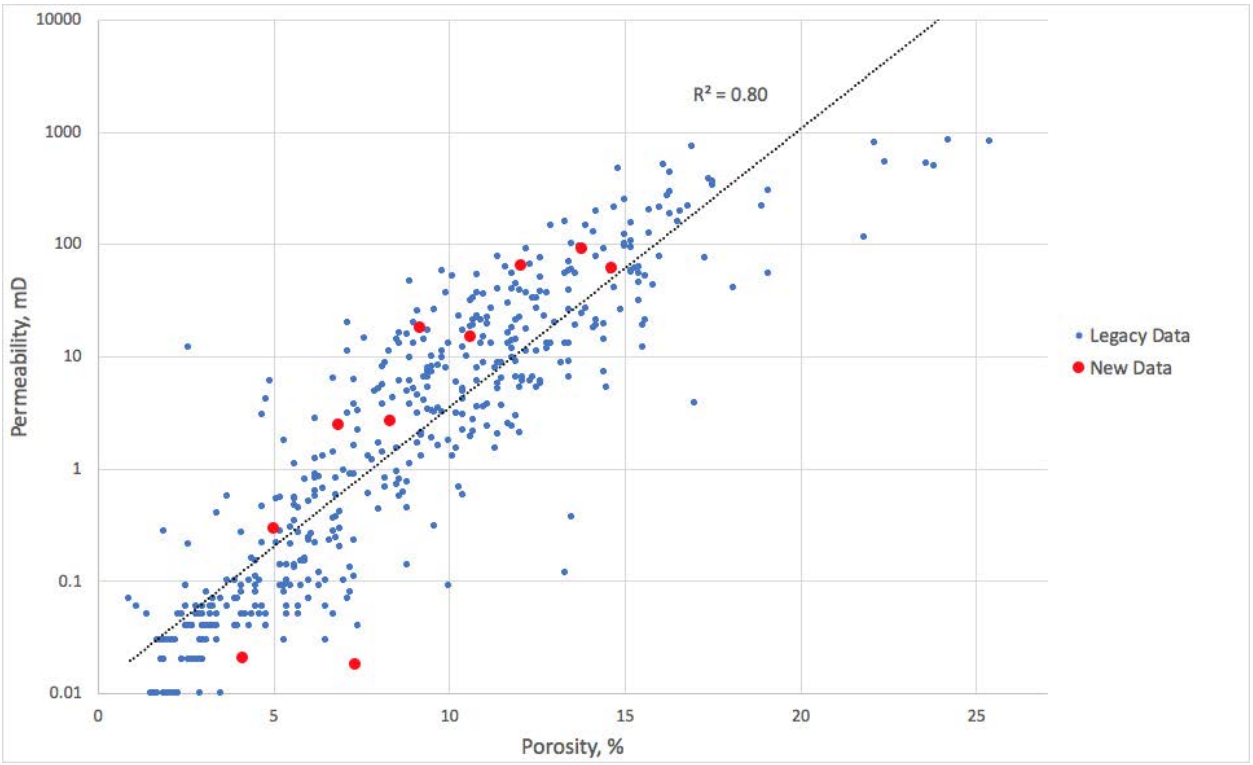

Figure 4.2.1b.. Semi-log plot of porosity versus permeability for the Nugget Sandstone. Published data (labeled "Legacy Data") are from wells with API numbers 3720385, 3720422, and 3722344. Data collected from Phase 1 investigations (labeled "New Data") are from well 3720422; data plotted are at 3570 psig

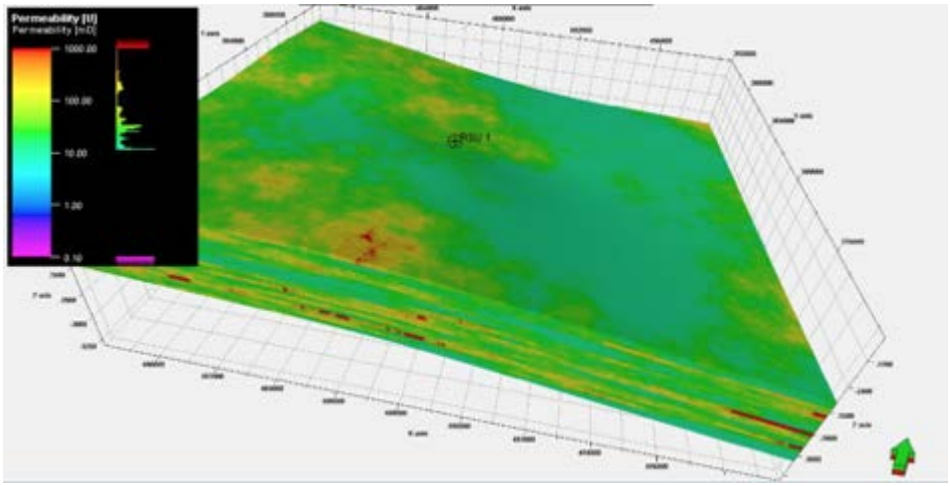

Figure 4.2.1c. Permeability distribution of the Nugget Sandstone (5x vertical exaggeration) within the 5 mi^2 study area. Permeability is relatively consistent, and generally >10mD; porosity averages 12.8%. Zones of higher permeability, both vertically and laterally, will impact plume migration

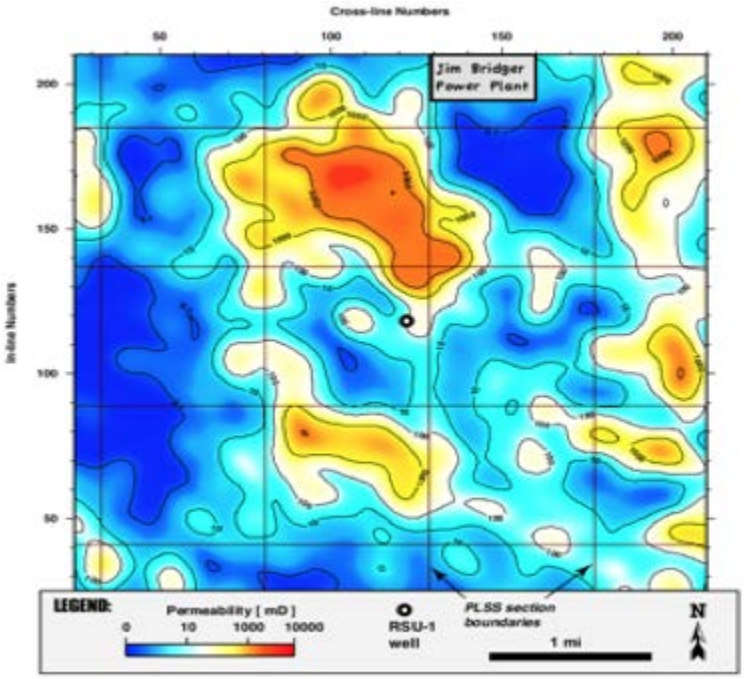

Figure 4.2.1d. Permeability map of the Nugget Sandstone derived from seismic interval velocity assuming: (1) laterally invariant velocity-porosity; (2) porosity-permeability relationships from WY-CUSP Test Well logs and cores; and (3) porosity is only factor affecting seismic interval velocity variations. Compartmentalization is visible in the map's permeability distribution

Weber Sandstone. At the study area, the Weber Sandstone is approximately 675 ft. thick and over 11,200 ft. deep and consists of two units: (1) an upper unit of fine- to medium-grained, cross-bedded sandstone and siltstone deposited in near-shore dune and interdune zones; and (2) a basal unit of carbonate, clastic carbonate and shale deposited in a shallow marine coastal setting. Only the 240 ft. thick upper unit has reservoir properties that are adequate for CO_2 injection and storage, though the laterally coalescing sand and calcareous, siliceous and evaporite cementation result in a highly heterogeneous reservoir rock. This heterogeneity is reflected in porosity and permeability core measurements, where porosity ranges from 1.7 to 8.8%, and permeability ranges from 0.001 to 13.8 mD (n=30 samples). Seismically derived permeability estimates range from a mode of 0.06 mD to a mean of 1.94 mD (Ganshin, 2013), which is consistent with the averaged measured permeability of 2.7 mD (McLaughlin and Garcia-Gonzalez, 2013). In contrast, the rocks of the basal unit can have relatively porous zones (>9% porosity), but permeability remains consistently low (<0.5 mD). Numerical injection simulations performed by CMI on the Weber reservoir show that long-term injection at moderate rates (0.5 million metric tons/year/well) is effective; at higher injection rates (1.0 million metric tons/year/well), reservoir pressure and migration into other formations could pose a risk (Jiao and Surdam, 2013).

Madison Limestone. At the study area, the Madison Limestone is approximately 400 ft. thick and occurs at depths greater than 12,200 ft. (McLaughlin et al., 2013). The formation consists of two units, an upper limestone that acts as a seal to the basal dolomitic reservoir. This dolomitic unit is identified as a prime CO_2 injection target (Surdam ed., 2013), and its thickest continuous reservoir interval is approximately 170 ft. at the study area. There are also three discontinuous dolomitic reservoir intervals below the thick zone, resulting in approximately 250 ft. of total reservoir interval. The average porosity and permeability within the thickest reservoir interval are 13.1% and 22.7 mD, respectively. However, the team observed that porosity and permeability varied by pore type, as the reservoir zones generally contain either intergranular or vuggy/moldic pore types. Porosity and permeability range from 0.001 mD to 82.6 mD in

intergranular sections, with 0.3 to 22.4% porosity. Permeability in moldic and/or vuggy dolostones ranges from 0.001 mD to 2245 mD with a porosity range of 0.3 to 19.8%. Observing the variance in reservoir character relative to pore type allowed for the development of property models that more accurately depict reservoir heterogeneity, resulting in less uncertainty in simulation results. *Importantly, injection results from previous studies (DE-FE0009202) of the Madison Limestone show that it has the capacity to safely and effectively store 25 million metric tons of CO_2 with only one injector well (1.0 million metric tons/year) over 25 years.* Similar to results from Weber injection simulations, pressure could also be a concern for the Madison reservoir, especially if it is locally confined.

Confining Systems: Pre-feasibility Phase I work identified and evaluated six significant confining systems using well log data and core analysis, including optical microscopy and mercury injection capillary pressure (MICP) assessments. Regional descriptions from a literature review have been compared with WY-CUSP test well (RSU #1) data to investigate lateral continuity and other geologic uncertainty. These data suggest the site has robust sealing units, with total confinement capacities that greatly exceed the storage need. The six confining systems are discussed below, followed by a MICP discussion.

Upper limestone facies of the Madison Limestone. At the study area, the reservoir intervals of the Madison Limestone are overlain by approximately 120 ft. of tight, micritic limestone. The sealing properties of this unit include low porosity (<0.42%) and permeability (<0.001 mD), and pore throats that are <0.3 µm (McLaughlin and Garcia-Gonzalez, 2013). This unit is likely highly variable regionally, though appears to be laterally consistent at the study area.

Amsden Formation. The Amsden Formation (418 ft. thick) overlies the Madison Limestone and is comprised of variegated marine shales with thin interbedded carbonate. The sealing properties of this formation at the study area include low porosity (<4.7%) and permeability (<0.005 mD), and pore throats that are <0.3 µm (McLaughlin and Garcia-Gonzalez, 2013). On the basis of prior CMI assessments (e.g, capillary entry pressures, thin section analysis, dissolved gas, isotopic and fluid analysis and vertical interference tests), the team has concluded that the Amsden Formation seals the Madison Limestone and hydraulically isolates this reservoir from the Weber Sandstone within the study area (Quillinan and Mclaughlin, 2013).

Chugwater and Dinwoody formations. The Triassic Chugwater and Dinwoody formations seal the top of the Weber and Phosphoria formations. This confining unit is a thick (984-1312 ft.) laterally extensive section of siltstone and shale with minor fine- to very fine-grained sandstones that is well-cemented by evaporite and carbonate. The sealing properties of these rocks at the study area include low porosity (<1.5%) and permeability (<0.001 mD), and pore throats that are <0.2 µm (McLaughlin and Garcia-Gonzalez, 2013). On the basis of core and thin section analysis and regional mapping, the team has concluded that the Chugwater-Dinwoody confining unit is both a local and regional seal which acts as a hydrologic divide between Paleozoic and Mesozoic reservoirs in the RSU (Quillinan and Mclaughlin, 2013; McLaughlin et al., 2014).

Gypsum Spring Formation. The Gypsum Spring Formation divides the overlying Sundance-Entrada reservoir and underlying Nugget Sandstone reservoir. The seal is 106 ft. thick and comprised of marine derived transgressive and regressive sequences. The Gypsum Spring may not be continuous throughout the study area (Love et al, 1993), so a hydrogeological connection could exist with the overlying Sundance-Entrada reservoir. Future work may identify this connection as a combined Nugget-Entrada reservoir complex with the Morrison Formation serving as the confining upper seal.

Morrison Formation. The Morrison Formation was deposited in a broad alluvial plain that covered large regions of western North America. At the WY-CUSP Test Well, it is 286 ft. thick and composed of variegated shales, with some interbedded sandstone and limestone layers. Regionally, the Morrison Formation is described as containing shales that are usually sandy and fissile, sandstones that are often calcareous and fine-grained, and thin limestone that separate the shales and sandstones. Sandy facies are present but not laterally continuous (Johnson, 2005). Isolated sandstone bodies (6-20 ft. thick) produce gas in some locations within the Green River Basin, though gas plays in the Morrison are discontinuous and isolated. The Morrison confining unit has not been well defined in the RSU region.

Upper Cretaceous Confining Unit. A thick laterally extensive confining unit is composed of the Upper Cretaceous shales including the Blair, Baxter-Steele, Frontier-Niobrara, Mowry, Muddy and Thermopolis Formations (Freethey and Cordy, 1991; Ahern et al. 1981, Collentine et al. 1981, Bartos and Hallberg 2010). At the WY-CUSP Test Well, this confining unit is 5,617 ft. thick (McLaughlin et al, 2013) and 2,762 to 8,379 ft. below the land surface. Rare water bearing zones occur within the confining unit; two sand intervals of 20 ft. in the Frontier Formation and a 15 to 5 foot sand interval in the Muddy Sandstone are reported. Based on correlative well log results from the WY-CUSP Test Well and extrapolation of regional TDS data, these minor sandy intervals are saline (TDS >10,000 ppm) and also confined by their parent shale unit. The confining unit is recognized as a major regional hydrogeologic barrier between the overlying Mesaverde aquifer system and the underlying hydrogeologic units of the Mesozoic formations (Clarey et al., 2010).

MICP Analysis: MICP analysis was performed during the pre-feasibility assessments on three samples from the Mowry Formation and two samples from the Morrison Formation, all collected from the USGS Core Research Center (CRC). Mowry samples are from well R567 (CRC catalog ID) and Morrison samples are from two wells, R616 and R567. For all samples, over 98% of pore throats by volume were shown to be nanopores (≤0.1 μm; Fig. 4.2e). Entry pressures for Mowry samples all exceeded 1000 psia, and were relatively consistent (between 1007-1120 psia). Entry pressures for Morrison samples were lower, between 528-979 psia. These data suggest that the Mowry seal could conservatively retain a CO_2 plume with nearly 1,000 feet of column height. Previous MICP experiments on samples from the Chugwater, Amsden and upper Madison confining intervals all recorded entry pressures >935 psia, with some samples approaching 3,000 psia. These units could safely confine large volumes of CO_2 in the study area's reservoirs.

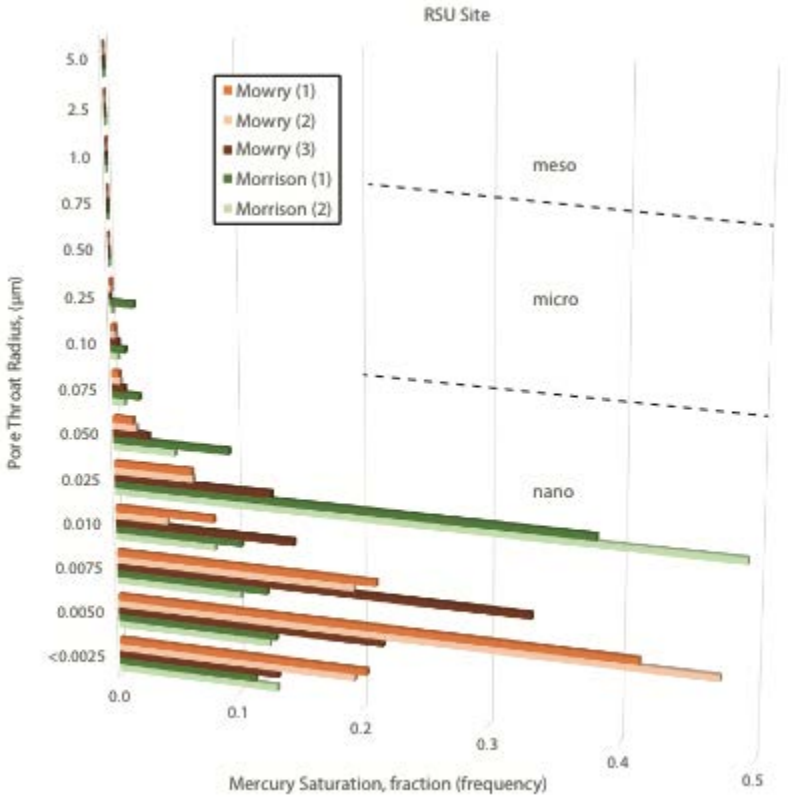

Figure 4.2.1e. Pore throat size histogram derived from MICP data for samples from sealing units

Wellbore Risk Analysis: There are a total of 17 wells within a 10-mile radius of JBP that penetrate the upper Mowry seal. The majority of sections (1 mi^2 units) do not exceed one well per section. Two exceptions are Section 8 of Township 0200N Range 1010W and Section 13 of Township 0200N Range 1030W, 1 and 9 miles southwest of JBP, respectively, both of which have two wells per section. The low density of wells -- generally less than 1 well per mi^2 -- is favorable for minimizing leakage risks. Nelson (2013) also conducted a study ranking wells with different levels of risk based on their plugged and abandonment date as well as local topography that could trap CO_2 on the surface in depressions; this study also addressed previous work that has ground-truthed wells in the area around JBP. The study produced two maps identifying wells that are potentially more likely to leak or cause a surface accumulation of CO_2 within 11 miles of the JBP.

Structural Elements: Within the study area, strata dip at ~5 degrees to the east-northeast. Structural confinement of the stacked storage section is defined by two main factors. First, very thick (>4000 ft.) Cretaceous shales overlie the reservoir systems. Because of the regional dip of 5 degrees, CO_2 plume migration up-dip is expected to be exhausted within a short distance, while still remaining contained under the overlying Cretaceous shale package. Confining units within the stratigraphic section of the stacked storage complex also dip to the east-northeast at ~5 degrees with no additional structural features, and are therefore expected to behave in a similar manner to the reservoirs. These formations are also proven to retain hydrocarbons at pressures above the hydrostatic gradient, locally and regionally.

Investigation of faults included field mapping and direct measurement in the high walls of the adjacent Bridger Coal Mine. Fault orientations viewed at the surface and within the coal mine high walls were compared with regional structural geology maps of the RSU. Relative fault displacement and orientation

were compared to regional structural trends to evaluate potential fault coherence at depth in the RSU. Regional structural trends used for comparison are determined from geological maps, satellite imagery evaluation, and subsurface geophysical data including seismic and well data. Surface evaluation of exposed faults revealed a mixture of hematite cement and silicic fluid sealing. Total depth of faults mapped on the surface was not determined. However, they share orientation with larger regional-scale faults which have segmented the RSU into discrete hydrologic units. It is expected that many of the surface faults viewed in this investigation represent a regional strain orientation and thus exist as splay faults to primary faults within the RSU structural domain. An example of a fault viewed in the Bridger coal mine high-wall is shown below in Figure 4.2.2. In future investigations the regional-scale compartmentalization of aquifers should be taken into consideration for sealing potential of injection reservoirs. The regional faults do not appear to produce formation waters and are considered sealing in this sense.

Figure 4.2.2. Normal faulting, highlighted by offsets in a coal seam, east of the JBP at the Bridger mine high wall.

Second, the RSU is regionally segmented into distinct hydrologic compartments by west to east trending transpressional faults. These segments have been recognized both as large-scale (miles) mapped faults on the RSU surface and by evaluation of fluids within younger Cretaceous reservoirs (i.e., Frontier-Niobrara and Muddy Formation), which indicate confinement. Dominant fracture orientations analyzed in core from the WY-CUSP Test Well are consistent with primary regional structures. Further geomechanical analysis in the Madison and Weber formations indicates that a minimal pore pressure increase will result in increased permeability anisotropy in the ENE-WSW orientation (Shafer, 2013). Additional faults, which are likely younger than the prominent west to east trending segments on the RSU, are identified as northwest trending strain compensation structures associated with relaxation of the greater RSU structure. Geophysical investigation by CMI (DE-FE00293020) suggests that both fault orientations are confining, and the larger west to east segmentation faults likely act as hydrogeologic seals. This compartmentalization behavior can likely be seen in the seismically derived Nugget Sandstone data that

was compiled during Phase I (Figure 4.2.1d). Evaluation of surface faults during pre-feasibility identified minor west to east trending surface faults with small (<1 meter) normal offsets.

Prospective Storage Resources: The four targeted reservoirs have sufficient criteria to warrant a commercial-scale feasibility assessment. These criteria include storage requirements -- including pore volume, salinity and closure (discussed below). *Previous studies confirmed that two deeper reservoirs at the RSU -- the Weber Sandstone and Madison Limestone -- alone have sufficient capacity to store 50+ million metric tons of CO_2 (Surdam editor, 2013).* However, comprehensive storage assessments have yet to be performed on all potential reservoirs, of which the shallower Nugget shows particular promise. During pre-feasibility, the team evaluated volumetric assessments of reservoir storage capacity using the DOE's best practice methodology for determining storage potential (after Goodman et al., 2011). The estimated potential of employing stacked storage near JBP suggests a volumetric CO_2 storage capacity between 6.7 (P10) and 17.1 (P90) million metric tons per square mile (Table 4.2.1a). These estimates indicate that the Nugget Sandstone has the highest storage capacity potential per volume, with nearly twice the potential capacity as that of the Madison Limestone for the P90 case. The Entrada Sandstone has the lowest estimated storage potential at the study area. Both the Nugget and Entrada formations, however, are worthy candidates for feasibility studies as the volumetric estimates in Table 4.2a are based on calculations from a limited dataset. Furthermore, studying these shallow reservoirs in the Project Area could help reduce "deep well" pressure management and economic risks associated with utilization of the RSU's deeper reservoirs for storage (Surdam et al., 2013; Nielsen et al., 2017).

Entrada Sandstone Storage Statistics (million metric tons/mi^2)		
P10	*P50*	*P90*
.14	.27	.47
Nugget Sandstone Storage Statistics (million metric tons/mi^2)		
P10	*P50*	*P90*
2.9	5.6	9.6
Weber Sandstone Storage Statistics (million metric tons/mi^2)		
P10	*P50*	*P90*
.7	1.2	2.1
Madison Limestone Storage Statistics (million metric tons/mi^2)		
P10	*P50*	*P90*
3.0	4.0	4.9

Table 4.2.1a. Storage estimates for the four targeted RSU reservoirs using the methodologies and E_{saline} variables from Goodman et al. (2011). The thickness of the porous sections of the Entrada, Nugget, Weber and Madison formations was calculated from WY-CUSP Test Well logs to best match local conditions. Average porosity values for the Weber and Madison formations are from McLaughlin and Garcia-Gonzalez (2013); average porosity for the Nugget Sandstone was calculated from regional core data and correlated with the density-neutron porosity log from the WY-CUSP Test Well; average porosity for the Entrada Sandstone was calculated using the density-neutron porosity log from the WY-CUSP Test Well

Section 4.2 References

Ahern J., Collentine M., and Cooke S. (1981) Occurrence and characteristics of ground water in the Green River Basin and Overthrust Belt, Wyoming. Report to U.S. Environmental Protection Agency by Water Resource Research Institute, University of Wyoming, vols V-A and V-B.

Bartos T.T. and Hallberg L. (2010) Chapter 5, Groundwater and hydrogeologic units. In: Copeland D. and Ewald E. (eds) Available groundwater determination technical memorandum, Green River Basin Water Plan II. Report to the Wyoming Water Development Commission.

Clarey K.E., Bartos T., Copeland D., Hallberg L.L., Clark M.L., and Thompson M.L. (2010) Available groundwater determination-Technical Memorandum. WWDC Green River Basin Water Plan II–Groundwater study, Level I (2007–2009).

Collentine M., Libra R., Feathers K.R., and Hamden L. (1981) Occurrence and characteristics of ground water in the Great Divide and Washakie Basins. Water Resources Institute, University of Wyoming, vols VI-A and VI-B.

Deng H., Stauffer P.H., Dai Z., Jiao Z., and Surdam R.C. (2012) Simulation of industrial-scale CO_2 storage: Multi-scale heterogeneity and its impacts on storage capacity, injectivity and leakage. *International Journal of Greenhouse Gas Control*, **10**, pp. 397-418.

Freethey G.W. and Cordy G.E. (1991) Geohydrology of Mesozoic rocks in the upper Colorado River Basin in Arizona, Colorado, New Mexico, Utah, and Wyoming, excluding the San Juan Basin. US Geological Survey Professional Paper 1411-C.

Ganshin Y. (2013) Predicting Permeability in the Target Reservoirs on the Rock Springs Uplift, Southwest Wyoming. In: Surdam R.C. (ed) *Geological CO_2 Storage Characterization*, Springer, pp. 169–190.

Goodman A., Hakala A., Bromhal G., Deel D., Rodosta T., Frailey S., Small M., Allen D., Romanov V., Fazio J., Huerta N., McIntyre D., Kutchko B., and Guthrie G. (2011) U.S. DOE methodology for the development of geologic storage potential for carbon dioxide at the national and regional scale. *International Journal of Greenhouse Gas Control*, **5**, pp. 952-965.

Jiao Z. and Surdam R.C. (2013) Advances in Estimating the Geologic CO_2 Storage Capacity of the Madison Limestone and Weber Sandstone on the Rock Springs Uplift by Utilizing Detailed 3-D Reservoir Characterization and Geologic Uncertainty Reduction. In: Surdam R.C. (ed) *Geological CO_2 Storage Characterization*, Springer, pp. 191-231.

Johnson E.A. (2005) Geologic assessment of undiscovered oil and gas resources in the Phosphoria Total Petroleum System, southwestern Wyoming province, Wyoming, Colorado, and Utah. In: Petroleum systems and geologic assessment of oil and gas in the Southwestern Wyoming Province, Wyoming, Colorado, and Utah, US Geological Survey Digital Data Series DDS-69-D.

Love J.D., Christiansen A.C., and Ver Ploeg A.J. (1993) Stratigraphic chart showing Phanerozoic nomenclature for the State of Wyoming. Wyoming Geological Survey Map Series 41.

McLaughlin J.F., Ganshin Y., Quillinan S., Bentley R., and Jiao Z. (2014) Mitigating Risks Associated with Long-term CCS: Characterizing the Geologic History and Heterogeneity of Sealing Strata, *Energy Procedia*, **63**, pp. 4999-5009.

McLaughlin J.F. and Garcia-Gonzalez M. (2013) Detailed Geologic Characterization of Core and Well Data from the Weber and Madison Formations and Associated Seals at a Potential CO_2 Sequestration Site in Southwest Wyoming: Defining the Lithologic, Geochemical, Diagenetic, and Burial Histories Relative to Successful CO_2 Storage. In: Surdam R.C. (ed) *Geological CO_2 Storage Characterization*, Springer, pp. 55-96.

McLaughlin J.F., Bentley R.D., and Quillinan S.A. (2013). Regional Geologic History, CO_2 Source Inventory, and Groundwater Risk Assessment of a Potential CO_2 Sequestration Site on the Rock Springs Uplift in Southwest Wyoming. In: Surdam R.C. (ed) *Geological CO_2 Storage Characterization*, Springer, pp. 33-54.

Nelson J.D. (2013) Assessment Tools for Assigning Leakage Risk to Individual Wells at a Geologic Sequestration Site in Wyoming. M.S. thesis, Department of Geology and Geophysics, University of Wyoming.

Nielsen C.M., Grimstad A.A., Drysdale R., and Williams J.D. (2017) Pressure control for managing and optimizing adjacent subsurface operations in large scale CCS. *Energy Procedia*, **114**, pp. 4787-4796.

Quillinan S.A. and McLaughlin J.F. (2013) Reservoir Fluid Characterization of the Weber Sandstone and Madison Limestone on the Rock Springs Uplift in Southwest Wyoming. In: Surdam R.C. (ed) *Geological CO_2 Storage Characterization*, Springer, pp. 151-167.

Shafer L.R. (2013) Assessing injection zone fracture permeability through the identification of critically stressed fractures at the Rock Springs Uplift CO_2 sequestration site. SW Wyoming, M.S. thesis, Department of Geology and Geophysics, University of Wyoming.

Surdam R.C. (ed) (2013) Geological CO_2 Storage Characterization: The Key to Deploying Clean Fossil Energy Technology, Springer, New York, NY.

Section 4.3: Hydrostratigraphy Description

Tom Moore and Scott Quillinan
Center for Economic Geology Research
School of Energy Resources, University of Wyoming
1020 E. Lewis Street, Energy Innovation Center
Laramie, WY 82071

The preferred on-site scenario would drill a test well (-108.776, 41.735) to further the fluid characterization of the two target reservoirs, the Entrada and Nugget sandstones.

For a formation to be considered for CCS, the formation must have a salinity exceeding 10,000 ppm. Salinity is measured via total dissolved solids (TDS). To gain an understanding of the salinity in the Entrada and Nugget target reservoirs, data were interpolated using inverse distance weighting (IDW) via ESRI ArcGIS. Using the USGS National Produced Waters Geochemical Database v2.2 (Blondes et al., 2016), salinity was estimated for the location of the proposed test well (-108.776, 41.735016) for the Entrada and Nugget formations.

The extent of the available data did not allow for interpolation of salinity for the Entrada formation, however, the nearest interpolation, 2.4 miles south of the proposed test well, predicts a salinity of 42,181 ppm (Figure 4.3.1). The formation salinity generally trends east to west, and it is likely similar to the predicted value to the south. The Nugget was predicted to have a salinity of 73,034 ppm (Figure .3.2). On the basis of this assessment both reservoirs appear to exceed the 10,000 ppm threshold and suitable for CCS. It should be noted that the dataset does not have good resolution in the study area, and samples should be taken using EPA methodology in future studies.

A previous study (WY-CUSP) characterized the Madison and Weber formation in depth and took a look at several other formation that lie above in the stratigraphic column. Quillinan and McLaughlin (2013) collected formation fluids from deep reservoir systems using the WY-CUSP Test Well and showed that Paleozoic reservoirs have a TDS >75,000 ppm. Analysis of resistivity curves in strata above have similar TDS values. All of which exceed the underground safe drinking water (USDW) standards. Local groundwater resources lie above the potential injection reservoirs and are hydrologically isolated by thick confining units. There are no sole-source aquifers as defined by EPA in the Study Area. The lowermost USDW within the Study Area consists of geologic units within the Mesaverde Group aquifer system: the Almond, Ericson, Rock Springs, and Blair formations. Freethey and Cordy (1991) estimated that the Mesaverde aquifers on the flank of the RSU have less than 500 ft. of saturated thickness and a TDS concentration of less than 1,000 ppm. Bartos et al. (2010) later refined TDS estimates to 342 ppm to 7,860 ppm. In the Study Area, the Mesaverde aquifers extend from the surface to a depth of approximately 4,150 ft. The main water-bearing zones lie at less than 1,000 ft. depth (McLaughlin et al., 2014). The Mesaverde aquifer is confined below by the Baxter-Mowry confining unit. The lateral continuity and greater-than-4,000-ft. thickness of this low-permeability material define a major hydrologic divide between the aquifers above and below the Baxter-Mowry confining unit, effectively isolating them (Ahern et al. 1981, Collentine et al. 1981, Freethey and Cordy 1991, Bartos and Hallberg 2010).

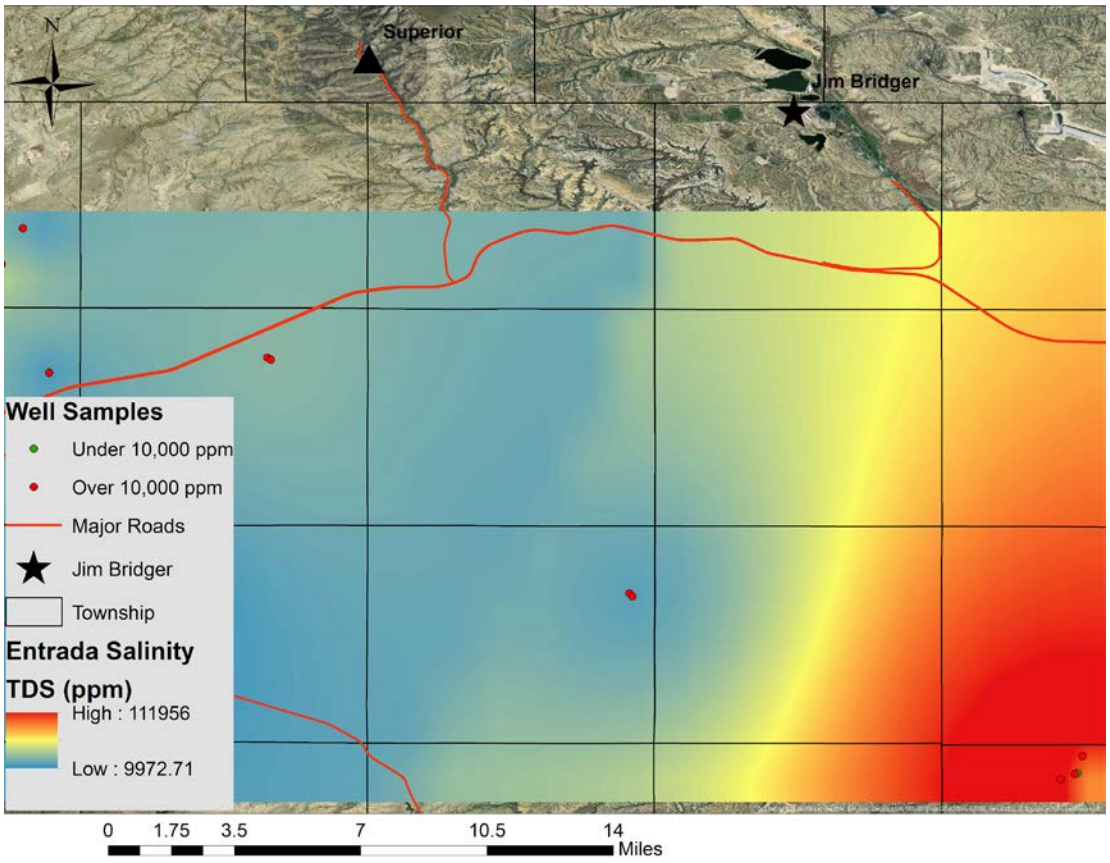

Figure 4.3.1. Salinity estimated using inverse distance weighting of the Entrada formation water quality samples

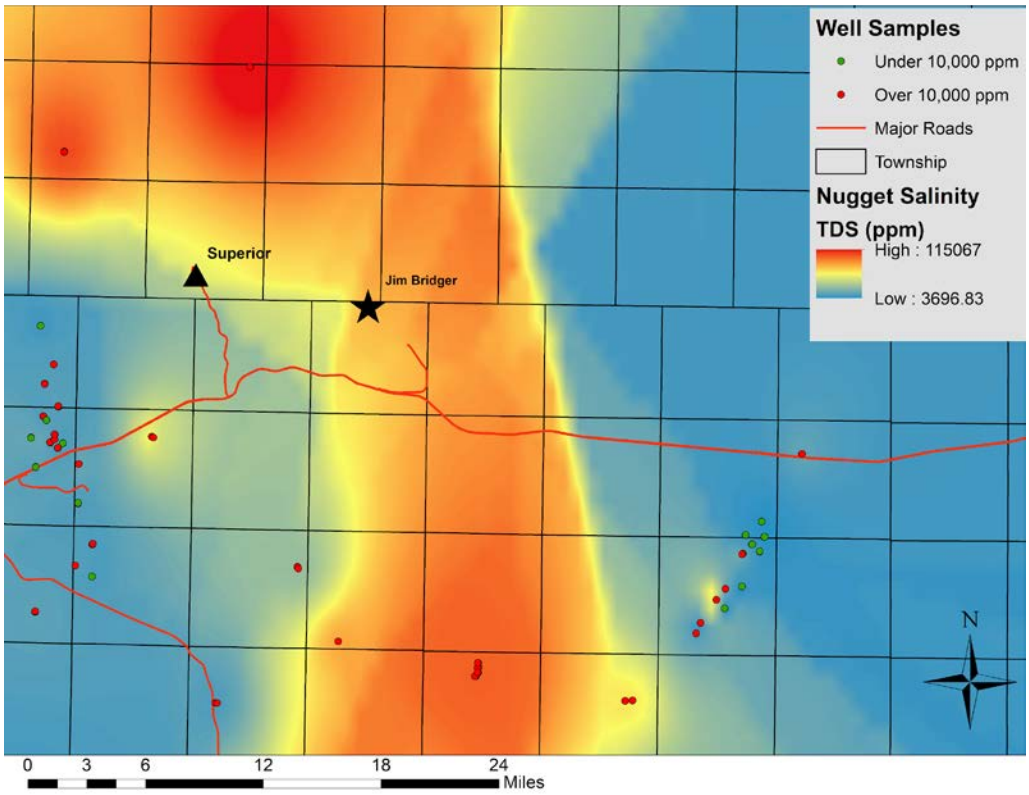

Figure 4.3.2. Salinity estimated using inverse distance weighting of the Nugget formation water quality samples

Section 4.3 References

Ahern J, Collentine M, Cook S (1981) Occurrence and characteristics of ground water in the Green River Basin and Overthrust Belt, Wyoming. Report to U.S. Environmental Protection Agency by Water Resource Research Institute, University of Wyoming, Laramie, vols V-A and V-B (p1.)

Bartos TT, Hallberg L, Clark M (2010) Chapter 6, Groundwater quality. In: Copeland D, Ewald E (eds) Available groundwater determination technical memorandum, Green River Basin Water Plan II. Report to the Wyoming Water Development Commission by the Wyoming State Geological Survey et al., p. 6-1–6-94

Bartos TT, Hallberg L (2010) Chapter 5, Groundwater and hydrogeologic units. In: Copeland D, Ewald E (eds) Available groundwater determination technical memorandum, Green River Basin Water Plan II. Report to the Wyoming Water Development Commission by the Wyoming State Geological Survey et al., p. 5-1 – 5-94

Blondes, M.S. Gans, KD. Rowan, E.L. Thordsen, J.J. Reidy, M.E. Engle, M.A. Kharaka, Y.K. Thomas, B. (2016). U.S. Geological Survey national produced waters geochemical database. https://energy.usgs.gov/EnvironmentalAspects/EnvironmentalAspectsofEnergyProductionandUse/ProducedWaters.aspx#3822349-data. Accessed: 8/1/2017.

Collentine M, Libra R, Feathers KR, Hamden L (1981) Occurrence and characteristics of ground water in the Great Divide and Washakie Basins. Water Resources Institute, University of Wyoming, Laramie. Vols VI-A and VI-B (p1.)

Freethey GW, Cordy GE (1991) Geohydrology of Mesozoic rocks in the Upper Colorado River Basin, in Arizona, Colorado, New Mexico, Utah and Wyoming, excluding the San Juan Basin, Regional aquifer-system analysis – Upper Colorado River Basin. U.S. Geological Survey Professional Paper 1411-C

McLaughlin, J.F., Ganshin, Y., Quillinan, S., Bentley, R. and Jiao, Z., 2014. Mitigating Risks Associated with Long-term CCS: Characterizing the Geologic History and Heterogeneity of Sealing Strata. Energy Procedia, 63, pp.4999-5009.

Quillinan, S.A. and McLaughlin, J.F., 2013. Reservoir fluid characterization of the Weber Sandstone and Madison Limestone on the Rock Springs Uplift in southwest Wyoming. In *Geological CO2 storage characterization* (pp. 151-167). Springer, New York, NY.

Section 4.4: Geophysical Description

Yuri Ganshin
Senior Research Scientist, Center for Economic Geology Research
School of Energy Resources, University of Wyoming
1020 E. Lewis Street, Energy Innovation Center
Laramie, WY 82071

We estimated the permeability in a 444-ft-thick sandstone unit within the Nugget Sandstone on the Rock Springs Uplift with the objective of increasing the accuracy of our CO_2 flow simulation program. We used core data collected in wells of the Brady Field (15 to 20 miles south from the RSU #1 well) to identify the porosity-permeability relationship for the Nugget stratigraphic interval. On the basis of this relationship and well log data, we constructed a continuous vertical permeability profile. The resulting statistical estimators of the permeability distribution led us to classify the Nugget Sandstone as good quality reservoir with a moderate to high degree of heterogeneity.

One of the most important steps in characterizing a geologic CO_2 storage site is the construction of 3-D volumes of seismic attributes. Interval velocity, anisotropy, coherency, and curvature attribute volumes were estimated for a 25-square-mile 3-D seismic dataset, creating a realistic 3-D model of storage reservoirs and seals. We correlated the key rock/fluid parameters from 1-D core, log, and VSP observations with seismic vertical profiles and horizon slices obtained for the most promising storage complexes in the Rock Springs Uplift. A specially designed automated velocity analysis technique was used to generate a high-density interval velocity volume. Seismically derived velocities were used to model spatial porosity distribution along the Madison and the Nugget reservoir units away from the RSU #1 well. Based on the derived porosity-permeability relationship for the Nugget sands, we modeled permeability distribution along the Nugget stratigraphic interval. We expect these porosity/permeability distribution maps, accompanied with structural framework, to be extremely useful for reservoir characterization and fluid flow modeling.

Predicting Permeability in the Nugget Sandstone Reservoir on the Rock Springs Uplift, Southwest Wyoming

Porosity-Permeability Relation

The most obvious control on permeability is porosity. However, permeability also depends upon the interconnectivity of the pores, and that in turn depends on the size and shape of grains, the grain size distribution, and such other factors as wetting properties of the rock and diagenetic history. For the Nugget Sandstone reservoir, some generalizations can be made:

- The smaller the grains, the smaller the pores and pore throats, and the lower the permeability; and
- Secondary porosity is negligible; thus, the bulk permeability is controlled solely by matrix (primary) porosity.

Under these assumptions and based on empirical knowledge (e.g., Archie 1950, Nelson 1994, Nelson 2004), permeability can be estimated from the relationship

$$\log(k) = a\varphi + b. \qquad (4.1)$$

Almost invariably for a consolidated sandstone, a plot of permeability (k) on a logarithmic scale against porosity (φ) results in a clear trend with a degree of scatter associated with the other influences determining the permeability. **Figure 4.4.1** shows a $\log(k)$-vs.-φ plot for the core samples from the

Nugget Sandstone (wells with API numbers 3720385, 3720422, and 3722344). There is a strong linear correlation (R^2=0.81) between log(k) and φ with a relatively steep trend that is characteristic of "tight gas sands" (Nelson 1994). Clearly, permeability can be predicted from porosity in such an environment.

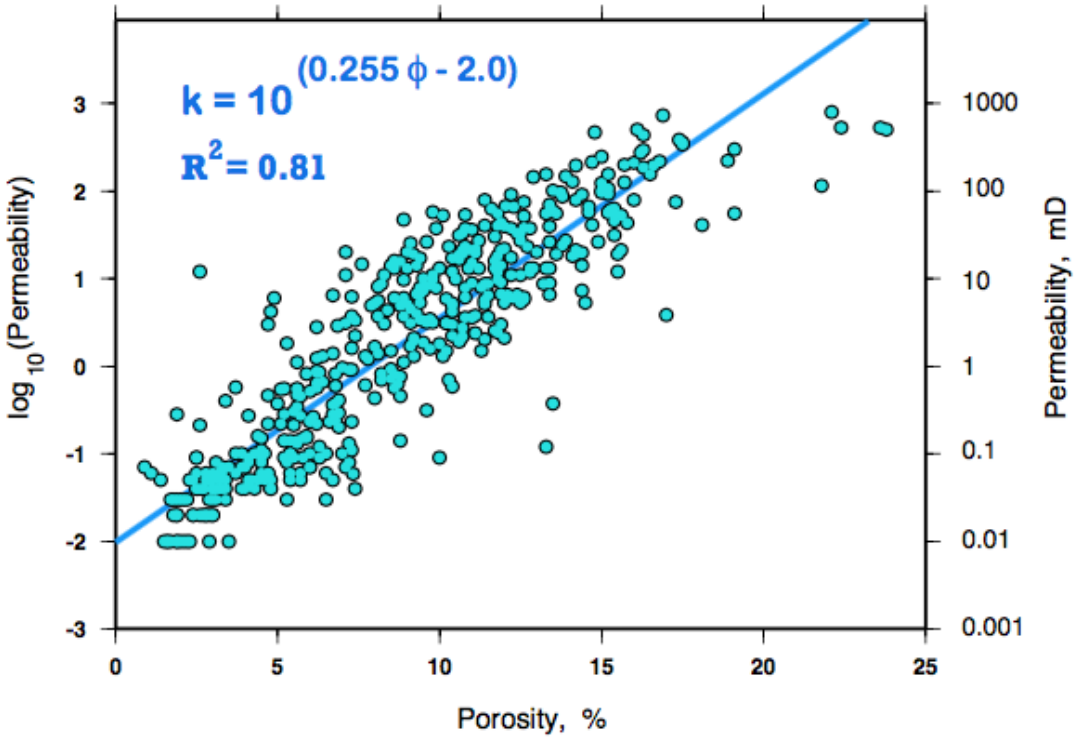

Figure 4.4.1. Semilog plot of permeability vs. porosity measurements for the core samples from the Nugget Formation, Rock Springs Uplift, Wyoming. API numbers of the sampled wells are 3720385, 3720422, and 3722344. The line of best fit, its equation, and coefficient of determination are shown in blue color.

With insertion of the regression coefficients into **Eq. 4.1**, the corresponding power-law equation for the Nugget Sandstone permeability will be:

$$k=10^{(0.255\varphi - 2.0)}. \qquad (4.2)$$

Porosity Estimation

We used **Equation 4.2** to calculate a continuous permeability profile for the Nugget Sandstone unit penetrated by the RSU #1 well, while the density log was used to calculate porosity. Density porosities were derived assuming a mono-component mineral composition (sandstone with matrix density r_{ma}= 2.65 g/cc) for the whole Nugget depth interval (9,216 – 9,660 feet). We also assumed the pore fluid density r_f= 1 g/cc, and then the final formula for porosity estimation is:

$$= 100*(r_{ma}- r_b)/r_{ma} \qquad (4.3)$$

Where r_b is bulk density as measured by the logging tool, and f is measured in percent.

The calculated porosity profile for the Nugget Sandstone and overlying strata is shown in **Fig. 4.4.2** (blue-colored track #6). It overlays the neutron porosity log that matches well the calculated density porosity values within the sandstone intervals (both the Entrada and Nugget Sandstones in **Fig. 4.4.2**). This match indicates that the neutron porosity tool was set-up to give the true porosity in water filled sandstone. A strong correlation between the measured neutron porosity and calculated density porosity curves for the Nugget stratigraphic interval indicates correctness of our assumption made about its mono-component mineral composition. To add more confidence to this statement, we performed facies classification based on log cluster analysis.

Petrofacies Analysis

It is critical for cluster analysis that log-derived facies represent only rock composition and texture. Therefore, we first used cross-plotting technique to visualize the calibration of wireline measurements with petrofacies, and thus to identify input logs for cluster analysis. Gamma ray intensity, photoelectric factor, and potassium-thorium content were particularly good at discriminating sandstone from siltstone and shale facies (**Fig. 4.4.3**). Overall, if a well log did not relate closely with petrofacies classes, as assessed in the cross-plots, then it was not selected for input. Additionally, we found that using too big number of input logs may generate confusing results, and trial and error approach, switching out curves, helped determine how each input affected the clustering outcome. The final selection of input logs was density, compressional velocity, photoelectric factor, gamma ray, potassium-thorium content, neutron porosity, and Vp-to-Vs ratio.

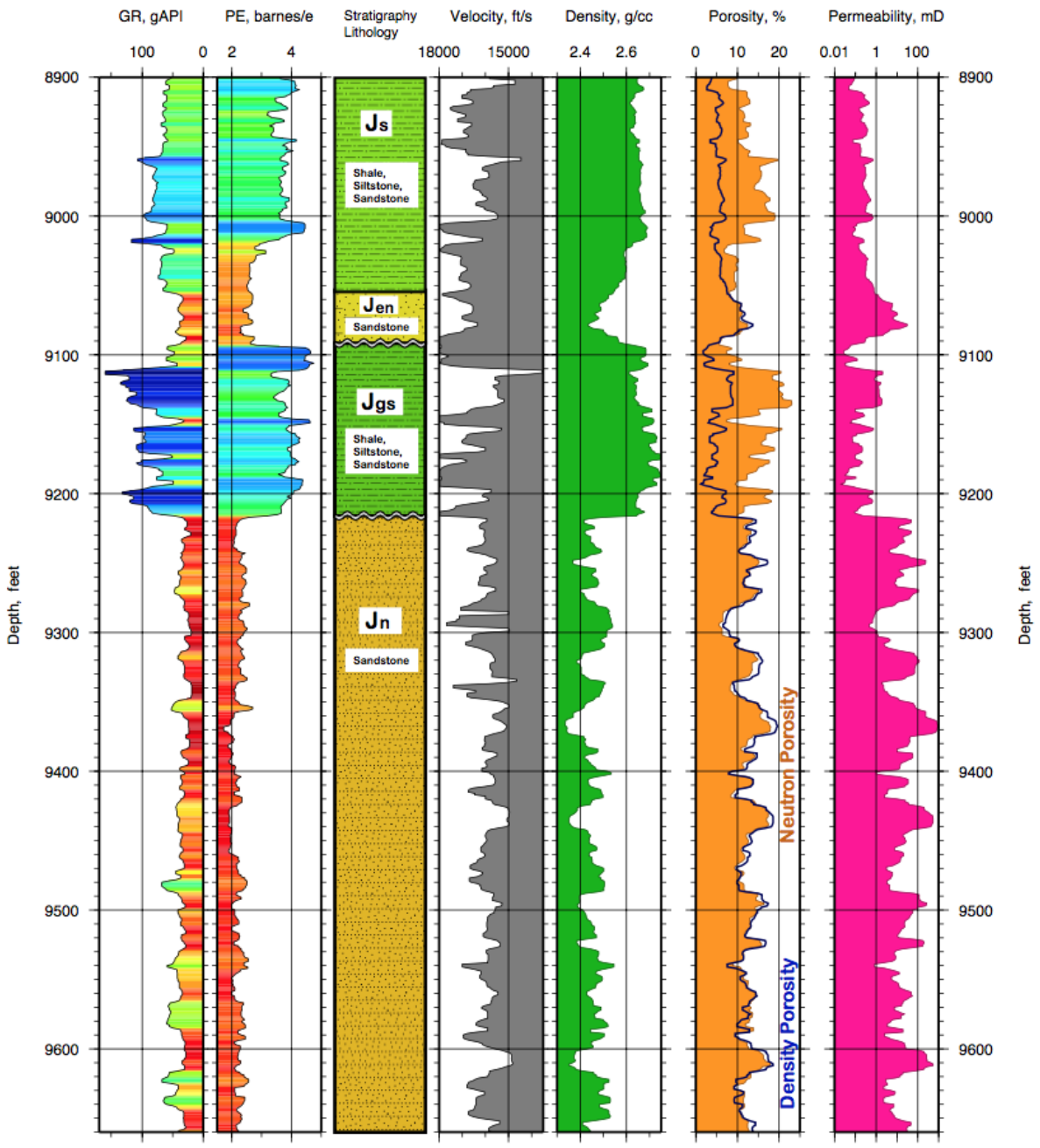

Figure 4.4.2. Interpreted wireline logs in the Nugget Sandstone and overlying strata in the RSU #1 well. Tracks from left to right are (1) gamma-ray, (2) photo electric section, (3) geological interpretation, (4) sonic velocity, (5) density, (6) neutron (orange) and density (blue) porosity, (7) modelled permeability. Note that density porosity estimates and permeability modeling were performed for rocks with sandstone matrix.

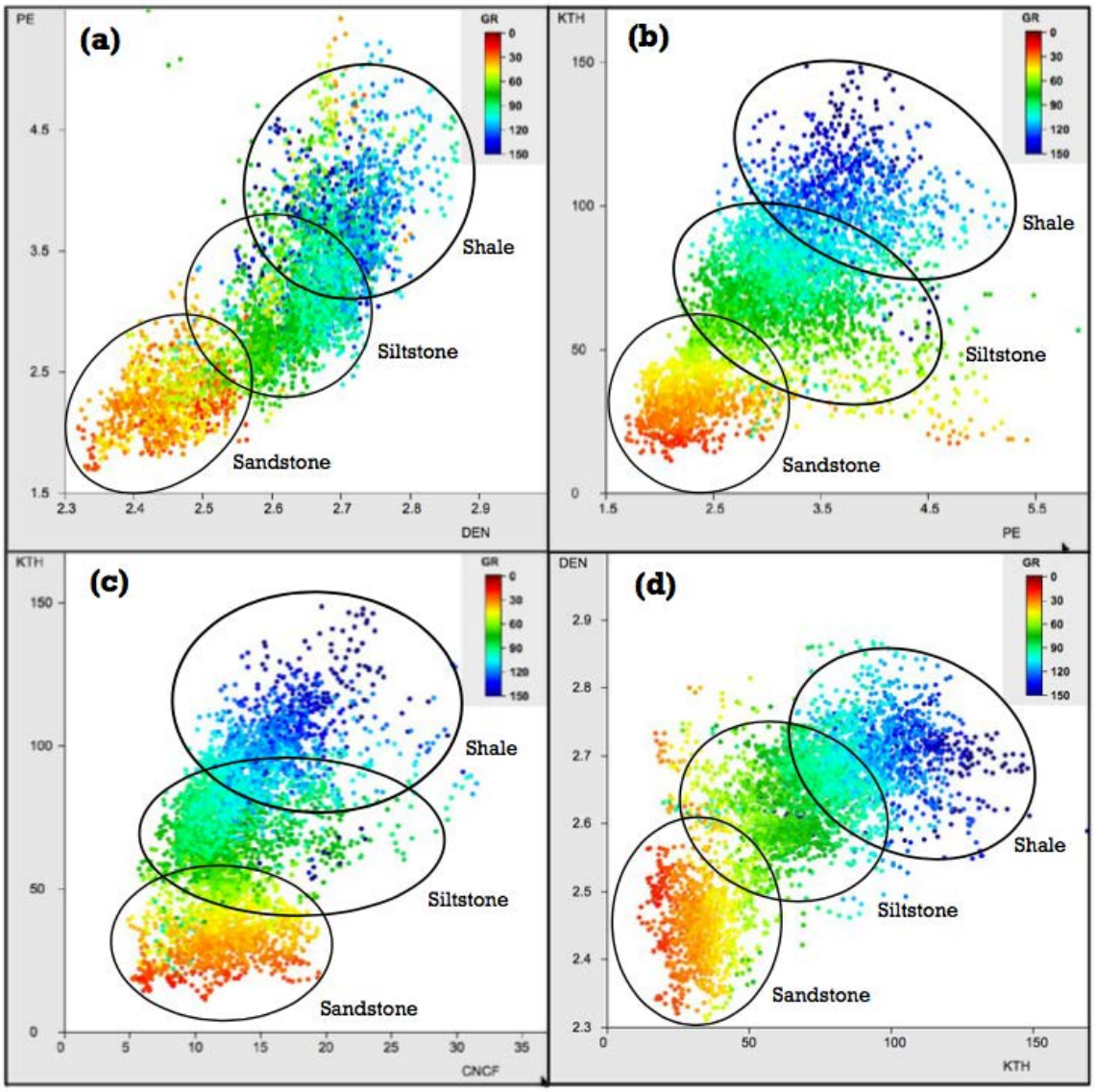

Figure 4.4.3. Petrofacies interpreted from cross-plots. (a) Photo Electric factor (PE) versus Density (DEN); (b) Potassium-Thorium content (KTH) versus Photo Electric factor; (c) Potassium-Thorium content versus Neutron Porosity (CNCF); (d) Density versus Potassium-Thorium content. The cross-plots are color coded by Gamma Ray intensity (GR). The measurements are from the RSU #1 well (8.531 - 10,890 feet depth interval), Rock Springs Uplift, Wyoming.

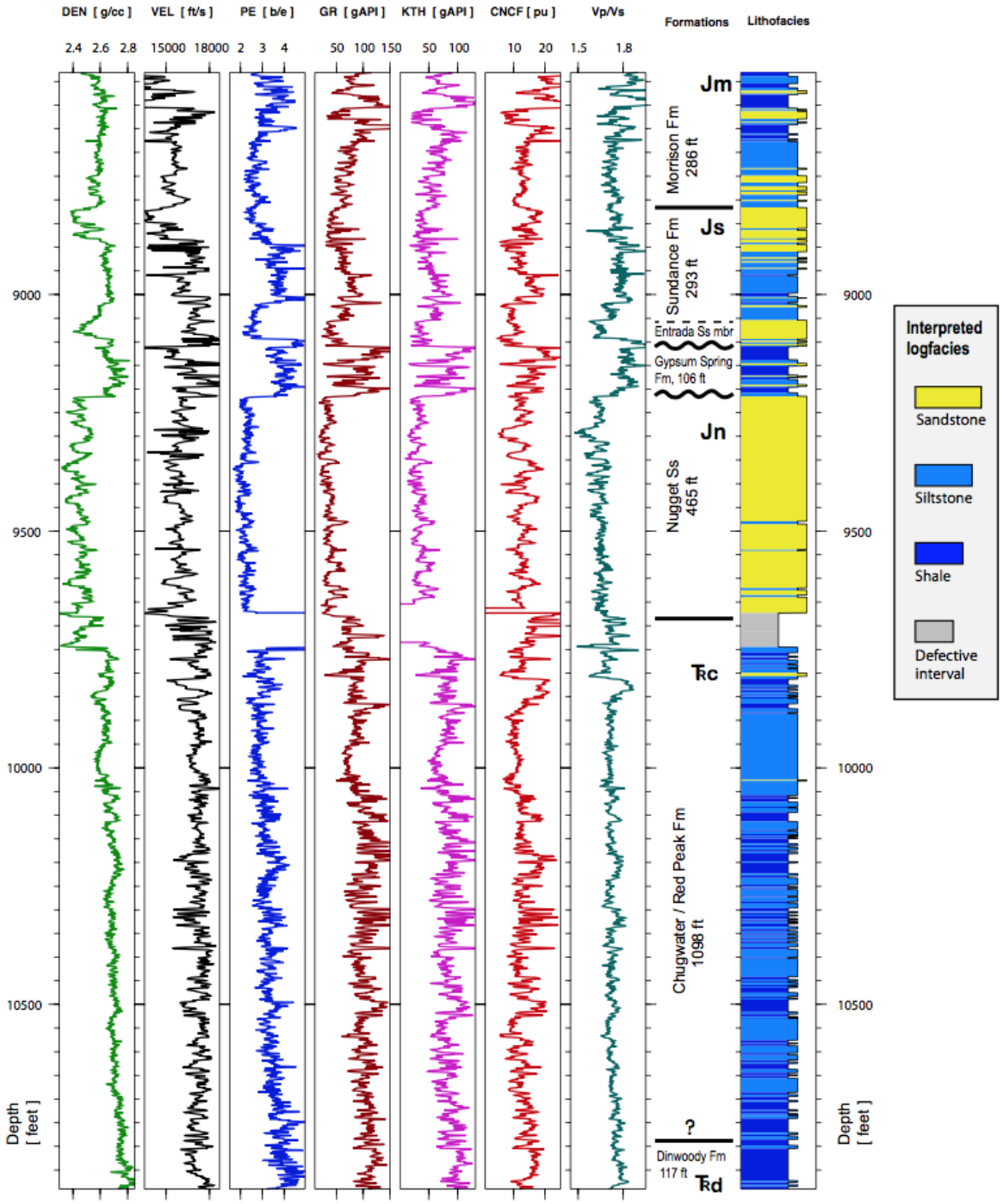

Figure 4.4.4. Interpreted wireline logs from the RSU #1 well (Rock Springs Uplift, Wyoming) and color coded logfacies profile (the rightmost panel) obtained from the logs cluster analysis.
Missed or defective data observed on some curves is due to the bit size change (from 8.75 to 6.125 in) at 9,672 ft depth.

Well logs were classified into logfacies using cluster analysis built on a very popular k-means algorithm (MacQueen, 1967), which attempts to minimize the average of the squared distances between the observations and their cluster centers or centroids. In our study, we defined logfacies using an interactive clustering routine 'CLUSTERS' that was developed at CMI and is available for free download from http://www.uwyo.edu/cmi/dgl-software/. The software utilizes the k-means method and is adapted to input multi-curve data stored as plain text files. Cluster analysis resulted in three logfacies: sandstone, siltstone, and shale. Clustering results were colored and scaled by logfacies and displayed next to the log data in style of a lithology column (**Fig. 4.4.4**). The lithofacies profile clearly reveals the lithological uniformity of the Nugget Sandstone unit drilled by the RSU #1 well.

Porosity-Velocity Relation

As seen in **Fig. 4.4.2**, strong correlation exists between the density and velocity logs within the Nugget Sandstone unit. Since density and porosity are linearly related through **Eq. 4.3**, we can expect similar type of linear dependence of log-derived velocity on porosity. To quantify this relationship, we generated a cross-plot of sonic velocity vs. density porosity and utilized regression method to obtain the best-fit linear trend (**Fig. 4.4.5**). Velocity of the Nugget Sandstone rocks tends to decrease linearly with porosity increase according to the equation:

$$\mathbf{V} = 18765 - 203f \qquad (4.4)$$

Where porosity f is measured in percent, and compressional velocity **V** - in ft/s, and the coefficient of determination R^2=0.63.

On the contrary, porosity of the Nugget sands can be estimated from velocity measurements using equation:

$$f = (18765 - \mathbf{V})/203 \qquad (4.5)$$

The last formula becomes especially handy when we attempt to model porosity distribution along the Nugget horizon from seismically derived compressional velocity values.

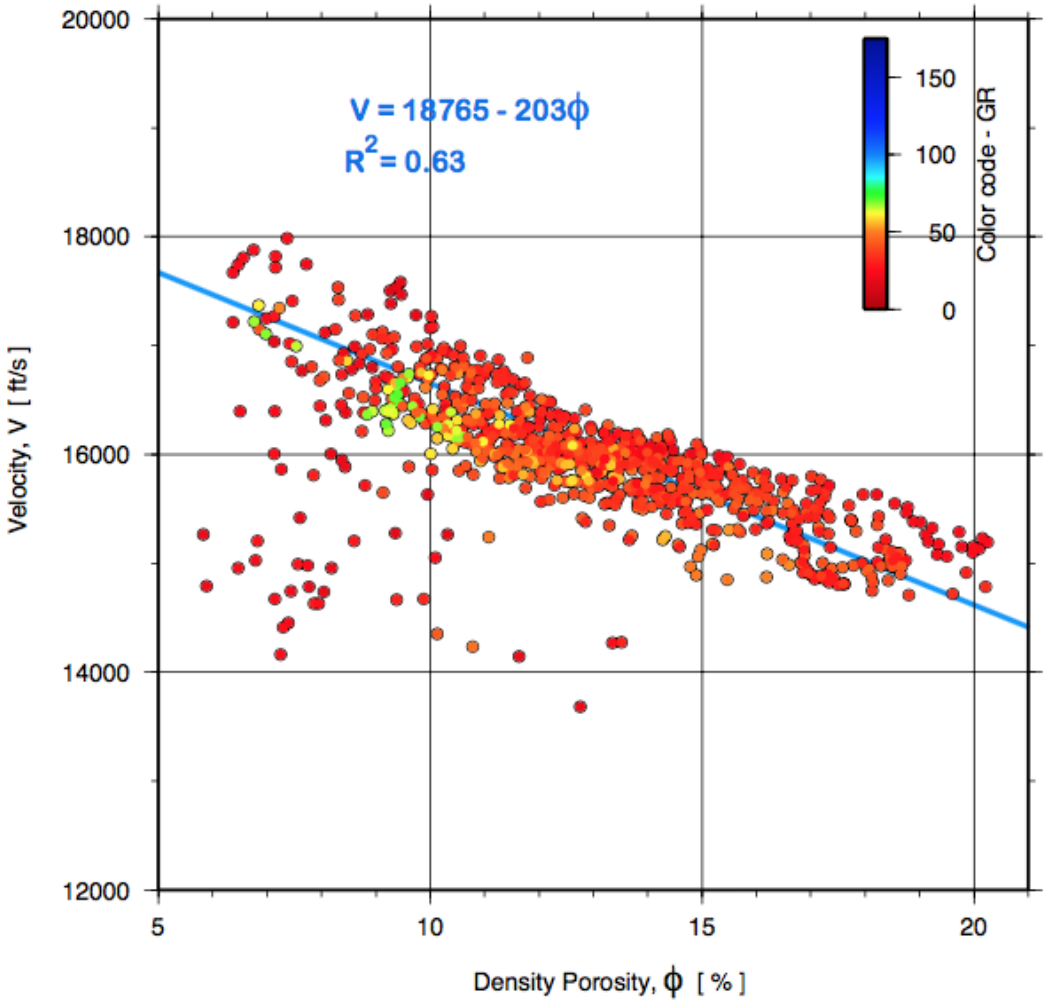

Figure 4.4.5. Sonic velocity vs. density porosity measurements for the Nugget Sandstone (9,216 - 9,660 ft depth interval), RSU #1 well, Rock Springs Uplift, Wyoming. The cross-plot is color coded by Gamma Ray intensity (GR). The line of best fit, its equation, and coefficient of determination are shown in blue color.

Log-derived Permeability Profile

The permeability profile shown in **Fig. 4.4.2** (the rightmost curve) is characterized by significant variability (about three orders of magnitude) even within the sandstones of the same formation. Most of permeability estimates for the Nugget sands lie between 1 and 1000 millidarcies. Although there are few intervals where permeability drops below 1.0 mD, the Nugget Sandstone in the study area can be classified as a conventional (not tight) formation.

Statistical Descriptors of Porosity and Permeability

Plots of petrophysical data vs. depth, e.g, those in **Fig. 4.4.2**, can be used to distinguish and separate geologic units. However, many modern flow simulation routines require a general quantitative reservoir descriptor obtained from data samples that are treated as random variables and are not attributed to a specific location. Both the probability and cumulative distribution functions (histograms) are common statistical tools that can be used to derive such a generalized descriptor of a formation.

Figure 4.4.6 shows histograms of the porosity distribution within the Nugget Sandstone, based on density log and sandstone matrix = 2.65 g/cc. To get the distribution and statistical averages we used 889 data samples from the 444-ft-thick interval, from 9,216 ft to 9,660 ft in depth. The porosity distribution (**Fig. 4.4.6** top panel) appear to be symmetrical in shape with very close values of different averaging estimators: the arithmetic mean = 12.85%, the geometric mean = 12.49%, the median = 12.74%, and the mode = 13%. We suggest using **12.5%** as the best porosity descriptor for the whole Nugget Sandstone unit penetrated by the RSU #1 well.

The corresponding permeability distribution, modeled with Eq. 5.2 is shown in **Figure 4.4.7**. Plotted on a logarithmic scale, the permeability is characterized by a multi-peak, slightly right-skewed distribution (**Fig. 4.4.7**). Unlike a symmetrical distribution, the skewed one has different averages produced by different estimators. In our case we have the following results: the arithmetic mean = 81.6 mD, the geometric mean = 18.9 mD, the median = 17.7 mD, and the mode = 25 mD. Mean is what most people commonly refer to as an average. However, for the Nugget Sandstone permeability, the arithmetic mean is 81.6 mD, which is much greater than the median value, 17.7 mD.

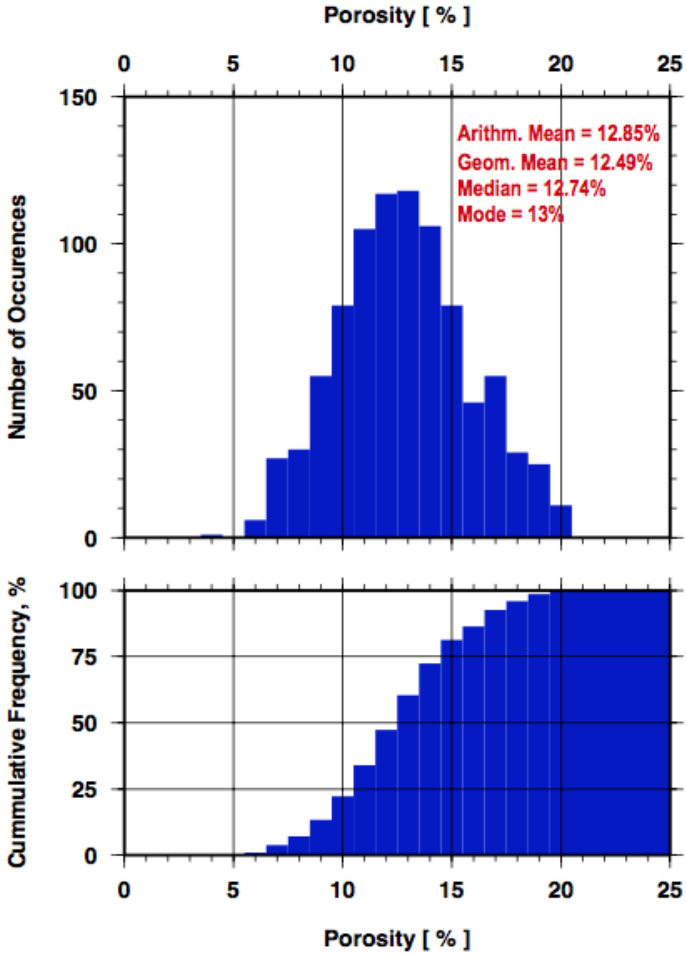

Figure 4.4.6. Porosity distribution within the Nugget Sandstone unit (9,216 - 9,660 ft depth interval; 889 data samples). Ordinary histogram (top); cumulative histogram (bottom).

Now, how well do these estimators represent the permeability population? According to Jensen et al. (2000), the geometric mean should produce a better estimate for a log-normal distribution. The Nugget Sandstone permeability distribution has close to a log-normal shape (only slightly asymmetric); therefore, we might use the geometric mean (18.9 mD) as a statistical permeability estimate for the whole stratigraphic unit. The median (17.7 mD) and mode (25 mD) values are very close to the geometric mean; hence, we conclude that ***20 mD*** (here, the rounded average of the geometric mean, the mode, and the median) would be the best permeability descriptor for the whole Nugget Sandstone section.

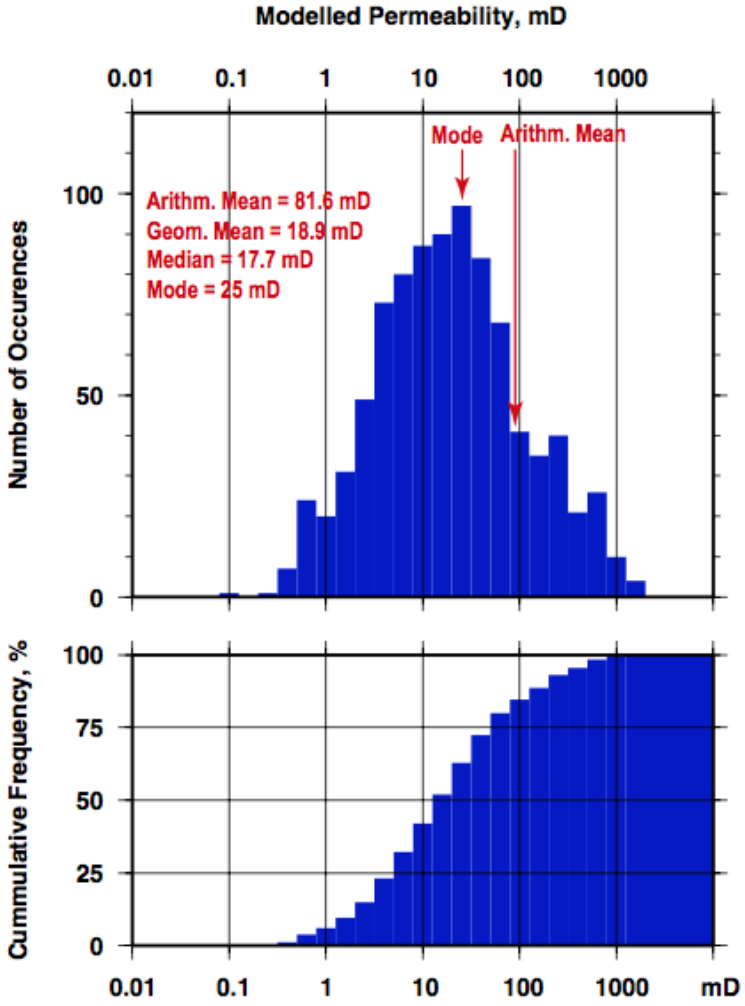

Figure 4.4.7. Permeability distribution within the Nugget Sandstone unit (9,216 - 9,660 ft depth interval; 889 data samples). Ordinary histogram (top); cumulative histogram (bottom).

The cumulative histogram can be used to determine the number of permeability values within a given range that have occurred (interval probabilities). As can be seen in **Fig. 4.4.7** (lower panel), 50% of the data (samples) have a permeability value ($k_{0.50}$) of about 17,7 mD or more; that is the median value. Only 5% of the data within the depth interval 9.216 ft to 9.660 ft have a permeability value lesser than 1.0 mD (**Fig. 4.4.7**).

The Dykstra-Parsons coefficient (V_{DP}) is commonly used in the petroleum industry as a measure of permeability variation or reservoir heterogeneity (Jensen et al. 2000). It is defined as

$$V_{DP} = k_{0.50} - k_{0.16} / k_{0.50} \quad (4.6)$$

where $k_{0.50}$ is the median permeability and $k_{0.16}$ is the permeability one standard deviation below the median on a log-probability plot. V_{DP} ranges between zero (0.0) for absolutely homogeneous reservoirs and one (1.0) for "infinitely" heterogeneous reservoirs. With a V_{DP} of 0.87 and average permeability of 20 mD, the Nugget Sandstone can be considered as good quality reservoir with a moderate to high degree of heterogeneity.

Lateral Permeability Distribution from Seismic data

A similar technique of permeability estimation (**Eq. 4.2**) can be applied to the lateral distribution of porosity values derived from surface seismic (**Ganshin and Surdam, 2013**). The result of permeability modeling for the Nugget Sandstone away from the RSU #1 well is shown in **Fig. 4.4.8**. Most of the area on the permeability map is blue and light blue, which correspond to permeability values below 10 mD (**Fig. 4.4.8**). Light colors (white to light yellow) correspond to permeability values in the range 10 to 100 mD. The RSU #1 well location appears to be within the light-colored area (10-100 mD) that matches the log-derived permeability estimates. Interestingly, there is a large area north of the test well location with the modeled permeability values in excess of 1000 mD. Another area with improved reservoir properties can be found about 1 mile south from the RSU #1 well (**Fig. 4.4.8**). It should be noted that permeability distribution along the Nugget stratigraphic horizon was derived from seismic interval velocity, which is inherently highly uncertain and possess resolution comparable with seismic wavelength (about 600 feet at the Nugget depth). Furthermore, we assumed porosity to be the only factor affecting interval velocity, while neglecting pore fluid variations within the Nugget reservoir. Also, we should note that the uncertainty in permeability model (**Fig. 4.4.8**) increases away from the RSU #1 well toward the periphery of the seismic study area. This is due to decreasing seismic fold coverage towards the edges of seismic survey, and the absence of control wells in that area.

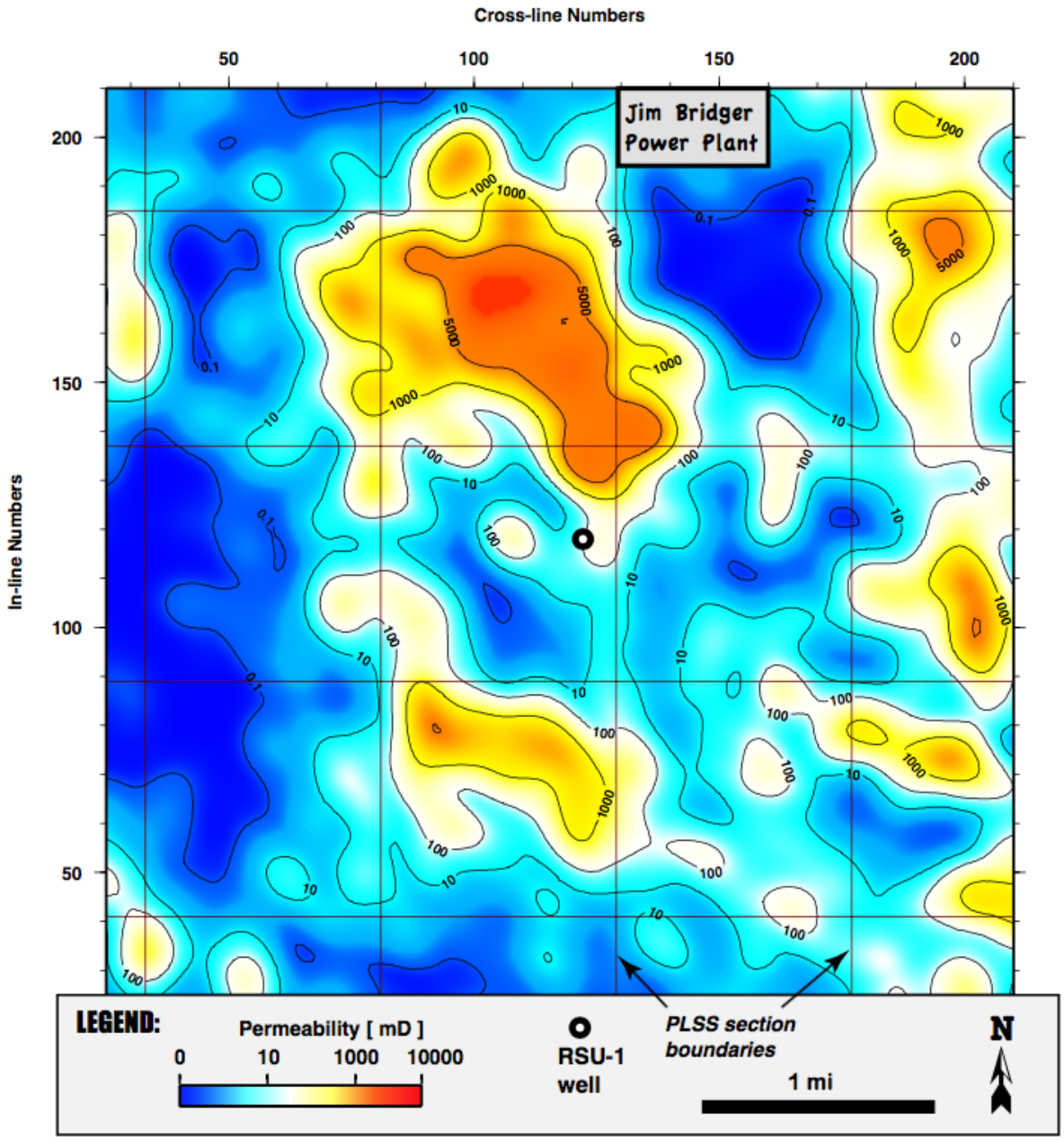

Figure 4.4.8. Permeability map of the Nugget Sandstone derived from seismic interval velocity assuming laterally invariant velocity-porosity and porosity-permeability relationships derived from RSU #1 well logs and cores. Note that porosity was assumed to be the only factor affecting seismic interval velocity variations.

Seismic Evaluation of the Carbon Sequestration Potential of the Deep Saline Reservoirs in the Rock Springs Uplift, Wyoming

Seismic Horizons

This study has emphasis on the following reservoir/seal systems that were considered by to be the most promising storage complexes in the Rock Springs Uplift (RSU):

- Madison Limestone (reservoir) and Amsden Formation (seal);
- Nugget Sandstone (reservoir) and Gypsum Springs Formation (seal); and
- Entrada Sandstone (reservoir) and Morrison Formation (seal).

We used seismic horizons within the Jim Bridger 3-D survey that correspond to the target formation tops based on the RSU #1 well Vertical Seismic Profile (VSP) and log data. Joint analysis of well logs, VSP, and surface seismic identified seismic horizons corresponding to the Morrison, Sundance, Nugget, Amsden, and Madison formations. The above-mentioned five reference horizons were tracked automatically within the 5 x 5 x 3-mile seismic amplitude volume at every grid sample, and the auto-tracking results were quality checked and edited manually at a coarser grid (10 x 10 samples). The Entrada Sandstone (~100 feet thick) and Gypsum Springs Formation (~200 feet thick) are too thin to be adequately imaged in reflected wavefield because of the band-limited nature of seismic method. Using the VSP data provided, each horizon was associated with a specific depth and the time difference between the horizons noted at the well. Using this fixed time difference between each reference horizon and its associated target depth/time, the artificial 'phantom' horizons were created corresponding to the Entrada and Gypsum Springs stratigraphic units.

Seismic Attributes

Roughly thirty seismic attributes were probed to establish their relevance to structural variations along the reference seismic horizons in the RSU Uplift (Ganshin and Surdam, 2013). The attributes were based on different input data (pre- and post-stack seismic amplitude), computational algorithms (instantaneous, windowed, etc.), and the nature of investigation (morphological vs. physical). Six out of thirty attributes were chosen for the continuity analysis of the reservoir rocks and confining strata (pre- and post-stack coherency, minimum curvature, dip azimuth and dip magnitude, and curvedness attribute (a combination of minimum and maximum curvatures)). Numerous horizon maps were prepared using the above-mentioned six attributes to investigate their variations along the reference and phantom horizons. The major fault/fracture zones were interpreted along the target horizons and correlated with the results of seismic velocity analysis (interval velocity and anisotropy parameters).

Seismic Velocity Analysis Technique

The methodology proposed in this study assumes anisotropic earth model (either VTI or isotropic-layered medium) and non-hyperbolic behavior of reflection curves. The algorithm seeks to create instantaneous velocity and anisotropic parameter from semblance estimates. Our objectives are twofold, (1) to estimate porosity by inverting effective velocity into the interval one, and (2) to obtain sandstone vs. shale distribution from anisotropic parameter.

Time imaging of reflection seismic data is drastically improved when dense velocity (***V***) fields are used. However, this is not enough to focus the large offsets, to migrate the steep dips, and finally, to take into account the anisotropy of the sediments. The estimation of an extra dense parameter field is required: the effective anisotropy parameter $\boldsymbol{\eta}$. In this study we used an original automatic dense bi-spectral scanning algorithm that is based on anelliptic approximations of the moveout equation in VTI media (Fomel,

2004). The algorithm allows maximizing the usage of information contained in far source-receiver offsets. The presented bi-spectral scan through the two moveout parameters provides ***V****nmo* and ***η*** fields as dense as the seismic. The lateral, pre-stack semblance coherency is another by-product of the algorithm. To convert ***V****nmo* to ***interval velocity V****int*, we propose a Dix-type inversion based on a simple linear regression. This scheme allows to control temporal resolution of the resultant ***V****int* volume by specifying minimum regression coefficient allowed for linear velocity models within a time interval. The proposed methodology leads to a stable and geologically plausible earth model, built upon the three attributes, ***V****int,* anisotropy, and coherency. The anisotropy parameter ***η*** can be used to discriminate between shales and sands in the subsurface. Interval velocity variations within horizon slices are important indicators of porosity and/or pore fluid changes. Areas of low coherency usually correlate with mechanically weakened zones like faults and fractures. Obtaining such information from surface seismic P-wave data has important implications for unconventional resources exploration, where natural gas (oil) cannot flow naturally, which makes drilling a risky business. The discussed velocity analysis technique does not require expensive or unusual acquisition procedures, the only requirement is presence of offsets exceeding the depth to the target. Compared with manual velocity picking, the automated approach is much faster and cheaper, especially in case of non-hyperbolic moveout. Importantly, the automated velocity analysis scheme provides additional information gained from 3D seismic survey that is extremely useful for reservoir characterization and development, and fluid flow modeling.

Vertical Sections through the volumes of seismic attributes

We used geophysical logs from the RSU #1 well (**Figures 4.4.9-a and 4.4.9-b**) to gain insight into velocity variations along the interpreted seismic horizons (**Fig. 4.4.10)**. The gamma ray, sonic, density, and neutron porosity log characteristics were used in the correlation analysis. Density porosities were derived assuming a multi-component mineral mixture with variable matrix densities that were interpreted from the neutron/density crossplot. The resultant velocity-porosity relationships were estimated from regression methods that fit linear trends for the pre-Cretaceous depth interval. On the basis of these petrophysical relationships, and considering negligible lithological variation along the interpreted seismic horizons, we predicted the velocity-porosity relationship for the three major lithologies (shale, sandstone, and dolostone) shown in Figure 4.4.11.

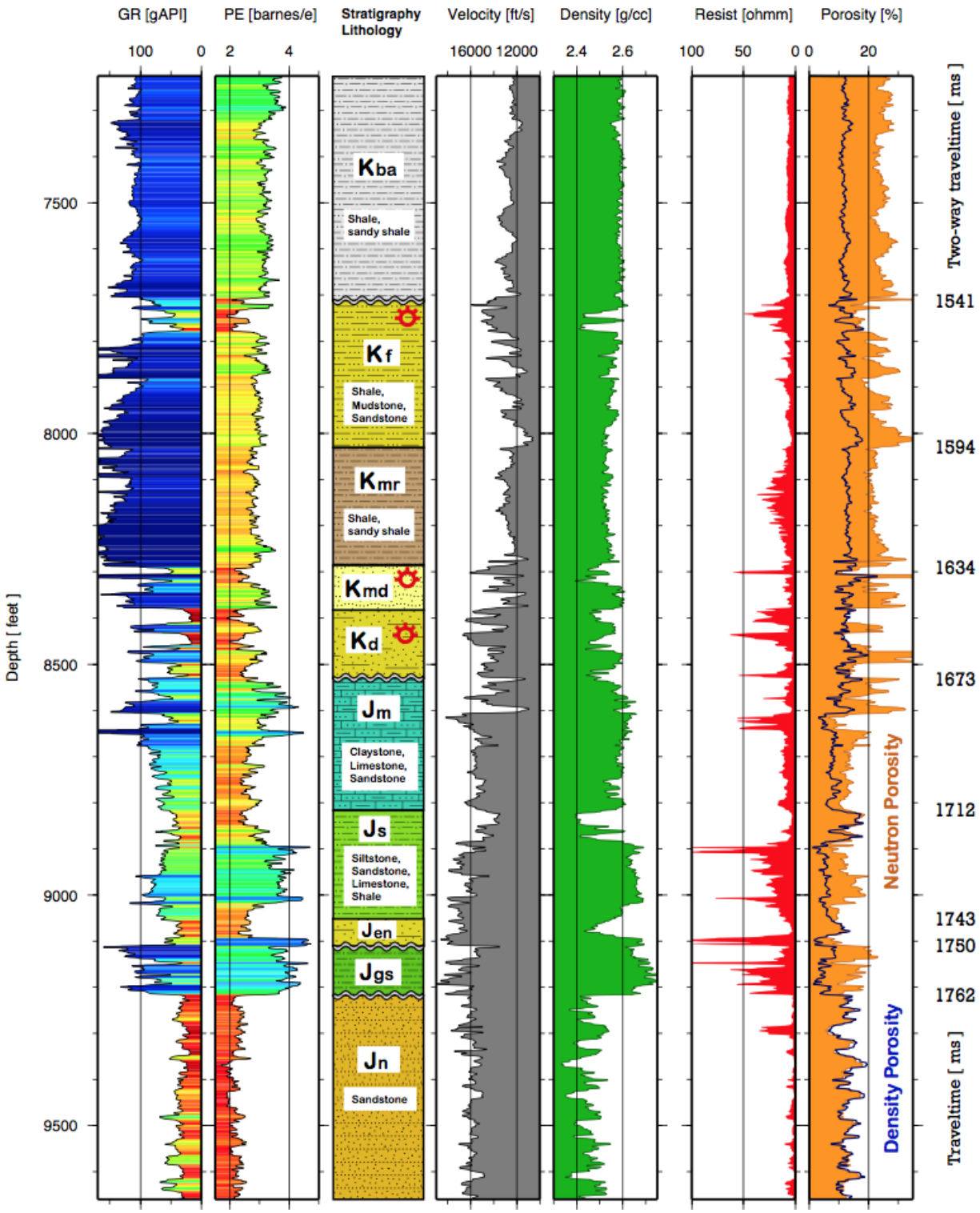

Figure 4.4.9a. Interpreted open-hole wireline logs from the RSU-1 well. Well lithology and stratigraphy was interpreted based on formation records and wireline logs characteristics.

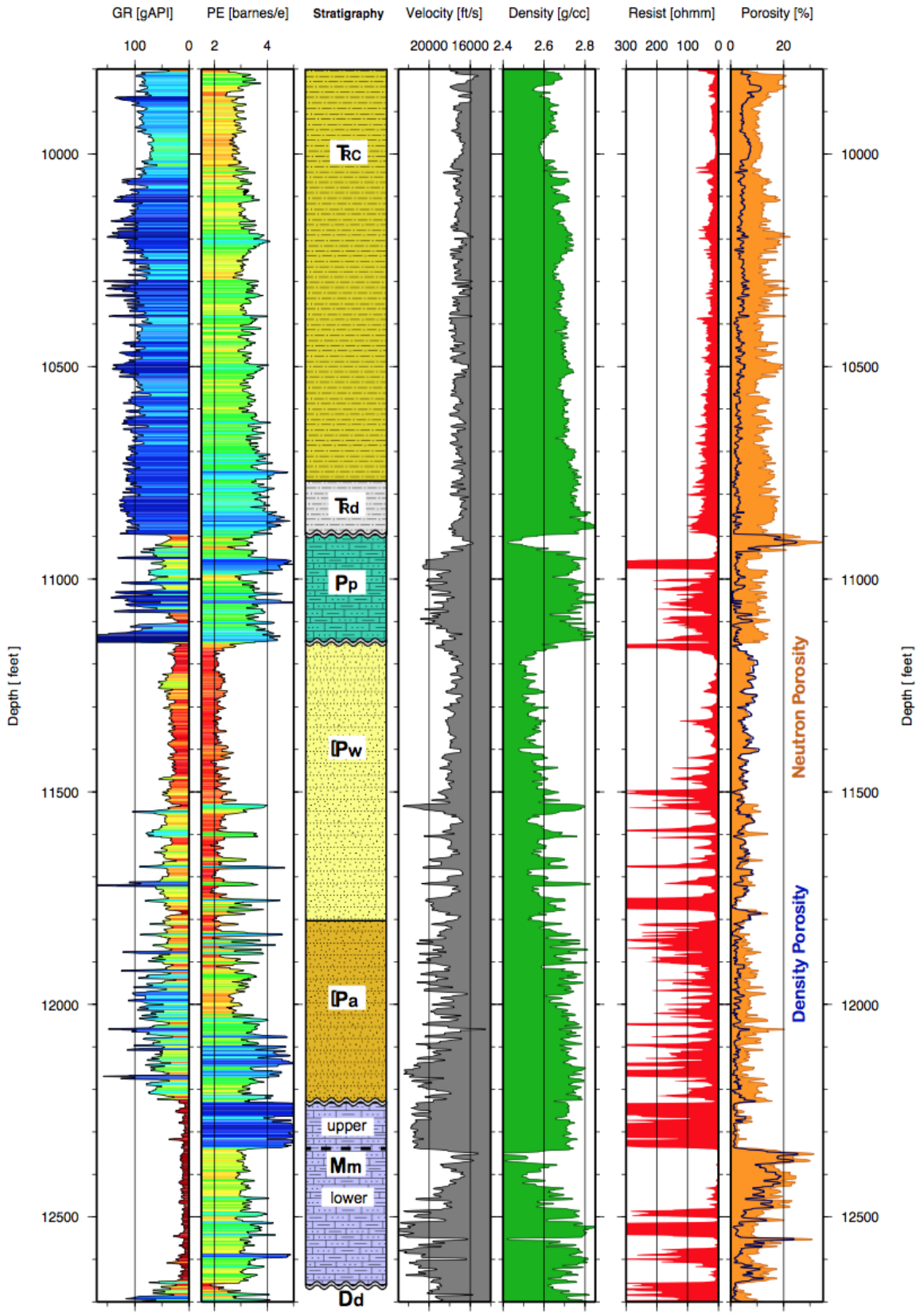

Figure 4.4.9b. Interpreted open-hole wireline logs (9800 - 12700 ft) from the RSU-1 well.

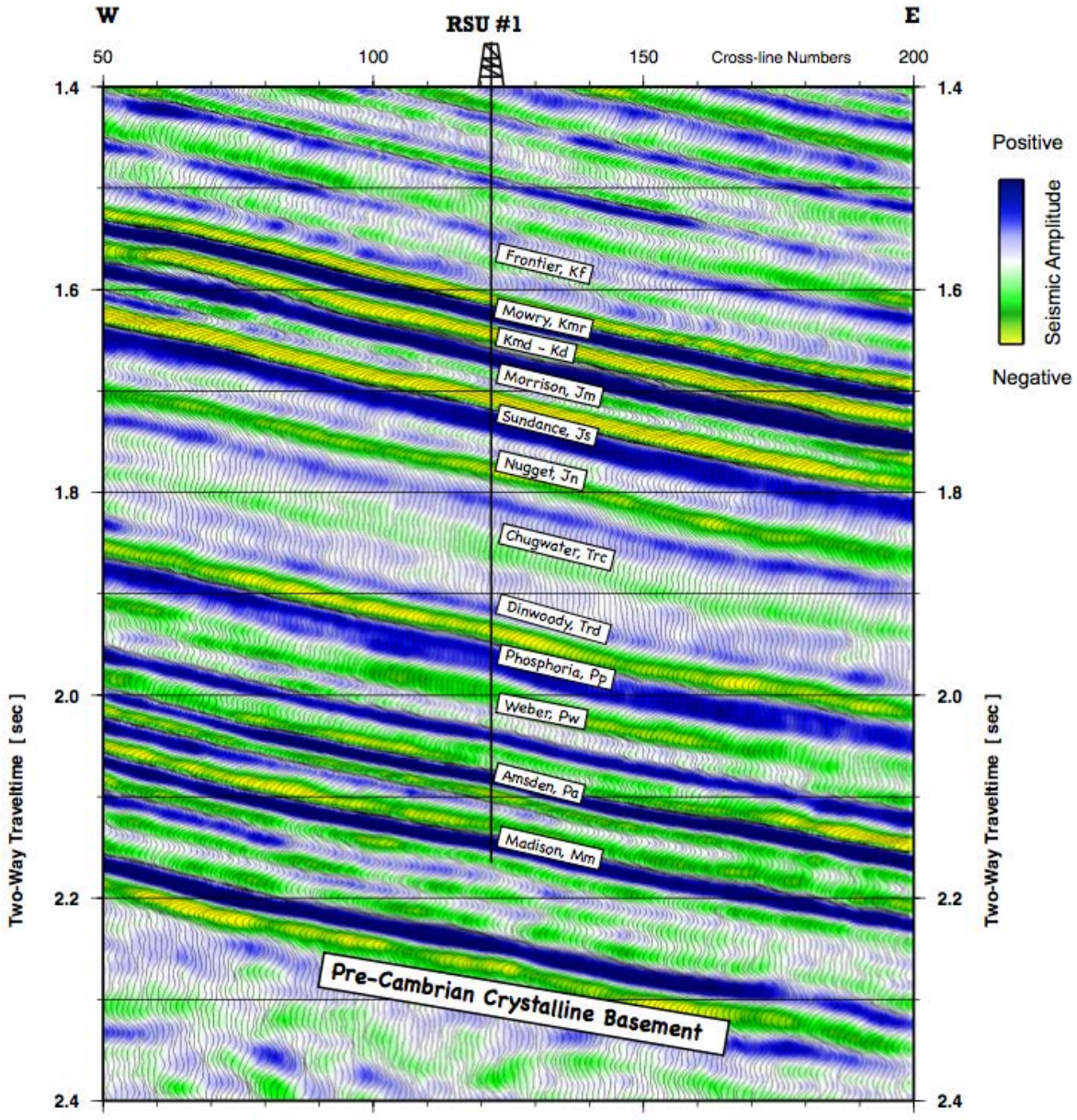

Figure 4.4.10. Interpreted west-east vertical section through the migrated seismic volume at the RSU #1 well location. Negative reflectivity wiggles - green and yellow, positive - blue color.

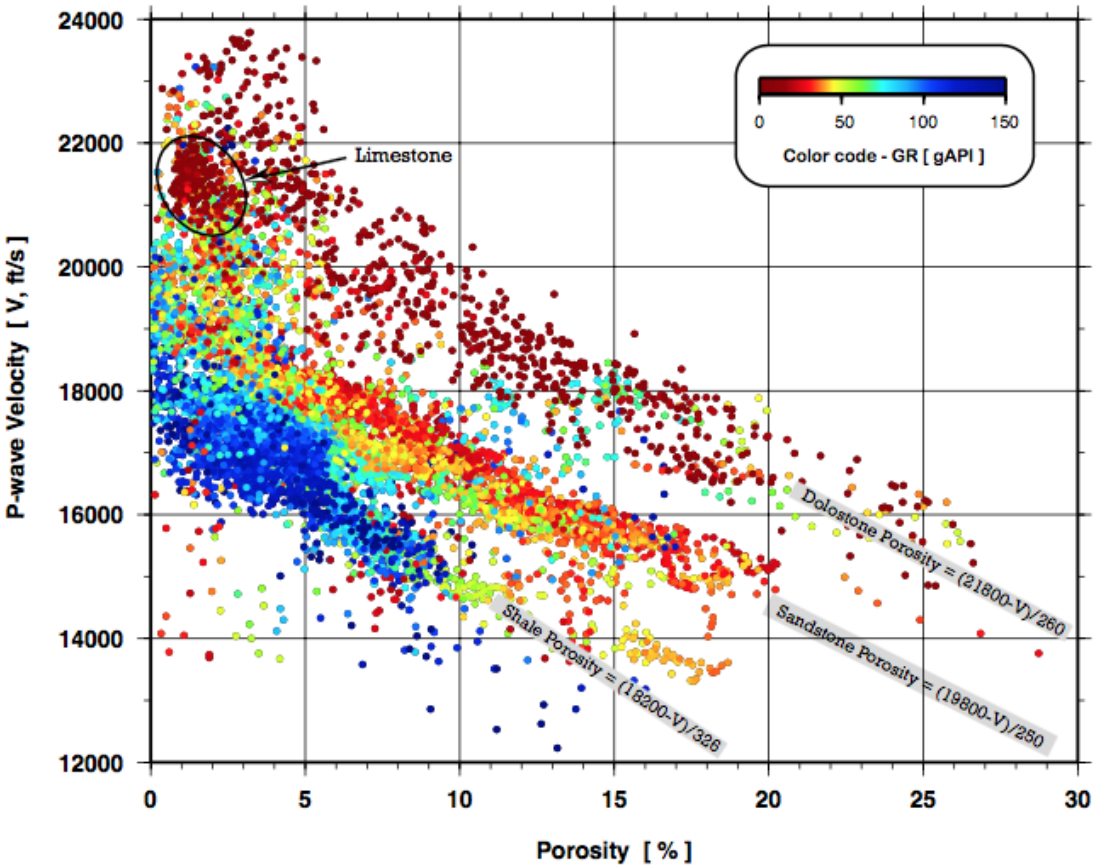

Figure 4.4.11. Sonic P-wave velocity versus density porosity crossplot color coded with the gamma ray log data, RSU-1 well. The measured depth interval is from 8,600 to 12,700 feet (pre-Cretaceous strata). Interpreted lithologies and the corresponding linear regression models are shown within the grey bars.

Automated velocity analysis using hyperbolic travel-time approximation was performed on the 3D seismic data acquired at the Rock Springs Uplift (RSU) in 2010 (Ganshin and Surdam, 2013). Seismic at RSU as well as in the Green River Basin in general is expected to behave in an **anisotropic** manner since the Mesozoic-age rocks are mostly represented by shales that are interlayered with thin beds composed of sandstone and siltstone. To extract additional information and value from the RSU seismic survey, automated nonhyperbolic velocity analysis routine was recently designed and tested. The DGL freeware (http://www.uwyo.edu/cmi/dgl-software/) enables a simultaneous estimate of parameters affecting reflection traveltime, ***V***nmo and anisotropy $\boldsymbol{\eta}$. As a result, dense volumes of interval velocity, semblance, and anisotropy attributes were calculated considering the case of VTI (Vertical Transverse Isotropy) model.

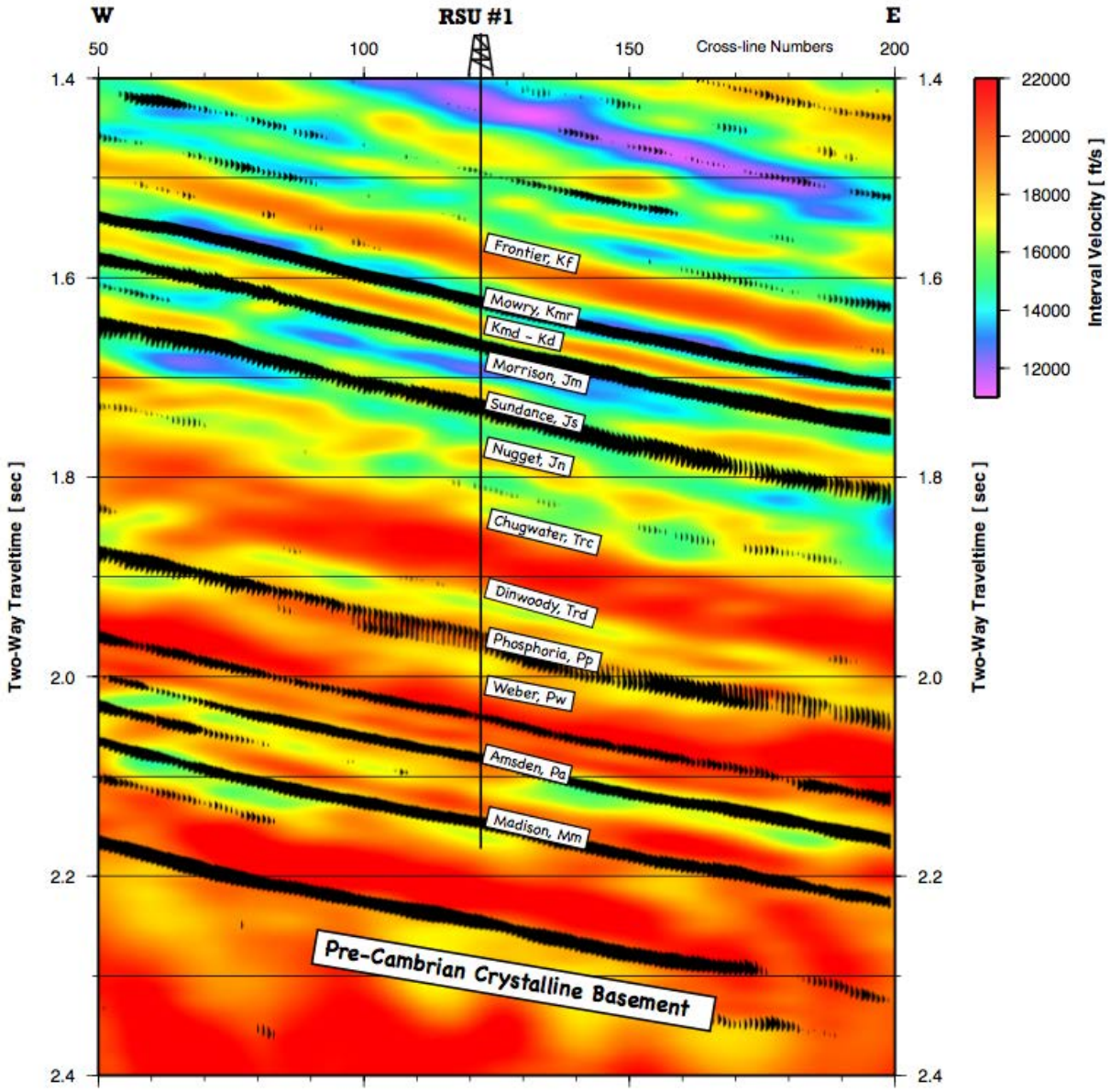

Figure 4.4.12. Interpreted west-east vertical section through the interval velocity volume at the RSU #1 well location. Positive reflectivity wiggles (black color) overlay the velocity image.

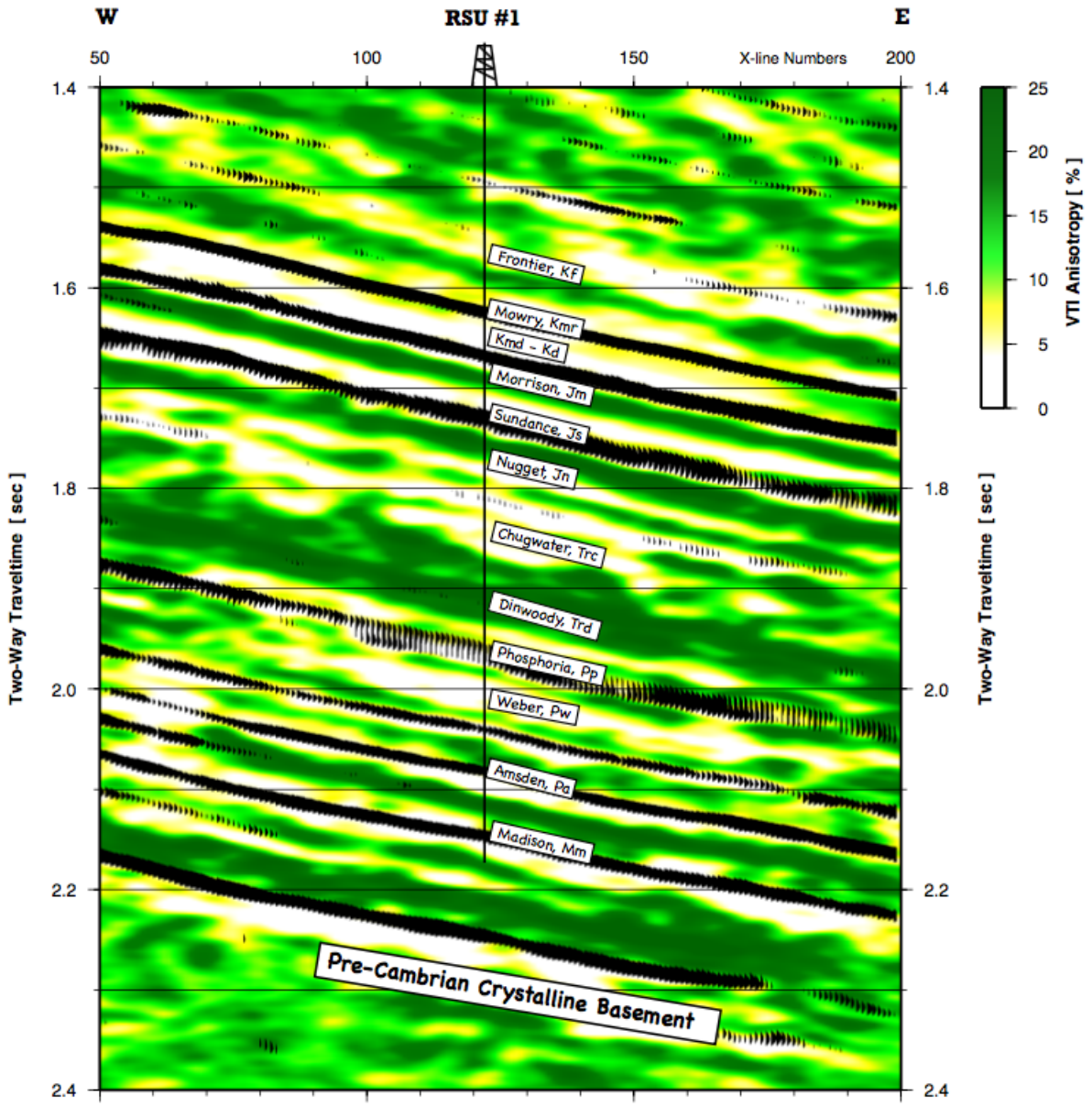

Figure 4.4.13. Interpreted west-east vertical section through the anisotropy parameter volume at the RSU #1 well location. Positive reflectivity wiggles (black color) overlay anisotropy image.

Figures 4.4.12, and **4.4.13** show west-east vertical sections through the interval velocity and anisotropy parameter volumes correspondingly. Note an abrupt increase in velocity at the top of Triassic Chugwater strata that corresponds to transition from siliciclastic to carbonate strata (**Fig. 4.4.12**). Also note that high-velocity sandstone reservoir rocks of the Cretaceous and Jurassic strata are imaged with red and yellow colors (e.g. the Frontier, Muddy-Dakota and Nugget), while shales are colored in green and blue (**Fig. 4.4.12**). The Weber Sandstone and the upper Madison unit are imaged with intense red color, corresponding to their high-velocity nature.

The anisotropy parameter η allows to discriminate shales from the massive rock formations such as sandstones and dolostones (imaged with yellow and white colors in **Figure 4.4.13**). Anisotropic shales

with high degree of sealing integrity can be distinguished by their intense green color in **Figure 4.4.13.** Particularly noticeable sealing interfaces are observed on top of the Madison Limestone, within the Triassic Chugwater and Dinwoody Formations, on top of the Nugget Sandstone (probably shales of the Gypsum Springs Formation), and within the Morrison Formation (**Fig. 4.4.13**).

Horizon slices related to the Madison storage complex

Unlike velocity-time profiles, such as that shown in **Fig. 4.4.12**, velocity distribution maps are associated with a specific seismic horizon (reflection) that commonly correlates with subsurface formation having constant lithology. Hence, variations in lithology are manifested mostly by *vertical* variations in velocity, while *lateral* velocity variations can be attributed to variable porosity, fracturing, and fluid content.

The upper Madison unit is represented by low-porosity and low-permeability limestone that is also characterized by increased velocity compared to the underlying dolostone unit (**Fig. 4.4.14**). Seismically derived interval velocities demonstrate this difference by comparing the two horizon slices, picked along the Madison stratigraphic level and the phantom horizon shifted in time by 20 ms (~180 feet). Compared to high velocity values in the upper Madison (**Fig. 4.4.14-a**), the interval velocity values of the low-Madison strata are relatively reduced especially in the up-dip direction (the southwest corner in Fig. 4.4.14-b). Moreover, the lower Madison unit possesses less uniform velocity distribution that may replicate uneven topography of the paleokarst features within the dolostone unit. Based on the dolostone trend-line shown in Figure 4.4.11, we mapped porosity separately for the upper and the lower Madison carbonate units (Fig. 4.4.15). The updip direction from RSU #1 well seem to be very promising for carbon sequestration into the lower Madison unit, since there are broad areas with reservoir porosity reaching 25% just one mile west and south from the well (Fig. 4.4.15-b). We speculate that the lower Madison dolomites were likely impacted by dissolution, resulting in the karst collapse features of both sub-horizontal and sub-vertical orientation. The underground karst cavities (secondary porosity) enhance the intergranular, primary porosity, and result in anomalously high porosity that is imaged with seismic waves. However, vertically oriented karst collapse features, the dissolution pipes, may serve as vertical conduits for the injected CO2 fluid. Faulting is another geological factor that may allow fluid to flow vertically through a low-permeability caprock. These vertical migration pathways, or seal bypass systems, must be determined beforehand the actual injection starts. We use volumetric seismic attributes, primarily coherence and curvature, to analyze the possibility of seal bypass systems occurrence in the vicinity of the RSU #1 well.

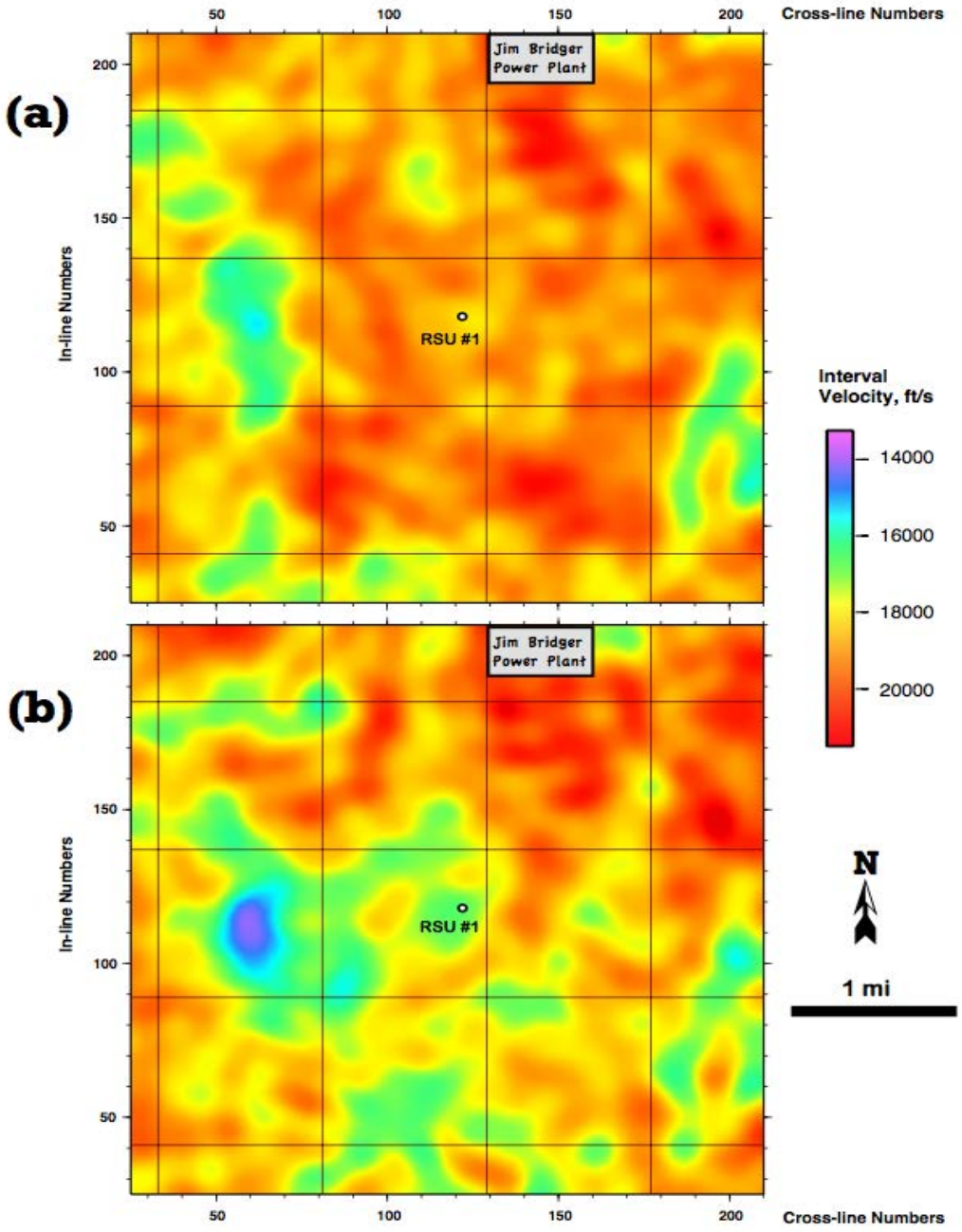

Figure 4.4.14. Velocity maps created on top of the stratigraphic intervals: (a) upper Madison, and (b) lower Madison. Note velocity decrease within the lower Madison rocks in the south-west (updip) direction from the RSU #1 well.

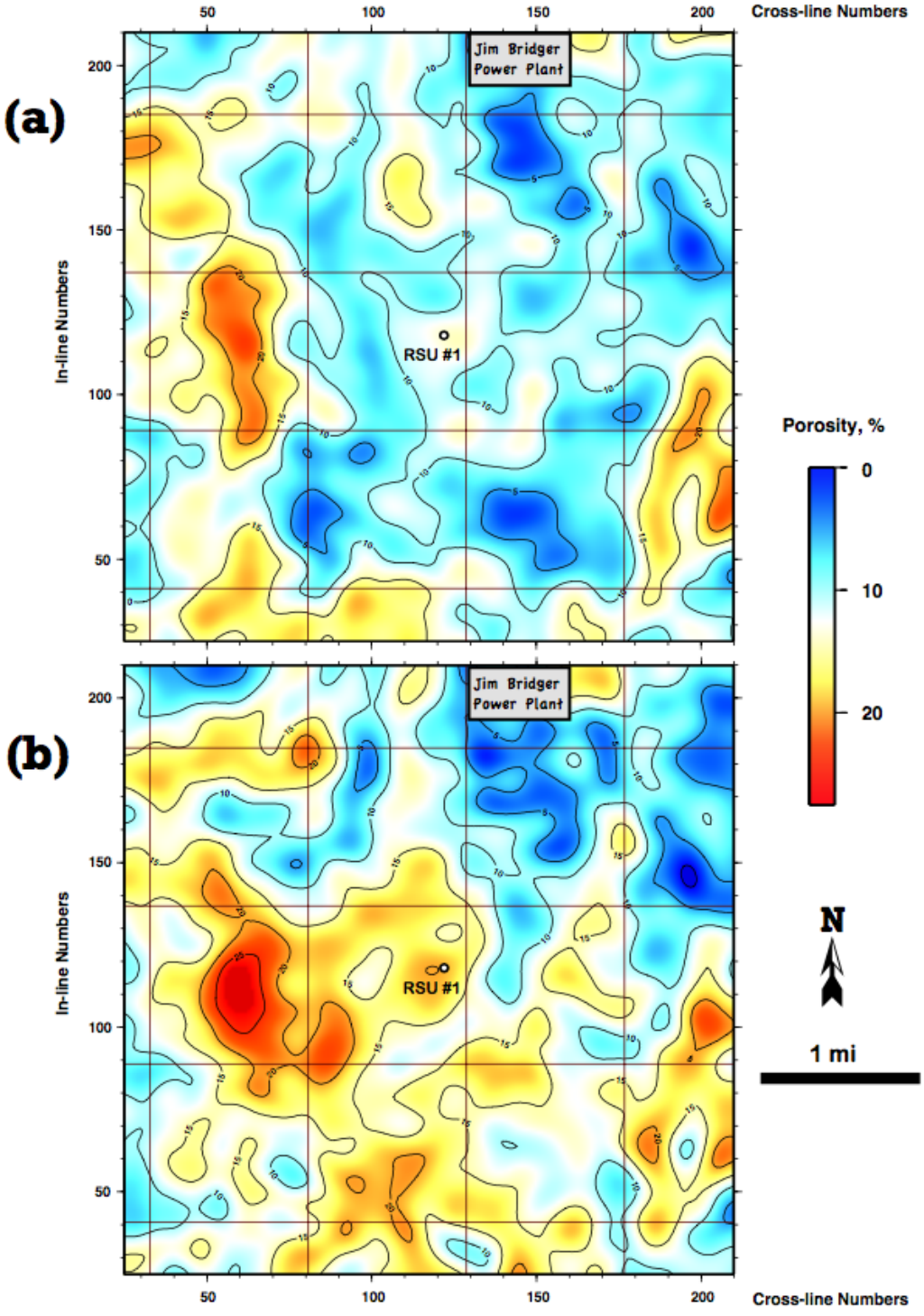

Figure 4.4.15. Porosity maps created on top of the stratigraphic intervals: (a) upper Madison, and (b) lower Madison. Note porosity increase within the lower Madison rocks in the south-west (updip) direction from the RSU #1 well.

The orthogonal system of faults is imaged in horizon slices picked at the Madison stratigraphic level through the coherency and curvature volumes (**Fig. 4.4.16**). As can be seen in the figure, the northwest-striking fault system is terminated within the study area by another system that is roughly orthogonal to the first one. A clearer image of geological features interpreted along the lower Madison seismic horizon is shown in **Figure 4.4.17**. The general northwest and southeast orientation of interpreted features along the Madison horizon is consistent with lineaments orientation visible on the digital elevation map of the Rock Springs Uplift (**Fig. 4.4.18**). We speculate that major discontinuities in seismic reflection data observable along the Madison horizon are related to structural deformation that occurred during the Laramide Orogeny. To get more confidence in interpretation presented in **Figure 4.4.17**, we constructed the along-strike profile through the seismic amplitude volume. Figure 4.4.19 shows southwest-northeast section with interpreted stratigraphic horizons and discontinuities. The section cuts seismic volume just north from the test well location. Note that the interpreted faults produce a noticeable displacement in the reflectivity patterns.

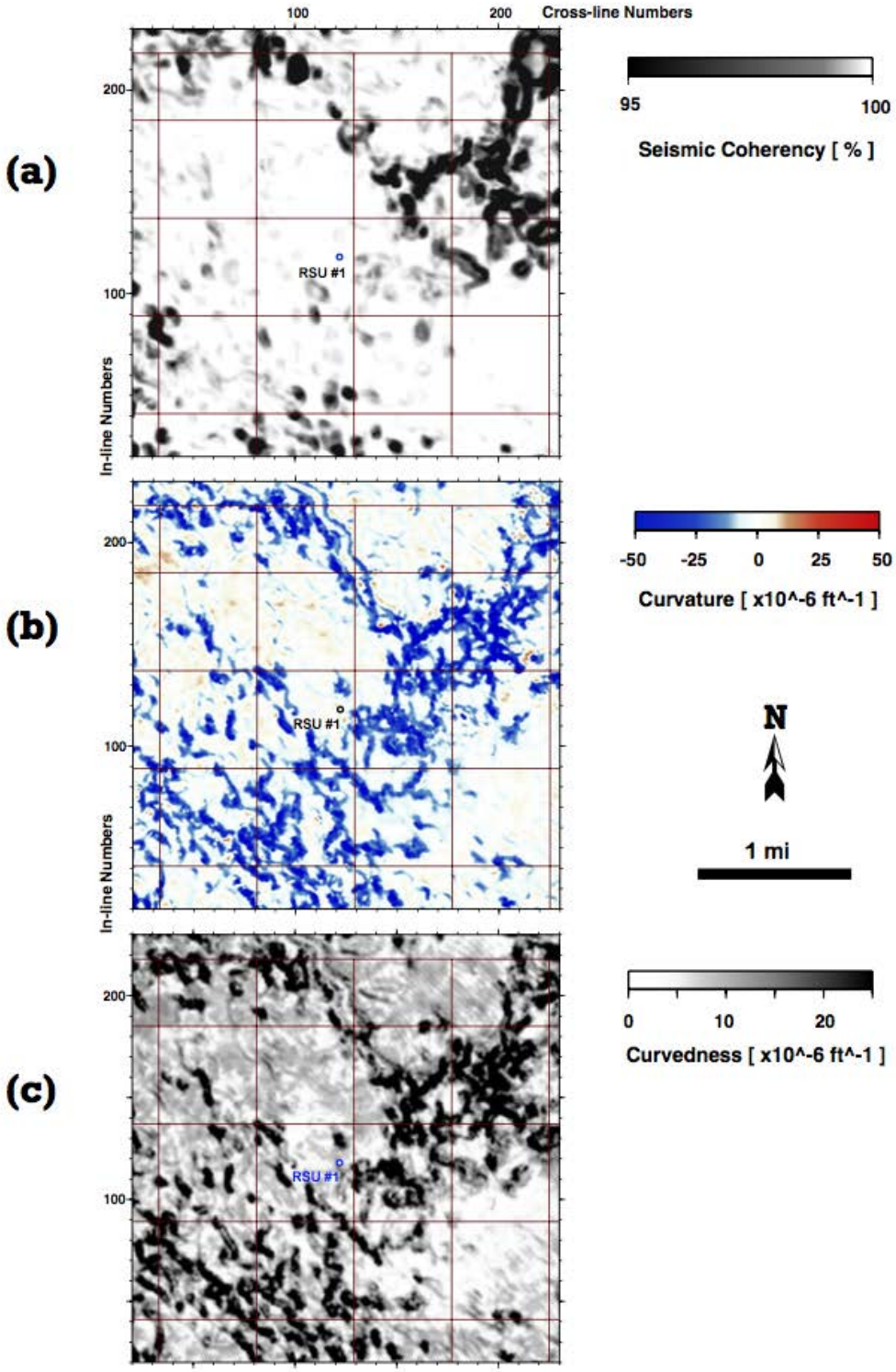

Figure 4.4.16. Reflection continuity maps calculated along the Madison stratigraphic horizon: (a) post-stack semblance coherency, (b) minimum curvature, and (c) curvedness. Note that dark-colored areas correspond to discontinuities within the Madison horizon.

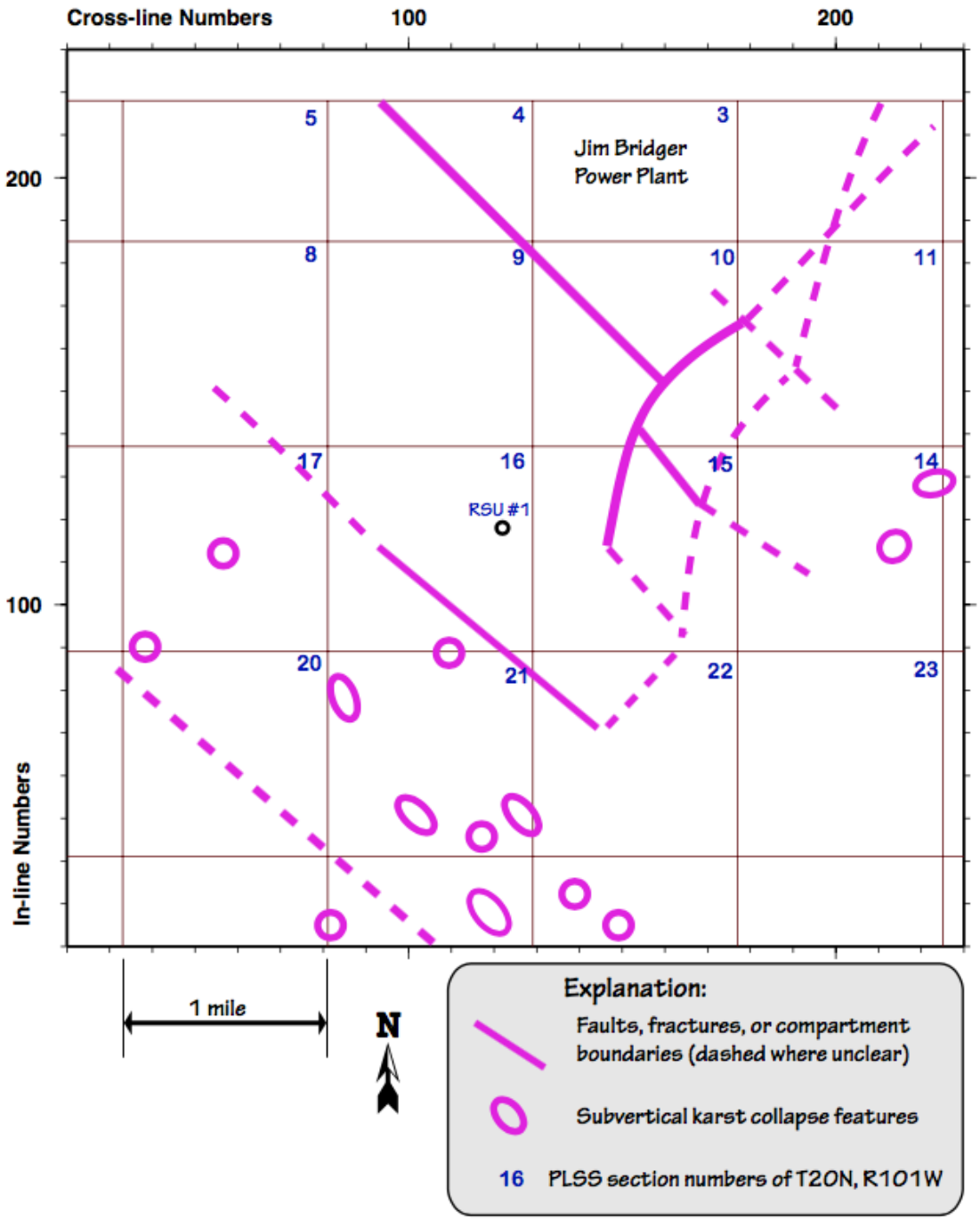

Figure 4.4.17. Geological features interpreted along the lower Madison horizon from seismic attributes analysis. In-line and cross-line numbers are from the Jim Bridger 3-D seismic survey.

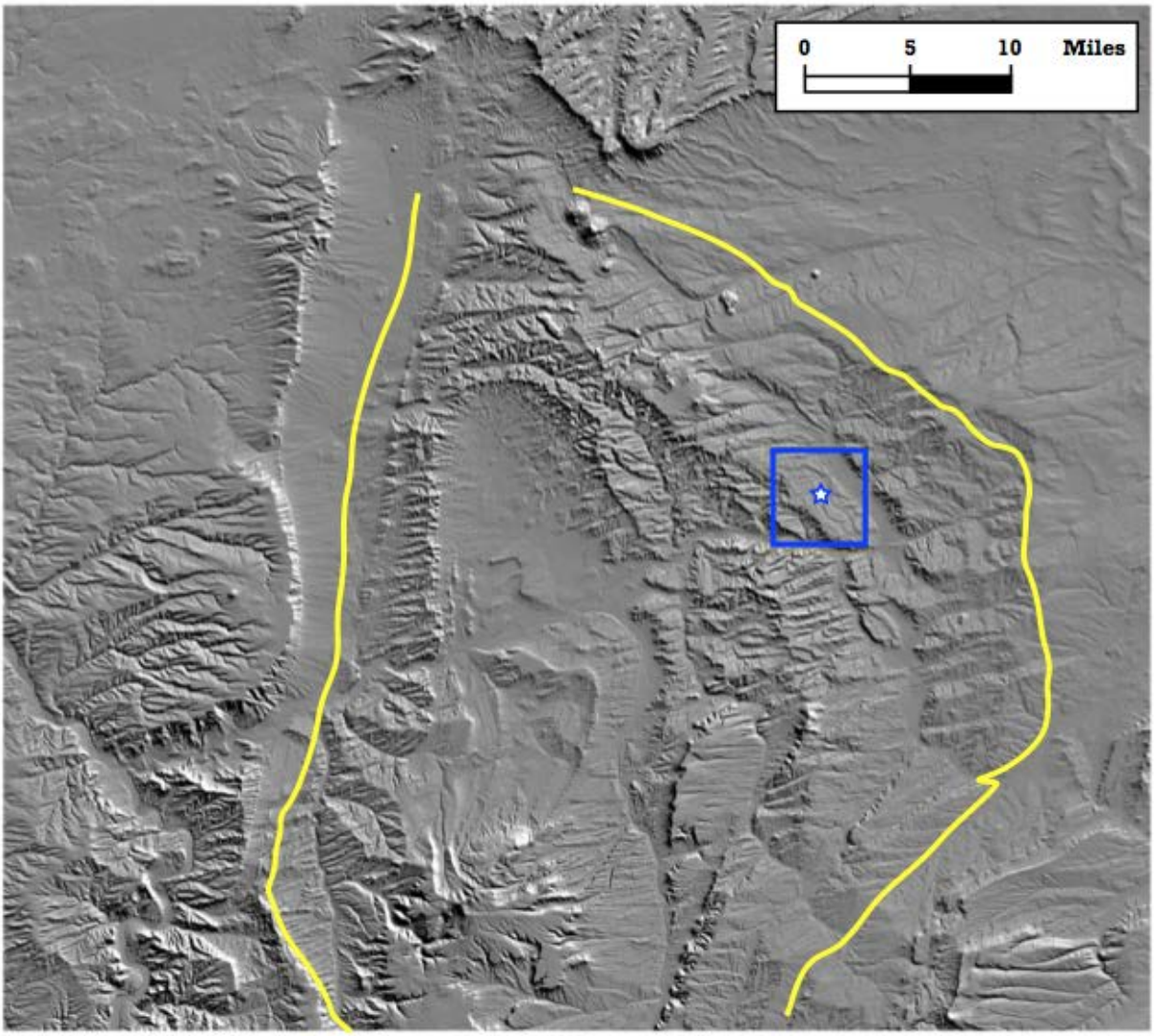

Figure 4.4.18. Digital elevation map of the Rock Springs Uplift with seismic survey outline (blue rectangle) and RSU #1 well location (blue star). Yellow contour outlines the surface expression of the uplift.

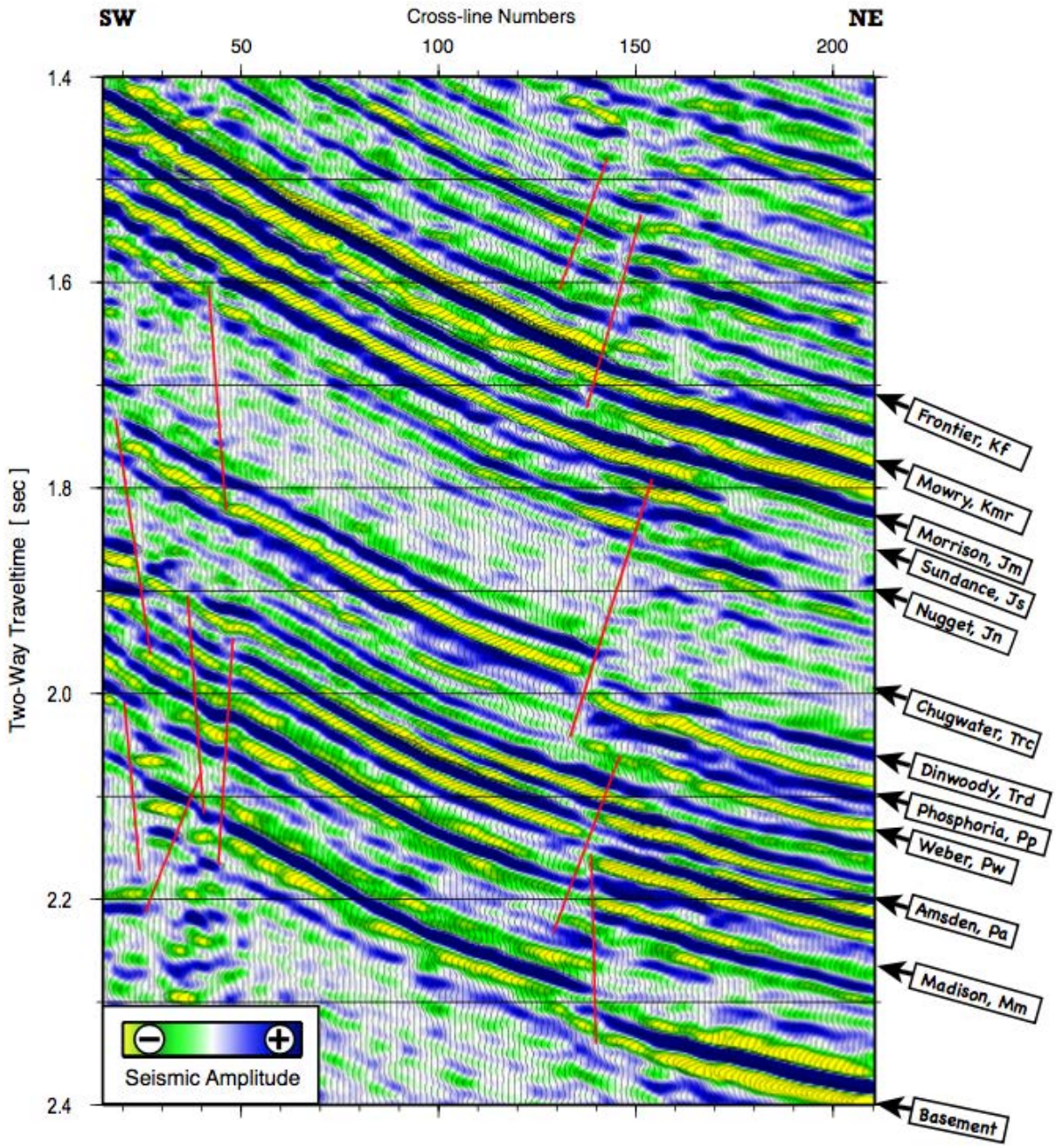

Figure 4.4.19. Interpreted SW-NE section through the migrated seismic amplitude volume (along-strike profile). Interpreted discontinuities in reflectivity pattern are shown with red lines.

Horizon slices related to the Nugget storage complex

We used the same bi-spectral (***V - Π***) velocity analysis technique to model velocity distributions for the Jurassic Nugget through the Morrison formations. These velocity distribution maps actually represent interval velocity models obtained from reflection seismic data. As in any modeling, our degree of confidence in identified features and their associated interpretation depends on the density of the modeled

data set. In this study, our measurements are sampled densely, 110 ft×110 ft×2 ms, and that makes our velocity models more precise (and probably more accurate) than those models produced for conventional stacking purposes.

Velocity distribution map obtained along the Nugget horizon is characterized by a broad range of modeled velocities, from about 13,500 to 20,500 ft/s (**Fig. 4.4.20-c**). This range exceeds the one derived from the sonic log (~15,000 to 18,000 ft/s) in the Nugget depth interval (**Fig. 4.4.2**). This discrepancy between the seismically derived and sonic velocities is not surprising since seismic velocity analysis possess big uncertainties due to multiple assumptions associated with the method. Although the velocity uncertainty is big, a relative distribution of high- and low-velocity values can be used for geological interpretation of large-scale features. There are two major low-velocity anomalies that are located about 1 mile south and north from the RSU #1 well (**Fig. 4.4.20-c**). Both of these anomalies, as well as a big area around the RSU #1 well are characterized with enhanced seismic coherency, which indicates good continuity of the Nugget reflecting horizon (**Fig. 4.4.20-a**). This quality control is required to gain more confidence in geological interpretation of seismically derived velocity anomalies. Hence, we disregard in our interpretation low-coherency (dark-colored) areas observed in **Figure 4.4.20-a**.

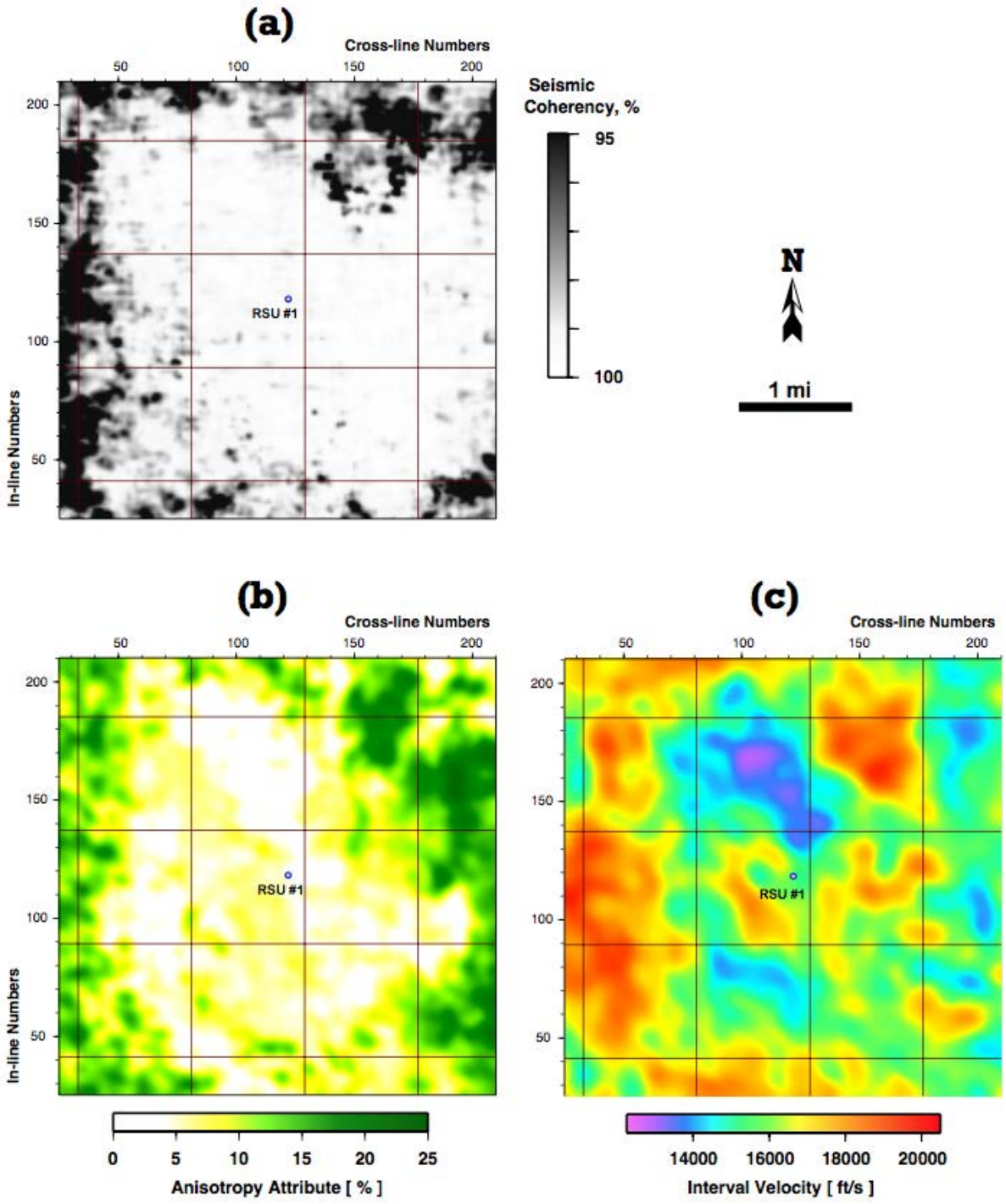

Figure 4.4.20. Seismic attribute maps calculated along the Nugget stratigraphic horizon: (a) post-stack semblance coherency, (b) anisotropy attribute, and (c) interval velocity. The anisotropy and velocity maps are outcomes of automated, non-hyperbolic seismic velocity analysis algorithm. Note that in the RSU #1 well vicinity, the Nugget Sandstone appears as a rather homogeneous, isotropic stratum with big velocity variations in it.

Figure 4.4.20-b shows spatial distribution of anisotropy parameter ***h*** that characterizes Nugget sandstone as a massive and relatively homogeneous stratum in the vicinity of the RSU #1 well. The areas northeast from well possess more anisotropy. A possible explanation is bed displacement resulting from faulting. Another possible explanation is relatively poor data quality in the northeast corner of the survey. To clarify the anomalous anisotropy parameter behavior northeast from the test well and its relation to the adjacent low-velocity anomaly, we performed coherency and curvature analysis along the Sundance horizon.

The Sundance horizon, located immediately above the Nugget, is characterized by a relatively higher reflection strength, which makes seismic attribute analysis on this horizon more sensitive to geological factors rather than to noise. Indeed, the northwest-striking fault in the northeast corner becomes obvious in seismic attribute maps calculated along the Sundance horizon (**Fig. 4.4.21-a**). There are several more faults striking in the same northwest direction that can be interpreted from the minimum curvature map (**Fig. 4.4.21-b**). An orthogonal system of faults can be also recognized in the curvature data that pass near the RSU #1 well location. However, existence of this last fault is uncertain because the dip azimuth map indicates change of the dip angle (from northeast to mostly north) right along its strike (**Fig. 4.4.21-c**). It seems more probable that a low-amplitude fold runs through the RSU #1 well with its strike orthogonal to the major, northwest-striking fault. A summary of the above discussion on structural framework is shown in **Figure 4.4.22-a.** More evidence of the northwest-striking fault existence can be found in **Figures 4.4.22-b** and **4.4.22-c.** These Figures show anisotropy attribute distribution along the Entrada and the Gypsum Springs phantom horizons. As it is expected, the Entrada sandstone unit appears to be mostly isotropic, and the Gypsum Springs shales are characterized with a high degree of anisotropy. And both of these units experience an abrupt change in properties in the northeast corner of the seismic survey. This change in properties may indicate structural deformation of the depositional surfaces associated with the Entrada and the Gypsum Springs horizon slices. In fact, as the structural relief increases, the anomalies on the horizon slice associated with the structure quickly dominate the image. We conclude that northwest trends observed in Figures 4.4.22-b and 4.4.22-c result from faulting that juxtaposed the Entrada reservoir facies and the Gypsum Springs shale. Figure 4.4.22-c also demonstrates high integrity of sealing rocks along the Gypsum Springs horizon for a very broad area around the RSU #1 well.

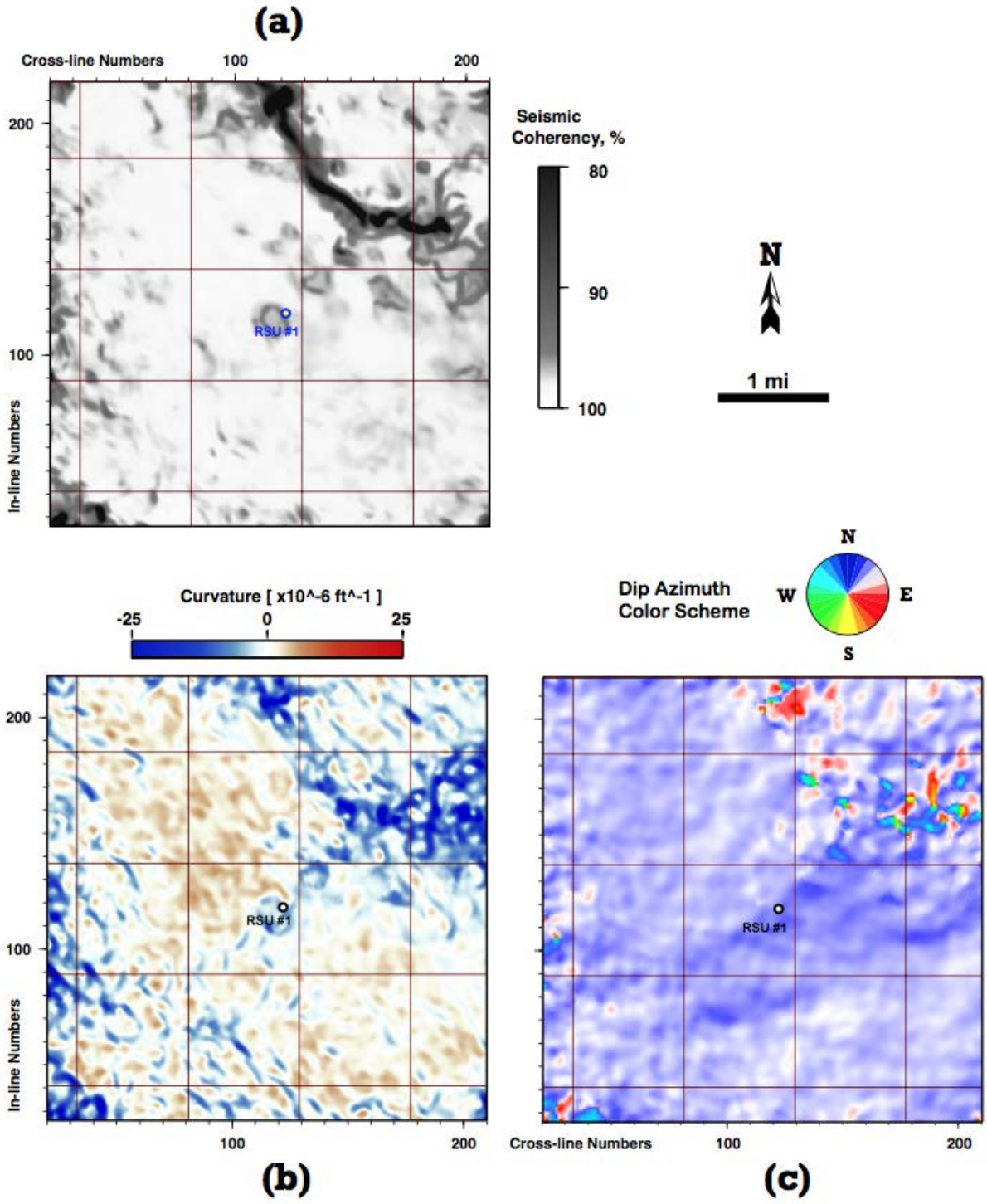

Figure 4.4.21. Seismic attribute maps calculated along the Sundance stratigraphic horizon: (a) post-stack semblance coherency, (b) minimum curvature, and (c) dip azimuth. Note a sharp discontinuity in seismic reflectivity northeast from the RSU #1 well.

Permeability and porosity are key parameters in reservoir flow simulation. When a velocity-porosity transform is available (as for the Nugget Sandstone unit), porosity can be inferred from seismic interval velocity. On the basis of petrophysical relationships shown in **Figure 4.4.5**, and considering negligible lithological variation along the interpreted seismic horizon, we modeled porosity distribution for the Nugget Sandstone that is shown in **Figure 4.4.23-a**. This porosity distribution model is based on assumption that velocity variations along a stratal surface (horizon slice) are solely dependent on rock porosity. Indeed, an interpreted reflection horizon is a reasonable approximation of a paleodepositional surface characterized by a constant lithology but we can't be sure that pore fluid content remains laterally unchanged over a big area. There are also other factors, as stratigraphic and facial changes, that may affect lateral seismic interval velocity variations.

In **Figure 4.4.23-a** we overlaid the faults interpreted along the Sundance horizon over the porosity map derived for the Nugget Sandstone. We find a strong correlation between the fault lines and zones where porosity changes abruptly. We conclude that faults may serve as compartment boundaries separating different reservoir facies of the Nugget Sandstone unit. The likely reason of facial variations along the Nugget is different pore fluid content in compartments composed with a fault/fracture network. The reservoir zones characterized by increased porosity (red color in **Figure 4.4.23-a**) are likely to be saturated with gas, while the blue-colored areas can be interpreted as water-saturated sandstones. If this interpretation is true, the permeability model shown in **Figure 4.4.23-b** is incorrect, since porosity was assumed to be the only factor affecting permeability. The lack of currently available data on permeability dependencies in the study area, do not allow us to create other permeability models for the Nugget storage complex. In fact, the permeability that necessarily has to be supplied in reservoir modeling seems to be the most elusive of reservoir properties and remains extremely uncertain.

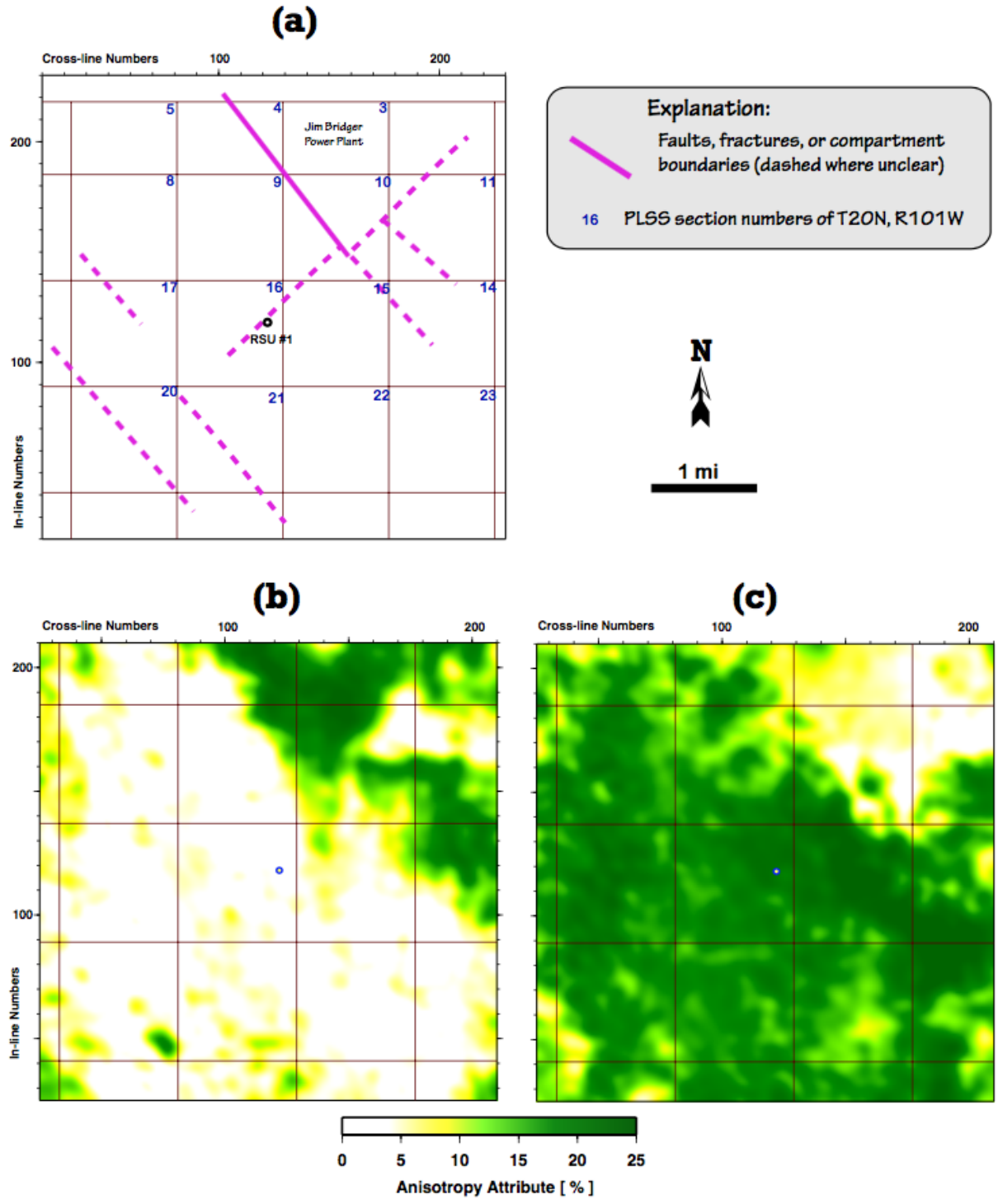

Figure 4.4.22. (a) Geological features interpreted along the Sundance seismic horizon from attributes analysis. (b) Anisotropy attribute calculated along the Entrada horizon, and (c) anisotropy attribute calculated along the Gypsum Springs horizon. Note lateral continuity of both, the Entrada sandstones and the Gypsum Springs shales.

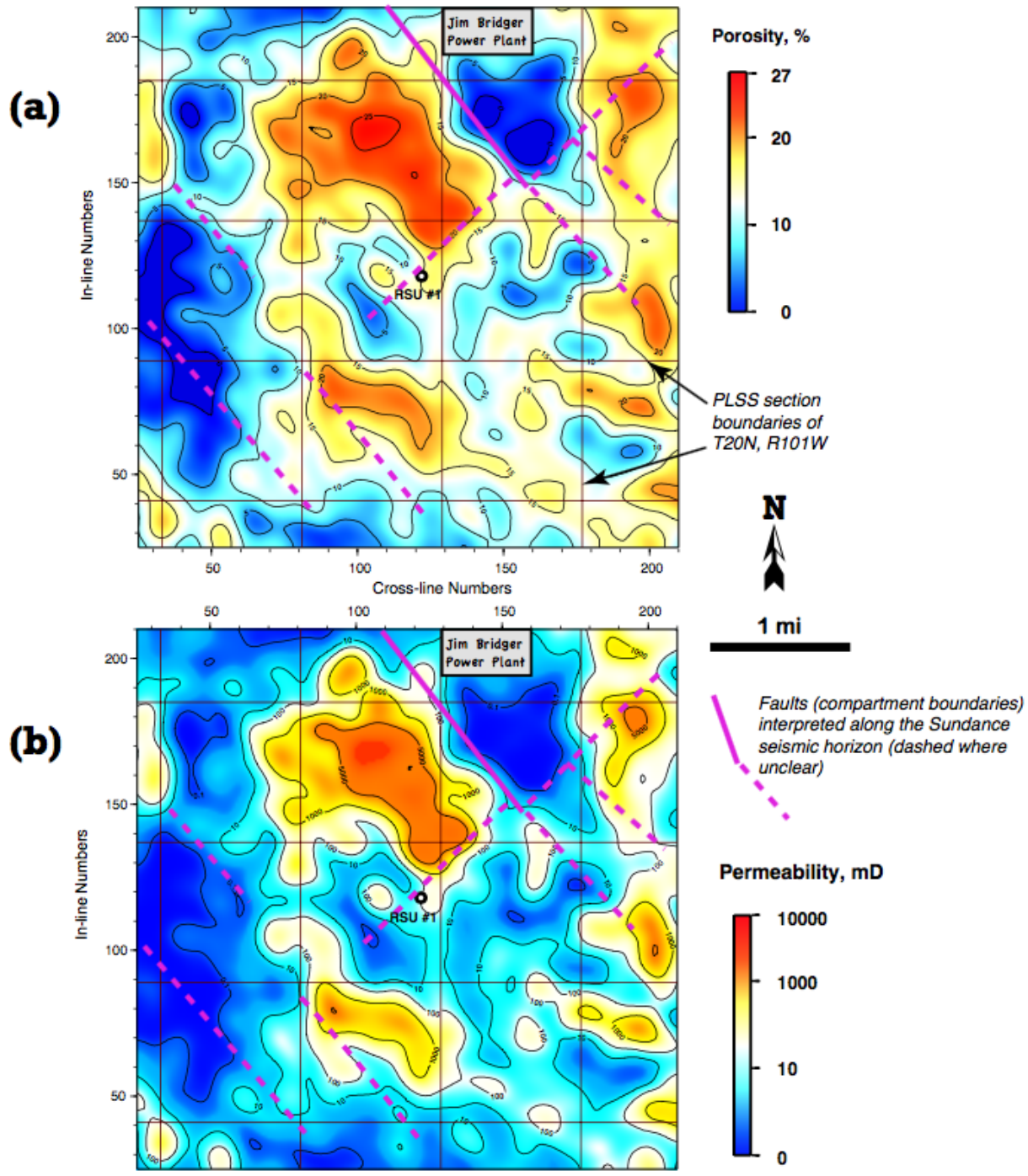

Figure 4.4.23. Porosity (a) and permeability (b) contour maps of the Nugget Sandstone derived from seismic interval velocity assuming laterally invariant velocity-porosity and porosity-permeability relationships derived from RSU #1 well logs and cores. Note that porosity was assumed to be the only factor affecting seismic interval velocity variations.

Section 4.4 References

Archie GE (1950) Introduction to petrophysics of reservoir rocks. American Association of Petroleum Geologists Bulletin 34(5): 943–961

Ganshin Yuri and Surdam Ronald, 2013, Utility of 3-D Seismic Attribute Analysis and VSP for Assessing Potential Carbon Sequestration Targets on the Rock Springs Uplift, Southwest Wyoming: in Ronald C. Surdam editor, Geological CO2 Storage Characterization, Chapter 7, pp. 97-150, Springer

Fomel Sergey, 2004, On anelliptic approximation for qP velocities in VTI media. Geophys. Prosp., 52: pp. 247-259.

Jensen JL, Lake LW, Corbett PWM, Goggin DJ (2000) Statistics for petroleum engineers and geoscientists, 2nd edn. Handbook of petroleum exploration and production, 2. Elsevier, Amsterdam

MacQueen, J. (1967). Some methods for classification and analysis of multivariate observations. Proceedings of the Fifth Berkeley Symposium on Mathematical Statistics and Probability, Volume 1: Statistics, 281--297, University of California Press, Berkeley, Calif.

Nelson PH (1994) Permeability-porosity data sets for sandstones. The Leading Edge (23): 1143–1144

Nelson, PH (2004) Permeability-porosity relationships in sedimentary rocks. The Log Analyst May–June:38–62

Section 4.5: Traditional Reservoir Modeling & Simulation

Heng Wang, Zunsheng Jiao, and Matthew B. Johnson
Research Scientist, Center for Economic Geology Research
School of Energy Resources, University of Wyoming
1020 E. Lewis Street, Energy Innovation Center
Laramie, WY 82071

Introduction

CO_2 emissions from fossil fuel consumption have caused a noticeable increase in CO_2 concentration in the atmosphere, which has been associated with climate change. Substantive CO_2 emission reductions might be possible through available sequestration technologies which utilize geologic storage of CO2 in oil reservoirs for CO2-EOR, depleted oil/gas reservoirs, unminable coal beds, and deep saline aquifers. This study investigates sequestration into saline reservoirs. As CO2 is injected into saline reservoirs, it flows through the porous spaces and displaces the water-wetting brine in a drainage-like process. In addition, the buoyant CO2 migrates laterally and upwardly, and the capillary effects such as snap-off lead to disconnection of the continuous gas phase into immobile blobs and ganglia, which is referred to as capillary or residual trapping. There are four dominant trapping mechanisms that contribute to the long-term storage of CO_2 in deep saline aquifers, including structural stratigraphic trapping, capillary residual trapping, solubility trapping, and mineral trapping. As CO_2 is injected into deep saline aquifers, larger-scale pressure buildup in the reservoir may limit injectivity and storage capacity, as elevated pressure decreases the difference between the bottom-hole pressure (BHP) of the injection well and reservoir pressure, which will reduce the injection rate. In addition, high reservoir pressure can affect caprock integrity, and increase the risk from leakage. One of the most efficient ways to manage formation pressure, and decrease risk from leakage, is to extract native brine. The extraction of native brine from storage formations can be used to control the reservoir pressure, thereby avoiding the possibility of leakage. Moreover, it can provide other benefits, such as increasing the storage capacity, controlling CO_2 plume size and shape, and with monitoring CO_2 plume size and determining leakage possibility.

Reservoir simulation is an effective way to describe multiphase flow (CO_2/water) during the CO_2 injection process, and to estimate the volumes that can be stored. Simulations also allow for the addition of water production wells to test ways in which CO_2 plume size and shape can be controlled, and CO_2 injectivity and storage capacity can be optimized. In this work, reservoir simulator Schlumberger Eclipse E300 (Eclipse 2016) is used to model CO_2 injection process in the Entrada and Nugget formations in an effort to characterize stacked storage potential in southwest Wyoming. These models are coupled with existing models of deeper saline reservoirs, for a full realization of the site's storage capacity, as well as the risks and challenges of long-term injection at the site. Schlumberger Petrel 2016 was used to build the static model using existing subsurface data from previous studies, and simulation cases were set up using the Petrel Reservoir Engineering (Petrel RE) module. We investigated the CO_2 injectivity and storage capacity with and without brine extraction.

Multiple units were focused in this report for the assessment of stacked storage of CO_2 at the study site at the Jim Bridger Power plant. This report divides the study into two parts; pre-feasibility investigations of the previously undefined Mesozoic Entrada and Nugget sandstones at the study site defined by scenario assessment and refined through geophysical evaluations. New data from these evaluations were coupled with a previous models developed during investigation of Paleozoic geologic reservoirs for longer duration CCS (50+ years) at the Rock Springs Uplift (RSU), the Weber and Madison formations. These analyses suggest that by employing a stacked storage strategy, two of the reservoirs (the Nugget and Madison formations) have the potential for safely storing 50+ million metric tons of CO_2 within the confines of the study site *if* injection is coupled with brine production.

Pre-Feasibility Storage Capacity Assessments of the Entrada and Nugget Sandstones at the JBP study site, Wyoming

To test dynamic storage simulations, we first needed to develop robust, heterogeneous property models. The initial focus us property model development for Phase I activities were the Entrada and Nugget sandstones. Data used to generate property models included petrophysical data from the RSU #1 well, which became the center point of the model, the seismic data described in the previous section, and regional subsurface data from hydrocarbon wells (Table X.1). These were then combined with existing models of deeper formations to test the potential of commercial-scale storage in a fully integrated property geologic model.

Zone	Seal/ Reservoir	Data Used	Average Thickness (ft)	Cut-offs	Average Porosity (%)	Average Permeability (mD)	Statistical Distribution Method
Sundance	Seal	PORZC Log	235	Forced 0	0	0	Sequential Gaussian Simulation
Entrada Sandstone	Reservoir	PORZC Log	54	No cut off	8	15.3	Sequential Gaussian Simulation
Gypsum Spring/Twin Creek	Seal	Seismic, PORZC Log	115	Forced 0	0	0	Sequential Gaussian Simulation
Nugget Sandstone	Reservoir	Seismic	465	No porosity less than 7%	13.7	31.8	Sequential Gaussian Simulation
Chugwater	Seal	Seismic	1214	Forced 0	0	0	Sequential Gaussian Simulation

Table 4.5.1. Data parameters and variables used to build property models

Entrada Sandstone

The Entrada Sandstone Model was created using Schlumberger Petrel Software and incorporated data Table 4.5.1. Because the seismic survey did not have the resolution to resolve attributes in the Entrada (due to its thickness), the top of the Morrison in the RSU #1 well and adjacent wells were used to generate control points for mimicking the slope in the study area. All subsequent horizons below the Morrison were picked using gamma ray and sonic logs, and then made to conform to the dip of the Morrison formation with grid cell increments of 150 x 150'. Units above and below the Entrada Sandstone (the Morrison and Gypsum Springs formations) where classified as seals, the entirety of the Entrada Sandstone was classified as reservoir rock. Within the model, five layers were generated within the Entrada Sandstone to be used to generate geostastically-relevant property variability spatially (Figure 4.5.1). Due to the lack of core data within the RSU #1 well of the Entrada Sandstone, porosity was determined from the PORZC log and distributed using the Sequential Gaussian Simulation method. All sealing horizons were set to zero porosity to simulate sealing rocks.

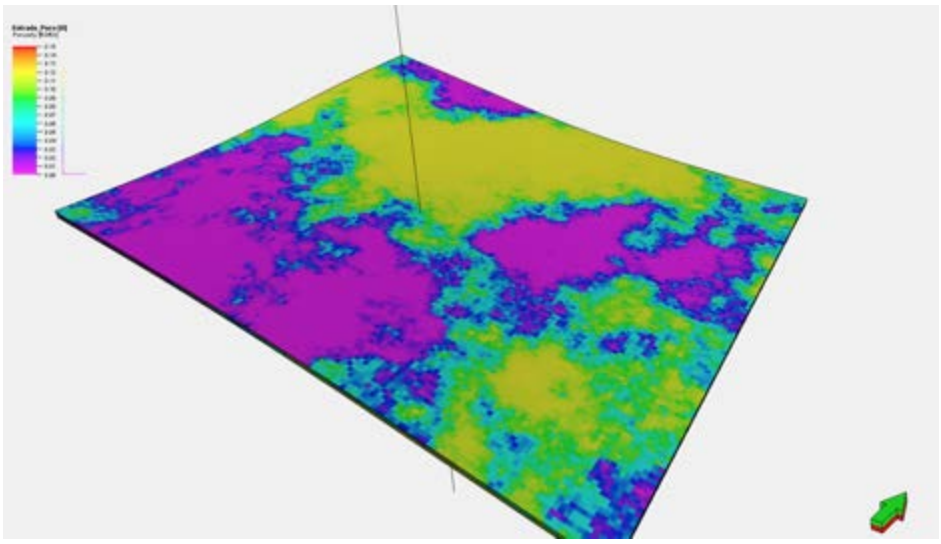

Figure 4.5.1. Entrada Sandstone porosity distribution based on the PORZC log. The black line represents the location of the RSU #1 well

Using core data from other Entrada wells, a porosity-permeability cross-plot was created and a trend line was established to determine realistic reservoir properties to best present the data (Figure 4.5.2). Using the function developed by the trend line in conjunction with the PORZC log, a permeability log was created for the formation at the RSU #1 well. Sequential Gaussian Simulation was then used to distribute these properties throughout the model (Figure 4.5.3). Sealing rocks were consider to be zero to simulate a no-flow boundary.

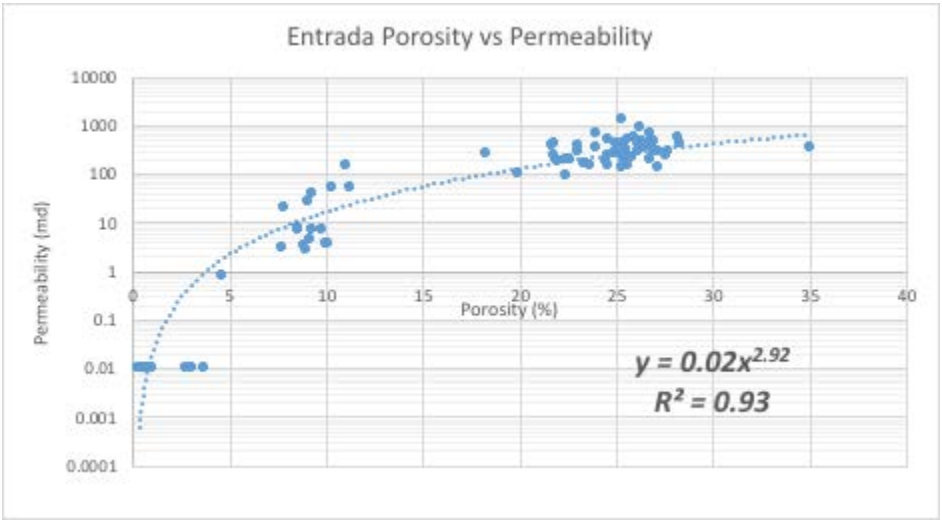

Figure 4.5.2. Graph showing the correlation between measured porosity and permeability from core sampled from regional Entrada Sandstone wells

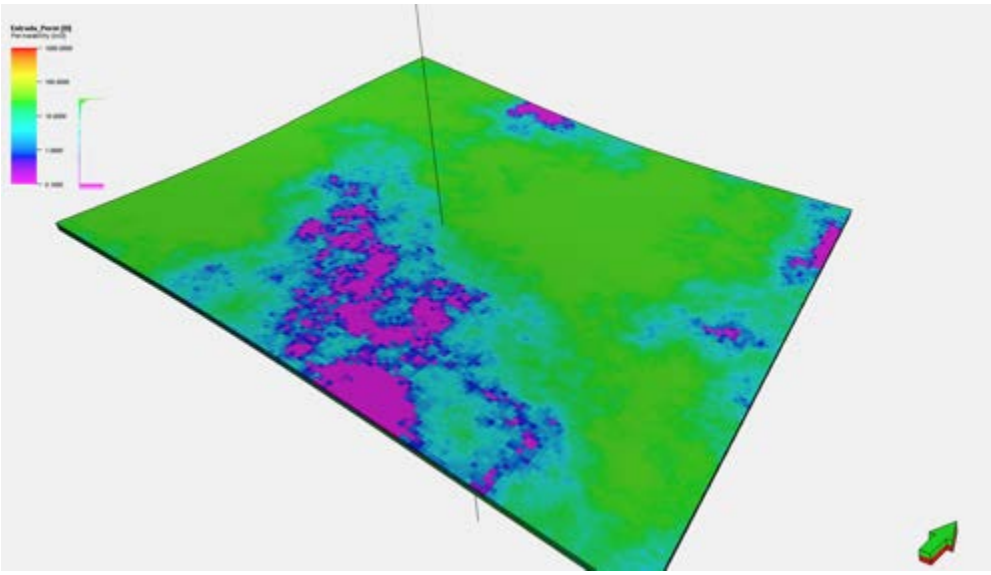

Figure 4.5.3. Entrada Sandstone permeability distribution. The black line represents the location of the RSU #1 well

Nugget Sandstone

The Entrada Sandstone model was created using Schlumberger Petrel Software and incorporated data from Table 4.5.2. The Nugget Sandstone is much thicker than the Entrada Sandstone, allowing for the incorporation of the RSU seismic data. Using data from the vertical seismic profile (VSP), a correlation between velocity and depth was obtained to tie the well logs to the seismic survey. A non-linear function was created using the data provided to obtain a much higher quality match (Figure 4.5.4).

Figure 4.5.4. Graph showing the relationship between two-way travel times (TWT) and measured depth. The blue line is the well data and the overlapping red line is the non-linear function used to develop the well ties. Note the clear overlap

Data from the RSU #1 well was then aligned with seismic data, and formation tops were picked within the seismic data by their relative geophysical log signature. Once identified, the formation was spatially tracked throughout the 3D seismic data field. Seismic horizons were then manually reprocessed and smoothed to remove peaks or artifacts that developed from the spatial expansion. The new horizons, along with well tops were used in the velocity modeling to convert the full seismic cube data from TWT to depths. Using the seismic data that is now converted inti the depth domain, seismic values were populated into a cell based format to being construction of the property models (Figure 4.5.5). Grid scale was set at 450 x 450', with the Nugget Sandstone having 10 layers of cells. Work previously done by Dr.

Yuri Ganshin (author of the previous section) suggests the relationship between velocity and porosity within the Nugget was as followed:

$$\text{Velocity} = 18{,}765 - 203 \times \text{Porosity}$$

Using this formulation, an initial porosity distribution was generated across the property model. Because of data quality within portions of the seismic data, Sequential Gaussian Simulation was used to fill in areas of non-realistic values to create a more representative (realistic) geologic interpretation. A porosity cutoff of seven percent was made to ensure the data did not populate unrealistically small values that are not observed in reservoir intervals (*see Subsurface Data section*). Core values were compiled from regional wells for porosity and permeability relationships (Figure 4.5.6). A non-linear function representative of the data derived from the porosity and permeability cross plot permeability was calculated and distributed spatially (Figures 4.5.7 and 4.5.8). All confining zones above and below the Nugget Sandstone had porosity and permeability values set to zero to represent sealing lithologies.

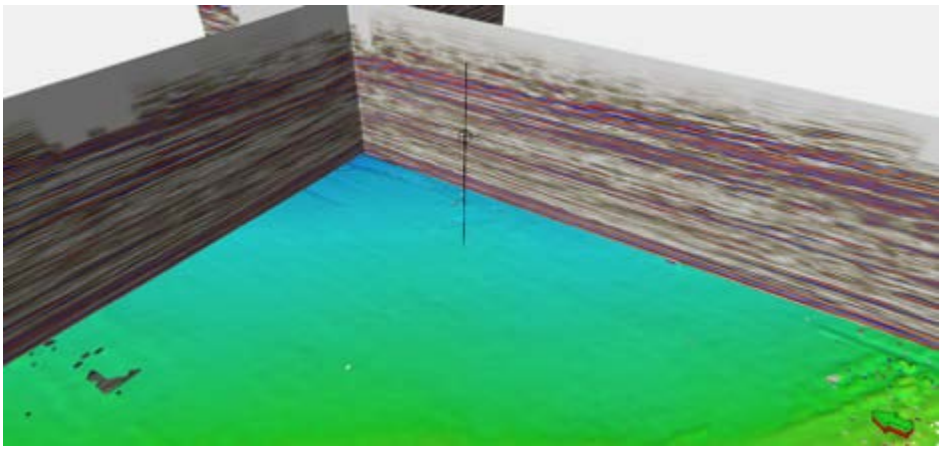

Figure 4.5.5. Image showing the Nugget Sandstone horizon tracked through the 3D seismic data with the RSU #1 well (black line) in the interpretation

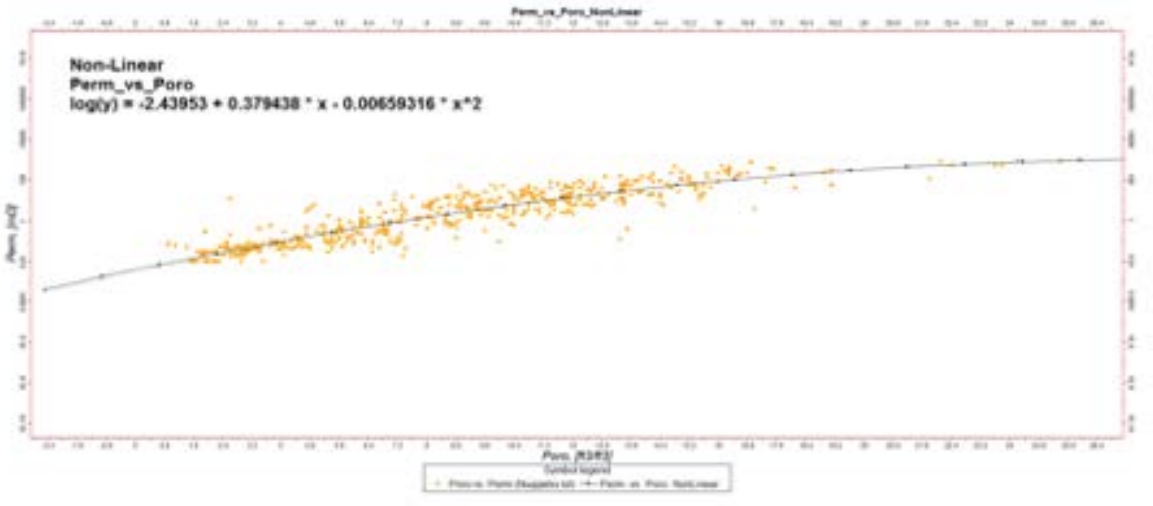

Figure 4.5.6. Graph showing the porosity and permeability cross-plot measured from Nugget Sandstone cores and their relationship to the derived function

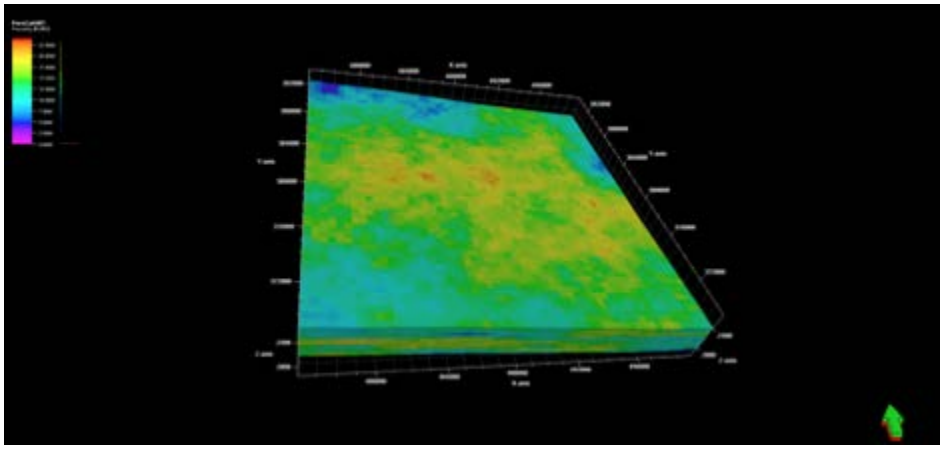

Figure 4.5.7. Image showing the porosity distribution of the Nugget Sandstone within the seismic cube. Porosity cut off was set at seven percent

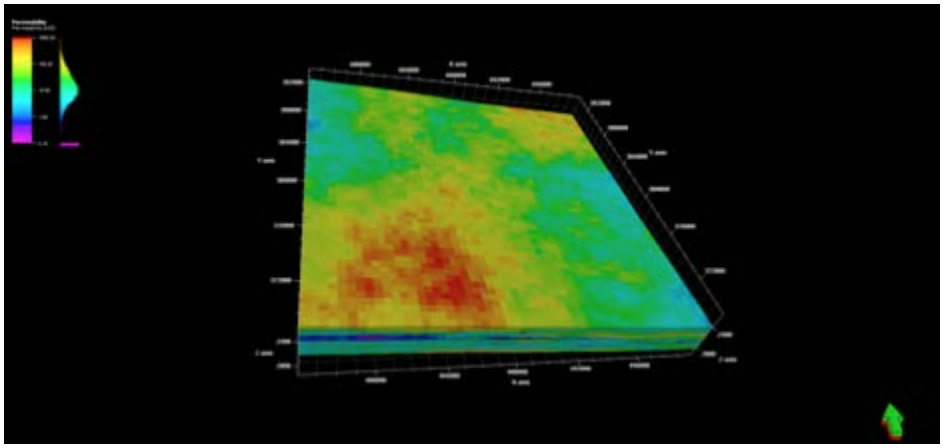

Figure 4.5.8. Image showing permeability distribution of the Nugget Sandstone

Dynamic Model Development

In order to assess the CO_2 storage potential at the Nugget and Entrada formations, compositional numerical reservoir models were built with an area of 19.8 km × 19.8 km and 21.3 km × 19.2 km, respectively. Table 4.5.4 summarizes the basic properties of the dynamic model. The RSU#1 well is located in the center of the model as defined as an injection well, and a brine production well is added in some experiments to study the pressure and injection response to water production. The well spacing between the injection and production wells is 3000 ft. Figure 4.5.9 shows the water-gas relative permeability curve used in this study. Figure 4.5.10 and Figure 4.5.11 shows porosity and permeability distributions of the Entrada and Nugget formation, respectively.

Table 4.5.4. Summary of the static model and parameters used for simulation

Parameter	Entrada	Nugget	Unit

Number of cells I direction	142	53	N/A
Number of cells J direction	128	56	N/A
Number of layers in K direction	5	10	N/A
Total number of active cells	145408	29680	N/A
Average I dimension	150	450	ft
Average J dimension	150	450	ft
Initial reservoir pressure	3600	4052	psi
Reservoir temperature	201	221	ºF
Average permeability	26.46	31.76	mD
Average porosity	9%	13.68%	N/A
Initial water saturation	100%	100%	N/A
Rock compressibility	1E-6	1E-6	1/psi
Designed injection rate	600,000	150,000	tonne/year

Injector bottom-hole pressure	6500	7000	psi

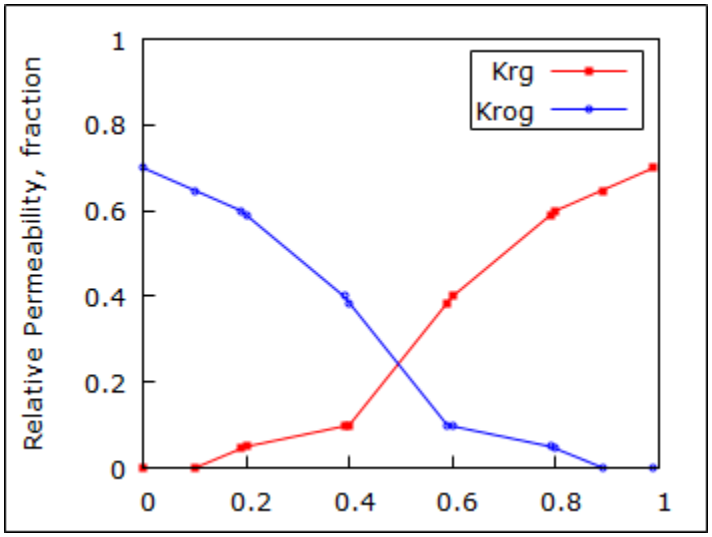

Figure 4.5.9. Relative permeability curve used for the Entrada and Nugget formation

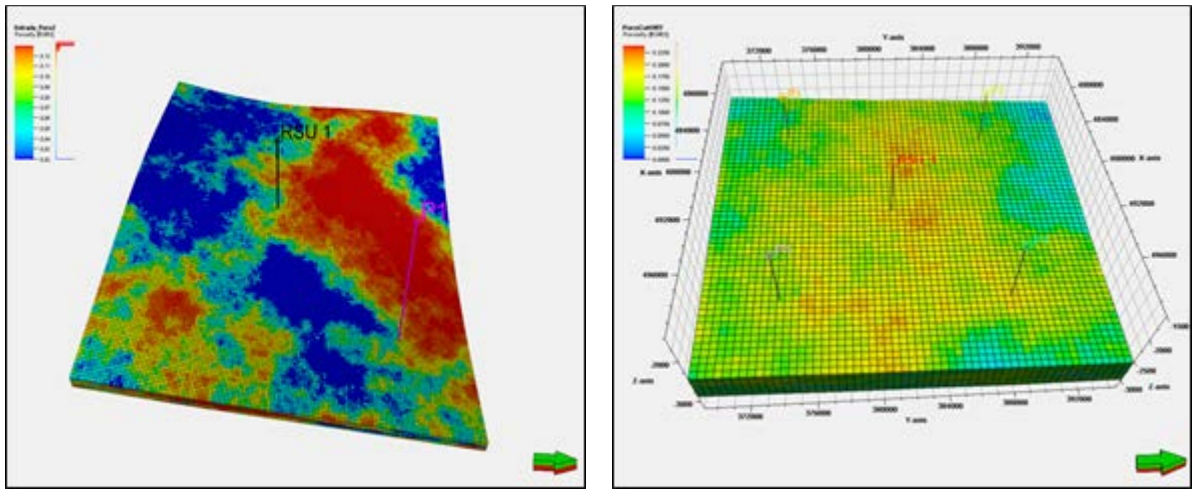

A **B**

Figure 4.5.10. Porosity distribution in the Entrada (A) and Nugget (B) formation. The average porosity is 9 and 13.7%, respectively

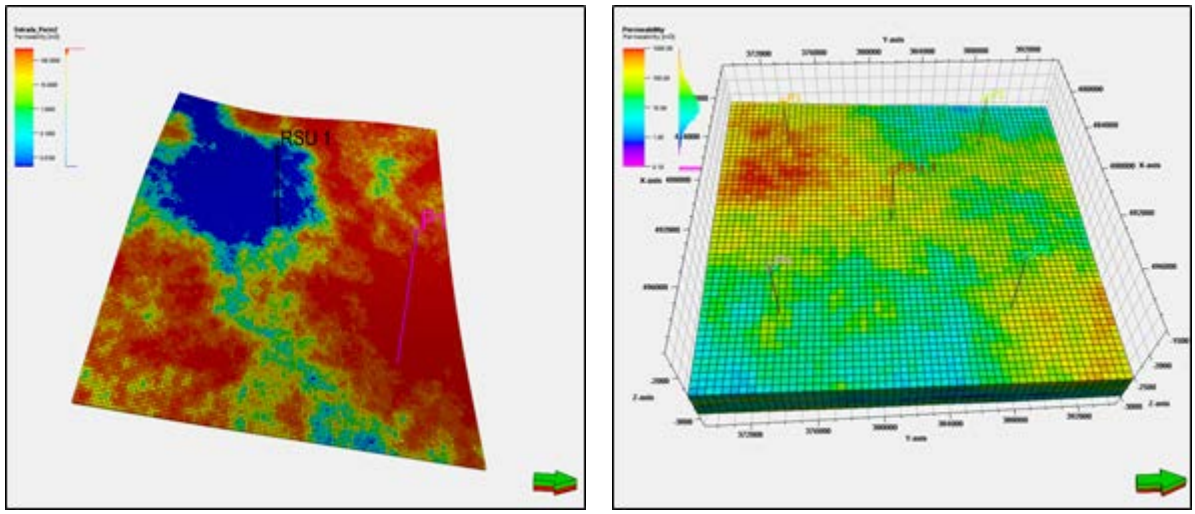

A **B**

Figure 4.5.11. Permeability distribution in the Entrada (A) and Nugget (B) formation. The average permeability is 120 and 31.7 mD, respectively

Dynamic Simulation Results

CO_2 Injection Experiments without Brine Co-Production: For these experimental simulations, CO_2 was injected through the well RSU #1 and no corresponding formation brine were be produced: these are one injection well experiments to determine direct reservoir response to injection. Figure 4.5.12 shows field average, CO_2 injection rate and cumulative injection volume of the Entrada and Nugget formations. At the beginning of injection, CO_2 injection rate for the Entrada formation equals 5282 MSCF/day, which is much smaller than designed injection rate (15927 MSCF/day). In addition, CO_2 injection rate decreases dramatically after injection, shown in Figure 4.5.12(A). After 6 years' injection, injection rate decreases to 42 MSCF/day (at Jan. 2026). After 25 years, total CO_2 injection volume is only 2.74E6 MSCF. One reason is that thickness of the Entrada formation is relatively small, and the pore volume is smaller compared with the Nugget formation. Moreover, porosity and permeability of the Entrada formation can be low and heterogeneous, especially around the injector, shown in Figure 4.5.11 (A) and 12 (A). The heterogeneity of porosity and permeability also results in the irregular distribution of the CO_2 plume, shown in Figure 4.5.5(A). Porosity and permeability of the Nugget Sandstone are more homogeneous (shown in Figures 4.5.12(B) and 4.5.13(B)) and the thickness is larger compared with the Entrada Sandstone. The CO_2 injection rate in the Nugget injection experiment keeps constant in the first 13 years. In April 2031, injection rate starts decreasing dramatically (Figure 4.5.13(B)). After another 10 years, CO_2 injection rate reaches 216 MSCF/day. Finally, total CO_2 injection volume is 1.58E8 MSCF. As shown in Figure 4.5.13 (B), the shape of the CO_2 plume is more regular (circular) compared with the Entrada formation. However, both cases cannot reach the CarbonSAFE Phase I target storage capacity because reservoir pressure increases very fast, risking seal failure. One injector well experiments show that it will likely be necessary to control reservoir pressure by extracting reservoir brine in order to hit target injection rates with the least number of wells.

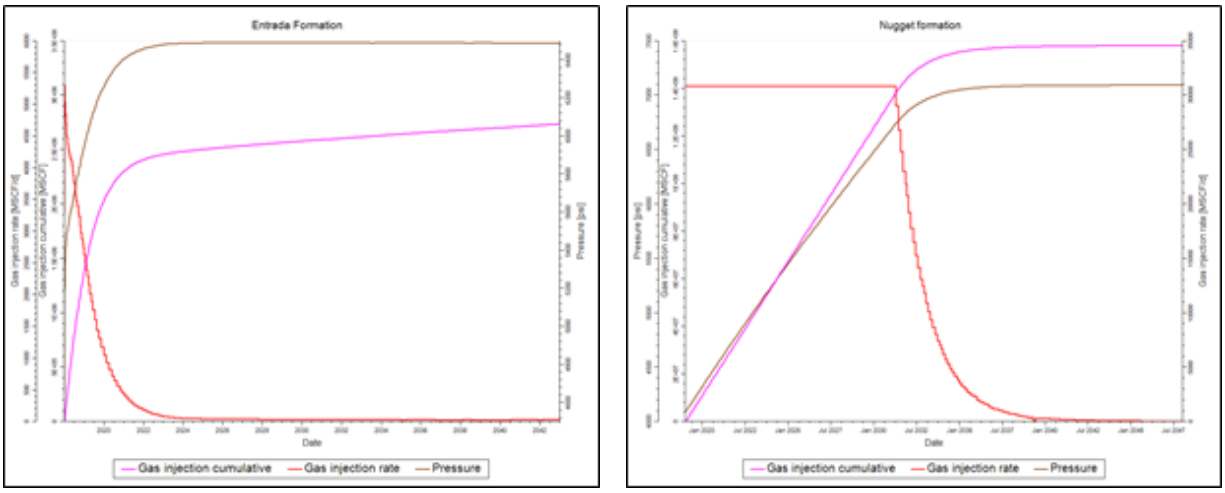

A **B**

Figure 4.5.12. Field average pressure, CO_2 injection rate and cumulative injection volume for Entrada (A) and Nugget (B) formation without brine extraction

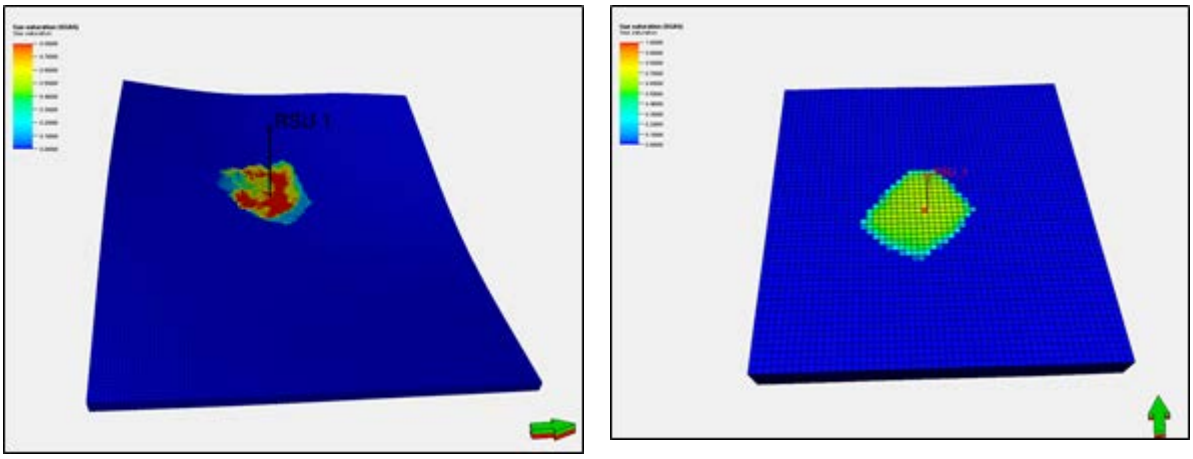

A B

Figure 4.5.13A and B. CO_2 saturation distribution for the base case after simulation. A: Entrada; B: Nugget

CO_2 Injection Experiments with Brine Co-Production: As shown in experiments with only an injection well, cumulative injection volume is constrained by reservoir pressure for both formations. It is therefore necessary to produce brine during or after CO_2 injection to optimize storage and decrease risk. In these next sets of experiments, we tested storage cases that include one injection well and one production well in which bottom-hole pressure is set as the constant of reservoir pressure.

Figure 4.5.14 shows the average pressure, water production rate, CO_2 injection rate and cumulative injection volumes for the Entrada (A) and Nugget (B) formations coupled with brine extraction. For the

Entrada Sandstone, the CO_2 injection rate decreases immediately after starting injection. The injectivity of CO_2 is limited due to the low permeability around the injector. With the inception of CO_2 injection and increased pressure, brine begins producing. After CO_2 injection rate reaches the minimum value (1982 MSCF/day), the CO_2 injection rate and brine production rate both increase slowly. Finally, the total CO_2 injection volume is 2.12E7 MSCF, which is much larger than the case without brine extraction. In this experiment, CO_2 is shown to break through to the production well (shown in Figure 4.5.15) in 2041, which would realistically halt all injection and production.

As the permeability of the Nugget Sandstone is greater and less heterogeneous across the reservoir, the CO_2 injection rate is much more constant than Entrada experiments. The brine production rate and reservoir pressure increase, reaching a plateau after 10 years of injection. These experiments show that the Nugget Sandstone is a much more applicable target for feasible CO_2 storage in commercial quantities.

The simulation results show that CO_2 injectivity and storage capacity are dependent on reservoir properties, such as permeability, heterogeneity and thickness. In addition, pressure management is crucial for CCS process optimization as it is shown to affect both CO_2 injectivity and storage capacity.

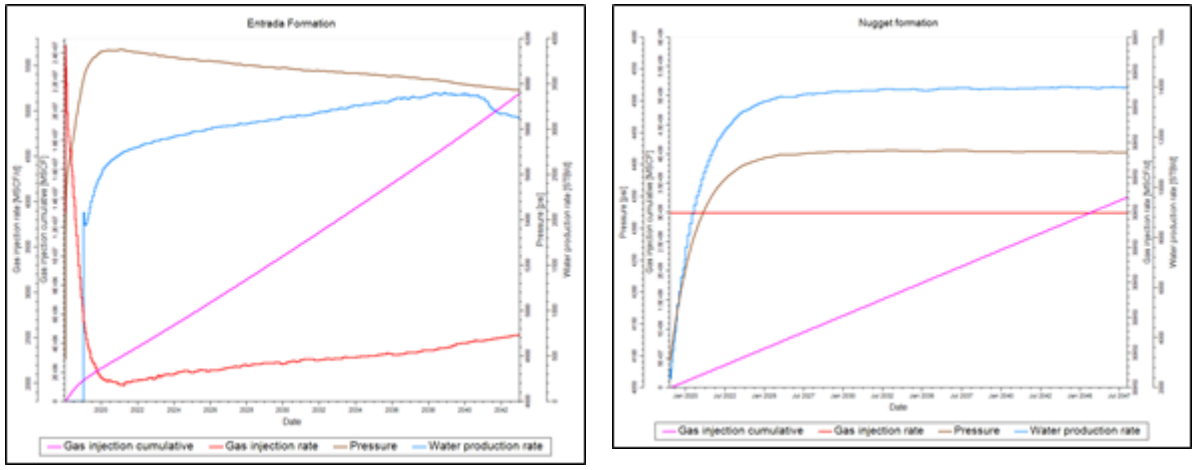

A B

Figure 4.5.14. Field average pressure, CO_2 injection rate and cumulative injection volume for Entrada (A) and Nugget (B) formation with brine extraction

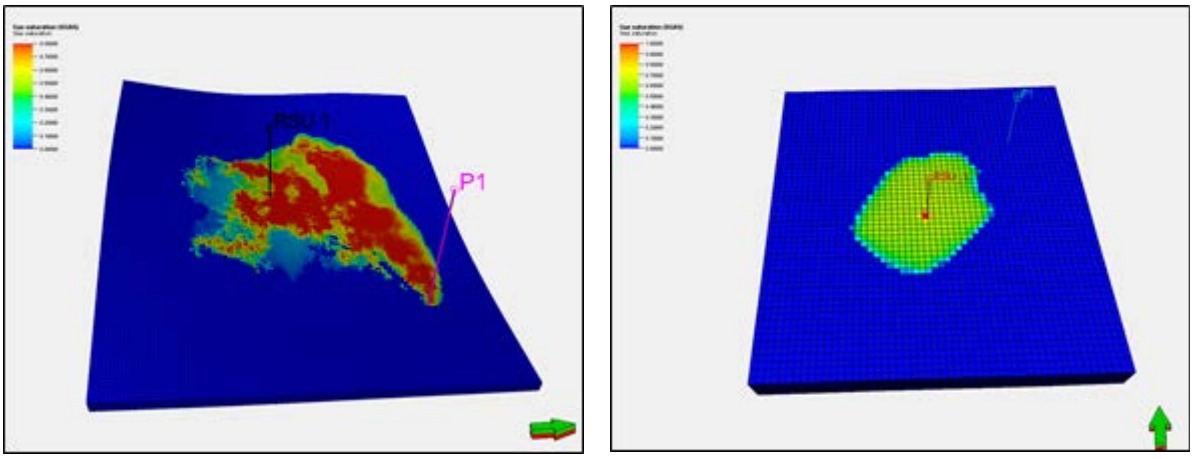

A **B**

Figure 4.5.15. CO_2 saturation distribution for the comparative case after simulation. A: Entrada simulation with one brine production; B: Nugget simulation with one brine production

Section 4.5 Conclusion

In this study, we investigated CO_2 injectivity and storage capacity in the Entrada and Nugget formation using compositional reservoir simulation techniques. The results show that --

For experiments without brine extraction, the target CO_2 storage capacity cannot be reached. For the Entrada Sandstone, the initial CO_2 injection rate is 5282 MSCF/day, which is smaller than the targeted CarbonSAFE injection rate. CO_2 injection rate decreases immediately after injection, and the overall injectivity within the Entrada is smaller due to reservoir properties, such as permeability and formation thickness. Relative to the Entrada formation, CO_2 injectivity within the Nugget Sandstone is much higher, showing it has more feasibility for injection. However, even the Nugget Sandstone would need to include brine co-production wells and several injector wells to reach the CarbonSAFE Phase I target storage capacity. Single injector well experiments prove that it will likely be necessary to control reservoir pressure by extracting reservoir brine in order to hit target injection rates with the least number of wells.

Pressure management by extracting brine during or after CO_2 injection is critical, as it also increases CO_2 injectivity and storage capacity. The designated CO_2 target injection rate can be reached for the Nugget Sandstone, and the reservoir pressure keeps constant after reaching a plateau. On the other hand, the designed injection rate for the Entrada formation will not be reached due to lower permeability, porosity and thickness, which limits CO_2 injectivity. Total CO_2 injection volume of the Entrada formation is 0.15 Mt without brine co-production and 1.2 Mt with brine co-production. However, the geologic heterogeneity of the Entrada formation makes it a great target formation for further CCS research, such as CO_2 migration in heterogeneity conditions. For the Nugget Sandstone, total CO_2 injection volume is 8.9 Mt without brine co-production and 15.0 Mt with brine co-production.

Heterogeneity of reservoir properties, like porosity and permeability affect CO_2 migration pathways and determine the overall CO_2 plume shape. Permeability within the Entrada is more heterogeneous, resulting in an irregular CO_2 plume, while the shape of the CO_2 plume within the Nugget formation is more regular (circular). In addition, the heterogeneity of reservoir properties accelerates CO_2 migration through high permeable pathways. As CO_2 viscosity is smaller than that of formation water, an unstable displacement of CO_2 creates an uneven CO_2 plume due to viscous fingering. CO_2 breaks through early if permeability

between the injector and the producer is high, such as the case within the Entrada formation, which reduces overall CO_2 storage capacity.

Regarding Pre-feasibility Storage Capacity Assessments of the Weber Sandstone and Madison Limestone, Wyoming

Regional geological CO_2 storage capacity assessments and numerical injection simulations investigated in previous studies at the study site (Surdam and Jiao, 2007; Surdam et al.2009, Stauffer et al., 2009b) suggest that geologic heterogeneity creates one of the largest uncertainties with respect to storage capacity. Heterogeneities in porosity and permeability are indicated to be the two most important variables, influencing storage capacity estimates, injection feasibility, CO_2 plume migration pathway, sealing strata integrity, reservoir pressure and displacement fluid management, and risk assessment. To evaluate uncertainties with respect to commercial-scale injection in deep reservoirs (Weber and Madison formations), heterogeneous property models were developed using core data, petrographic observations, laboratory measurements, log data, and seismic attribute data which then provided the basis simulation investigations. Simulations for these reservoirs were run over longer time scales to help understand the impacts to reservoir and seal pressure over differing rates, as these were assumed to be the site's largest risk.

Modeling domains and dynamic injection simulations

The simulation domain is 8 km (x) × 8 km (y) × 3.6 km (z), and is discretized into 291,954 tetrahedral nodes with horizontal spacing of 150 m and 37.5 m around the injection well. The variable vertical resolution is reduced to 10 m in order to capture relative small vertical correlation length reservoir and seal formations. The formations dip to the southeast at an angle of 5 degrees and an azimuth of 130 degrees. Injection of CO_2 into the Weber Sandstone and Madison Limestone is assumed to be at a constant temperature (45 ◦C) and a constant injection pressure of 18.5 MPa at the well head. Injection pressure at the penetrated reservoirs is below 65% lithostatic, and is comparable to the maximum sustainable injection pressure estimated by Rutqvist et al. (2007), who analyzed coupled fluid flow and geomechanical fault-slip under conditions of hypothetical compression and extension stress.

The bottom of the simulation domain is a designated no-flow boundary. The top and west and south boundaries of the simulation domain are designated open for flow in and out. Down dip boundaries to the north and east are closed (i.e. designated no-flow). Constant temperatures are held at the top (54°C) and bottom (110°◦C) of the domain, which is equivalent to a specified geothermal gradient of 23°C /km. The fixed side boundaries will allow for an estimate of the amount of water that must be produced to ensure that the injection site does not impact surrounding parcels of land (i.e. plume is contained). Initial CO_2 concentrations in injection well nodes were set at zero. Simulations incorporate the CO_2 density model (Duan et al., 2008) and solubility model of CO_2 in brine (Duan et al., 2006) into transport models.

CO_2 Storage feasibility assessments of the Weber Sandstone and Madison Limestone

Simulations on injection into the Weber Sandstone show that porosity and permeability have a significant effect on injection feasibility. Injection rates of 1 Mt/year, 0.75 Mt/year, 0.5 Mt/year, and 0.3 Mt/year were investigated, but the rate of only 0.3 Mt/year appears feasible. Higher injection rates caused the simulation to fail due to elevated formation pressure. With the injection rate of 0.3 Mt/year, 15 Mt CO2 could be feasibly stored within the Weber Sandstone over 50 years (~7.5 t over the 25 year lifespan of CarbonSAFE), though 19 Mt of formation water must be removed (Figure 4.5.16). The pressure changes are not uniformly distributed and mainly occur around the injection well and in the down dip directions where boundaries are closed. There are no pressure elevations in the up dip directions where the boundaries are open to fluid flow (Figures 4.5.17 and 4.5.18).

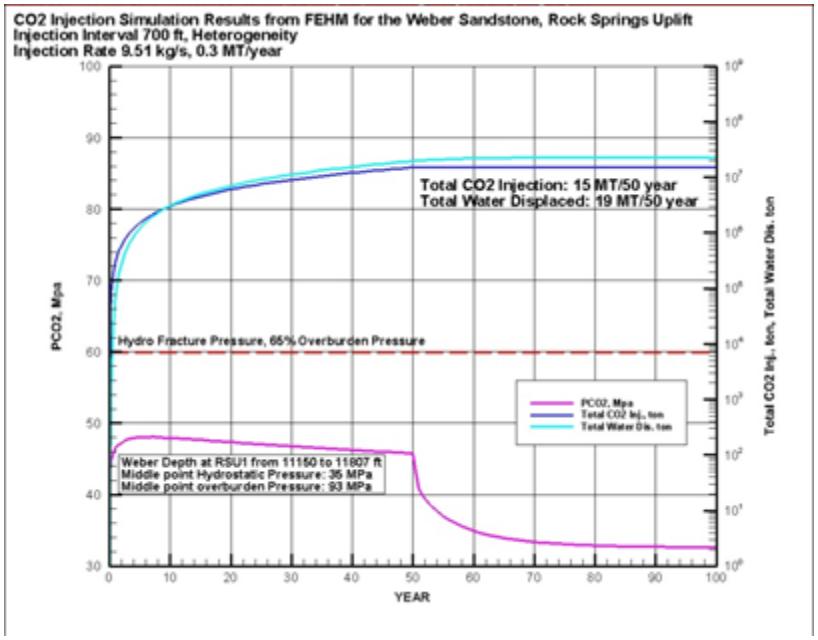

Figure 4.5.16. FEHM CO_2 injection simulation results for the Weber Sandstone. The injection rate of 9.51 kg/s is constant for 50 years, and monitored 50 years post CO_2 injection

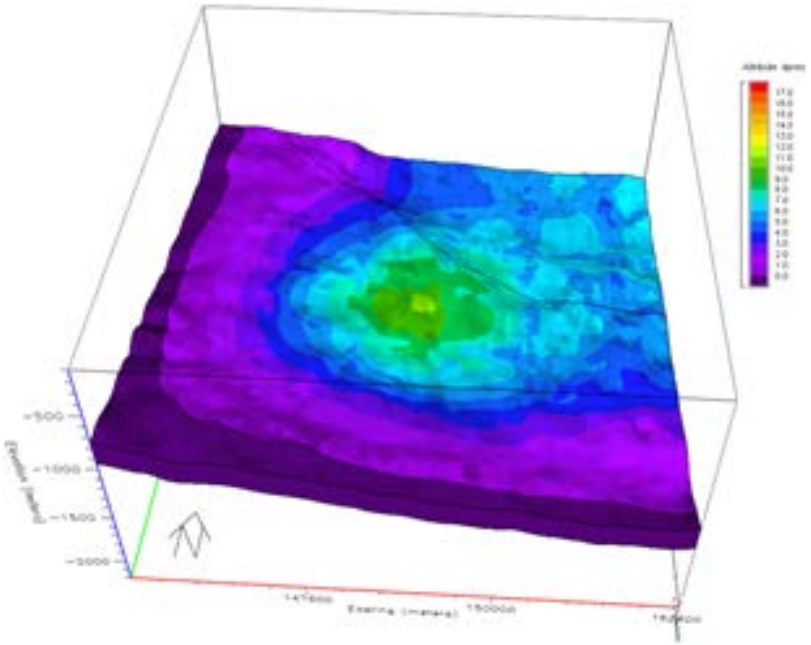

Figure 4.5.17. The pressure changes within the Weber reservoir at the end of the CO_2 injection simulations

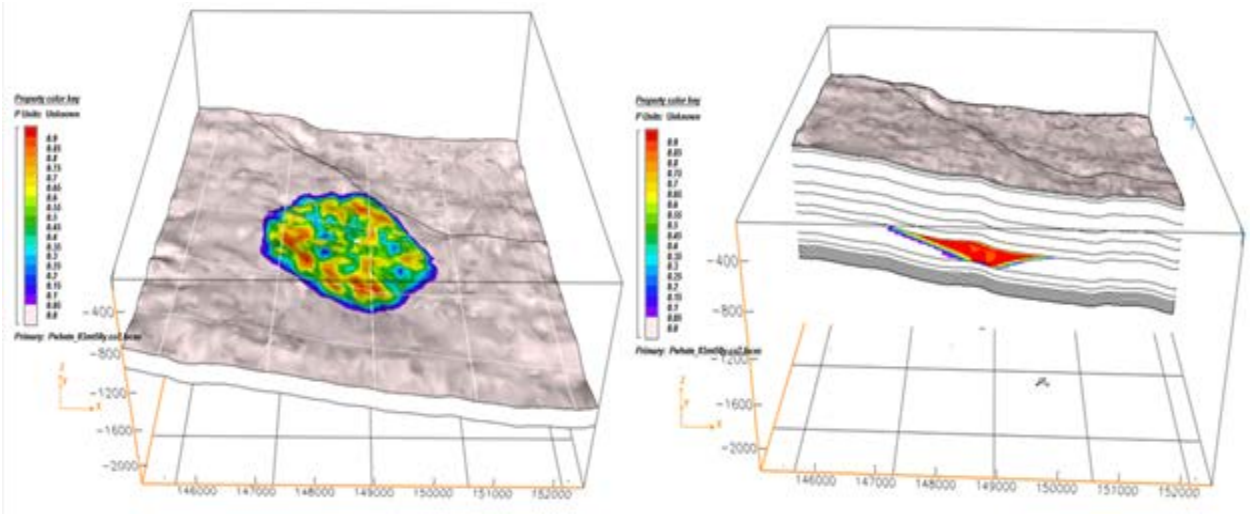

Figure 4.5.18. The incline view (A) and cross section of the CO_2 plume in the Weber Sandstone after 15 Mt CO_2 was injected into the reservoir

Relative to the Weber Sandstone, the Madison Limestone appears to provide an injection reservoir that is more feasible for CCS. Reservoir property within the Madison Limestone are highly heterogeneous and captured in the model: porosity ranges from less than 1% to over 20%, and permeability ranges from 0.001 md to over 100 mD. Simulations focused on an injection interval of 250 feet in the middle Madison Limestone. Injection response was tested using three wells located within the higher, medium, lower reservoir quality areas in an effort to fully test feasibility (Figure 4.5.19).

Though injection works better in the area of high porosity and permeability, formation water must be produced to create accommodation space and to keep the reservoir pressure below the fracture pressure in all three scenarios. Reservoir pressures increase rapidly at the start of injection in all scenarios, and quickly attenuates to the reservoir hydrostatic pressure about 10 years after injection ceases. Injectivity and storage capacities differ significantly among the three wells. At the highest reservoir quality well, 50 Mt CO_2 could be injected and safely stored in the Madison Limestone during a 50 year period with an injection rate of 31.71 kg/s and 57 Mt of formation water displaced (Figure 4.5.20). For the medium reservoir quality well, only 25 Mt CO_2 could be injected and safely stored in the Madison Limestone during a 50 year period with an injection rate of 15.85 kg/s and 25 Mt of formation water displaced (Figure 4.5.20). At the lowest reservoir quality well, only 10 Mt CO_2 could be injected and safely stored in the Madison Limestone during a 50 year period with an injection rate of 6.34 kg/s and 12 Mt of formation water displaced (Figure 4.5.20).

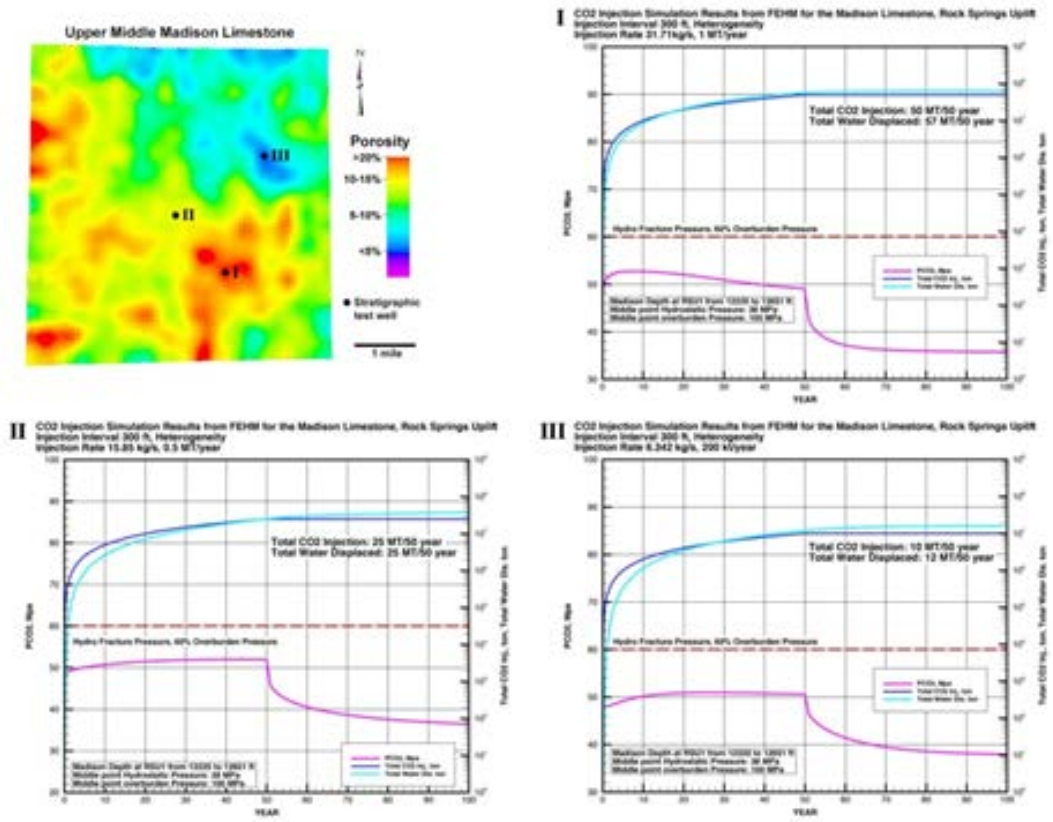

Figure 4.5.19. FEHM CO_2 injection simulation results for the Madison Limestone, using three wells and injection rates of 31.71 kg/s, 15.85 kg/s, and 6.34 kg/s (I, II and II respectively). Note that the reservoir pressures elevate quickly as injection starts, but kept below the hydro-fracture pressure threshold due to co=production of formation brines. After injection ceased, the reservoir pressure attenuated back to original pressure within 10 years

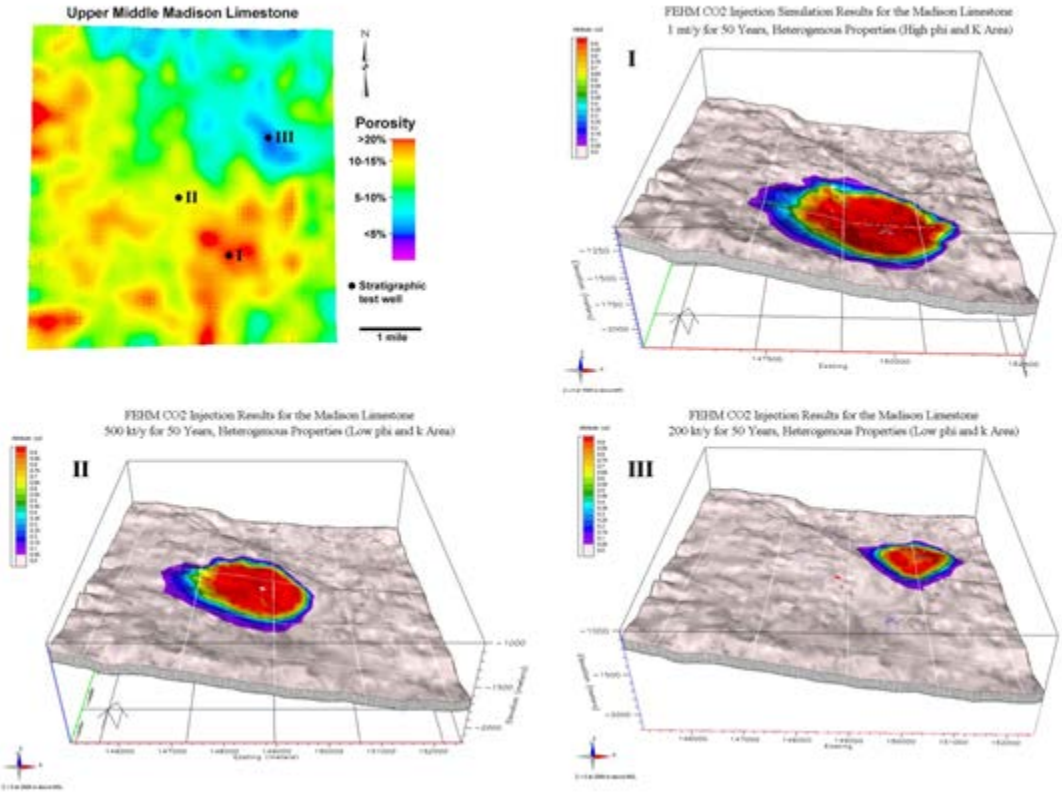

Figure 4.5.20. The CO_2 plume distributions using injection rates of 1 Mt/year in a single injection well in the higher reservoir quality area (I), 0.5 Mt/year in the medium reservoir quality area (II), and 0.2 Mt/year in the lower reservoir quality area (III)

The plumes of injected CO_2 are shaped differently relative to the rate and well placement (Figure 4.5.20). CO_2 plumes in all scenarios show some expansion at the plume top due to buoyancy. None of the plumes pass the domain boundary.

***

Reservoir heterogeneity has a significant effect on CO_2 injectivity and storage capacity of the targeted saline aquifers, and well injectivity is highly dependent on the local permeability distribution in the storage formation. Therefore, pre-feasibility studies should focus on determining the best reservoir zones within a study area, and build experiments with those parameters. For the middle Madison limestone and selected interval (eolian facies) in the Weber Sandstone with higher quality reservoir domains, the injection rate can be as high as 1 Mt per year, whereas in the lower quality reservoir domains, the injection rate could be lower than 0.2 Mt per year. Coupled with modeling done on the Nugget and Entrada reservoirs, we suggest that the Madison and Nugget formations are feasible targets for injecting 25+ Mt over 25 years within the confines of the study site, with brine co-production identified as the best way to reduce pressure risk, control plume migration and optimize storage potential.

Section 4.5 References

Bowker, K.A., and W.D. Jackson, 1989, The Weber Sandstone at Rangely Field, Colorado: in Coalson, E.B. et al, eds., Petrogenesis and petrophysics of selected sandstone reservoirs of the Rocky Mountain region, Rocky Mountain Association of Geologists, p. 65-80.

Duan, Z., Hu, J., Li, D., Mao, S., 2008. Densities of the CO2-H2O and CO2-H2O-NaCl systems up to 647 K and 100 MPa. Energy & Fuels 22, 1666–1674.

Duan, Z., Sun, R., Zhu, C., Zhou, I.-M., 2006. An improved model for the calculation of CO2 solubility in aqueous solution containing Na+, K+, Ca2+, Mg2+, Cl−, and SO42−. Marine Chemistry 98, 131–139.

Han, W.S., Stillman, G.A., Lu, M., Lu, C., McPherson, B.J., Park, E., 2010. Evaluation of potential nonisothermal processes and heat transport dur-ing CO2 sequestration. Journal of Geophysical Research 115, B07209, http://dx.doi.org/10.1029/2009JB006745.

Hein, J.R., Perkins, R.B., McIntye, B.R., 2004. Evolution of thought concerning the origin of the phosphoria formation, western US phosphorate field. In: Hein, J.R. (Ed.), Life Cycle of the Phosphoria Formation: From Deposition to Post-Mining Environment. Elsevier, pp. 19–42.
Love et al, 1993Love, J. D., Christiansen, A. C., and Ver Ploeg, A. J., 1993, Stratigraphic chart showing Phanerozoic nomenclature Survey Map Series MS-41, 1 sheet., 1 p.

Miller, T.A., V. V. Vessilinov, P.H. Stauffer, K. H. Birdsell, and C. W. Gable, 2007, Integreation of geologic frameworks in meshing and setup of computational hydrogeologic models, Pajarito Plateay, New Mexico. New Mexico Geological Society Guide Book, 58th Field Conference, Geology of the Jemez Mountains Region III.

Neuzil, C.E., 1994. How permeable are clays and shales? Water Resources Research 30, 145–150.

Piper, D.Z., Link, P.K., 2002. An upwelling model for the Phophoria sea: a Per-mian, ocean-margin sea in the northwest United States. AAPG Bulletin 86 (7), 1217–1235.
Pruess, K., Muller, N., 2009. Formation dry-out from CO2 injection into saline aquifers: 1. Effects of solid precipitation and their mitigation. Water Resources Research 45, W03402, http://dx.doi.org/10.1029/2008WR007101.

Stauffer, P.H., Surdam, R.C., Jiao, Z., Miller, T.A., Bentley, R.D., 2009a. Combining geologic data and numerical modeling to improve estimates of the CO2 sequestration potential of the Rock Springs Uplift, Wyoming. Energy Procedia 1, 2717–2724.

Stauffer, P.H., Viswanathan, H.S., Pawar, R.J., Guthrie, G.D., 2009b. A system model for geologic sequestration of carbon dioxide. Environmental Science & Technology 43, 565–570.
Stauffer, P.H., Stein, J.S., Travis, B.J., 2003. The correct form of the energy balance for fully coupled thermodynamics in water. Los Alamos National Laboratory Report, LA-UR-03-1555, pp9.

Surdam, R.C., Jiao, Z., Stauffer, P.H., Miller, T., 2009. An integrated strategy for carbon management combing geological CO2 sequestration, displaced fluid production, and water treatment. Wyoming State Geological Survey. Challenges in Geologic Resource Development No. 8.

Surdam, R.C., Jiao, Z., 2007. The Rock Springs uplift: an outstanding geological CO2 sequestration site in southwest Wyoming. Wyoming State Geological Survey. Challenges in Geologic Resource Development No. 2.

Surdam, R.C., Jiao, Z., Stauffer, P.H., Miller, T.A., 2011. The key to commercial-scale geological CO2 sequestration: displaced fluid management. Energy Procedia 4, 4246–4251.

Robert C. Burruss, Sean T. Brennan, Philip A. Freeman, Matthew D. Merrill, Leslie F. Ruppert, Mark F. Becker, William N. Herkelrath, Yousif K. Kharaka, Christopher E. Neuzil, Sharon M. Swanson, Troy A. Cook, Timothy R. Klett, Philip H. Nelson, and Christopher J. Schenk, 2009, Development of a Probabilistic Assessment Methodology for Evaluation of Carbon Dioxide Storage,USGS Open File Report 2009-1035

Yang, Y., Aplin, A.C., 2010. A permeability-porosity relationship for mudstone. Marine and Petroleum Geology 27, 1692–1697.

Zyvoloski, G.A., Robinson, B.A., Dash, Z.V., Trease, L.L., 1997. Summary of the models and methods for the FEHM application – a finite element heat-and mass-transfer code. Rep. LA-13307-MS, Los Alamos National Laboratory, Los Alamos, New Mexico.

Zyvoloski, G. A., Z. V. Dash, and S. Kelkar, “FEHM: Finite Element Heat and Mass Transfer Code,” LA-11224-MS (1988). NNA.19900918.0013.

Section 4.6: Identification of Future Characterization Activities

Fred McLaughlin[1] and Dylan Esquivel[2]
1. Center for Economic Geology Research
School of Energy Resources, University of Wyoming
1020 E. Lewis Street, Energy Innovation Center
Laramie, WY 82071
2. WellDog
1525 Industry Dr, Laramie, WY 82070

To advance the program's objective of validating commercial-scale CO_2 sequestration at the study site beyond pre-feasibility, the following characterization activities are described. Future characterization activities will focus on a study area to the west/southwest of JBP (Figure 4.6.1). To meet future phase project objectives of characterizing lesser-defined Mesozoic reservoir/seal couplets, we suggest drilling a stratigraphic test well through the Nugget Sandstone at a location east of the JBP (Figure 4.6.1). The objective of the stratigraphic test well are two-fold with respect to characterization; to collect core and fluid data from understudied Mesozoic reservoirs and to perform downhole, in-situ reservoir and seal tests to characterize responses to fluid injection and stress.

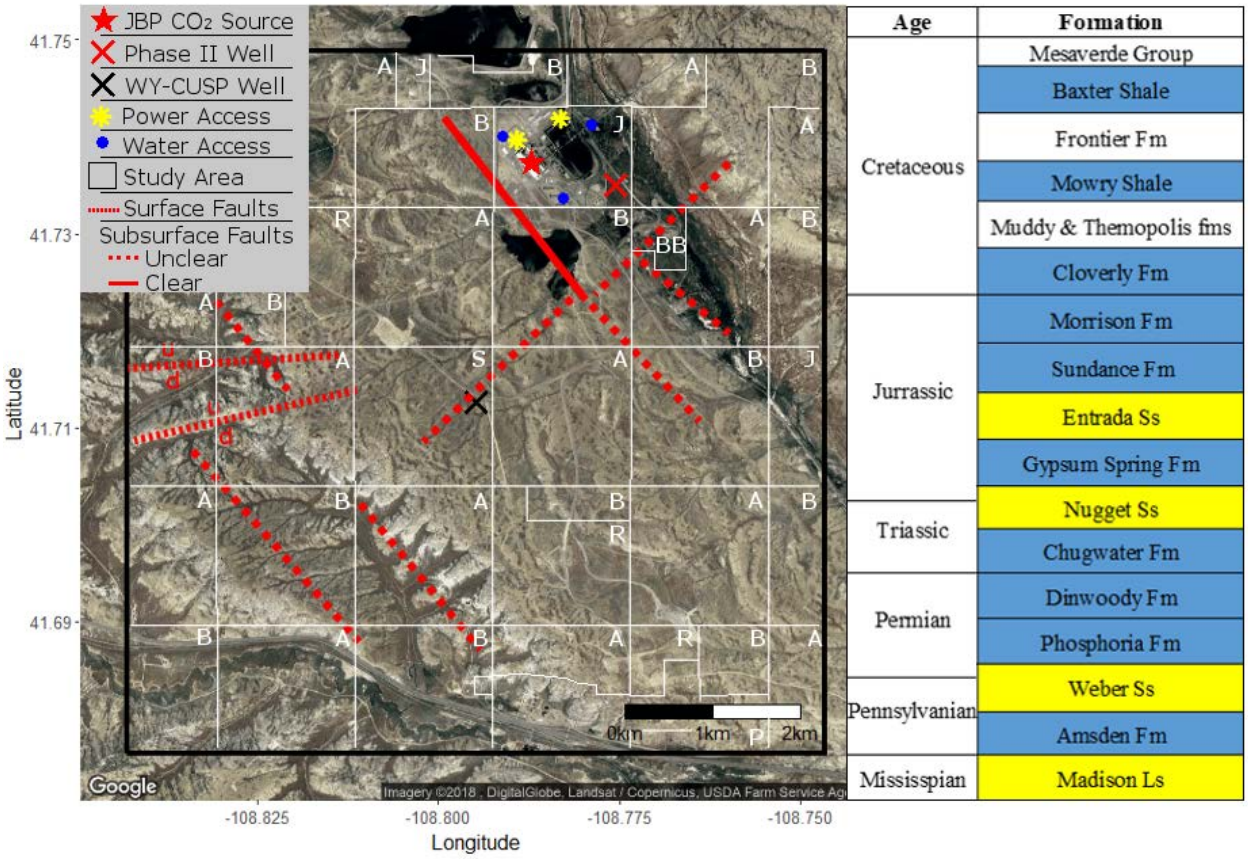

Figure 4.6.1. The Study Area within the 25 square mile seismic survey surrounding the previously drilled WY-CUSP Test Well. Surface ownership delineated in white includes (J) Jim Bridger, (B) BLM, (A) Anadarko, (S) State, (BB) Black Butte, and (P) Other Private property. Ages and formations within the storage complex are shown on the right, including the target reservoirs (yellow) and seals (blue). The proposed future phase characterization well (labeled Phase II well) location on JBP property is marked

with a red "x". Access to utilities (power and water) are also marked. Two naturally-cemented surface faults were mapped during Phase I investigations (fine-dashes). Seismically derived faults have been projected to the surface but occur at varying depths.

Future phase characterization should include core collection and analysis. Core samples should be collected from understudied Mesozoic reservoir intervals (Entrada and Nugget sandstones) and confining unit intervals (Baxter and Mowry shales and the Gypsum Springs formation). Collected core should be professionally processed (e.g., slabbing, cataloging, and spectral log analysis for borehole log correlations). Once processed, the core should be analyzed for petrographic, petrophysical, geomechanical and geochemical character to better understand factors that influence storage capacity and the long-term containment of CO_2. Rock analyses should include: (1) routine porosity and permeability measurement paired with mercury injection capillary pressure (MICP) tests; (2) optical microscopy thin section analysis; (3) x-ray fluorescence; (4) x-ray diffraction coupled with Rietveld refinement; (5) scanning electron microscopy (FE SEM); (6) geomechanical analysis using a triaxial press; (7) steady and unsteady-state relative permeability core plug CO_2 flooding (including pre- and post-flood Nuclear Magnetic Resonance (NMR)) from reservoir intervals; and (8) fluid inclusion volatile assessment of cuttings from the future phase stratigraphic well and the WY-CUSP test well. These analyses will provide/identify porosity (via analyses 1 and 7), pore distribution (via analyses 1, 2, 5), permeability (via analyses 1,7), sealing capacity (via analyses 1 and 7), CO_2 injection response and trapping mechanisms (via analysis 7), mineral character and distribution (via analyses 2, 3, 4, 5), diagenesis and thermal history (via analyses 2, 4, 5), mechanical strength and fracture gradient (6), and confinement history of reservoirs within the Study Area (via analysis 8).

Formation fluids should be sampled from the Nugget and Entrada sandstones. Characterization of the formation fluid would provide the baseline for UIC well permitting requirements and MVA. It may also help characterize reservoir confinement, and is a necessary input for core experiments and dynamic modeling. Fluid analyses should include: (1) field measurements (e.g., pH, oxidation reduction potential, total dissolved solids, temperature); (2) major, minor, and trace element geochemistry; (3) isotopic ratios (O, H, C, and Sr); and (4) exsolved gases. Fluid measurements from the Mesozoic reservoirs should be compared to fluid collected from the WY-CUSP test well, which show that the site's deeper reservoirs are sequestered from inter-formational mixing and meteoric recharge; similar evaluations must be performed for the site's Mesozoic reservoirs for future phase characterization.

Petrophysical well logs should be acquired from the future phase well, with the following logs identified as necessary for advancing characterization: spectral gamma ray, triple combination, VSP, dipole sonic, electric log, nuclear magnetic resonance, pulsed neutron and cement bond. These data should be correlated with core and seismic data, and interpreted to populate geologic property models.

One of the greatest data needs for advancing future characterization activities at the study site were determined to be downhole well tests. Well tests: (1) provide insight into reservoir characteristics at a distance from the wellbore, thereby dramatically improving understanding of target formation behavior over time during injection; and (2) would help determine potential flow boundaries within the Nugget Sandstone and other reservoirs enhancing subsurface characterization data. Understanding reservoir compartmentalization relative to fault character (permeable, impermeable, semi-permeable) and spacing is a critical component for determining injection, risk mitigation and pressure management strategies. Production and injectivity tests should be performed to allow for direct calculation of near-well permeability, anisotropy, radius of investigation (influence), reservoir fracture gradient and maximum allowable rates for production or injection. Monitoring data (both pressure and temperature) can be collected remotely from a permanent downhole gauge before, during and after well testing. These data

will be used to: (1) refine pressure management and MVA strategies; and (2) inform dynamic simulations. The monitoring equipment also could be repurposed in future project phases.

After collecting future phase characterization data, refined storage estimates, CO_2 plume migration rate and extent, risk assessment and site performance strategies should be determined by updating pre-feasibility heterogeneous property models and performing dynamic injection simulations. Injection simulations should be performed using Eclipse and/or Computer Modelling Group's software packages and to evaluate the response of injecting 50+ million metric tons of CO_2 over 25 years relative to the new data collected from core, fluid, well logs and in-situ well tests from the future phase well. Outcomes from these models should then be used to determine additional future phase activities, such as determining optimal well spacing, safe CO_2 injection volumes and rates, well quantity, and help to engineer well completion strategies for utilizing stacked reservoirs for storage. Risk models should be updated using the NRAP-IAM-CS tool.

To help determine the capital needs of future phase activities, final costings and design of a stratigraphic test well were put collected with respect to downhole testing, sampling and completion. The well was designed to be utilized beyond next phase and is fully cased throughout for potential reuse as an injection, monitoring or production well. A number of tests were included in future phase costs, as one of the primary purposes of this well would be testing the boundaries of the reservoir systems. The understanding of boundaries is important to determine the potential size of the compartment targeted for greenhouse gas sequestration, along with confirming that the boundaries, in this case faults, are sealing. We expect that both production and injectivity tests will allow direct calculation of the permeability, radius of investigation (influence) and maximum allowable rates for production or injection. These tests, along with the proposed rig spec, coring, logging, and other formation tests are including in the costing and were anticipated in the wellbore design and completion costs (Tables 4.6.1 and 4.6.2; Figure 4.6.2).

Item	Days	Qty	Unit Price	CPI ADJ	Industry ADJ	Cost	Cost Share	Required Funding	Totals
GrandTotal	**80**			**5.1%**	**28.6%**				**3,796,188**
Operator Representative (Principal)	55		2,000			110,000	22,000.00	88,000	
Operator Representative (Senior)	55		1,600			88,000	17,600.00	70,400	
Wellsite Geologist	115		1,200			138,000	27,600	110,400	
Drilling Engineer	115		2,500			287,500	57,500	230,000	
Per diem lodging	340		100			34,000		34,000	
Per diem meals	340		59			20,060		20,060	

Wellsite Professional Services									**552,860**
Conductor Casing		120	42			5,100		5,100	
Surface Casing		2000	28			57,400		57,400	
Production String Casing		10000	14			142,600		142,600	
Conductor Cementing		1	11,781			11,781		11,781	
Surface Cementing		1	35,379			35,379		35,379	
Production String Cementing		1	57,648			57,648		57,648	
Casing									**309,908**
Mobilization/Demobalization		1	210,000			210,0000		210,000	
Crew Subsistence	80	18	100			8,000		8,000	
Drilling Rig	80		14,900			1,192,000		1,192,000	
17.5 in. GTX Steeltooth Tricone Drill Bit, IADC 115	1	28,200			28,200		28,200		
12.25 in. GT Steeltooth Tricone Drill Bit, IADC 117		2	14,250			28,500		28,500	
8.5 in. GX Steeltooth Tricone Drill Bit, IADC 117			8,900			35,600		35,600	
Drill Rig Related									**1,502,300**
Solids Control Chemicals		1	3,000		858	3,858		3,858	
Mud		1	98,837		28,294	127,131		127,131	
Water / Mud Disposal		3000	4		1	15,435		15,435	

Cuttings Hauling		40	110	5		4,623		4,623	
Solids & Control									**151,049**
Infrastructure		25	495	25		13,003		13,003	
Pads/Roads		1	80,000			80,000		80,000	
Crew Trailers		34	75	3		2,679		2,679	
Wellhead		1	17,650			17,650		17,650	
Site Reclamation		1	19,908	1,010		20,919		20,919	
Well Site Related									**134,252**
OH Logging Services		1	270,000			270,000		270,000	
CH Logging Services		1	750,000			75,000		75,000	
DST		2	65,000			130,000	30,000	100,000	
Water Samples		4	2,600		744	13,377		13,377	
Coring		1	200,000			200,000		200,000	
Stimulation Treatment		1				50,000		50,000	
Logging Services									**708,377**
Completion Rig		1	78,440		22,455	100,895		100,895	
Perforating		1	35,000			35,000		35,000	
Plug Cement		1	50,000		14,313	64,313		64,313	
Plug Rig		1	78,440		22,455	100,895		100,895	
Permanent Downhole Gauges		1	40,207			40,207		40,207	
CTU		5	6,000			30,000		30,000	
Completions Related									**371,311**
Fuel		15000	2	0.11		32,626		32,626	
Pump		0	356,500		102,057				
Safety		1	31,883	1,618		33,501		33,501	

Miscellaneous									**66,128**

Table 4.6.1. Costs associated with drilling a future phase well at the study site, as well as costs associated with downhole testing and sample collection.

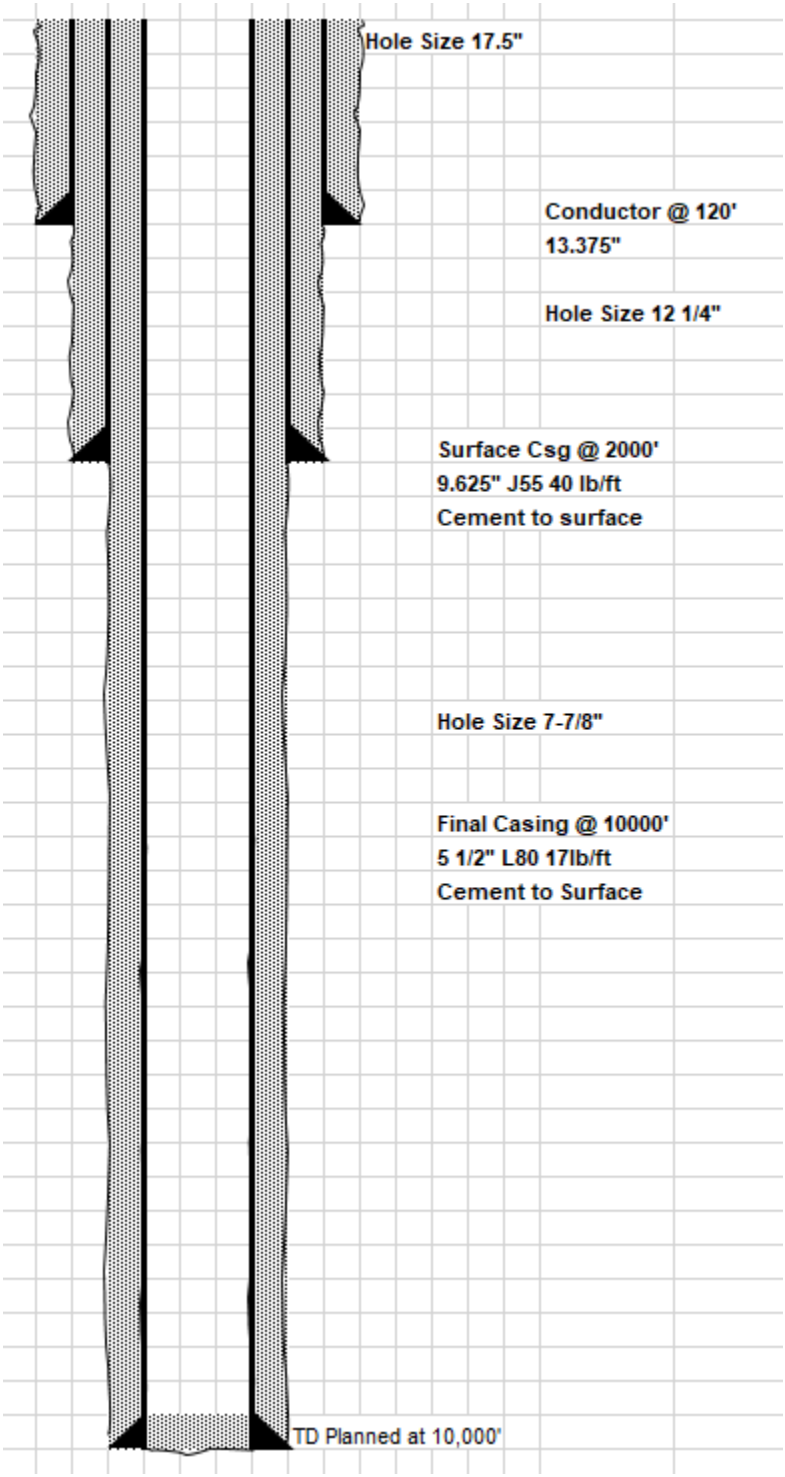

Figure 4.6.2. Well schematics diagram of a future phase well to be placed adjacent to JBP (Figure 4.6.1). This well would be anticipated to be completed at 10,000' in order to focus study on the site's Mesozoic reservoirs. Well design favors reuse in additional phases (Table 4.6.1).

Rig Specs: Capable of efficiently drilling depths of 13,000'
Using 4-1/2" drill pipe
National-55 Drawworks with Parmac 342-A Hydromatic Brake powered by Three D-353E Caterpillar Diesel Engines rated 425 HP each with National C-245 -80 Torque Converters.
136' x 18.6' BHL International Inc. Cantilever Mast with 12' clearance under Rotary Beams. Capacity 550,000#.
NOV TDS – 11SA Top Drive System
2-Emsco F-1000 6" x 10" Triplex pumps, independently driven by a Caterpillar 3508 Diesel engine rated at 915 HP.
20-1/2" Emsco Rotary Table.
BOPs - To meet operator's requirements
300 KW Three Phase 110-480V AC Generator with D353 Caterpillar Engine.
300 KW Three Phase 110-480V AC Generator with D353 Caterpillar Engine.
Vapor Proof Lighting System.
2 - Steel Mud Tanks: 960 Bbl. System.
2 – Brandt 3-panel King Cobra Linear Shakers
6,600' 4-1/2" Grade E 16.60#, 4,960' 4-1/2" Grade E 20#, and 2,000' Grade G 16.60# Drill Pipe with

4-1/2” Extra Hole Connections.
3 - 7 ½” OD X 2 ½” ID X 30’ Long Drill Collars with 6 5/8” Regular Connections.
18 6-3/8” OD x 2-13/16” ID x 30’ long Drill Collars with 4-1/2” Extra Hole Connections.
400 Bbl. Water Tank.
125 HP Boiler.
Skid Mounted Pushers Quarters.

Table 4.6.2. Suggested drilling rig schematics diagram for the future phase well to be placed adjacent to JBP (Figure 4.6.1).

Chapter V: NRAP Modeling and Validation

George J. Koperna, Anne Oudinot
Advanced Resources International, Inc.
4501 Fairfax Drive, Suite 910

Review of NRAP Tools

The United States Department of Energy, National Energy Technology Laboratory (USDOE-NETL) is sponsoring research as part of the Carbon Storage Assurance Facility Enterprise (CarbonSAFE) initiative. This program seeks to mitigate carbon emissions from the burning of fossil fuels and addresses key research gaps in the deployment of large-scale (50+ million metric tons) CCS.

USDOE-NETL requested that awarded projects evaluate a suite of sponsored reduced order modeling tools designed to help stakeholders evaluate and then mitigate potential risks associated with subsurface injection of CO_2. Developed by the National Risk Assessment Partnership (NRAP), these tools assess environmental risks associated with leakage and induced seismicity for reservoirs, confining units, wells, and aquifers. This report outlines their use in relation to the CarbonSAFE Phase I project at UW's RSU study area.

To support this request, this report describes in detail the ten available NRAP reduced-order models, their use, required inputs and the available outputs. Out of the ten tools, only two of the ROMs were further studied in application to the RSU CarbonSAFE project.

With numerical models being generated to assess CO_2 storage capacity in the Entrada formation as part of the Rock Springs Uplift CarbonSAFE Project, the Reservoir Evaluation and Visualization (REV) tool was analyzed with available ECLISPE/ Petrel datasets. The initial phase of the evaluation which consisted in getting the tool to run was made difficult by compatibility issues and the existence of various versions of the tool. Once that issue was resolved, the tool functioned properly. However, the results obtained didn't fully compare with simulator results. While the computed CO_2 saturation and differential pressure plume sizes seem consistent with the reservoir simulation outputs, the visual display of the plumes is faulty and require some support from the NETL NRAP personnel.

WLAT (only focusing on the multi-segmented wellbore ROM option) was chosen for testing because it allows for the modeling of leakage of CO_2 and brine along wells with multiple thief zones. The results suggest that CO_2 migration into overlying zones will be limited and little or no migration is expected into shallow aquifers or to the atmosphere.

5.1 Site Background

The RSU study area is located within the Central Greater Green River Basin, just northeast of Rock Springs, Wyoming (**Figure 5.1**). The site is strategically located near a large diameter CO_2 transmission pipeline as well as PacifiCorp's coal-fired JBP. The study area and its deeper sediments have been characterized, and the Madison and Weber sandstones were found to be a significant storage target. However, these studies indicated deep storage could be cost prohibitive with regard to wellfield development and compression.

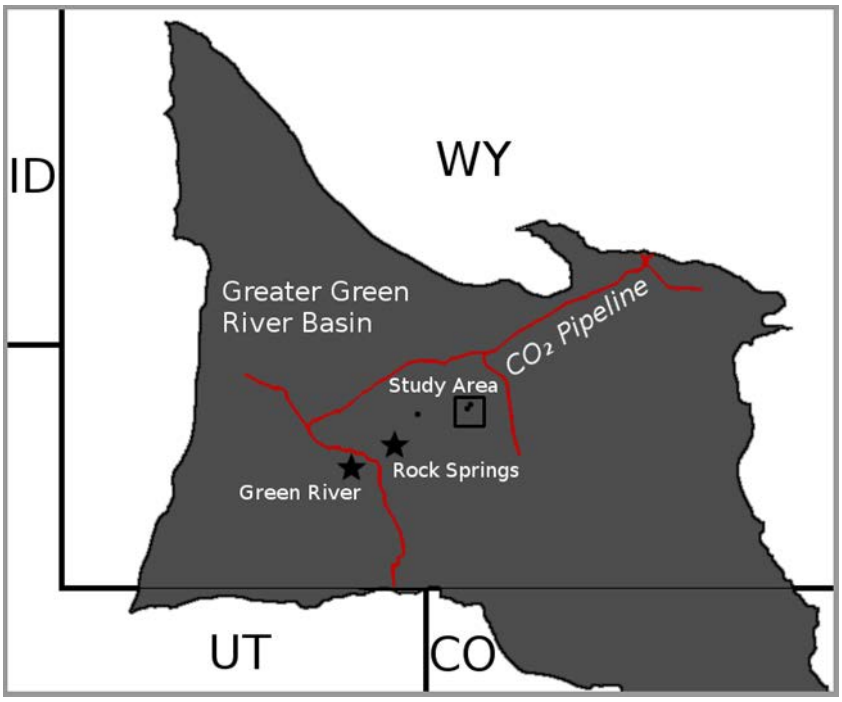

Figure 5.1. RSU Study Area (McLaughlin and Coddington, 2017)

The major goal of this current study is to characterize the shallower subsurface, identifying the formations that may be able to accept 50+ million metric tons of anthropogenic CO_2 and the sealing formations that would trap it in place. Should suitable storage and cap rock formations be identified the Jim Bridger Plant, which is the largest source of anthropogenic CO_2 in the State of Wyoming, along with the plants proximal CO_2 transmission infrastructure, could make this a storage hub for the Rocky Mountain Region.

NRAP Tools

There are ten NRAP tools (listed below) available for use and evaluation of this project. The following sections discuss the tools, their input parameters, and their expected output. Several of the tools were selected to test datasets collected from the ongoing work of the CarbonSAFE Phase I project at the RSU test site. They were the Reservoir Evaluation and Visualization Tool (REV) and the Well Leakage Analysis Tool (WLAT).

NRAP Tools:

- Aquifer Influence Model (AIM)
- Designs for Risk Evaluation and Management (DREAM) Tool
- Ground Motion Prediction Applications to Potential Induced Seismicity (GMPIS)
- Multiple Source Leakage Reduced-Order Model (MSLR)
- NRAP Integrated Assessment Model–Carbon Storage (NRAP-IAM-CS)
- NRAP Seal Barrier Reduced Order Model (NSEALR)
- Reservoir Evaluation and Visualization Tool (REV)*

- Reservoir Reduced-Order Model Generator RROM- Gen
- Short-Term Seismic Forecasting (STSF)
- Well Leakage Analysis Tool (WLAT)*

** Tools that were selected to be tested using datasets from the RSU test site.*

The following discussions highlight use of the two NRAP tools employed in this study. Similar descriptions of the remaining eight tools can be found in the Appendix.

5.2 Reservoir Evaluation and Visualization Tool (REV)

Introduction. The REV tool is a numerical modeling post-processing visualization tool that uses time-lapse CO_2 saturation and pressure outputs from various specific reservoir simulators to generate CO_2 saturation maps and pressure differential (as compared to initial reservoir pressure) maps based on a user-specified threshold. A threshold is being defined as a minimum value for the parameter evaluated. If a grid cell in the model has a value above the user-specified threshold, this cell is considered to be inside the plume.

Input. REV accepts inputs, from eight different simulators listed below. While each simulator is different, REV requires from each two types of information: a grid file (contains description of the model grid) and a dynamic file (contains time-lapse CO_2 saturation and pressure information). Sample files are provided for some of the simulators and their format is also described in the manual.

- Two-Phase Three Dimensional (TP3D),
- Finite Element Heat and Mass (FEHM),
- Computer Modeling Group-Generalized Equation of State Model (CMG-GEM),
- NRAP-Integrated Assessment Model-Carbon Storage (NRAP-IAM-CS),
- Transport Of Unsaturated Groundwater and Heat 2 (TOUGH2),
- Subsurface Transport Over Multiple Phases (STOMP),
- Exploration Consultants Limited Implicit Program for Simulation Engineers (ECLIPSE) and
- PETREL (ECLIPSE's pre and post-processor).

Figure 5.2 shows the REV input/output tab with a drop-down menu to select the simulator (CMG-GEM chosen here as an example). Zipped files can also be loaded into the model and REV will unzip them automatically.

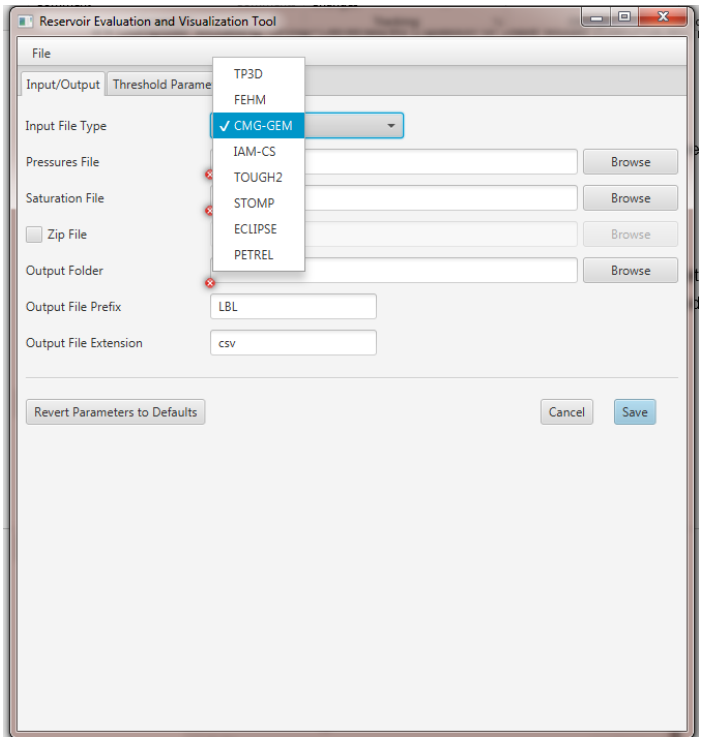

Figure 5.2. REV Input/Output Tab

There are three types of threshold that can be defined by the user.

- critical CO_2 saturation to detect areas of free phase CO_2 in the formation,
- differential pressure to detect areas of elevated pressure, and
- saturation-pressure product.

Multiple thresholds can be specified at the same time, **Figure 5.3.**

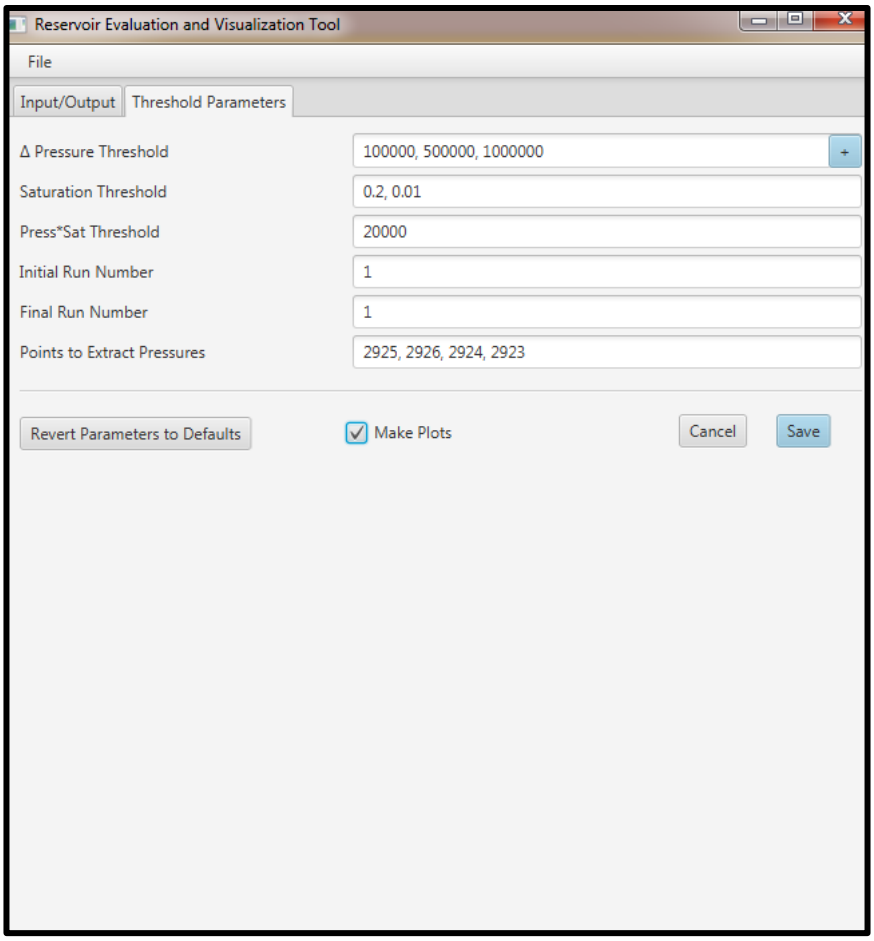

Figure 5.3. REV Threshold Parameters Tab

Output

REV outputs come in two different formats:

- Graphical display of differential pressure and saturation maps versus time. These files will have a png (portable network graphics) extension, **Figure 5.4**. Figure 5.4 shows the evolution of the differential pressure plume (or area of increased pressure of 0.5MPa or more than initial pressure) at various times over the life of the injection project. Any grid block in the plume will be colored in red whereas any grid block outside the plume will be colored in blue.

- Quantitatively, for each threshold input (differential pressure, saturation, and pressure saturation product), a csv (comma separated value) file will be generated with the computed maximum plume area at each time step.

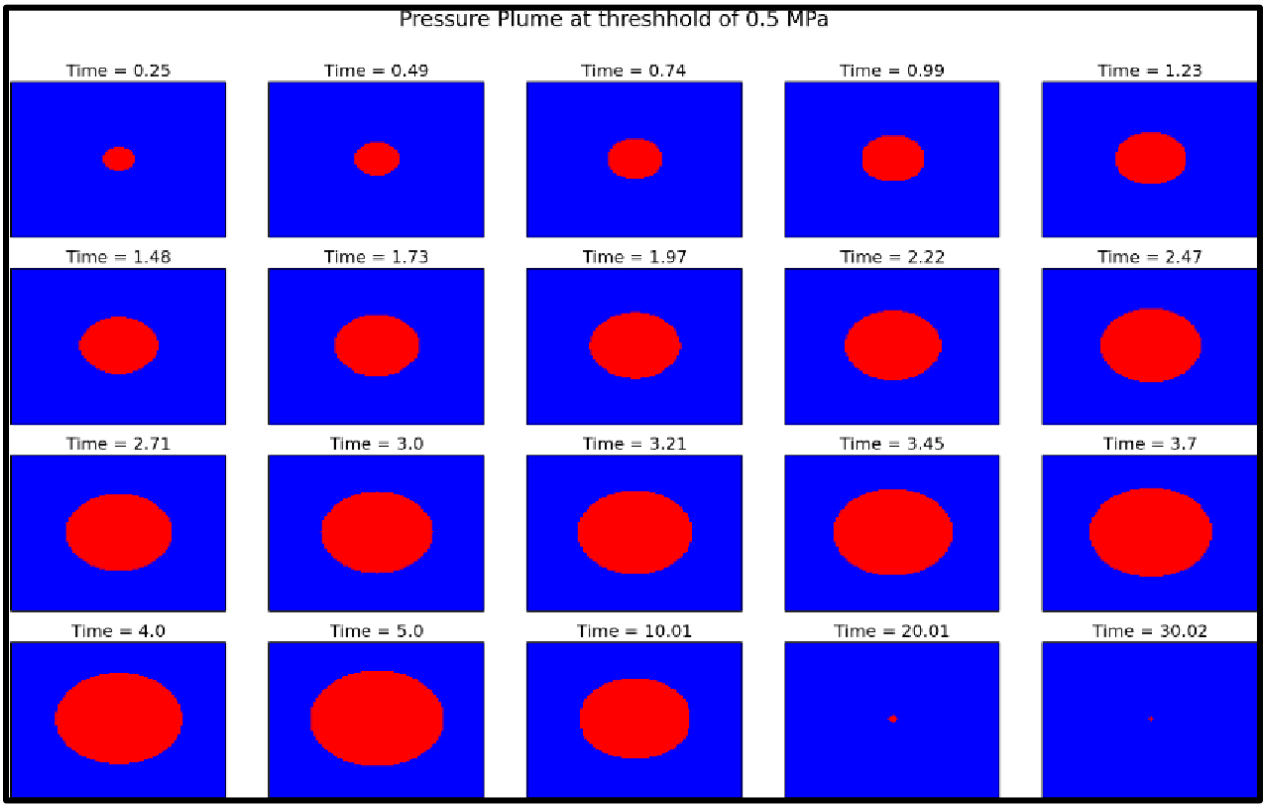

Figure 5.4. Example of Visualization from Sample File– Pressure Plumes

5.2.2 Well Leakage Analysis Tool (WLAT)

Introduction. This standalone tool contains four Reduced Order Models (ROMs) focused on the analysis of wellbore leakage from geologic CO_2 storage operations: (1) Cemented Wellbore Model; (2) Multi-segmented Wellbore Model; (3) Brine Leakage Model; and (4) Open Wellbore Model. For all models, the outputs consist of plots of leakage rates of CO_2 and brine and can be saved in a text file format for external use. **Figures 5.5 to 5.8** show the main input tab for each reduced order model as well as the output plots.

5.2.2.1 Cemented Wellbore Model

The model treats multiphase flow of CO_2 and brine up a leaky well. It is based on a library of simulations which were run with detailed full-physics FEHM (Finite Element Heat and Mass) code (Zyvoloski, 2007)[1]. The FEHM transfer simulations are 3D, multiphase solutions and heat and mass transfer of water and supercritical, liquid and gas CO_2. It assumes that Darcy's flow is applicable to each phase. The model can handle leakage to an overlying aquifer, thief zone or to the atmosphere. The model has some limitations: geochemical and geomechanical reactions (such as CO_2 dissolution in brine) are not taken into account and brine density stays constant with pressure and temperature. Some values are currently hard-wired in this version of the tool (such as aquifer and upper layer characteristics).

The input parameters include the field properties (upper shale, shallow aquifer, thief zone, reservoir and wellbore), and some additional parameters (type of calculation for the leakage and graphic output parameters), **Figure 5.5**.

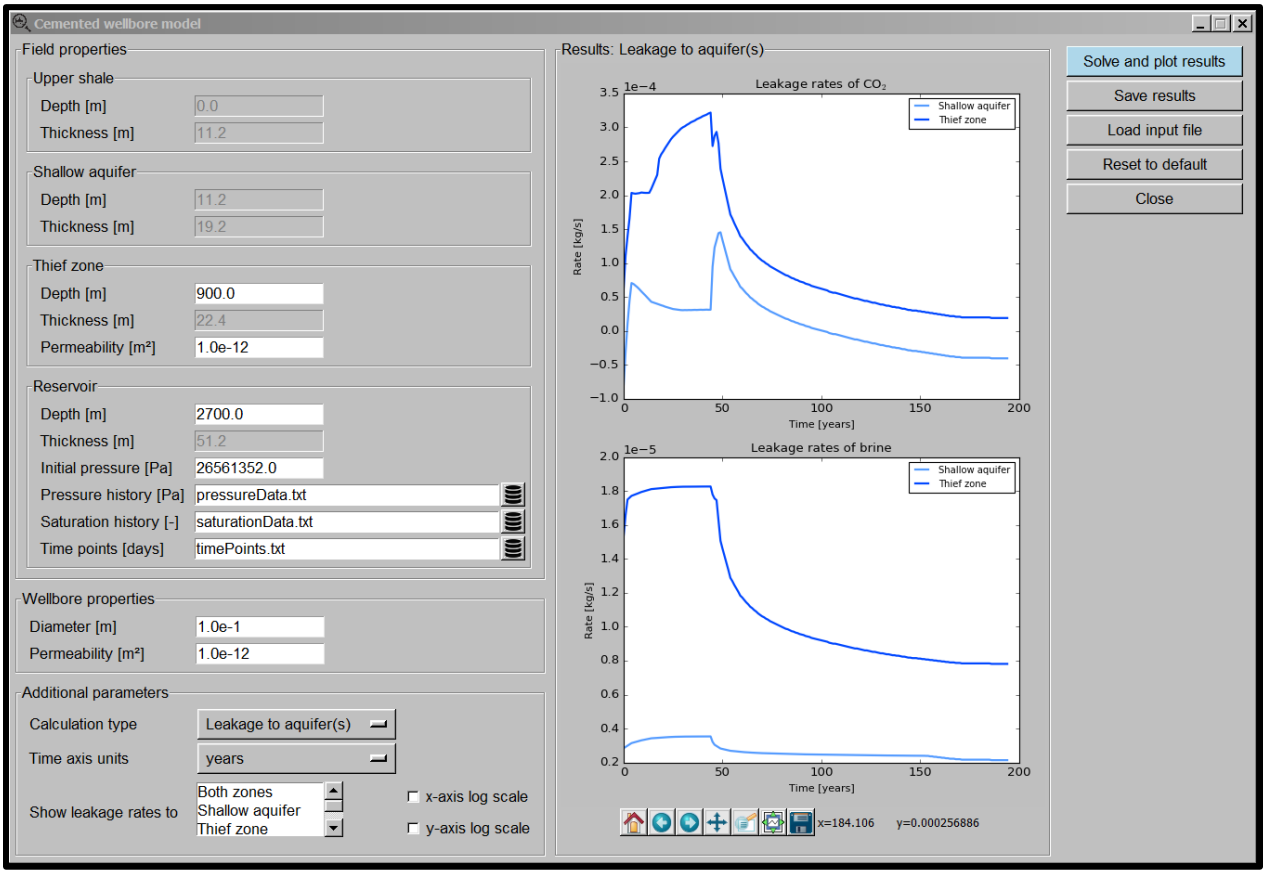

Figure 5.5: WLAT Main Screen for Cemented Wellbore Model

5.2.2.2 Multi-Segmented Well Model

Like the Cemented Well Model, this tool treats multiphase flow of CO_2 and brine up a leaky well but in the presence of multiple aquifers and thief zones. The model is based on work by Nordbotten and Celia (2005)[2]. The two main assumptions of the model are vertical equilibrium of the pressure distribution and the existence of a sharp interface between the CO_2 and the brine phase. The model is focused on flow across large distances and hence does not account for leakage in flow paths such as cement fractures, cracks or annuli. Additionally, it is assumed that leakage occurs in the annulus between the outside of the casing and the borehole. Each individual formation penetrated by the well is assigned an effective permeability. One dimensional multi-phase version of Darcy's law is used to represent flow along the leaky well.

The inputs for the multi-segmented well model are divided into 8 sections including but not limited to shale layers (up to 30) characteristics, aquifers' characteristics, reservoir characteristics, leaking well, CO_2 and brine properties, **Figure 5.6**.

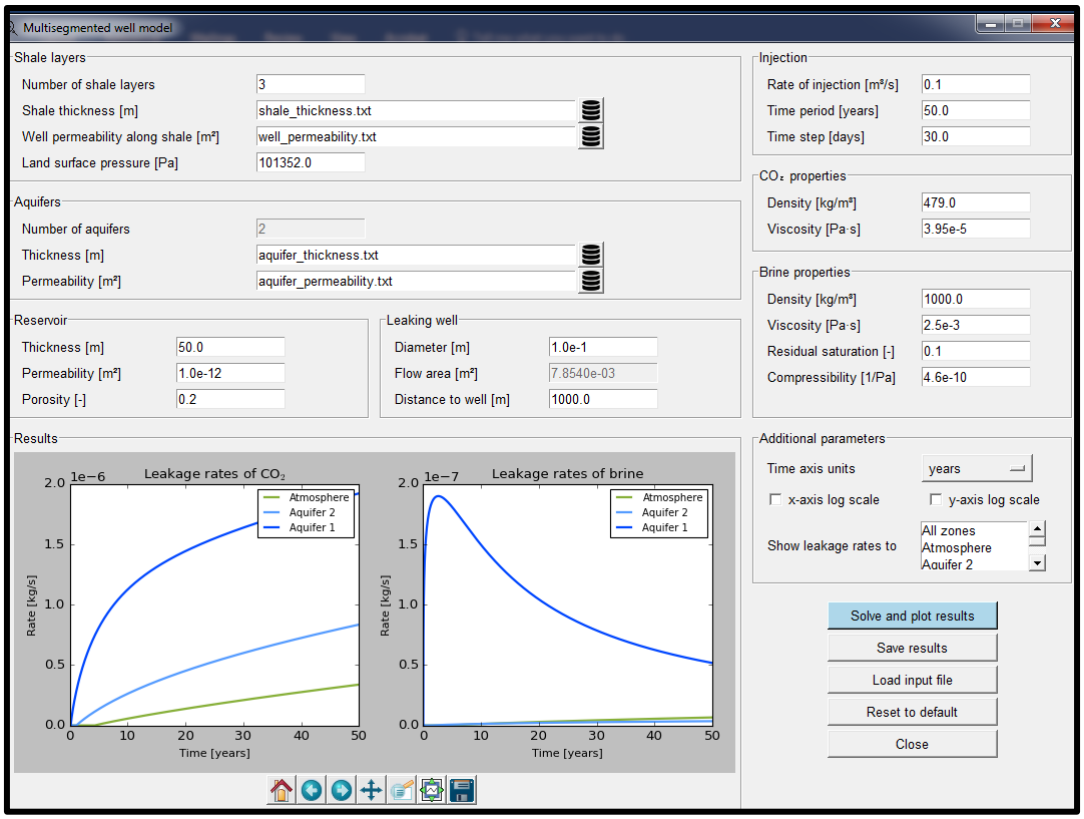

Figure 5.6. WLAT Main Screen for Multi-Segmented Well Model

5.2.2.3 Brine Leakage Model

The Brine Leakage Model focuses on the geochemical processes which are taking place inside the wellbore. It assumes that the fractures inside the cement can seal themselves after being in contact with the acidic brine. The model allows the user to simulate different case scenarios of fracture sealing (permeability decrease due to precipitation) or leaking (permeability increase due to dissolution). An important assumption is flow in series, meaning that the fracture zone contains three different zones of permeability: an unaltered cement zone followed by a precipitation zone and a dissolution zone. Some of the model limitations include the fact that the model only takes into account the brine flow but not the CO_2 phase flow and considers the brine properties (such as density and viscosity) to be constant as a function of pressure and temperature.

The main inputs required are well properties, fracture geometry, permeability and brine properties, **Figure 5.7**.

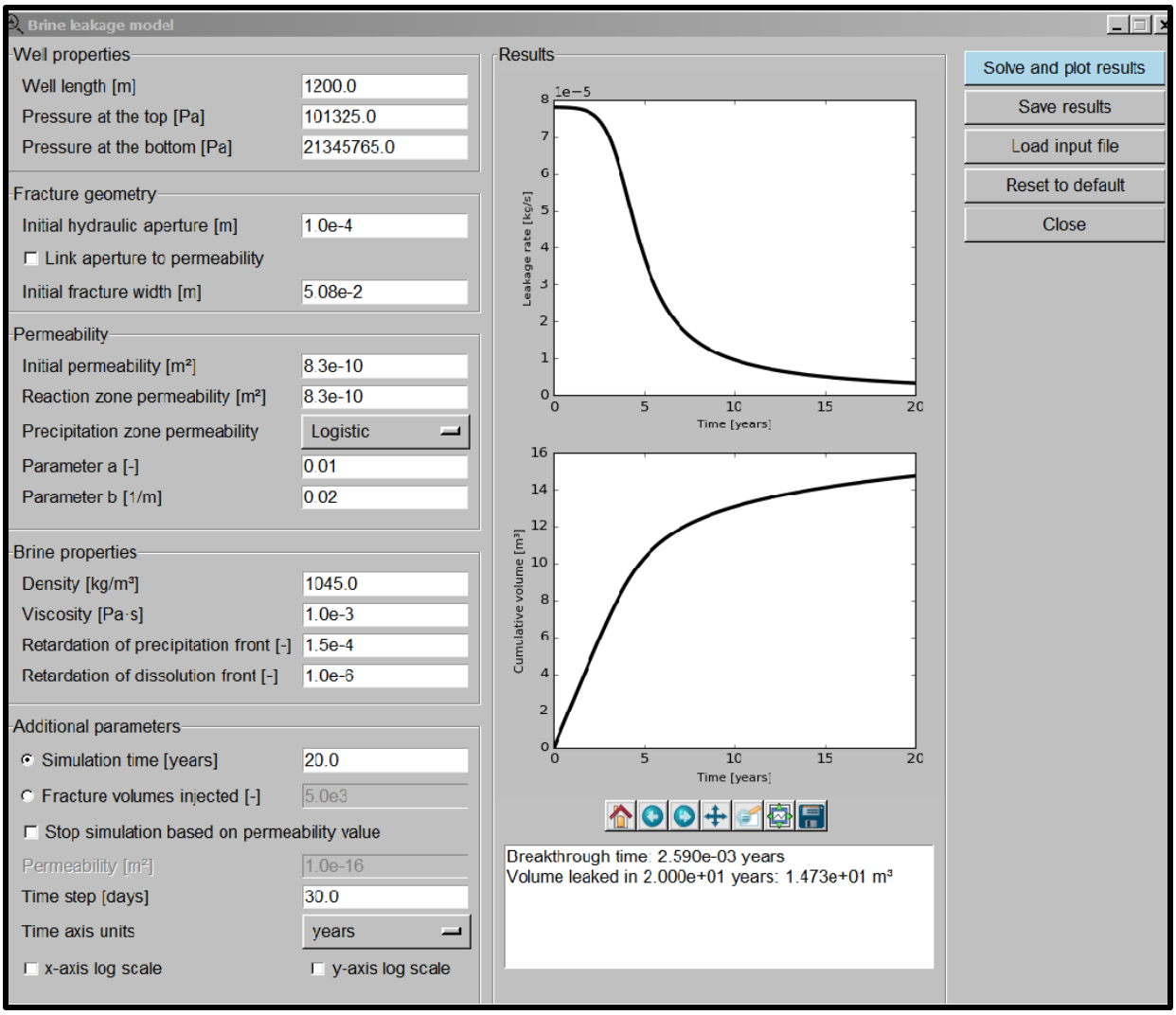

Figure 7. WLAT Main Screen for Brine Leakage Model

5.2.2.4 Open Wellbore Model

This model treats the non-isothermal flow of CO_2 and brine up an open wellbore using the drift-flux approach (Pan et al., 2011)[3]. The model allows for phase transition of CO_2 from supercritical to gaseous. It is worth noting that the model should only be applied to estimate the leaking rate through an open wellbore for a short initial transient period but should be used with caution for longer period times as it does not consider time dependent reservoir pressure at the bottom of the leaking well. The model is incorporated into NRAP-IAM-CS. The inputs are limited to field properties (aquifer properties are currently hard-wired values and reservoir) and wellbore properties, **Figure 5.8.**

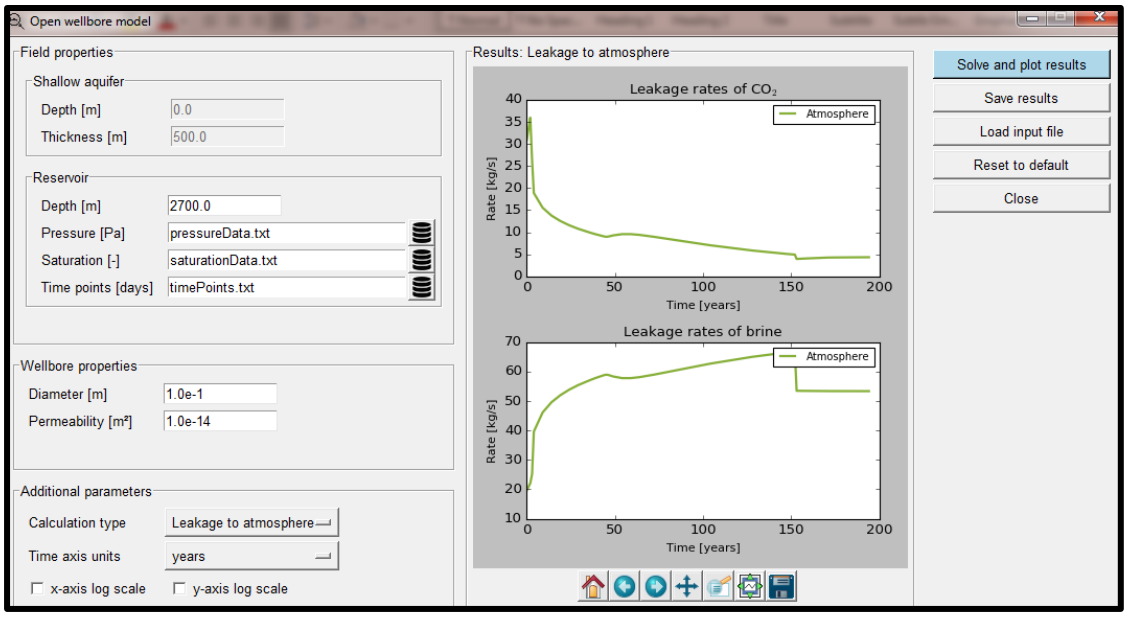

Figure 5.8. WLAT Main Screen for Open Wellbore Model

5..3 NRAP Tools Computer Requirements

Table 5.1 summarizes the list of the reviewed reduced order models with their corresponding computer requirements for use. This also highlights the drawbacks that might be encountered when a model requires other supporting software to be downloaded (GoldSim is required for NRAP-IAM-CS and NSealR for example) or an operating system not always available to the user (STSF is only available on Linux or Mac only for example).

Table 5.1. ROMs Computer Requirements

	OS	Requirements
AIM	Windows 64-bit	Java Version 8 or newer
	Linux and OSX	Oracle JRE version 8u41 and the R scripting language
DREAM	Windows 64-bit	Java Version 8 or newer
	Mac	
GMPIS	Windows 64-bit	Java Version 8 update 46 or newer
MSLR	Windows 64-bit	Java Version 8 update 50 or newer
NRAP-IAM-CS	Windows 2003/ XP/ Vista / 7	GoldSim 11.1.02 is required
NSealR	Windows 2003/ XP/ Vista / 7	GoldSim 11.1.02 is required
REV	Windows 64-bit	Java Version 8 update 40 or newer
RROM-Gen	Windows 64-bit	Java Version 8 update 40 or newer
STSF	Mac or Linux	Java Version 8 update 40 or newer
WLAT	Windows	Java Version 8 or newer

ROM Evaluation

5.3 REV Evaluation

At the time the NRAP tools were to be evaluated with project data, numerical models were being generated to assess CO_2 storage capacity. With pressure and saturation maps over time being an output of this assessment, evaluation of the REV (Reservoir Evaluation and Visualization, section 2.0 of this report) tool was a logical extension for the project team. It is worth noting that the version of the REV to be tested is supposed to be the publicly available version 2016-11-1-2 which can be downloaded from the NETL EDX website. However, this version turned out to be unusable due to version compatibility issues with the simulator. An updated version of the tool, version 2017-03-1-2-1 (not publicly available) was provided and solved the issue. All the testing described below uses version 2017-03-1-2-1 of the tool.

For this storage capacity assessment, Schlumberger's reservoir simulator Eclipse was used to model the CO_2 injection process into the Middle Jurassic Entrada sandstone formation. Schlumberger's Petrel 2016 (pre and post processor for Eclipse) was used to build the static model. The case chosen for this evaluation looked at injecting 300,000 tons of CO_2 over a period of 30 years into the Entrada formation through one central injector with a second well producing water to control reservoir pressure and maximize the injected volume. With that configuration, the well is able to inject at a constant rate over the full injection period. **Figure** 5.**9** shows a 3-D view of the model with the location of the injector (labeled RSU1) and the producer (labeled P1). The model covers an area of 4 miles by 3.5 miles.

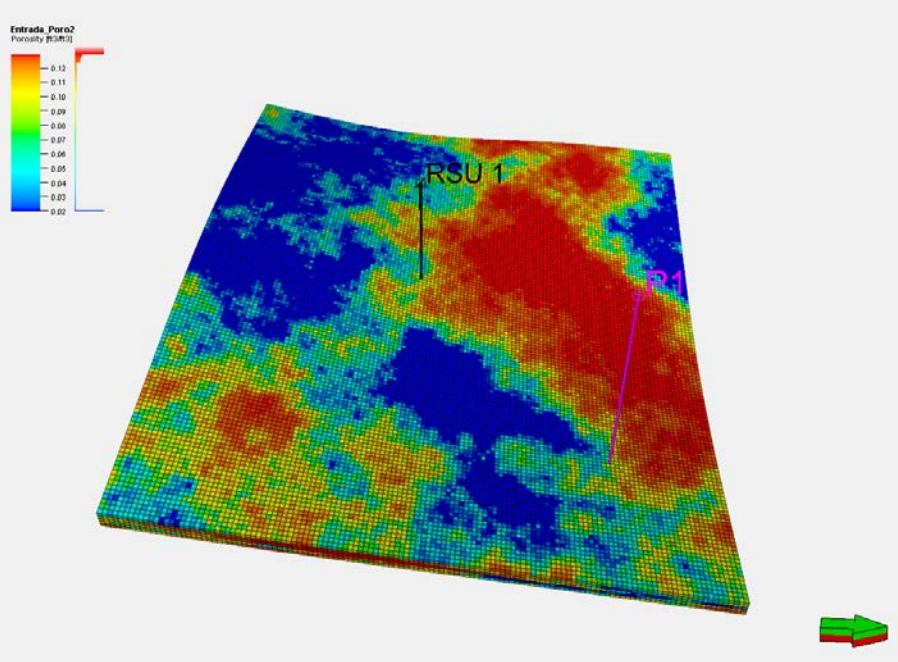

Figure 5.9. Petrel Model 3D View

REV uses as inputs time-lapse reservoir pressure and saturation maps from the simulation work and provide as outputs differential pressure and CO_2 saturation plumes based on a threshold defined by the user. If a grid cell has a value at or above the defined threshold, it will be considered inside the plume. Eclipse and Petrel (simulator and pre/post processor) output files can be interchangeably used as inputs

for REV. While the input files will be different, the resulting differential pressure and saturation maps generated by REV will be identical. For this exercise, both Eclipse and Petrel were evaluated.

The first step of the process consists in generating the required input files to be loaded into REV. For Eclipse, two types of files, FGRID and FUNRST, are required whereas for Petrel, FGRID and GRDCL are required. The FGRID file contains the complete grid description of the model whereas the FUNRST (Eclipse) and the GRDCL (Petrel) files contain the dynamic properties. It is worth noting that the tool (**Figure 5.10**) requests a GRDCL file whereas the correct file extension coming from Petrel is GRDECL.

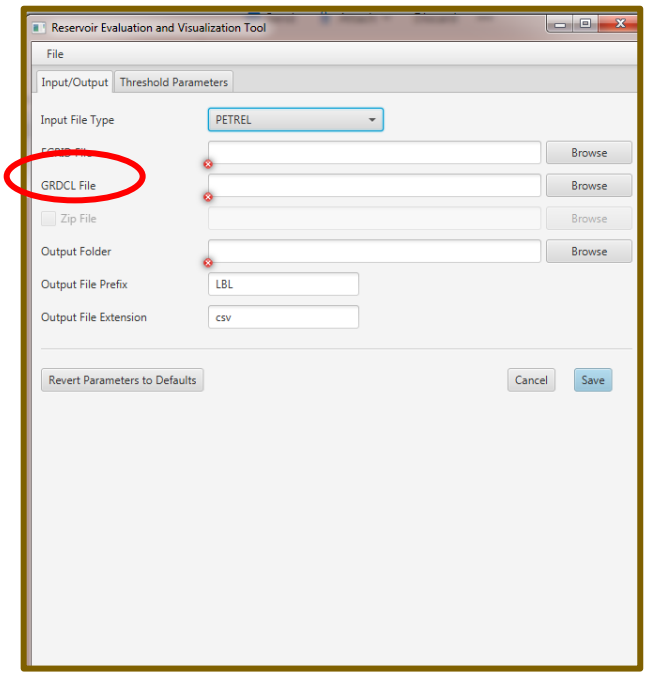

Figure 5.10. REV Petrel Input Tab

At the early phase of the testing, the FGRID files (static files defining the model grid) could not be generated (neither with Eclipse nor with Petrel) but EGRID extension files only. Loading of the EGRID files was unfortunately returning an error message. After some effort, it was figured out that the version of ECLIPSE/ Petrel used could not generate the required REV file format and only ECLIPSE E300 could be used to produce the FGRID file.

Once the static file (FGRID) was generated, the dynamic file (containing the time-lapse pressure and saturation data) had to be imported into the tool and Eclipse was tested first. As described in the REV manual, the FUNRST file should be as follows: “The FUNRST file will have the keywords “PRESSURE” and “SGAS” for each time step, where time steps have an associated “SEQNUM”’ and “DOUBLEHEAD” section (from ECLIPSE).” After thoroughly studying the FUNRST file generated by Eclipse 300, all the necessary keywords mentioned above could be found but “DOUBLEHEAD” could not be located in the file. As such, the tool was giving an error message and the dynamic properties could not be properly loaded. The NRAP support team was made aware of the issue but the problem could not be resolved on time for redaction of this report. The next step was then to move on to trying to load Petrel inputs instead of Eclipse inputs as these can be used interchangeably, meaning FGRID (static file) and GRDECL (Petrel dynamic file with time-lapse CO_2 saturation and pressure) files. These were successfully loaded into the tool.

The second step in the process consists in defining the differential pressure and CO_2 saturation threshold (lower limit), **Figure 5.11.** For this exercise, an initial differential pressure minimum value of 100 psi (over initial pressure) and a CO_2 saturation minimum of 0.01 (or 1% gas saturation) were chosen. As stipulated in the manual, the tool doesn't deal with units. Because the simulation units are in pound per square-inch (psi) and feet, thresholds have to be defined in the same units. As mentioned above, any grid cell with an increase in pressure of 100 psi over initial pressure will be considered as being inside the pressure influenced area and any grid cell with a gas saturation higher than 0.01 will be considered inside the CO_2 plume.

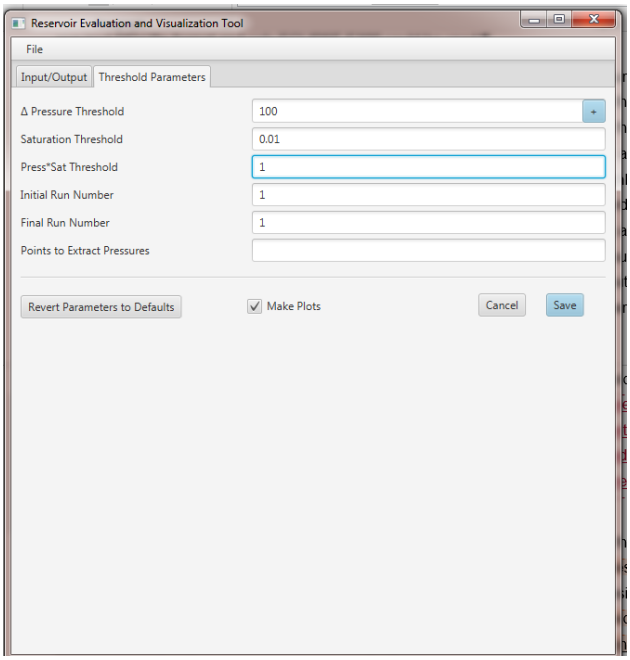

Figure 5.11. REV Petrel Threshold Tab

Once the analysis is running, the DOS windows on **Figure 5.12** appears and remains the same. This DOS window does not show the status of the process and remains idle until the conclusion of the visualization effort. As a reference, the Petrel pressure and saturation maps were initially output on a monthly basis over the 30 years injection period and after processing the visualization over from Friday to Monday, the program was terminated and restarted with yearly timesteps. The tool was able to render results within five minutes

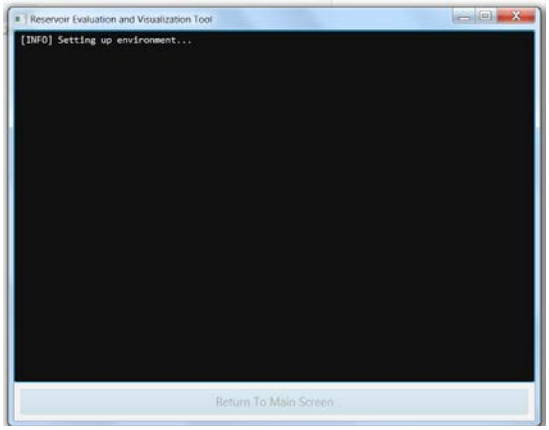

Figure 5.12. REV DOS Windows

Figure 5.13 shows the gas saturation map (maximum gas saturation scale is 0.8 or 80%) after 30 years of injection from Petrel while **Figure 5.14** shows the corresponding gas saturation maps from REV at various time steps (roughly on a yearly basis) with a defined minimum CO_2 saturation value of 0.01. The saturation map at the end of the 30-year injection period will be the last image of the REV series of maps (highlighted in red on **Figure 5.14**). The saturation plumes displayed by the REV tool are not representative of the Petrel output. NRAP support at NETL was contacted regarding this difference but this issue had not be resolved prior to the preparation of this report.

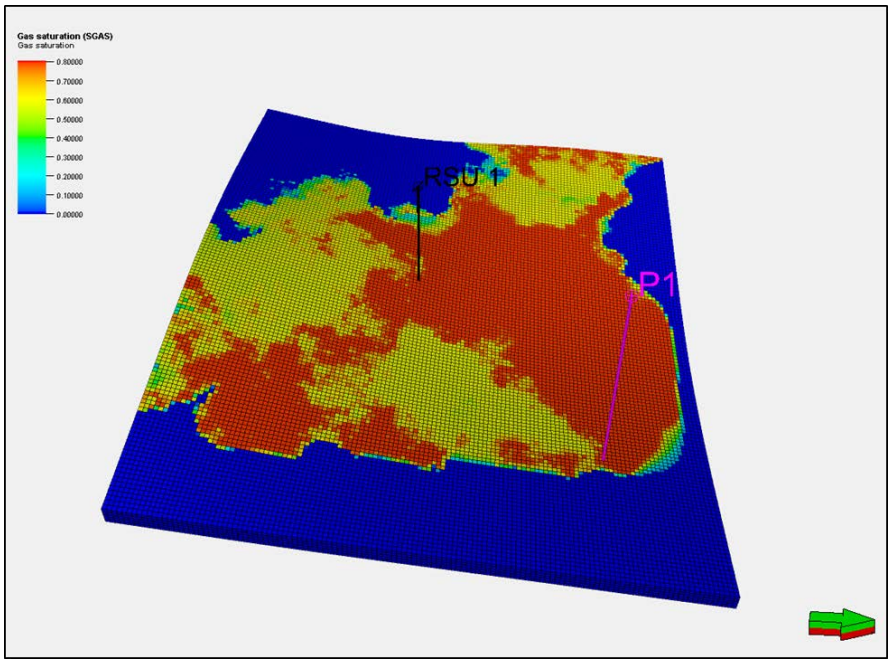

Figure 5.13. Petrel Gas Saturation Map at End of 30-year Injection Period – Entrada Formation

Figure 5.14. REV Gas Saturation Maps – Entrada Formation

Next, a comparison of the differential pressure maps from REV with the Petrel pressure maps was made. **Figure 5.15a** shows the initial pressure in the model (with an average of 4052 psi), and **Figure 5.15b** (scale from 4200 to 4600 psi) shows the pressure at the end of the 30-year injection period (with an average of 4404 psi) or an increase of about 350 psi over the area with a higher pressure zone around the injector and a lower pressure zone around the producer. In addition, **Figure** 5.**16** shows an intermediate map with the pressure after one year of injection.

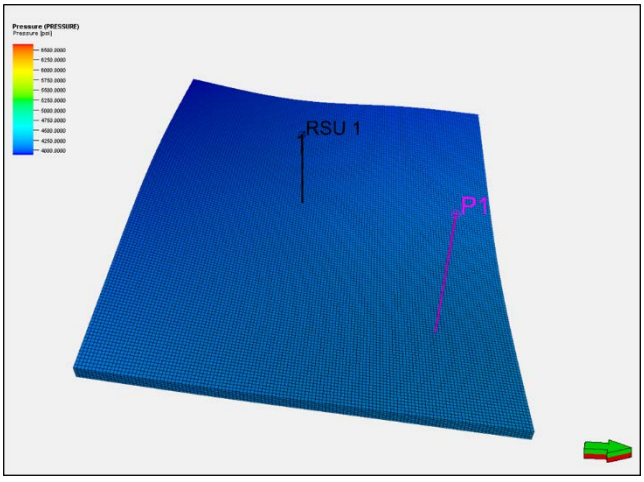

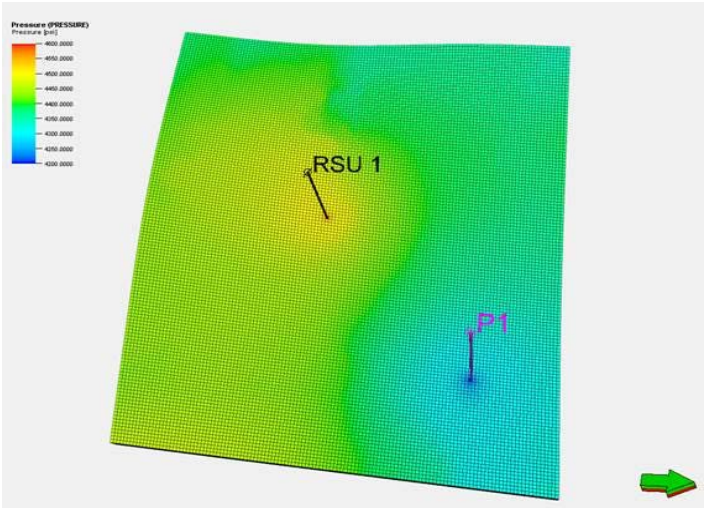

Figure 5.15. a) Petrel Initial Pressure Map; b) Petrel Pressure Map at End of 30-year Injection Period

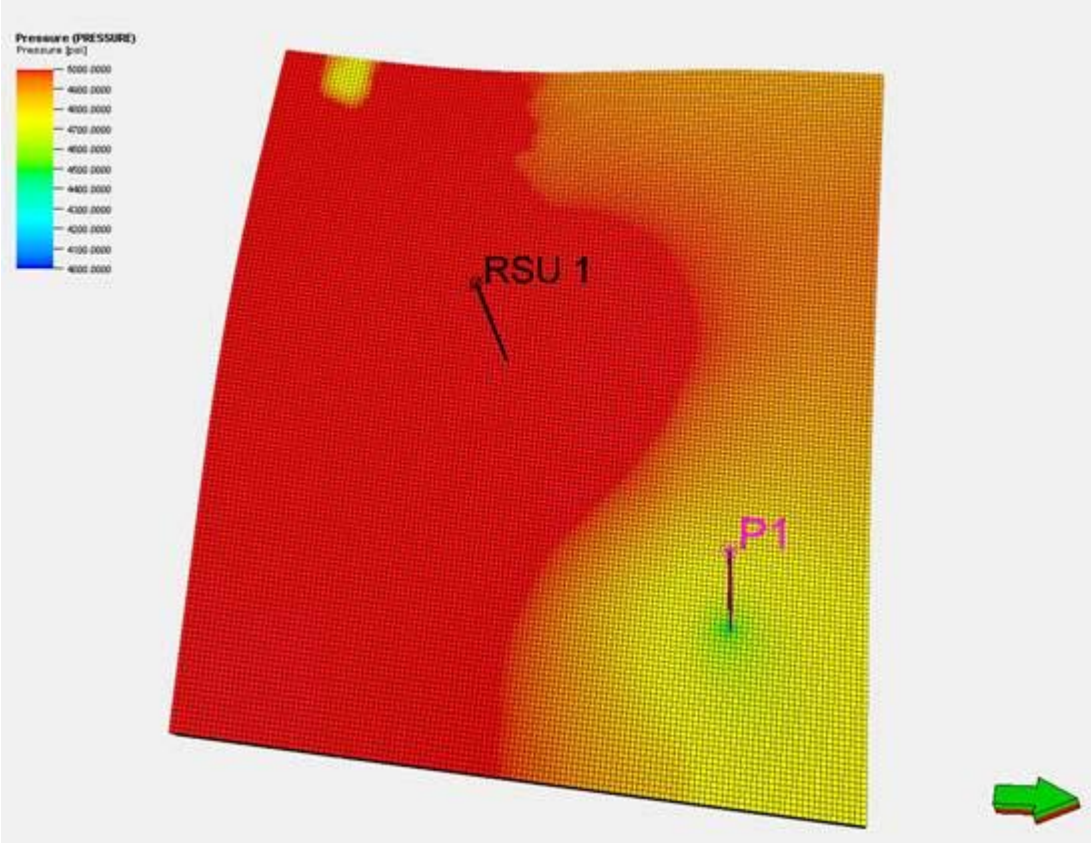

Figure 5.16. Petrel Pressure after 1 Year of Injection

Figure 5.17 shows time-lapse pressure maps roughly on a yearly basis from REV with a differential pressure threshold of 100 psi (any grid block with a pressure value more than a 100 psi over initial pressure will be considered in the plume). The plume covers the full area from the beginning to the end of the 30-year injection period. As mentioned previously, REV does not deal with units, the Petrel model being in pound per square inch (psi), the thresholds have to be specified in psi and the maps will be generated in psi. However, the title exhibits MPa instead. Analyzing the results, they are consistent with the Petrel output (**Figure 5.15b and Figure 5.16**) indicating the pressure differential is greater than 100 psi. However, there is no definition of the pressure interface indicating areas of elevated pressure.

Figure 5.17. REV Pressure Plumes at 100 psi Threshold

In an effort to try to improve the results, analyses were run with an additional differential pressure threshold of 300 psi, knowing that the incremental in pressure at the end of the injection period is on average 350 psi. **Figure 5.18** shows the differential pressure results for a threshold of 300 psi. The area with an increase in pressure greater than 300 psi after one year of injection (highlighted in green) covers the whole area which is consistent with the pressure increase on **Figure 5.16**. Looking at the evolution of the pressure influenced area over time, the pressure stays elevated around the injector and decreases around the producer. While it is difficult to compare the plume at the end of the 30-year simulation (highlighted in yellow) with the Petrel map (as there is no plume per say), the area around the injector shows to be at least 300 psi above initial pressure while the area around the producer shows to be less than 300 psi above initial pressure, which is consistent with **Figure 5.15b**. However, the vertical limit between the blue and the red area (respectively out and in the pressure plume) does not seem very representative of the Petrel results.

Figure 5.18. REV Pressure Plumes at 300 psi Threshold

In addition to the differential pressure and saturation maps, the maximum size of the plumes is also given as a REV output as shown on **Figure 5.19.** For a differential pressure threshold of 300 psi, the maximum pressure plume (which covers the full model area) is 408 million square meters when the model is actually 408 million square feet. Despite the unit issue previously mentioned, the values are consistent. However, for a CO_2 saturation threshold of 0.01, the tool outputs a maximum area of 261 million square meters (so actually 261 million square feet considering the unit issue corrected), which should hence cover more than half of the whole area, but comparing with **Figure 5.14**, that area is almost null showing an inconsistency between the computed plume area and the graphic display.

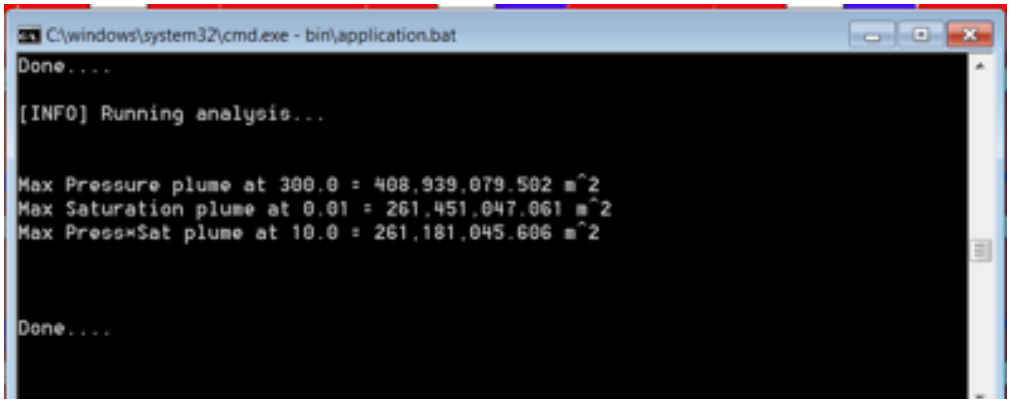

Figure 5.19. REV Analysis Plume Sizes – Entrada Formation

Recommendations:

The following is a list of comments and recommendations based on findings from the study:

- Only one version of the REV tool is available to users. However, updated ROMs are provided to users experiencing difficulty. Known issues should be identified to the users and patches provided via the EDX portal.
- Eclipse and Petrel sample input files are not provided with REV. Even though there is a succinct description of the files in the manual, being able to compare project files versus sample files would allow users to quickly notice differences in file format due to various releases of the simulators.
- It would be very useful if the manual stipulated which version of each simulator is supported by the tool. With regular updates to reservoir simulators in the industry, file formats change and hence can render the tool unusable.
- It would be very helpful to be able to see the progress of the analysis with something similar to a progress bar
- A unit issue was discovered during the analysis. While units from the simulation are field units, REV outputs are in metric.
- There is a display issue for the differential pressure and saturation maps which needs to be further investigated.

5.3.2 WLAT Evaluation: Multi-segmented Wellbore Reduced Order Model

In addition to REV, input well data, provided by the University of Wyoming, were available to test the multi-segmented wellbore model option of WLAT and are summarized in **Table 5.2**. The WLAT is a standalone tool that contains four reduced-physics models or reduced-order models (ROMs) for well leakage. The multi-segmented wellbore ROM estimates the leakage rates of brine and CO_2 along wells with the presence of overlying aquifers (or "thief zones") and intervening confining units (shales). Notably, the ROM allows for input of injection rates from an injection well and distances between the injector(s) and a leaking well. The ROM calculates reservoir pressure buildup (which is not reported as an output).

The simulated RSU leaking well was 6.5 inches in diameter with a cross sectional flow area of 33 square inches. Cement effective permeabilities along the shale interfaces ranged from 0.01 to 10 millidarcies. Aquifer permeabilities were 10 to 100 millidarcies. The corresponding stratigraphic model is represented in **Figure 5.20**. For this exercise, the distances between the injection well(s) and the leaky well were varied between 32 ft. (10 meters) and 3,280 ft. (1,000 meters). The injection rate was 106 million standard cubic feet per day (5,550 metric tonnes per day, or 2 million metric tonnes per year) for 25 years. The total injected volume is 50.1 million metric tonnes.

Table 5.2. WLAT Input Data

Interface Input names (unit)	*Input Values in the Column Below*
CO2 Properties:	
Density (kg/m^3)	728.7
Density (lb/ft^3)	46
Viscosity (Pa*s)	6.21E-05
Viscosity (cp)	6.21E-02
Brine Properties:	
Density (kg/m^3)	1027
Density (lb/ft^3)	64
Viscosity (Pa*s)	3.97E-04
Viscosity (cp)	3.97E-01
Residual saturation	0.4
Compressibility (1/Pa)	4.35E-10
Injection:	
Rate of injection (m^3/s)	34.61
Rate of injection (ft^3/day)	105,595,110
Time Period (years)	25
Time step (days)	1
Reservoir:	
Thickness (m)	465
Thickness (ft)	1526
Permeability (m^2)	8E-14
Permeability (Darcy)	0.081
Porosity (-)	0.128
Leaking Well:	
Diameter (m)	0.23
Diameter (in)	9
Flow Area (m2)	0.041547565
Flow Area (in2)	64
Distance to well (m)	5000, 1000, 500, 100, 10
Distance to well (ft)	16404, 3280, 1640, 328, 32
Aquifer:	
Number of Aquifers	5
Thickness (m)	465, 89, 46, 98, 249
Thickness (ft)	1526, 292, 151, 322, 817
Permeability (m2)	10^-13, 10^-13, 10^-13, 10^-14, 10^-14
Permeability (Darcy)	0.1, 0.1, 0.1, 0.01, 0.01
Shale layers:	
Number of Shale layers	6
Shale Thickness (m)	32, 87, 31, 76, 1000, 508
Shale Thickness (ft)	105, 285, 102, 3281, 1011
Well Permeability along shale (m2)	10^-17, 10^-14, 10^-13, 10^-16, 10^-15, 10^-14
Well Permeability along shale (Darcy)	1.0E-5, 0.01, 1.01, 1E-4, 0.001, 0.01
Land surface pressure (Pa)	101500
Land surface pressure (Psi)	14.7

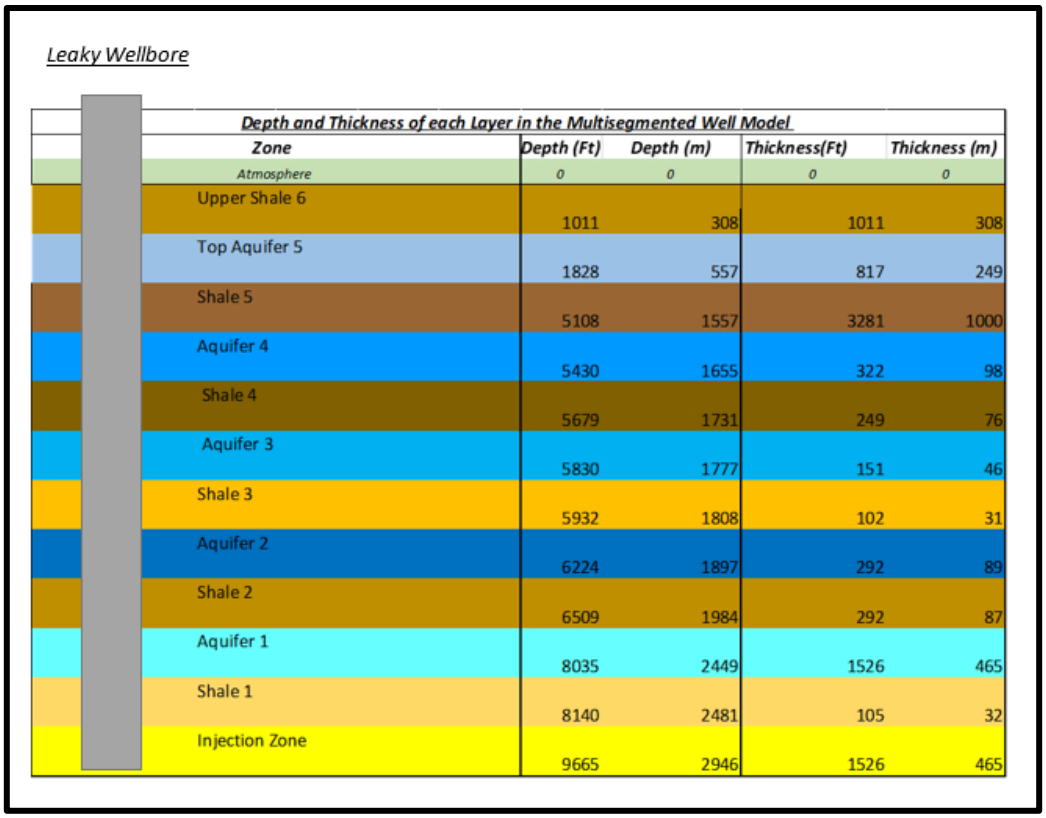

Depth and Thickness of each Layer in the Multisegmented Well Model

Zone	Depth (Ft)	Depth (m)	Thickness(Ft)	Thickness (m)
Atmosphere	0	0	0	0
Upper Shale 6	1011	308	1011	308
Top Aquifer 5	1828	557	817	249
Shale 5	5108	1557	3281	1000
Aquifer 4	5430	1655	322	98
Shale 4	5679	1731	249	76
Aquifer 3	5830	1777	151	46
Shale 3	5932	1808	102	31
Aquifer 2	6224	1897	292	89
Shale 2	6509	1984	292	87
Aquifer 1	8035	2449	1526	465
Shale 1	8140	2481	105	32
Injection Zone	9665	2946	1526	465

Figure 5.2.: Schematic of Injection Zone, Confining Unit (Shales) and Thief Zones (Aquifers) Depths

The leakage rates for CO_2 and brine for the base 10 meter well spacing case are shown in **Figures 5.21 and 5.22,** respectively. The cumulative CO_2 leakage over 25 years from the injection zone is 10,760 tonnes or 0.02% of the total CO_2 injected volume of 50.1 million metric tonnes. All of the CO_2 leakage remains in aquifers (thief zones) and there is no CO_2 leakage into the shallowest aquifer or to the atmosphere in this or any of the cases. Increasing distances between the injector and the leaky well results in less CO_2 leakage out of the reservoir, and extended times for CO_2 to breakthrough. The time that is

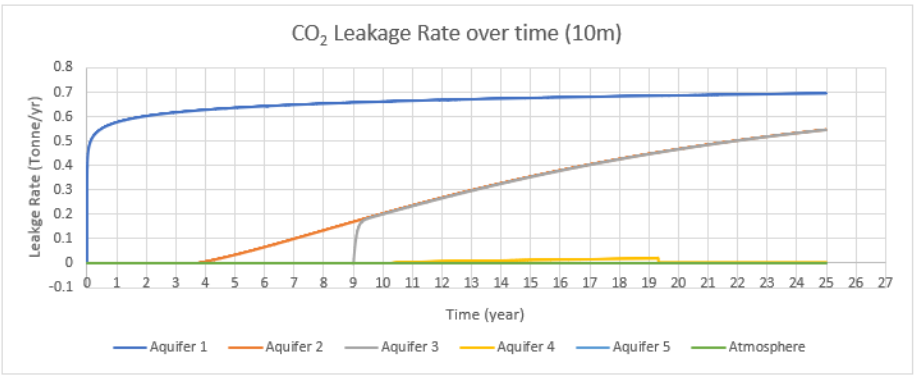

	Aquifer 1	Aquifer 2	Aquifer 3	Aquifer 4	Aquifer 5	Atmosphere	Total Leakage out of Reservoir
Total Leakage (Tonnes)	6043	2420	2250	46	0	0	10759
Total Percentage of Reservoir Leakage	0.12%	0.05%	0.04%	0.00%	0.00%	0.00%	0.21%

took for Aquifer 1 to start leaking CO_2 into the zone at 32 ft. distance is 1.4 minutes, or, effectively instantaneously.

Figure 5.21. CO_2 Leakage Rates – 10 Meters Distance Between Wells

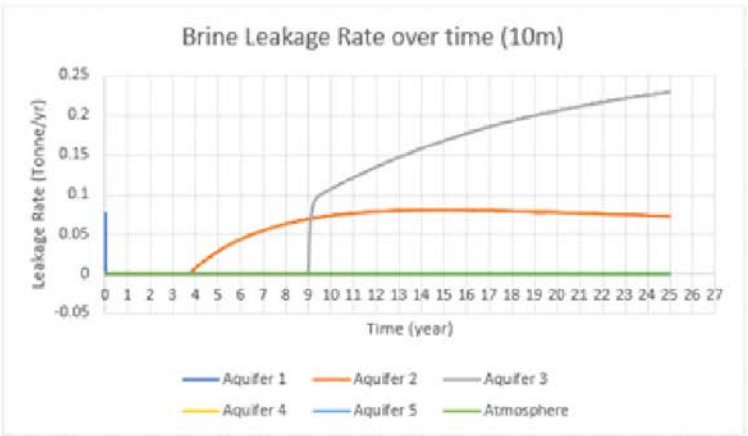

	Aquifer 1	Aquifer 2	Aquifer 3	Aquifer 4	Aquifer 5	Atmosphere	Total Leakage out of Reservoir
Total Leakage (Tonnes)	5	529	1024	0	0	0	1558

Figure 5.22. Brine Leakage Rates – 10 Meters Distance Between Wells

Increasing the distance from leaking well to the CO_2 injector to 328 ft. (100 meters), results in less leakage overall for both CO_2 and brine, as expected. Most of the CO_2 leakage is going into aquifer 1 (first aquifer above the injection zone) with 4,480 tonnes leaking over the 25-year injection (**Figure 5.23 and 5.24**). The total leakage of CO_2 from the reservoir is 7,461 tonnes, or 0.015% of the total injection. The leakage starts in aquifer 1 only 2.5 hours after injection starts while for aquifers 2,3, and 4 it takes 5,11, and 13 years respectively.

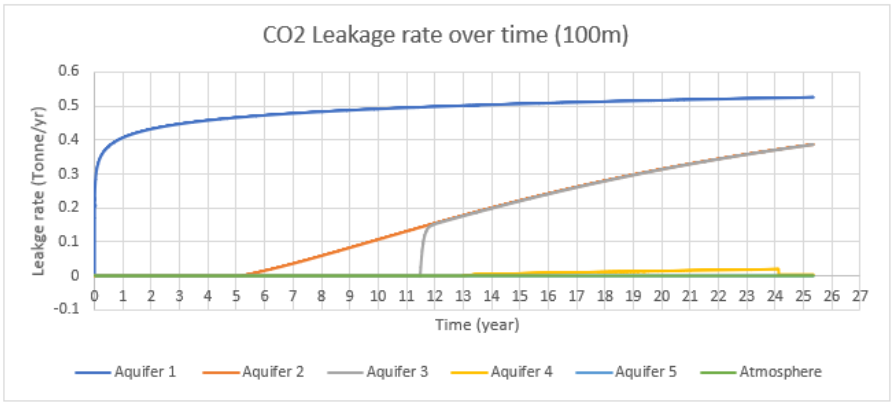

	Aquifer 1	Aquifer 2	Aquifer 3	Aquifer 4	Aquifer 5	Atmosphere	Total Leakage out of Reservoir
Total Leakage (Tonnes)	4480	1550	1384	48	0	0	7461
Total Percentageof Reservoir Leakage	0.088%	0.030%	0.027%	0.001%	0%	0%	0.15%

Figure 5.23. CO_2 Leakage Rates – 100 Meters Distance Between Wells

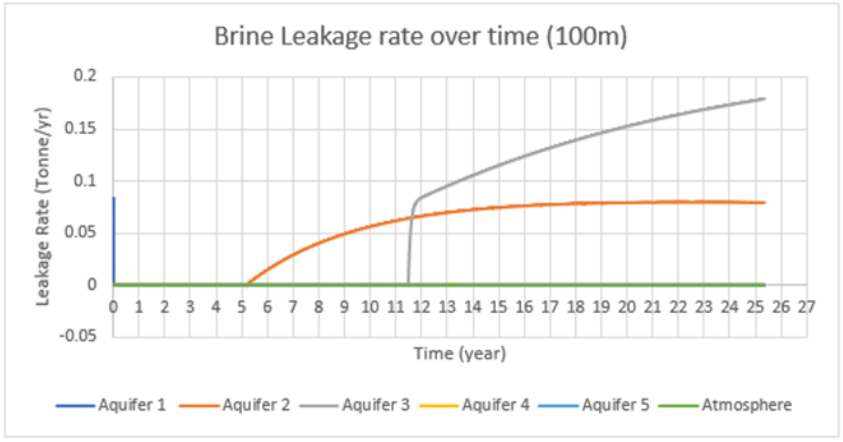

	Aquifer 1	Aquifer 2	Aquifer 3	Aquifer 4	Aquifer 5	Atmosphere	Total Leakge out of Reservoir
Total Leakage (Tonnes)	7	470	684	0	0	0	1161

Figure 5.24. Brine Leakage Rates – 100 Meters Distance Between Wells

The trends mentioned previously still apply for distances of 500 meters and 1,000 meters between the injector and the leaky well. **Table 5.3** summarizes the time for leakage to occur for each aquifer at each of the 4 distances analyzed. With a distance of 1,000 meters (3,280 ft) between the injector and the leaky well, it would only take 10 days for the CO_2 to leak into the first aquifer.

The results of the WLAT multi-segmented wellbore ROM analysis of potential leakage from a hypothetical well in an RSU injection scenario suggest that the volumes of CO_2 leakage along wellbore will be modest. It should be noted that the model assumes Darcy flow through cement or along a cement interface and does not consider cases where the cement is fractured, degraded, or there are cement-casing or cement-formation annuli that would allow for elevated rates of leakage. As such, the results suggest that wells with cement coverage over some/most of the confining units will limit CO_2 leakage to manageable levels. That said, breakthrough of CO_2 at the leaking well, even at distances of 3,280 ft,

occurs within days of injection. This is likely unrealistic and suggest that improvement can be made on the reservoir CO_2 simulation aspect of the ROM.

Table 5.3: Summary of Time for Leakage

Distance from Leaky well to Injector	Aquifer 1	Aquifer 2 (years)	Aquifer 3 (years)	Aquifer 4 (years)	Aquifer 5 (years)	Atmosphere (years)
10 m (33 Ft)	1.4 minutes	4	9	10	Never	Never
100 m (328 Ft)	2.5 hours	5	11	13	Never	Never
500 m (1640 Ft)	2.5 days	7	14	16	Never	Never
1000 m (3280 Ft)	10 days	8	16	18	Never	Never

Recommendations:

The following is a list of comments and recommendations based on findings from the study:

- A stated assumption in the WLAT multi-segmented ROM is that leakage is treated as flow through porous media using Darcy's law. The flow model in the cement does not take into account flaws in the cement leading to high permeability zones such as annuli or fractures which could significantly alter CO_2 leakage rates.
- Breakthrough of CO_2 at the leaking well seem unrealistically fast and the reservoir CO_2 simulation of the ROM should be reviewed
- In the multi-segmented wellbore ROM, CO_2 density and viscosity properties appear to be held constant (i.e. the input values) for the entire vertical length of the well. CO_2 density (and viscosity) will dramatically decrease up hole relative to hydrostatic pressure, thus increasing its buoyancy drive, consequently increasing the leakage drive.
- The tool should be tested against industry tools for benchmarking purposes.

Recommendations

This report describes in detail the ten available NRAP reduced-order models, their use, required inputs and the available outputs. Out of the ten tools, only two of the ROMs were further studied in application to the Rock Springs Uplift CarbonSAFE project.

With numerical models being generated to assess CO_2 storage capacity in the Entrada formation as part of the Rock Springs Uplift CarbonSAFE Project, the Reservoir Evaluation and Visualization (REV) tool was analyzed with available ECLISPE/ Petrel datasets. The initial phase of the evaluation which consisted in getting the tool to run was made difficult by compatibility issues and the existence of various versions of the tool. Once that issue was resolved, the tool functioned properly. However, the results obtained didn't fully compare with simulator results. While the computed CO_2 saturation and differential pressure plume sizes seem consistent with the reservoir simulation outputs, the visual display of the plumes is faulty and require some support from the NETL NRAP personnel.

WLAT (only focusing on the multi-segmented wellbore ROM option) was chosen for testing because it allows for the modeling of leakage of CO_2 and brine along wells with multiple thief zones. The results suggest that CO_2 migration into overlying zones will be limited and little or no migration is expected into shallow aquifers or to the atmosphere.

Section V References

Zyvoloski, G. A. *FEHM: A control volume finite element code for simulating subsurface multi-phase multi-fluid heat and mass transfer*; Report LAUR-07-3359; Los Alamos National Laboratory: Los Alamos, NM, 2007.

Nordbotten, J. M.; Celia, M. A.; Bachu, S.; Dahle, H. K. Semianalytical Solution for CO_2 Leakage through an Abandoned Well. *Environmental Science & Technology* **2005,** *39*, 602–611.

Pan, L.; Webb, S. W.; Oldenburg, C. M. Analytical Solution for Two-Phase Flow in a Wellbore Using the Drift-Flux Model. *Advances in Water Resources* **2011a,** *34,* 1656–1665.

Douglass, J.; Edwards, B.; Convertito, V.; Sharma, N.; Tramelli, A.; Kraaijpoel, D.; Cabrera, B.; Maercklin, N.; Troise, C. Predicting ground motion from induced earthquakes in geothermal areas. *Bull. Seis. Soc. Am.* **2013,** *103,* 1875–1897.

Abrahamson, N.; Silva, W. Summary of the Abrahamson & Silva NGA Ground-Motion Relations. *Earthquake Spectra* **2008,** *24*, 67–97.

Boore, D.; Atkinson, G. Ground-Motion Prediction Equations for the Average Horizontal Component of PGA, PGV, and 5%-Damped PSA at Spectral Periods between 0.01 s and 10.0 s. *Earthquake Spectra* **2008,** *24*, 99–138.

Britter, R. E.; McQuaid, J. D. *Workbook on the dispersion of dense gases*; Contract Research Report 17 Health and Safety Executive, Sheffield, UK, 1988.

Ogata, Y. Statistical-models for earthquake occurrences and residual analysis for point-processes. *J. Am. Stat. Assoc.* **1988,** *83,* 9–27.

Bachmann, C. E.; Wiemer, S.; Woessner, J.; Hainzl, S. Statistical analysis of the induced basel 2006 earthquake sequence: Introducing a probability-based monitoring approach for enhanced geothermal systems. *Geophys. J. Int.* **2011,** *186,* 793–807. DOI:10.1111/j.1365-246X.2011.05068.x.

Appendix 1: NRAP Tools Review

1.1 Aquifer Influence Model (AIM)

Introduction. The AIM tool predicts the size of a CO_2 leak into an overlying aquifer. Two reduced order models (ROMs), one an unconfined carbonate model and the second a confined alluvium model, can be employed to perform the numerical calculations. Monte Carlo techniques are used to review the results in a probabilistic context.

The software application accepts input data for a specific ROM. The major input panels are leak rate models, aquifer characteristics, and control parameters. The tool has been developed as an early stage screening tool where "site specific knowledge is expected to be low and only moderate levels of accuracy should be expected."

Input/Output Data. At a high level, the input variables may be grouped into three categories. They are 1) the leakage locations and their number, 2) the rate of flow of brine and CO_2 at those positions, and 3) the characteristics of the aquifer into which the leakage occurs. AIM results are given in terms of the plume size for each of nine water quality facets (pH, total dissolved solids, four trace metals and three organic compounds, **Figure 27**) as well as the flux of CO_2.

Figure 25 show the tab for inputs of the leakage rate model. At the bottom of the tab, a drawing of the leak scenario explains what each parameter corresponds to and what an acceptable range for each parameter is. As highlighted in red, several scenarios (input by the user) will be run using Monte-Carlo probabilistic techniques.

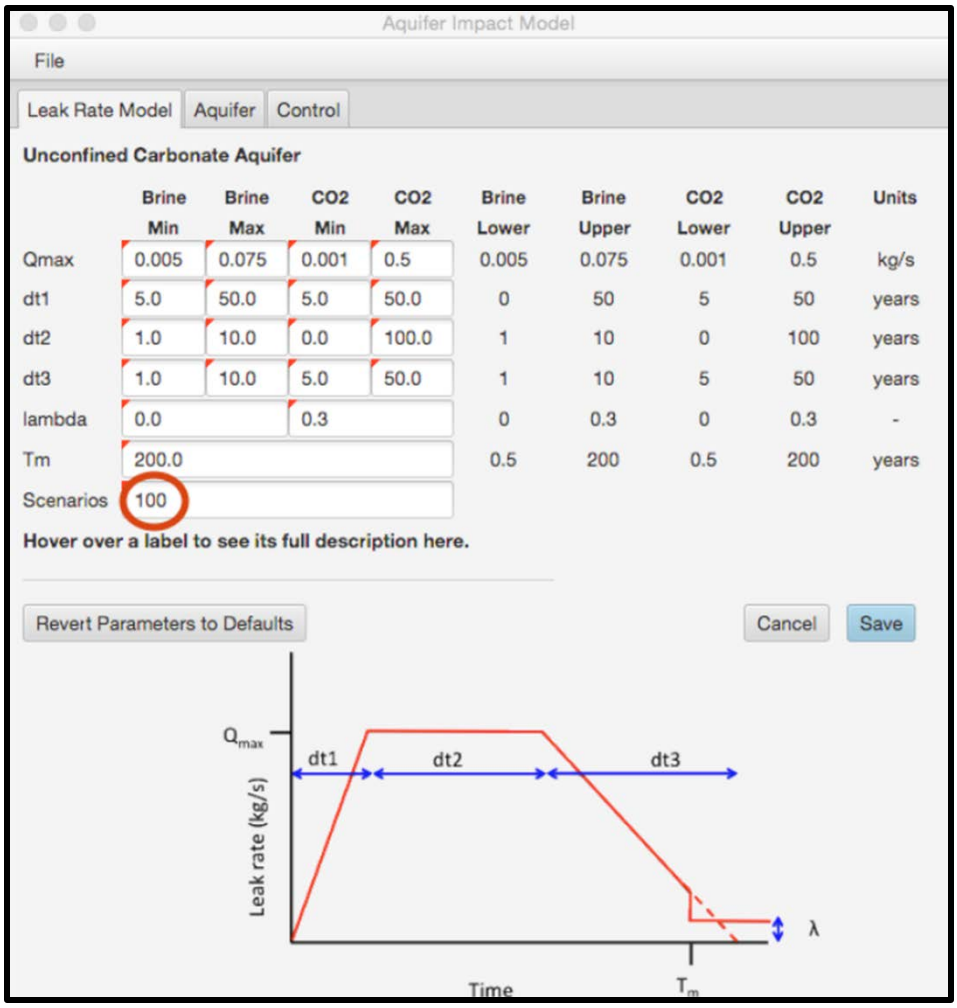

Figure 25: Leak Rate Model Tab and Inputs

Figure 26 shows the numerous inputs necessary to describe the aquifer for each option (unconfined carbonate or confined alluvium).

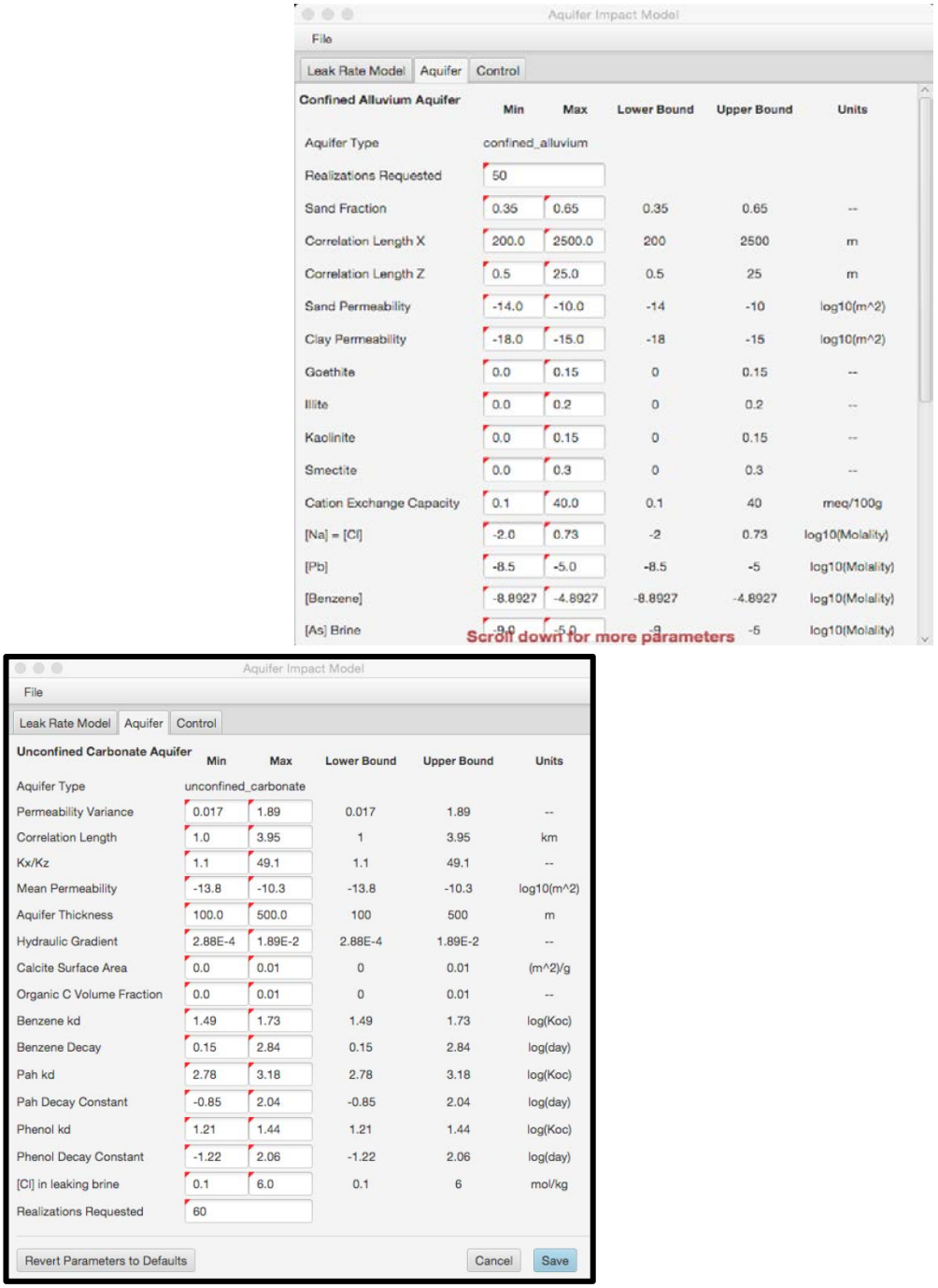

Figure 26: a) Unconfined Carbonate Aquifer and b) Confined Alluvium Aquifer Tab and Inputs

Note: to convert from m^2 to Darcy multiply by 1.013249966e+12

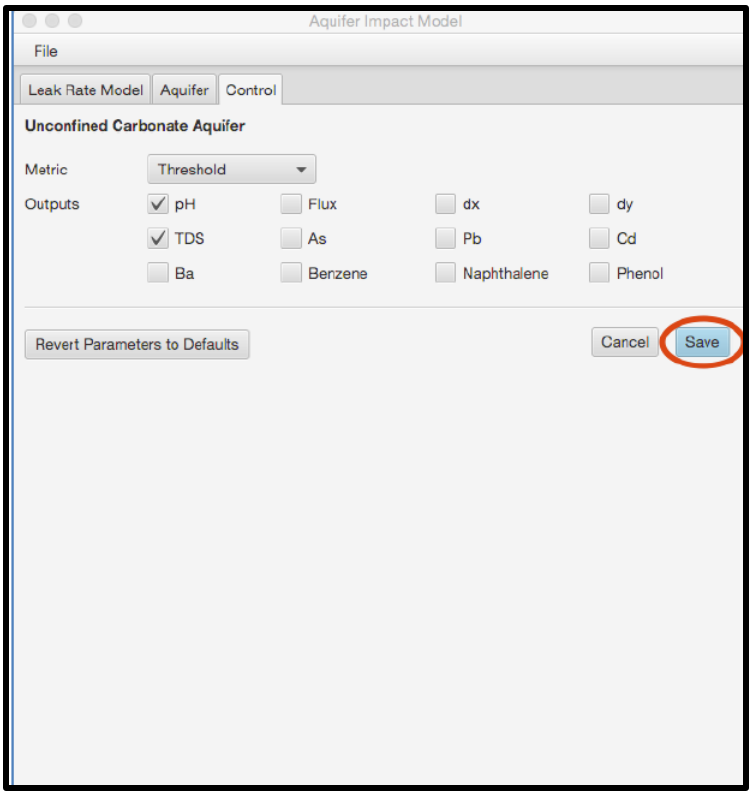

Figure 27: Control Tab and Inputs

1.2 Designs for Risk Evaluation and Management (DREAM) Tool

Introduction. The DREAM software application was constructed to be a monitoring program design tool to minimize the time to first detection of a subsurface CO_2 leak. When executing the program, there are three components that comprise the software: (1) a Java input and execution wizard; (2) a results visualization protocol; and (3) a results plotting tool.

Input/Output Data. DREAM leverages user-provided CO_2 leakage modeling results to optimize the outlay of monitoring tools and wells available. These inputs may include any modeling results developed from physics-based, porous media flow models, including pressure, temperature, gas saturation, etc. The various windows/panes for the software are described below.

DREAM Welcome. The software opens to the welcome window, which contains links to the software development manual, references and acknowledgments.

Input Directory. This pane requests the directory containing the CO_2 leakage simulation output files in HDF5 format. If the output files are not currently in HDF5 format, the Launch Converter button can be used to convert the ASCII data into the desired structure.

Porosity. The porosity of the system is required to calculate aquifer volumes. Additional zones can be provided along with porosity data from an external file. This data can be saved for future use elsewhere.

Scenario Weighting. Modeled leakage scenarios, which have been created in subfolders for input, are listed and are each assigned a default weighting of 1.0. This represents the likelihood of the potential leakage scenario. The larger the number is the greater the potential for leakage.

Leakage Criteria for Monitoring Parameters. Based on the flow modeling output of the imported simulations, DREAM will generate a table of monitoring parameters. The application requires the monitoring technology to be deployed for each selected parameter, the total cost, the detection criteria and the ranges for the detection criteria. In addition, the triggering nodes (elements that meet the detection criteria) can be found and the solution spaces (set of nodes where leakage is present) selected. The leakage nodes and the optimum monitoring locations can be viewed through the Launch Visualization button.

Minimum Triggered Monitoring Devices. Input the minimum number of sensors required.

Configuration Settings. The application designs the monitoring program based on user input specifications regarding the total sensor budget and number of wells. If well spacing limitations are known, this can be input, as well.

Exclude Locations. Should monitoring nodes be excluded from the configuration, they may be deselected on this pane. If the user has incorporated a Google map of the storage site, this can also be used to confirm locations.

Run DREAM. Prior to running the software, output directories and best achievable monitoring protocols (no budget) are available to manage the output and set the expectation prior to running the requested number of configurations to determine the budgeted monitoring optimization.

Formatted software output accepted for DREAM input includes NUFT (Non-isothermal, Unsaturated Flow and Transport Model), STOMP (Subsurface Transport Over Multiple Phases), and TECPLOT (which is a post-processing simulation tool).

While executing, two windows pop up to show progress. The first is the DREAM visualization window, which shows the monitoring configuration being tested. The second is a window with four performance plots showing the time to detection results for new configurations, the best configurations, each realization, and the percentage leak detected. The program generates several useful output files in .CSV format for user review. **Figure 28** shows an example from the Visualization Tool.

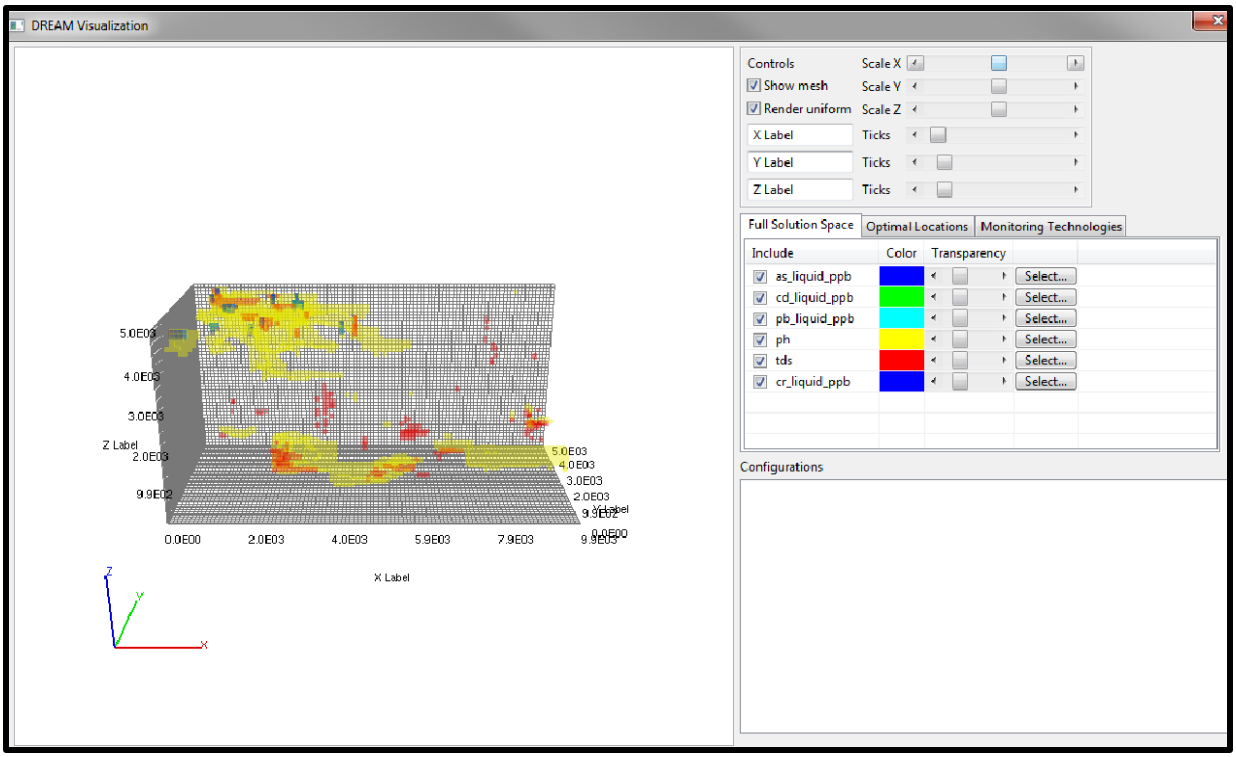

Figure 28: DREAM Visualization Tool – Full Solution Space

1.3 Ground Motion Prediction Applications to Potential Induced Seismicity (GMPIS)

Introduction. The GMPIS tool predicts the distribution of potential ground movement due to induced seismicity (IS) caused by CO_2 injection and accompanied by accelerated/triggered tectonic-related seismicity. Because of the limited seismicity data due to CO_2 injection, ground motion prediction equations were adapted and developed from data derived from active geothermal sites (Douglas et al, 2013)[4] to obtain peak ground acceleration and peak ground velocity. The database includes nearly 4,000 records from Switzerland, Germany, France, the Netherlands, California, and Iceland. One limitation to the tool is that induced seismicity is regionally dependent. Because of the lack of data on injection IS, global IS data with uncertainties have to be applied via a simplified site amplification model. The site amplification models of Abrahamson and Silva (2008)[5] and Boore and Atkinson (2008)[6] were incorporated to adjust the ground motion prediction equations (GMPEs). These models estimate the shallow shear-wave velocity, typically in the upper 30 meters (Vs30) with direct measurements based on geology, slope or terrain and other local velocity observations.

The major input panels for the ROM include a Master, description of induced seismicity characteristics and description of tectonic seismicity characteristics.

Input/Output Data. At a high level, the input variables may be grouped into three categories. They are: (1) the location of the site; (2) for induced seismicity, the properties of the induced earthquake; and (3) for the tectonic seismicity, fault characteristics and properties of the earthquake.

1.3.1 Site Location

The Master tab allows the user to define the bounding coordinates of the studied area as well as the number of evenly spaced sites in that area. The user can also upload personal topographic maps in the model. This tab allows for specific outputs to be generated such as a ShakeMap (maps of ground motion from the USGS Earthquake Hazard Program) or a detailed output. **Figure 29** shows the 'Master' tab in the GMPIS model.

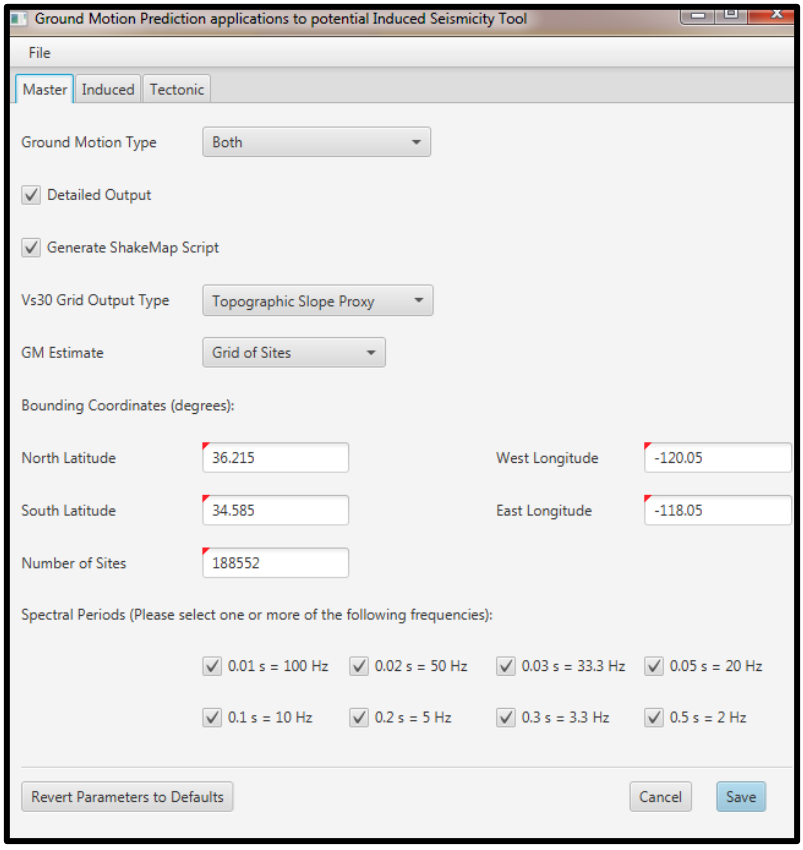

Figure 29: GMPIS "Master" Input Page

1.3.2 Induced Seismicity Characteristics

Under the induced tab, characteristics pertinent to the earthquake induced by the CO_2 injection are input. These are the earthquake coordinates as well as its magnitude and its depth. The user specifies which site amplification method to be used for site specific corrections (Abrahamson and Silva or Boore and Atkinson). **Figure 30** shows the 'Induced' tab.

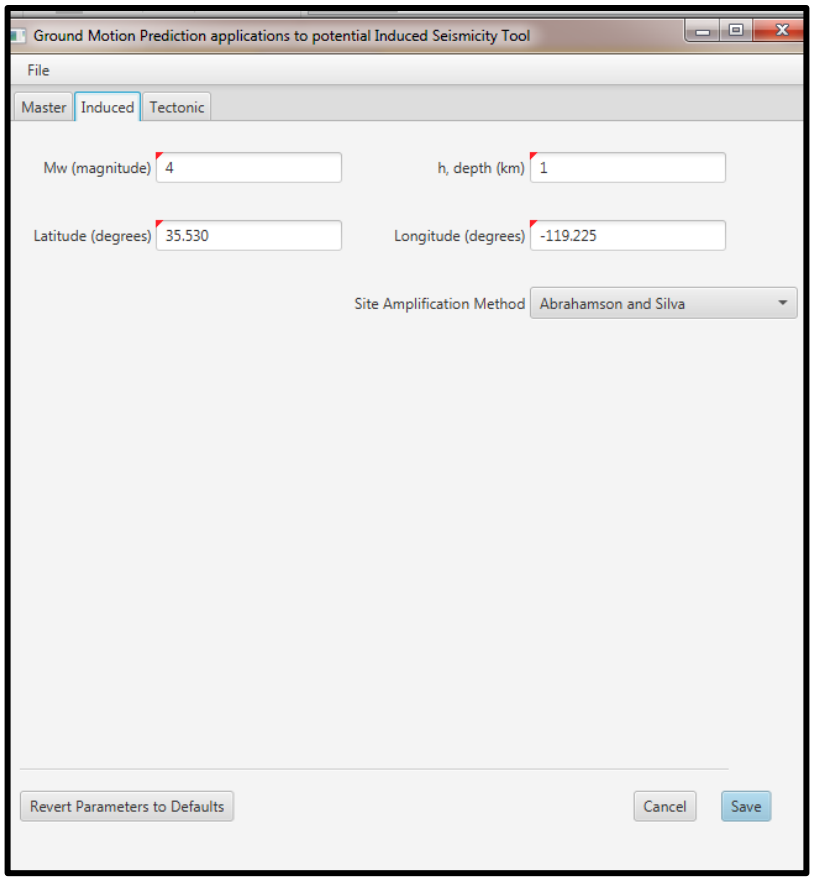

Figure 30: GMPIS "Induced" Input Page

1.3.3 Tectonic Seismicity Characteristics

Under the 'Tectonic' tab, the characteristics of the rupture surface (fault), which was triggered during CO_2 injection, are input. These include the type of fault, the fault dip, exact coordinates along the fault, the top depth of the fault as well as the magnitude of the triggered earthquake. **Figure 31** shows the 'Tectonic' tab.

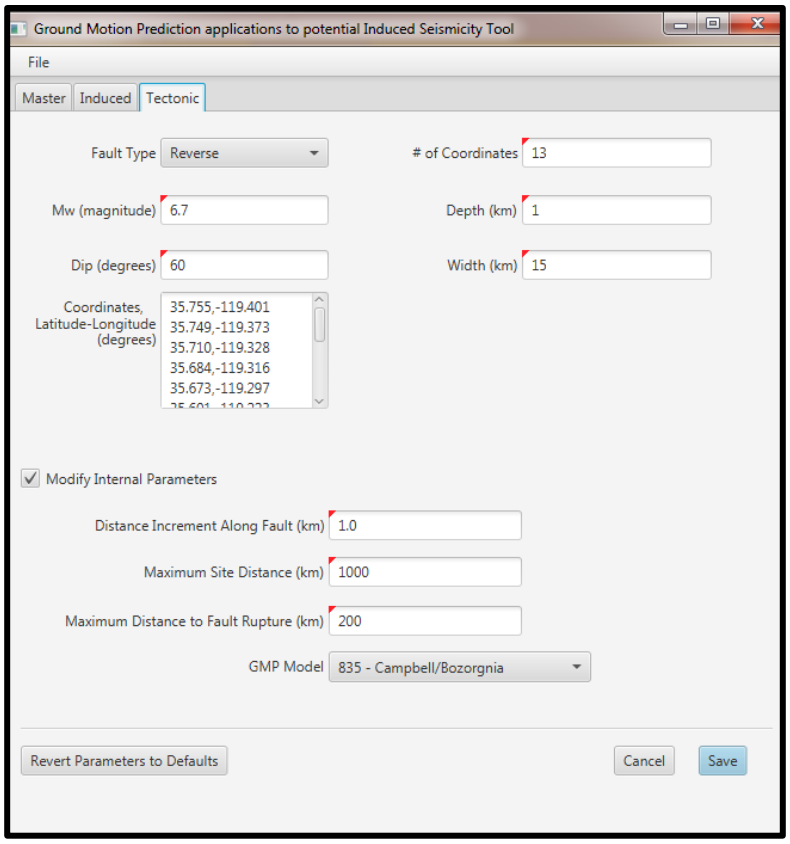

Figure 31: GMPIS "Tectonic" Input Page

1.3.4 GMPIS Outputs

GMPIS simulation results are a flat file containing peak ground velocity and acceleration at each defined location over the area of interest as well as input files for graphic packages.

1.4 Multiple Source Leakage Reduced-Order Model (MSLR)

Introduction. The MSLR tool predicts if receptors are within a critical radius of eventual multiple CO_2 leakage sources. The MSLR is developed as both a built-in tool in the NRAP-IAM-CS (Integrated Assessment Model for Carbon Storage) and as a standalone module. The Britter and McQuaid (1988)[7] correlations for predicting plume extent and concentration of dense gases during potential gas releases were used, but are only applicable to single source releases. A superposition approach was developed to handle multiple leakage sources. This tool is mainly intended for scoping studies.

Input/Output Data. The main inputs to the MSLR are CO_2 leakage rates, wind speed, leakage sources' location, receptors' locations (limited to 100) and the critical CO_2 concentration (the threshold concentration limit above which CO_2 is considered to become hazardous).

1.4.1 MSLR Main Inputs

The model main inputs include atmospheric conditions (temperature and pressure to compute air density and wind speed) as well as the source of the CO_2 leakage temperature (to compute CO_2 density), and time. The main inputs are shown on **Figure 32**.

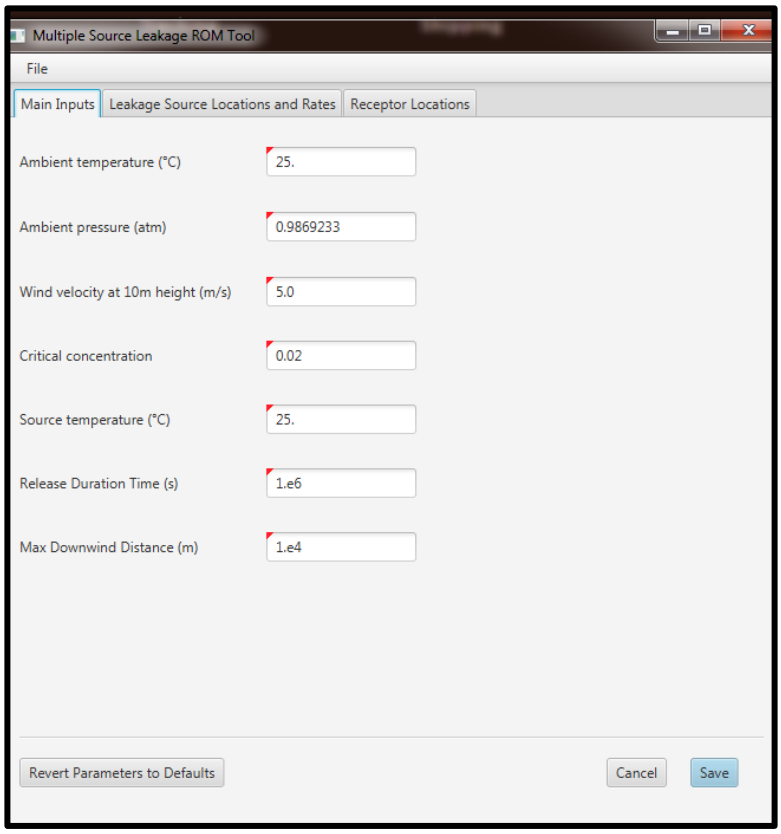

Figure 32: MSLR Main Input Tab

1.4.2 MSLR Leakage Source Locations and Rates

Up to 1,000 sources of CO_2 leakage can be input in the model. For each source, location (coordinates) and leakage rate are required. If the ROM is used as part of the NRAP-IAM-CS model, leakage locations and rates can be passed from other modules. If the ROM is used as a standalone, the information need to be entered into the 'Leakage Source Locations and Rates' tab as illustrated in **Figure 33**.

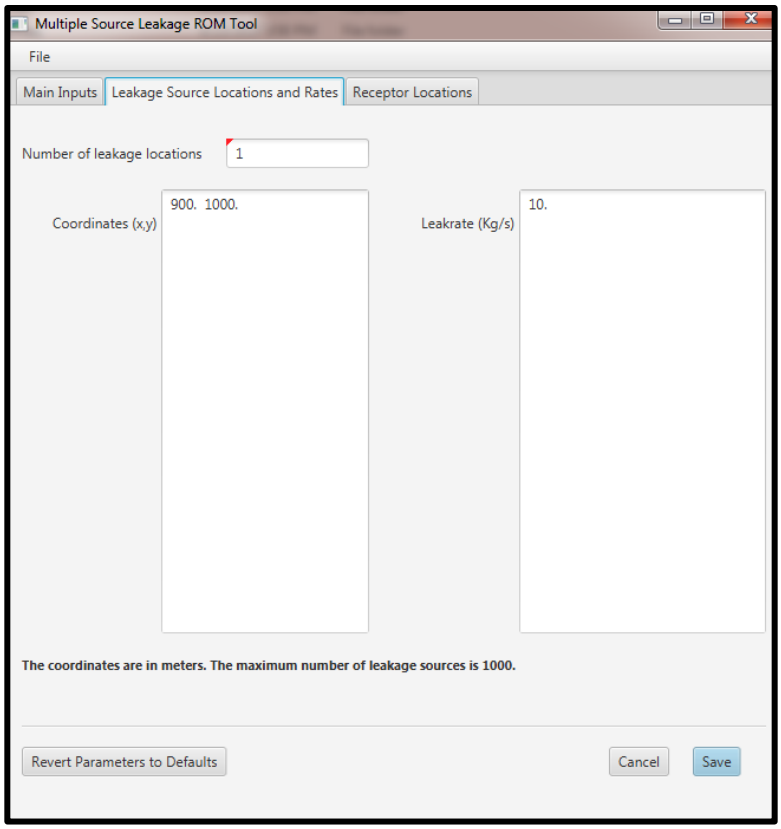

Figure 33: MSLR Leakage Source Locations and Rates Tab

1.4.3 MSLR Receptor Locations

Up to 100 receptors (locations at which the user wants to know if the dense gas concetration exceeds the critical value defined) can be defined. If the ROM is used as part of the NRAP-IAM-CS model, receptor locations are provided through a specific text file. If the ROM is used as a standalone, the information need to be entered into the 'Receptor Locations' tab as illustrated in **Figure 34**.

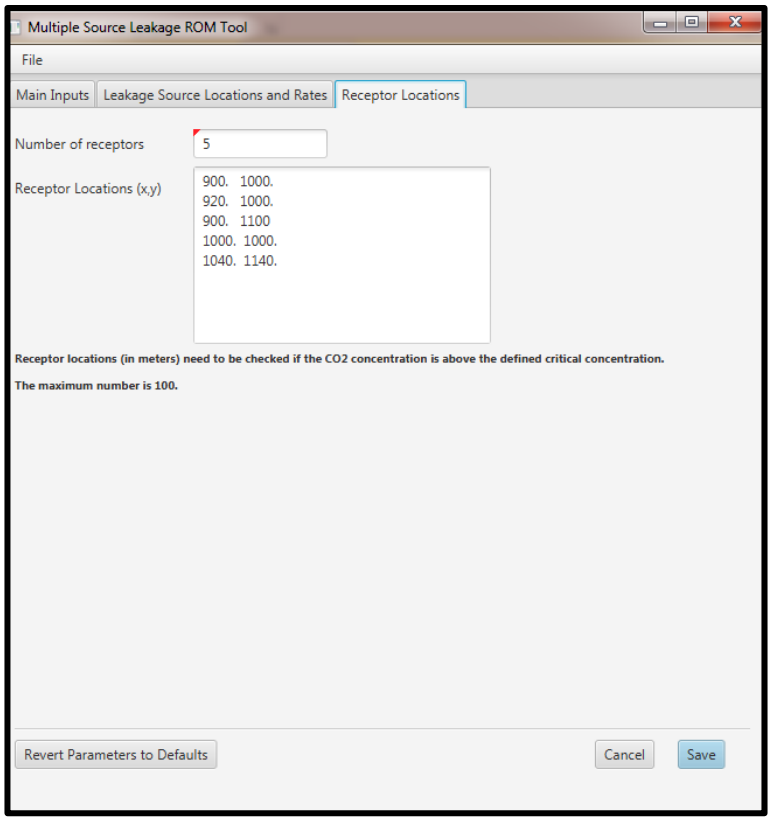

Figure 34: MSLR Receptor Locations Tab

1.4.4 MSLR Outputs

If used as a standalone evaluation tool, MSLR results are in the format of a text file (graphical outputs are currently not available) and include the list of the receptors where the critical CO_2 concentration has been reached as well as the critical radius of each leakage zone to define the critical zone. When used within the NRAP-IAM-CS, graphic visualization is available.

To prove the validity of the superposition method and Britter and McQuaid monograph built into MSLR, the model has been tested against Fluidyn-PANACHE (family of software modules for modeling atmospheric flows) for single and multiple source releases. Results are in very good accordance and can be viewed in the tool's user manual.

1.5 NRAP Integrated Assessment Model–Carbon Storage (NRAP-IAM-CS)

Introduction. The NRAP-IAM-CS software is constructed to provide probabilistic simulations modeling the long-term fate of CO_2. Several ROMs make up the program, allowing subsurface modeling to be conducted within the storage reservoir, through leakage pathways, and in shallower reservoirs. This does include leaky wellbores. Modeling results are provided in terms of volumes in place, plume extent, and impact on other resources, such as shallow groundwater wells or the atmosphere.

GoldSim is required to be installed in order to run the model, which must be purchased or provided as an academic or 30 day evaluative license (available at: https://www.goldsim.com/Forms/Evaluation.aspx).

Input/ Output. NRAP-IAM-CS can operate in two modes. The first type is a scoping level input array that employs simplified model geometry and constant geologic properties. Later, when more data is available, the model can be run in a detailed mode to describe the spatial variability of subsurface properties, well locations, and leakage pathways.

Model input data can be categorized as follows:

1. Scenario Type and Inputs
    a. Direct leakage to atmosphere through wells (requires reservoir, legacy wells and land surface information)
    b. Leakage to groundwater through wells (requires reservoir, legacy wells, shallow aquifer and intermediate reservoir and land surface information)
    c. Area of review (requires reservoir, seal, legacy wells and land surface information)

Once the type of scenario has been chosen, the site needs to be described.

2. Site Characteristics
    a. Simple (built-in model)

One main assumption for the simple site is that there is one single injection well. The CO_2 injection rate can be specified by the user but will be limited by the maximum frac pressure, if reached. Main reservoir inputs include depth, thickness, permeability, porosity, water and CO_2 residual saturations (constant or distributed).

    b. Complex

A lookup table option is available for the complex option and allows the user to import spatially variable inputs such as land surface elevation, reservoir elevation, thickness, permeability, temperature, CO_2 saturation, dissolved CO_2 concentration and pressure. All inputs must be generated on a 100 by 100 grid.

3. Wellbore Characteristics

NRAP-IAM-CS uses the wellbore leakage WLAT reduced-order model (described in section 1.3.10) to calculate CO_2 and brine leakage rates.

    a. Locations options

This is a very flexible option which allows the user to input coordinates for existing well(s) or let the software generate random location(s) for a specified number of wells over a specific area using a normal distribution.

    b. Permeability options

Three permeability options are available, which include: constant cement permeability for all the wells, variable permeability using available distribution options or an open wellbore model (refer to section 2.2.4 of the WLAT Reduced Order Model for more details).

4. Shallow Aquifer and Intermediate Reservoir

The simulations for the shallow aquifer plumes are from multiphase reactive chemistry models using the FEHM (Finite Element Heat and Mass) and STOMP (Subsurface Transport Over Multiple Phases) models. The shallow aquifer and intermediate reservoir section requires the input of physical and hydrologic and geochemical parameters

a. Physical parameters
b. This section allows the user to fill in physical properties such as elevation, thickness, pressure, temperature, permeability and porosity for each of the shallow aquifer and the intermediate reservoir Hydrologic and geochemical parameters

This section allows the user to fill in a complex table of inputs for 16 different aquifer hydrologic (permeability, permeability anisotropy, aquifer thickness, etc.) and geochemical (benzene, pH and phenol decay constants for example) parameters. Each of these parameters can be defined as constant or a distribution can be selected which will be applied during Monte Carlo analysis.

5. Surface Environment Characteristics (land surface information)

In this section, the leakage from the wells or/and faults that make it to the atmosphere is input into the atmospheric dispersion model which computes the changes in CO_2 concentration above the sequestration site based upon external factors (such as wind speed, ambient temperature and ambient pressure). More details are provided in Appendix 1, section 1.4 on the MSLR (Multiple Source Leakage Reduced Order Model) tool.

Leakage and impact results are provided in five sub-classifications. They are CO_2 and brine leakage, CO_2 and brine leakage: multi-variate statistics, aquifer impacts results, and aquifer impacts: multi-variate statistics and atmospheric dispersion results.

Using GoldSim output and the results viewer, animations of contour plots or three-dimensional realizations can be seen.

1.6 NRAP Seal Barrier Reduced Order Model (NSEALR)

Introduction. NSEALR models the flow or leakage of CO_2 through low permeability formations overlying storage horizons. These strata, often called cap rocks or confining units, are a primary characterization criterion that must be input in order to quantify leakage/seepage potential from storage pools. The model currently assumes a 1D (vertically), two-phase flow of CO_2 through a brine saturated rock under CO_2 supercritical conditions.

GoldSim is required to be installed in order to run the model, which must be purchased or provided as an academic or 30-day evaluative license (available at: https://www.goldsim.com/Forms/Evaluation.aspx).

Input/ Output. As can be seen on **Figure 35**, there are 7 different sections for inputs, the top 5 for seal-related properties and the 2 additional sections for general reservoir parameters.

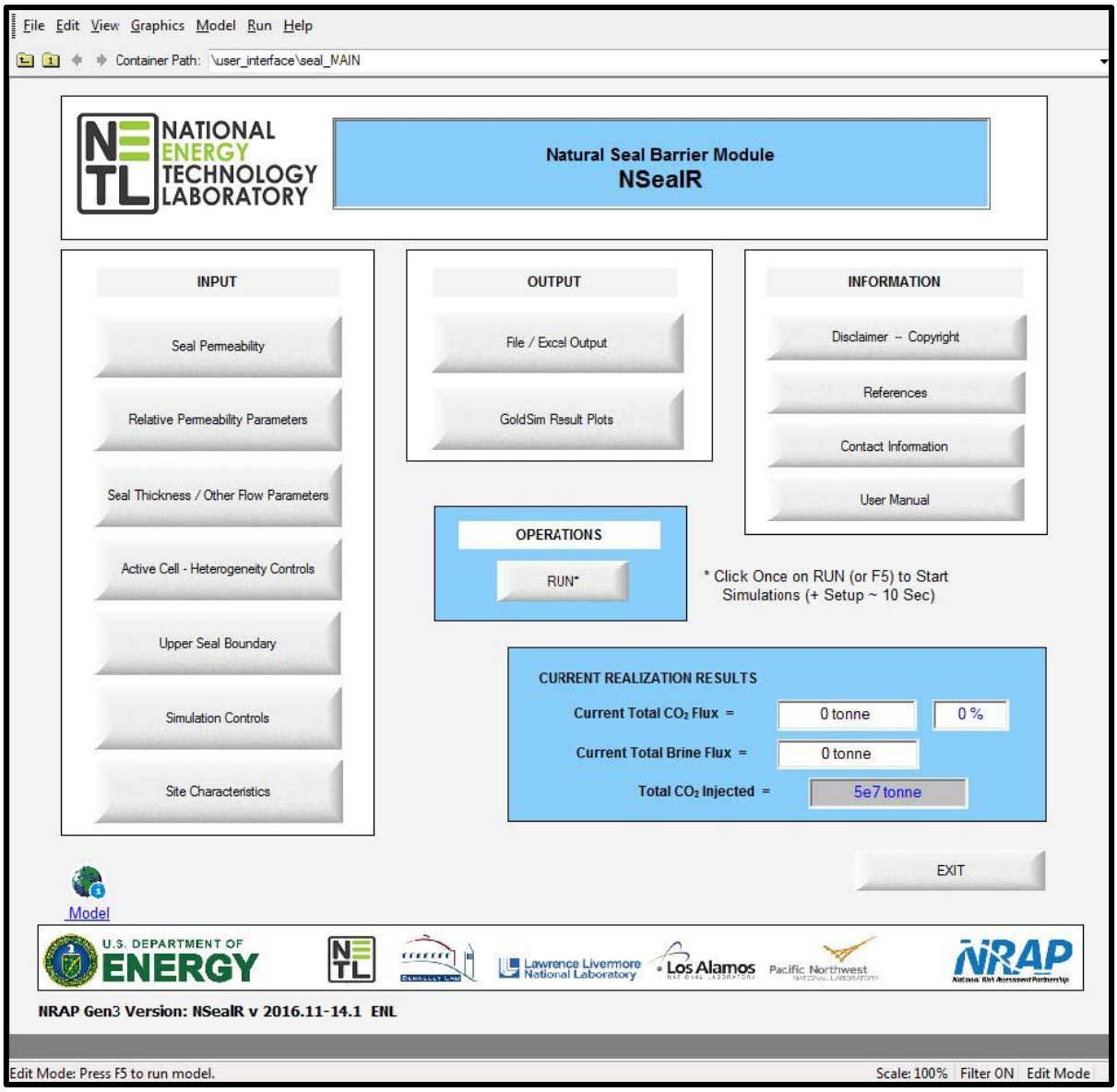

Figure 35: NsealR Main Dashboard

1.6.1 Seal Permeability

There are 5 different options available for a seal permeability model: (1) constant flux; (2) user defined constant permeability and porosity for each cell; (3) definition of permeability and porosity across the area of interest using stochastic distributions; (4) user defined equivalent permeability and porosity for each cell using the fractured rock model and (5) a user defined permeability map input using a text file. Additional information regarding the different permeability models can be found in Appendix A of NSealR's user manual. All the required inputs are shown on **Figure 36**.

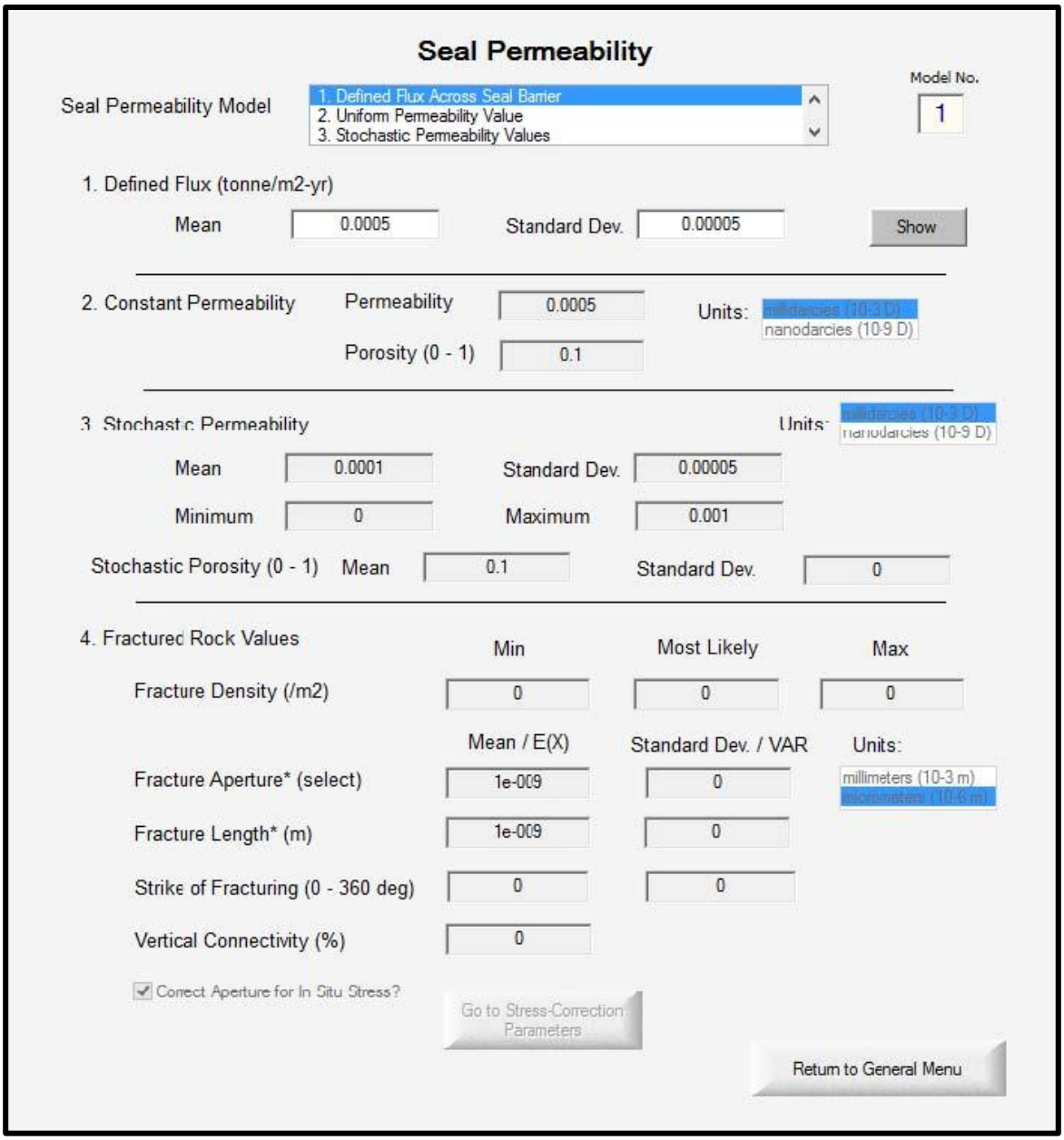

Figure 36: Seal Permeability Dashboard

1.6.2 Two-Phase Flow and Relative Permeability

Two-phase model parameters can be entered as a single value or as a variable value (using a uniform distribution). The model currently supports four different two-phase models: Purcell Model, Brooks-Corey model, van Genuchten-Mualem model and LET general model. These relative permeability model are all described in great details in Appendix C of NSealR's user manual. **Figure 37** highlights all the inputs required.

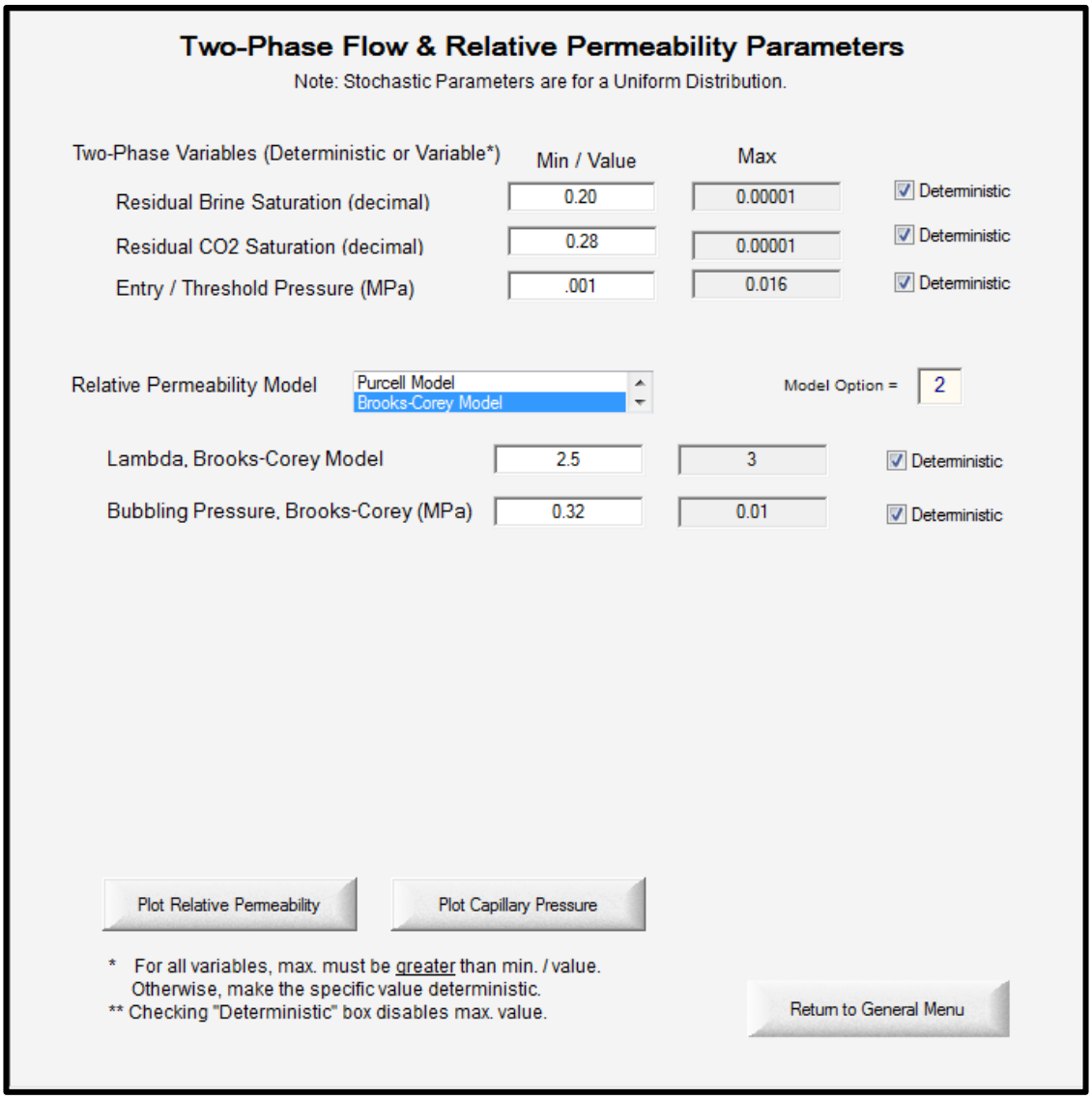

Figure 37: Two-Phase Flow and Relative Permeability Dashboard

1.6.3 Seal Thickness and Reference Parameters

The seal thickness can be defined via three different options: constant value through the formation, probabilistic distribution or an array of user-defined values input from an external text file. In addition, four reference parameters are defined here: the salinity of the brine in the seal, the brine pressure at a specified depth, the reference depth and temperature. Other required parameters are shown on **Figure 38**.

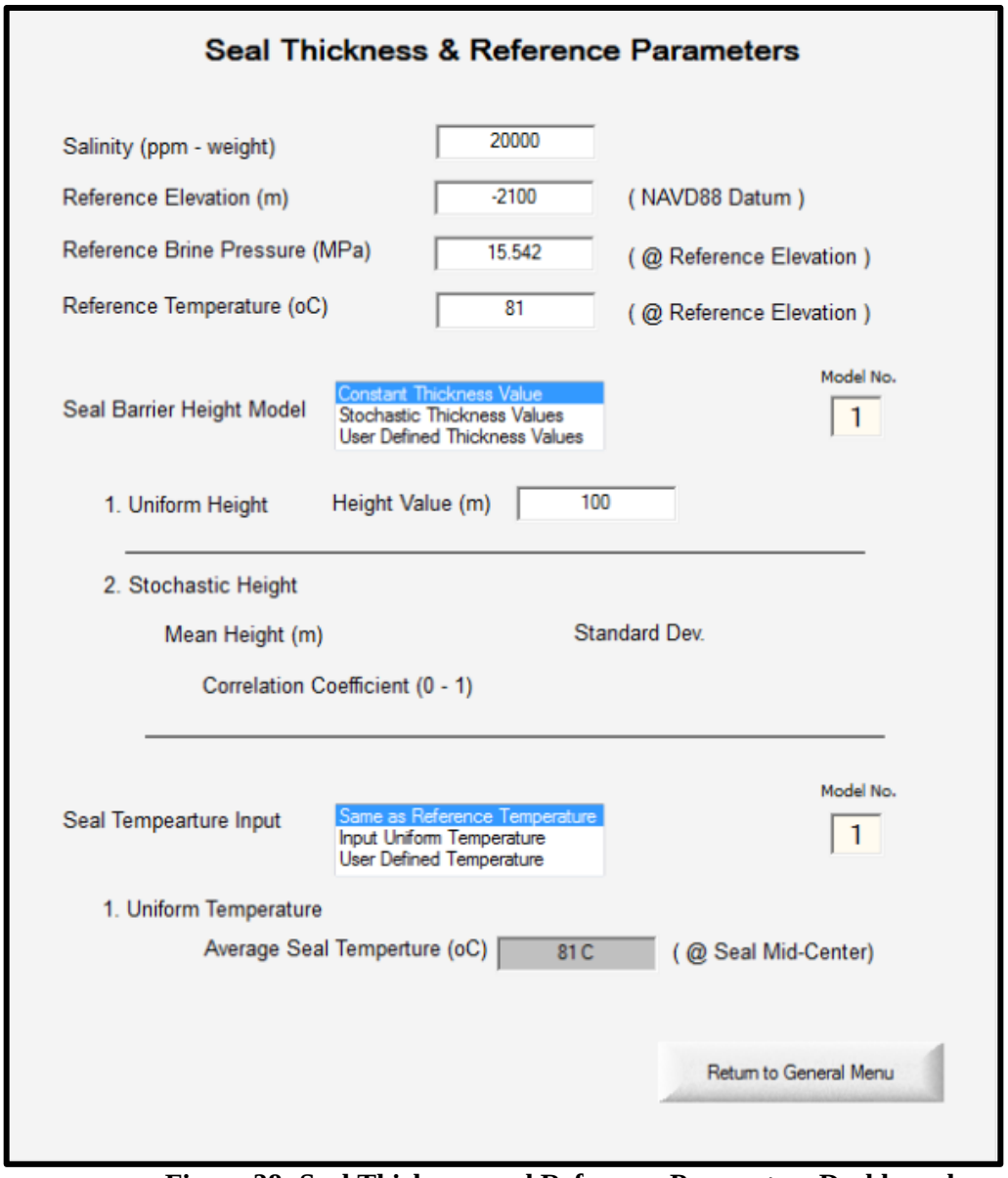

Figure 38: Seal Thickness and Reference Parameters Dashboard

1.6.4 Active Cell Definition and Heterogeneity Controls

The active cell option allows the user to limit the flow to certain areas across the seal horizon, basically generating a sub-model. The required parameters for that option are shown in **Figure 39.**

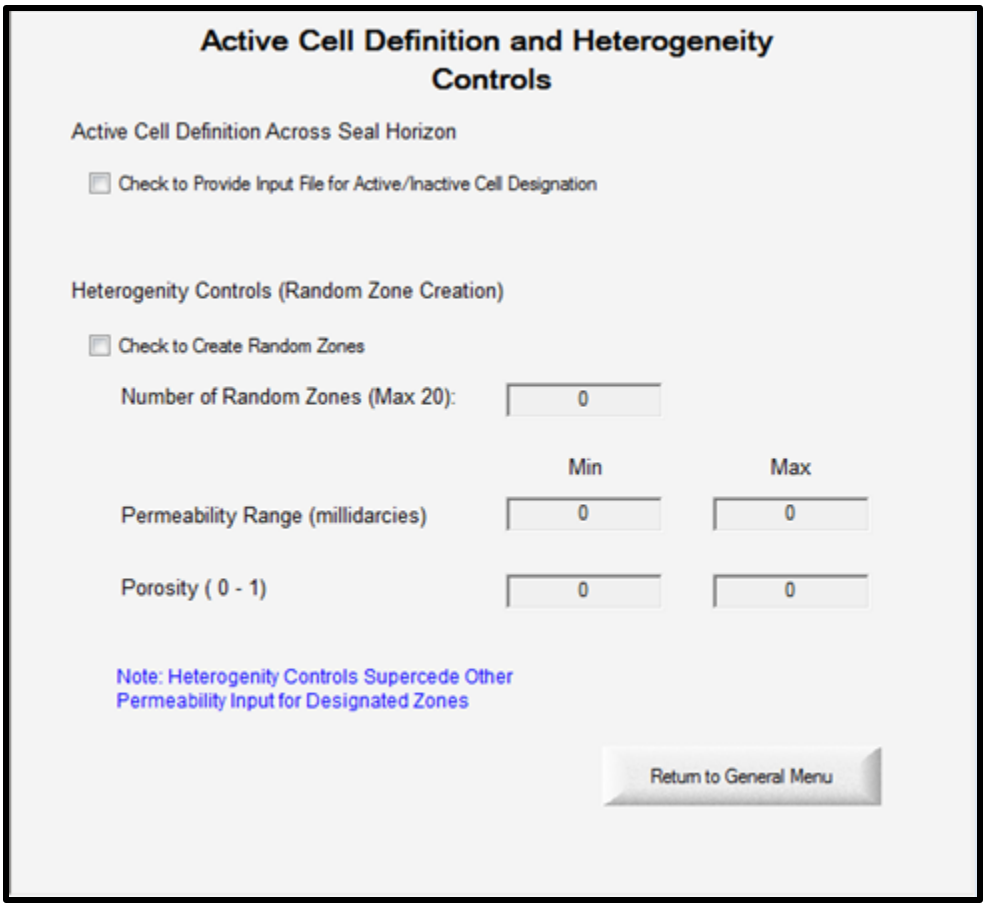

Figure 39: Active Cell Definition and Heterogeneity Controls Dashboard

1.6.5 Upper Seal Boundary Definition

The last form allows the user to define the pressure and saturation conditions at the top of the seal horizon. Three options are available for input:

- static conditions,
- a function that computes the pressure and saturation conditions at the top of the seal as a function of the corresponding values at the bottom,
- and user defined values which allows values from a text file to be imported.

The required parameters for the upper seal boundary definition are shown on **Figure 40**.

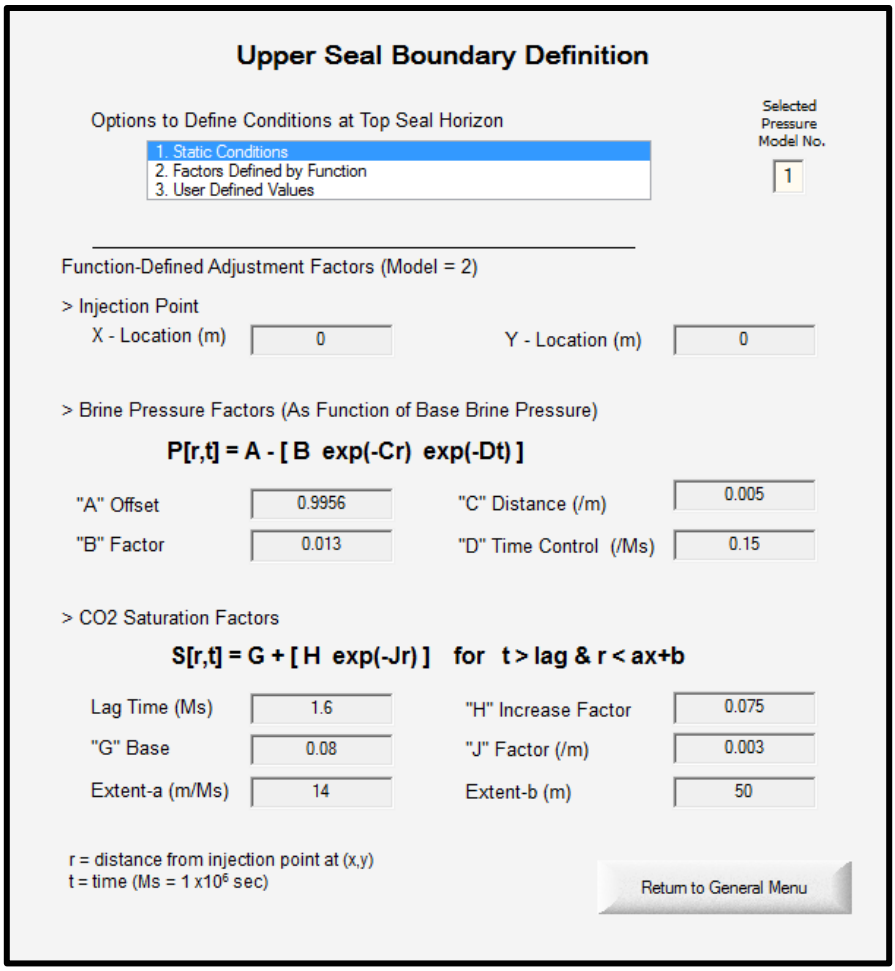

Figure 40: Upper Seal Boundary Definition Dashboard

1.6.6 Ouputs

The results are available in the form of text files and Excel files and are as follows:

- Brine and CO_2 mass flux at specific time intervals
- Brine and CO_2 mass flux for the entire 100*100 grid at a specific time interval

If GoldSim is being used, brine and CO_2 mass flux can be plotted versus time. Additionally, plots of the distribution of the total brine and CO_2 mass flux at the top of the seal horizon at the end of each simulation can be generated. 3D visualization is also available in GoldSim.

1.7 Reservoir Reduced-Order Model Generator RROM-Gen

Introduction. RROM-Gen is a utility program which uses reservoir simulation parameters (inputs and outputs) from 7 different simulators and converts them to a format acceptable for NRAP-IAM-CS.

1.7.1 RROM-Gen Inputs

RROM-Gen accepts inputs from 7 different simulators:

- TP3D (Two Phase Three-Dimensional model)
- FEHM (Finite Element Heat and Mass model)
- CMG-GEM (Computer Modeling Group, Generalized Equation-of-State Model)
- TOUGH2, (Transport Of Undersaturated Groundwater and Heat 2 model)
- STOMP, (Subsurface Transport Over Multiple Phase model)
- ECLIPSE (Exploration Consultant Limited Implicit Program for Simulation Engineering) and
- PETREL (Schlumberger Exploration and Production software platform).

Depending upon the simulator chosen, one or several files need to be read. The data is manipulated (by using bi-linear interpolation) to be converted to a 100*100 grid size, which is the only grid size accepted by NRAP-IAM-CS and translated into the appropriate file format. The grid has the option to be regular (meaning all grid blocks have the same size) or linear (the size of the grid blocks can be defined and is especially useful if a grid refinement was applied to the original grid) The units are also converted if needed as NRAP-IAM-CS accepts only meters, MPa and years. If the original grid is not oriented with the coordinate system, a rotation will be applied to re-orient the grid. The various options for inputs are shown on **Figure 41**.

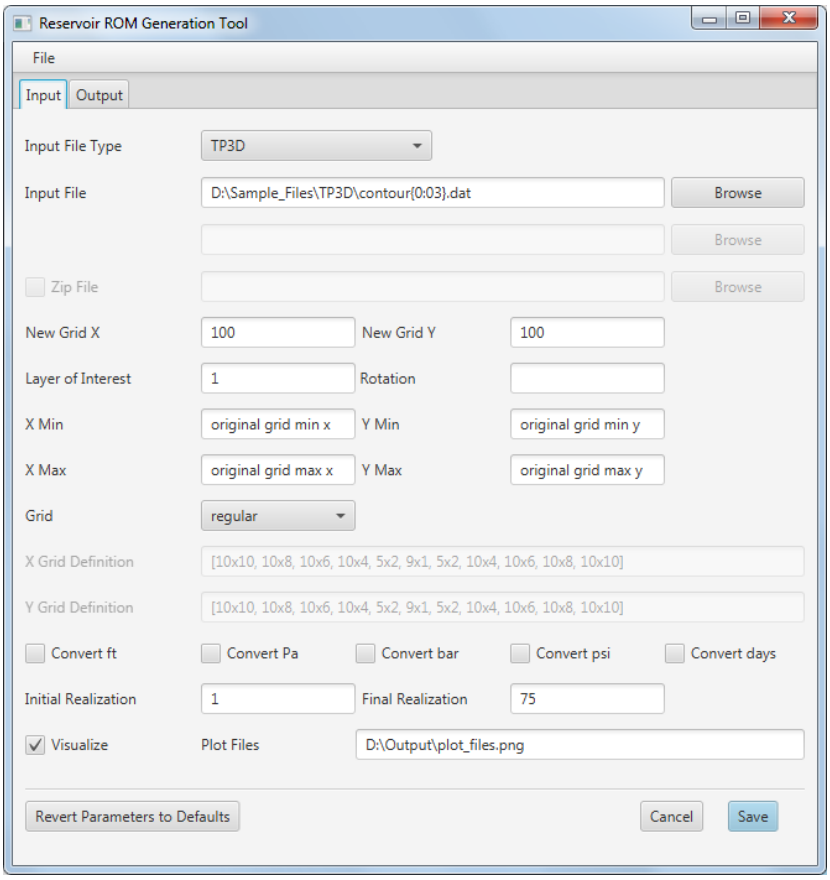

Figure 41: RROM-Gen Inputs Tab

1.7.2 RROM-Gen Outputs

RROM-Gem has 2 required outputs (pressure and saturation) and 4 optional (elevation, dissolved CO_2, temperature and permeability), **Figure 42**.

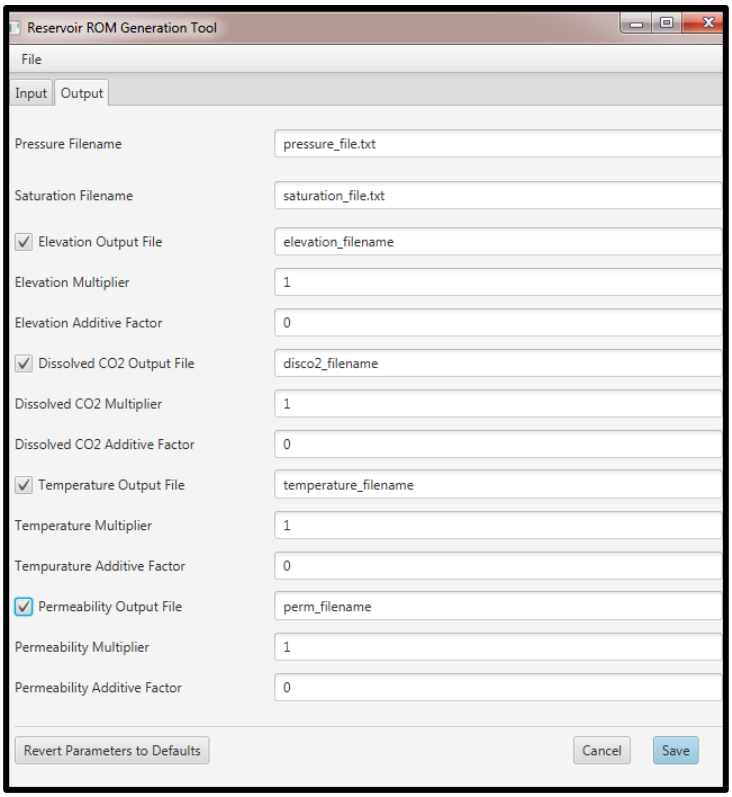

Figure 42: RROM-Gen Outputs Tab

1.8 Short-Term Seismic Forecasting (STSF)

Introduction. The reduced order model was developed to simulate induced seismicity associated with the underground storage of CO_2. The tool is an adaptation of the ETAS (Empirical Type Aftershock Sequence) model (Ogata, 1988)[8] that was originally designed to model the rate of aftershocks after a main large shock. To adapt the model to the behavior of induced seismicity, an additional rate of aftershocks term has been included by Bachman et al. (2011)[9] to account for the external forcing due to the injection.

Input/ Output. The tool only uses two input files, the seismic catalog and the flow file. The seismic catalog contains the recorded magnitude and location of seismic events as a function of time. The user has the option to either use the provided catalogue or create its own. Six different injection parameters can be used as inputs from the flow file to run the simulations: downhole flowrate, surface flowrate, downhole pressure, surface pressure, and flow in, which all vary versus time. The last option, constant, is not time dependent. In addition, event magnitude and Guttenberg-Richter law (relationship between the magnitude and the number of earthquakes of at least that magnitude) parameters are also required. Outputs come in the form of two text files and will forecast the number of seismic events occurring in a specified range of magnitudes during a specified time frame. **Figure 43** shows STSF input tab.

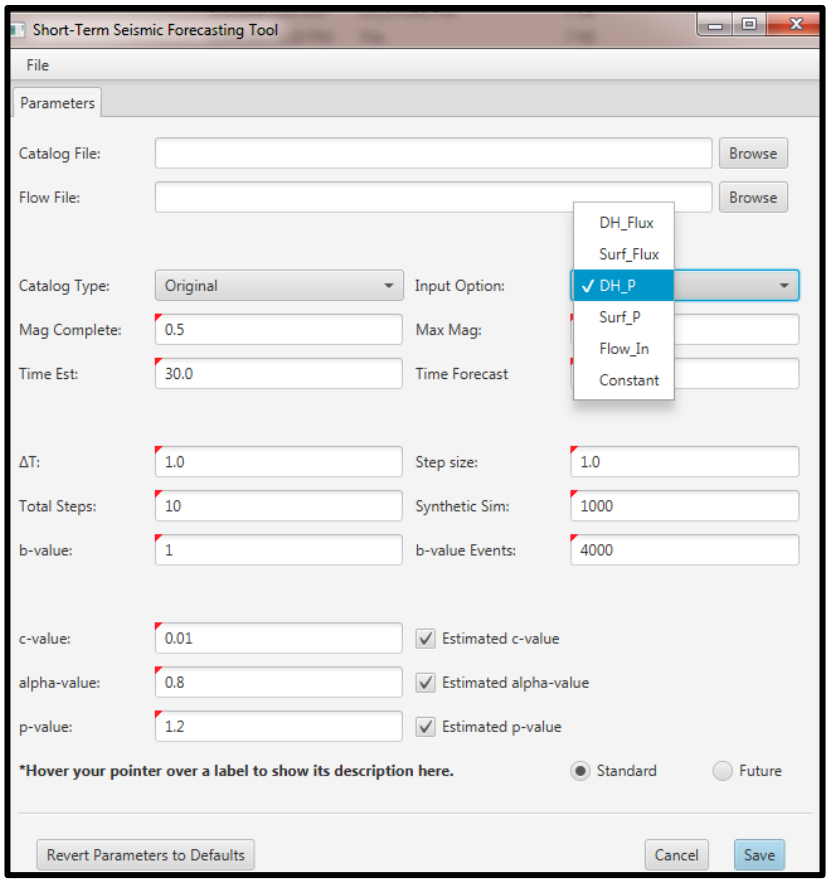

Figure 43: STSF Input Tab

Appendix 3: Sargent & Lundy CO_2 Capture Feasibility Report

CARBONSAFE PROJECT

PACIFICORP JIM BRIDGER POWER PLANT

CO_2 CAPTURE FEASIBILITY MEMO

FINAL
For Use

December 11, 2017
S&L Project No.: 13658-001

Prepared by:

55 East Monroe Street • Chicago, IL 60603 USA • 312-269-2000

LEGAL NOTICE

This report ("Deliverable") was prepared by Sargent & Lundy, LLC (S&L), expressly for the sole use of University of Wyoming and PacifiCorp, Rocky Mountain Power (jointly referred to as Client) in accordance with the agreement between S&L and Client. This Deliverable was prepared using the degree of skill and care ordinarily exercised by engineers practicing under similar circumstances. Client acknowledges: (1) S&L prepared this Deliverable subject to the particular scope limitations, budgetary and time constraints, and business objectives of the Client; (2) information and data provided by others may not have been independently verified by S&L; (3) the information and data contained in this Deliverable are time sensitive and changes in the data, applicable codes, standards, and acceptable engineering practices may invalidate the findings of this Deliverable. Any use or reliance upon this Deliverable by third parties shall be at their sole risk.

CO_2 CAPTURE FEASIBILITY MEMO

Sargent & Lundy (S&L) was retained by the University of Wyoming ("University") to evaluate a large-scale carbon storage project in Wyoming as part of Phase 1 of their DOE-funded CarbonSAFE project. The overall purpose of the Phase 1 project is to conduct pre-feasibility studies for a commercial-scale CO_2 geological storage complex.

As part of this project, the University is developing a strategy for an integrated capture and storage project, which includes identification of a potential source site. The University has engaged PacifiCorp, the Owner and Operator of the Jim Bridger Power Plant (Jim Bridger), to participate in the CarbonSAFE project as the host site.

To support Phase 1 of this project S&L is evaluating the high-level feasibility of implementing CO_2 capture at Jim Bridger. Based on S&L's experience with performing feasibility analyses for CO_2 integration at existing power plants, Jim Bridger is believed to be a good candidate for installing CO_2 capture technology to provide compressed/concentrated CO_2 for the CarbonSAFE project.

CO_2 Capture Background and Considerations for Feasibility

This feasibility evaluation is based on a traditional, commercially-available MEA (amine-based) process. S&L considers commercially available processes to be those that have been demonstrated during slipstream tests or have been implemented on permanent installations treating a quantity of flue gas that is at least equivalent to 5 MWe. The following technologies are commercially available:

- Fluor – Econamine FG Plus™
- Mitsubishi Heavy Industries (MHI) – KM-CR Process® with KS-1™ solvent
- Shell – Cansolv

A typical amine-based CO_2 capture system consists of a quencher, an absorber column, and a stripping column; in addition, a booster induced draft (ID) fan is typically required in retrofit applications to overcome the pressure loss through the slipstream.

A CO_2 capture facility can have a large impact on an existing facility, and the following criteria need to be evaluated to determine the feasibility and cost of installing a CO_2 capture system:

1. Location and Siting Considerations – The major process equipment and balance of plant (BOP) systems included in a complete CO_2 capture facility require a very large footprint.
2. Process Considerations – Sulfur dioxide (SO_2) and other pollutants can have a detrimental impact on the effectiveness of the amine reagents in a CO_2 capture facility. As such, in order to optimize the design and minimize reagent degradation, vendors typically limit the incoming SO_2 emissions to about 5 ppm.

3. Steam Requirements – The regeneration energy comes from low quality steam, which can be provided by the unit's existing steam cycle or by a new steam generation unit (if the existing steam cycle does not have sufficient capacity).

4. Process and Cooling Water Requirements – The CO_2 capture system consists of a large quantity of heat exchangers used for process cooling as well as intercoolers. Process water will also be required for operation of the CO_2 island equipment for makeup to the amine solution, water wash of amine vapor, and miscellaneous uses. .

5. Auxiliary Power Requirements – The CO_2 capture and BOP systems include a significant quantity of pumps, compressors, fans, and other components which will result in high auxiliary power consumption. The primary power consumer is the compressor, which pressurizes the CO_2 stream to the required pipeline pressure. The auxiliary power can either be provided by the existing unit or a new power generation unit (if spare capacity is not available, or the associated unit derate is not acceptable to the station).

Station Background

Jim Bridger is located in Point of Rocks, Wyoming in un-incorporated Sweetwater County and consists of four nearly identical coal-fired units commissioned between 1971 and 1979. Each unit is rated at approximately 570 MW (gross capacity) and burn a western bituminous coal. All four units are equipped with electrostatic precipitators (ESPs) for particulate control and wet flue gas desulfurization (WFGD) for SO_2 control. One of the major differences between the units at Jim Bridger is the recent implementation of selective catalytic reduction (SCR) technology for NO_X control on Units 3 and 4.

Future requirements for SCR technology on Units 1 and 2 are uncertain at this time; depending on future demand and regulatory uncertainty, Units 1 and 2 may cease coal operations sooner than Units 3 and 4. While the units have already been in operation for approximately 40 years on average, it is expected that with proper equipment maintenance and upgrades, these units will be capable of continued operation for many years. Due to the longer potential lifetime of Units 3 and 4 based on unit age and recently completed AQCS upgrades, this feasibility assessment is limited to these two units.

The potential CO_2 production rate will depend on the scale of the CO_2 capture facility, which could range from a small slipstream from a single unit to100% of the flue gas from both units. Based on a typical system design capture efficiency of 90%, annual CO_2 capture per unit would be approximately 3 million tons per year, assuming a 60% capacity factor for the capture island itself.

Location and Siting Considerations

As discussed above, a very large footprint is required for a CO_2 capture facility. The Jim Bridger property has sufficient land available within the existing property line. Sufficient space for a CO_2 capture facility is located adjacent to Unit 4, which is ideal for a CO_2 capture system associated with Unit 3 and/or 4. This area is

approximately 20 acres and with only minor relocation of pre-fabricated buildings would be available for a large-scale CO_2 capture system.

Due to the proximity to Unit 4, the most cost-effective treatment cases would be associated with Unit 4. Unit 3 can be easily integrated into the system with incrementally more ductwork and piping to tie-in to the Unit 3 flue gas stream and utilities. Furthermore, Unit 4 has additional ID fan capacity for the base plant flue gas draft loss, which provides some additional operating margin for the unit in the future in comparison to Unit 3.

Process Considerations

One major benefit of the Jim Bridger units is that they are already equipped with wet FGD systems, which limits the amount of SO_2 and SO_3 in the flue gas; therefore, only polishing in the quencher system is required to support the amine-based CO_2 capture system. If no SO_2 controls were present, a new FGD system would be required to pre-treat the flue gas upstream of the CO_2 capture system, which dramatically increases the cost of the system and the necessary footprint.

Steam Requirements

Typically for a CO_2 capture facility, low quality steam will be extracted from the crossover between the IP and LP sections of the existing turbine and supplied to the CO_2 island. The associated condensate from the reboiler exit will be returned to the main condenser.

Based on S&L experience with similar Units and steam turbines, it is expected that Jim Bridger Units 3 or 4 would be capable of supplying the required process stream without affecting turbine performance. This is expected to be true even at the maximum steam extraction rate that would be needed for treating 100% of the flue gas.

While extraction of this quantity of steam would derate the gross output of the turbine, and potentially the quantity of saleable power, it is expected to be less of an issue at Jim Bridger as the units are not currently base loaded (i.e. selling power at 100% MCR). The cost of the steam would then equate only to the cost of the coal to generate the steam and plant O&M cost rather than resulting in a loss in revenue for the plant (due to reduced sales of electricity) or additional capital expense to install an alternative steam source, which can be quite costly.

Process and Cooling Water Requirements

As discussed above, a CO_2 capture system requires a significant quantity of cooling water, typically a new cooling tower would be installed to provide process cooling to the CO_2 capture system heat exchangers even at a facility, like Jim Bridger, which has existing cooling towers. Depending on the current operation of the cooling towers, it may be possible to supply the required cooling loads using the existing cooling towers; however, this would need to be further studied based on their current operation.

At Jim Bridger, makeup water will be supplied from the existing raw water sources. At this time, the available capacity of the Jim Bridger raw water supply has not been evaluated; however, the expected quantity of makeup

water is expected to be relatively small and is not anticipated to be a fatal flaw based on the current and future operation of the plant. This quantity of makeup water required and the available capacity of raw water should be evaluated as part of a feasibility study.

Auxiliary Power Requirements

As discussed above, a CO_2 capture system has a very high auxiliary power demand, primarily due to the compressors. This can be provided by the existing facility if sufficient capacity is available or alternatively by an alternative source. In some cases an alternative source of power can also provide steam for regeneration.

Similar to the steam requirements, adding auxiliary load to an existing power plant can reduce the quantity of saleable power, it is expected to be less of an issue at Jim Bridger as the units are not currently base loaded (i.e. selling power at 100% MCR). The cost of the power would then equate only to the cost of the coal to generate the power and O&M cost rather than resulting in a loss in revenue for the plant (due to reduced sales of electricity) or additional capital expense to install an alternative power source, which can be quite costly.

Feasibility of CO_2 Capture at Jim Bridger

Based on this high level feasibility evaluation, Units 3 and 4 at the Jim Bridger Power Plant are good potential candidates integration of a CO_2 capture facility in conjunction with Wyoming's CarbonSAFE project. In fact, the current configuration and operation of the units result in a more cost-effective host site than other facilities which may not have sufficient land, emission control equipment and spare capacity.

This feasibility evaluation was performed based on S&L's experience with both CO_2 capture technologies and the PacifiCorp Jim Bridger Power Plant. A more detailed study is recommended to fully evaluate the extent of capture that is feasible at Jim Bridger as well as the cost of constructing and operating the system.

Appendix 3: Plan for assumption of long-term liability for stored CO_2

Carbon Management Institute
Plan for assumption
of
long-term liability for stored CO_2

for

PROJECT AWARD # DE-FE0029302: Integrated Pre-Feasibility Study of a Commercial-Scale CCS Project in Formations of the Rock Springs Uplift, Wyoming

II. Executive Summary

This memo sets forth the Carbon Management Institute's (CMI's) plan for assumption of long-term liability for stored CO_2 at the Rock Springs Uplift, Wyoming Commercial-Scale CCS project site.

A. Process: The approach to address long term liability can best be described as having three parts: (1) risk minimization; (2) scenario analyses to estimate residual liability; and (3) financial risk management instrument design and management.

B. Project Structured to Minimize Risk

The risk management posture of the Rock Springs Uplift project uniquely positions the project to qualify for favorable long-term risk management financing solutions. The risk reducing characteristics embedded in the very structure of the proposed program, combined with a well-defined legal and regulatory environment unique to the State of Wyoming, including clear criteria and a history of successful and safe management of enhanced oil recovery (EOR) under the law, and extensive experience with other oil and gas extraction, pipeline and other CO_2 injection activities, create conditions that allow this project to be designed to a theoretical zero expected loss standard.

Specifically, siting of the Rocky Springs Uplift project was chosen to minimize overall liability exposure through (1) placement of injection wells on land sections owned by the State of Wyoming; (2) site selection criteria focused on superior geology; (3) site selection using community information focused on minimizing impacts; (4) operational criteria managing pressure loading into the reservoir; (5) engineered site characteristics[1] designed to conform to the IPCC estimate which projects >99.9% storage security

[1] Lackner KS, Brennan SA, Matter J, Park A-HA, Wright A, van der Zwaan, BCC (2012), The urgency of the development of CO_2capture from ambient air, Proc Natl Acad Sci, August 14, 109, 33, 13156–13162.

(virtually a zero leakage standard); and (6) prioritization of re-use of CO_2 over storage as a project goal – minimizing reservoir inputs and exposures as a matter of operational rule.

C. Loss Scenario Analyses

Loss scenario analyses will be developed in a manner consistent with accepted practices in the insurance and finance industry for property and casualty loss modeling.

Designing the project to theoretical zero expected loss standard allows the storage liability underwriting process to focus on discrete loss modeling activities and create a price efficient solution because no regular losses are expected as part of the normal course of operations – leaving loss scenario analyses to be focused on the unexpected and unintended event scenario only.

The loss modeling outputs will be used to create an expected loss table with assigned probabilities based upon project characteristics.

Those expected loss tables will be converted into funding stream requirements and assigned cost of capital and other customary finance charges to determine funding requirements over time.

D. Instrument Design and Implementation

The ability to structure necessary financial instruments and obtain sufficient market capacity responsive to the maximum probable loss arising directly out of release of injected CO_2 from the insured reservoir will be dependent upon both scenario based loss analyses discussed above and an underwriter's assessment of characteristics that drive loss exposure including but not limited to: financial market conditions, injection site geology, maximum injection volume and over time and in the aggregate, legal considerations, site infrastructure, injection pressure, and related operations, operator performance and loss history. The number of parties with ownership interest in the pore space, ground water, surface water and other resources and assets on State of Wyoming lands will also constitute critical conditions considered during the underwriting process.

The ultimate instrument design will be a structure that accrues available limits of liability as exposure builds consistent with the loss scenarios.

Limits of liability will be designed to reflect maximum probable loss for this low frequency risk profile.

Given the ultimate expected declining risk profile over time, the instrument may also have to address the possibility of excess funding allocation upon liability termination.

Given the project plan's structure to a zero expected loss standard, CMI plans to manage long-term liability risks through a combination of insurance instruments and user fee funded

and structured financial instruments. CMI also plans on continuing to engage the Wyoming Legislature on the issue of long term liability management to address limitations on market capacity and related indemnity. In such discussions, CMI will emphasize the reasonableness of a possible sun-setting liability policy approach that would designed to track with the well documented real risk reductions that occur in properly designed and managed storage reservoirs over time.

III. Introduction and Relevant Background

Wyoming geology, Wyoming legal framework and project specific engineering and operational standards at the Rock Springs Uplift site minimize and bound any potential legal liability arising out of planned CCS and CCUS operations. In fact, the entire project is structured to a 'zero loss' posture meaning that should a loss arise from CO2 leaking from the reservoir, such a loss would be both unexpected and unintended by project design.

This risk management posture when combined with an overall program and process that connects project location, design, operational risk management, state liability framework and community risk management converges to minimize maximum possible and maximum probably liability scenarios.

a. Project design is keyed to a zero loss scenario. This project structure affirms a solid understanding of the sequestration process as well as operational risks and mitigation criteria. Site selection criteria applied in this design reduces both the possible and probable maximum exposure should an unexpected and unintended CO2 release event manifest from the storage reservoir.

b. In theory, risk management is predicated on forecasting the range of possible outcomes, determining what influences and drives the outcomes, recognizing that forecasts can be wrong, identifying the consequences of being wrong, and then, establishing risk management policies, procedures and tools to reduce risk and optimize risk mitigation.

c. In practice, the Rocky Springs Uplift project was designed using such risk management criteria in a manner to reduce risk by design and create risk mitigation opportunity as a core operational matter.

d. All models used to identify and quantify risk have limitations – however small – to leave a residual risk of loss. The long term CO_2 liability program designed for the Rocky Springs Uplift was designed to be responsive to such contingent, unexpected and unintended risks.

e. The long term liability program approach is designed to respond to residual risks modeled including but not limited to those arising out of CO_2 leakage which could cause bodily injury or property damage, including environmental damages, to third parties not involved (not in privity) with the Rocky Springs Uplift project.

f. The long term storage liability program will be designed to mitigate moral hazard (e.g. avoid incentives to increase risk because of the presence of the risk management product).

g. The CO_2 liability management program will be designed to meet financial responsibility criteria up to an estimated maximum probable loss scenario.

h. Existing Wyoming law and policy, geology and infrastructure form a substantially reduced probable loss scenario than those found with storage location alternatives

including but not limited to: (1) offshore locations where international law schema and natural resource liability abound; (2) in states with no CO_2 pipelines that lack positive performance and loss history with gas management; (3) states with no permitted EOR operations – which creates a substantial permitting risk; and (4) in states with no CCS laws where confusion about regulatory rules could enhance or cloud responsibility and liability for storage management criteria.

IV. Relevant WY State Law Issues

See the separate legal analysis.

V. Risk Management and Liability Transfer Tool Options

a. Types of Tools

In general, four classes of risk transfer products exist:
1) traditional indemnity products which are typically only available to risks where there is a number sufficient to create a pool,
2) retained risk (or self-insured) products, that are often used where moral hazard and / volatility are difficult to manage or knowledge of the risk is proprietary
3) independent event triggered (also known as parametric insurance) products, often used where loss adjustment processes or expenses make a traditional product impractical and
4) structured products – which typically combine characteristics of several products – often used where low frequency catastrophic risk is desired to be transferred but operating risk is most efficiently retained.

b. Scenario Based Analyses Used To Inform Policy Structure Choice and Critical Characteristics - Including Limits of Liability and Triggers

Risk management structures will be chosen by CMI that balance the desire to maximize coverage and optimize cost efficiency. Scenario based analyses will be developed to inform limitation of liability requirements and other terms of the policies structured. The limits of liability for the program will be designed to have a reasonable relationship to the maximum probable loss estimated by the scenario analyses.

A careful evaluation of the embedded and engineered risk management characteristics of the Rocky Springs Uplift project suggest that a structured program with excess layer indemnity coverage would be the most efficient and effective tool for risk transfer for the long term portion of the program. However, as actual scenario analyses proceed, an alternate structure may be deemed more efficient.

Precise limits of liability and triggers will be determined in the next phase of the project.

VI. Risk Transfer Marketplace

The risk transfer marketplace globally and in North America is robust. In the United States in 2016, according to the latest report from the Federal Insurance Office dated September 2017[2], the Property and Casualty (P&C) direct written premiums (DWP) for all US insurers in 2016 were approximately $610 Billion. Approximately $294 Billion of this DWP was collected from the commercial sector. The 2016 P&C surplus was approximately $712 Billion. Commercial insurers regularly share risk with the oil and gas industry across all matter of operations. Further engagement with respect to injection technology for the insurance industry is consistent with parts of the specialty insurance industry.

VII. Planned CCS RM Framework & Components

a. CMI plans to develop a risk management framework in two (2) phases: operational and Long-Term Stewardship.

b. **Operational Phase** – This phase of risk management would address risks arising out of project siting, operation (compression and injection), and delimited closure.

   i. Single Goal Financial Instruments – Surety Bonds, Insurance, Letters of Credit, Self-Insurance (Financial Test, Corporate Guarantee) will be reviewed to determine which instrument is most responsive to loss scenarios for this work phase. Funds consistent with maximum probable loss projections resulting from the scenario based analyses will be collected using a metric driving risk – such a injection volume or pressurization or other reasonable risk

   ii. Cost Estimation Requirements – As noted above cost estimations informing requirements for limits of liability and risk premium loading factors will be informed using scenario based loss analyses.

   iii. Delimiting Requirements for Issuing Institutions – capital adequacy, credit rating and regulatory compliance issues applicable to the issuance of the risk management instruments chosen will inform qualification parameters for issuers of the chosen risk management instruments. Obviously, any instrument issuer must be legally permitted to issue in Wyoming – but specific credit quality requirements may also be desired to assure ability to pay in the unlikely event of loss.

c. **Long-Term Stewardship Phase Liability Tool**– Post-Injection, Post-Site Certification – Post-Closure: Three-Part Solution – Safety Board, CCS Trust, Enabling Legislation

   The Rocky Springs Uplift project will address long term liability by reducing risk as part of the project structure. After operational risk reduction steps are taken, (1) a Safety Board may be established to monitor, verify an audit ongoing risk reduction activities; (2) a CCS Trust account will be established as further described to create an accrual fund to pay for risk management instruments that will hold long term liability related to CCS storage; and (3) enabling legislation will be sought to limit the duration and magnitude of the liability to reflect the maximum probable loss as established by scenario analyses referenced above and the reduction of risk over time established by the technical evaluation of the risk profile.

[2] https://www.treasury.gov/initiatives/fio/reports-and-notices/Documents/2017_FIO_Annual_Report.pdf

Background Charts

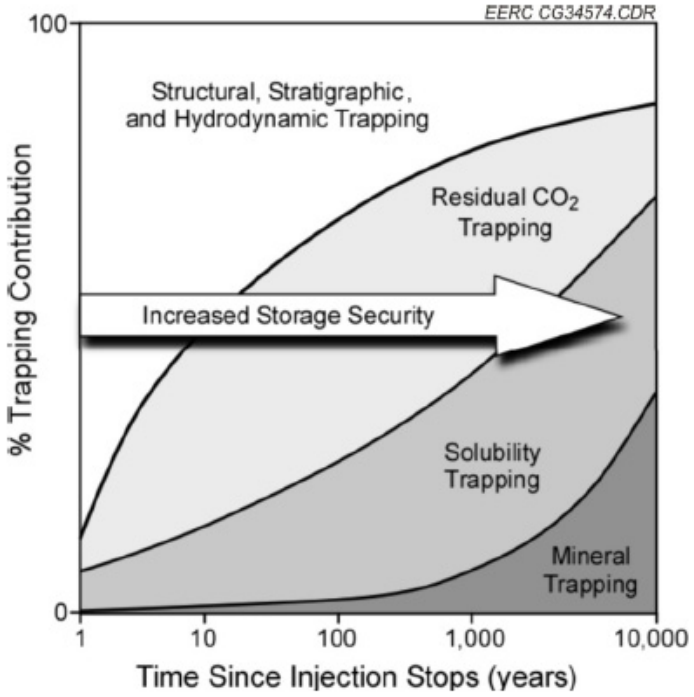

Figure 3. Storage security of the different trapping mechanisms and their relationship with time (IPCC, 2005).

Figure 1. CCS Project Lifecycle [29]

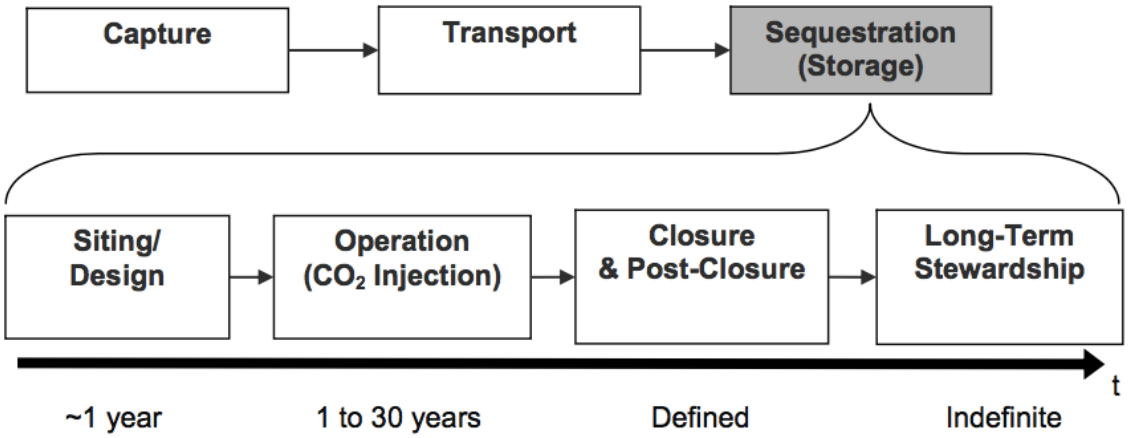

Figure 2. Risk Profile Curve for CCS Sites[32]